Serum Stable Carbohydrate-Oligoethyleneamine Copolymers for Nucleic Acid Delivery

Karina Kizjakina

Dissertation submitted to the faculty of the Virginia Polytechnic Institute and State University in partial fulfillment of the requirements for the degree of

Doctor of Philosophy
In
Chemistry

Theresa M. Reineke
Paul R. Carlier
Kevin J. Edgar
Maren Roman
S. Richard Turner

01/20/2011
Blacksburg, VA

Keywords: nucleic acid delivery, glycopolymers, oligoethyleneamines, trehalose, PEG.

Serum Stable Carbohydrate-Oligoethyleneamine Copolymers for Nucleic Acid Delivery

Karina Kizjakina

ABSTRACT

The delivery of nucleic acids at the tissue and cellular levels remains one of the major hurdles in this scientific area. Since nucleic acids are bulky macromolecules and unstable in the presence of nucleases, vehicles are required to compact them into nanosized particles, offer protection from degradation *in vivo*, and release the therapeutic cargo at the desired location. Polycationic vehicles are good candidates for these purposes since they can be chemically modified to tune the desired properties in nanoparticle formulations.

We designed a family of trehalose-oligoethyleneamine copolymers that showed promising plasmid DNA (*p*DNA) transfection results in the presence of serum proteins. A diazidotrehalose monomer was copolymerized with linear oligoethyleneamines of varying length and containing alkyne end-groups via step-growth Cu(I)-catalyzed azide-alkyne cycloaddition polymerization resulting in a series of trehalose copolymers with a range of secondary amines (from 4 to 6) within the polymer backbone. Upon electrostatic complexation of the polycations and *p*DNA in aqueous medium, nanosized particles were formed, and their sizes and zeta-potentials were characterized via dynamic light scattering (DLS). The glycopolymers were tested for *p*DNA binding, toxicity, cellular uptake, and transfection efficiency *in vitro*. Characterization of these polymers revealed a

significant influence of minor structural modifications on bioactivity. In general, all of the polymers efficiently bind *p*DNA at low nitrogen to phosphate (N/P) ratios forming nanoparticles below 100 nm in size and demonstrated cellular uptake and transfection. Polymers comprised of trehalose moieties and four secondary amines in the repeat unit showed the greatest promise in *p*DNA delivery *in vitro*. Because of its large hydration volume, we hypothesize that trehalose contributes to particle stabilization in serum.

The trehalose-based polymers with four secondary amines (**Tr4**) were subsequently modified with PEG (5kDa). This modification lead to the development of well-defined polymeric structures with PEG moieties selectively incorporated at the ends of linear trehalose-oligoethyleneamine polycations. The study of the effect of this modification on bioactivity revealed that there were no significant difference in the toxicity profiles within this series of PEGylated and non-PEGylated materials; however, overall results suggest that both modified and unmodified trehalose-oligoethyleneamine copolymers have a great promise for stem cell-based and regenerative therapies.

ACKNOWLEDGEMENTS

First, I would like to thank my advisor Dr. Theresa M. Reineke for the great opportunity to do innovative research in her group in both University of Cincinnati and Virginia Tech. Thank you, Dr. Reineke, for the support and faith in my abilities. Thank you for the opportunities to participate in national conferences and invaluable advice on giving interesting and well-organized presentations. I would like to thank Dr. James Mack and Dr. Apryll M. Stalcup, my committee members in the University of Cincinnati, and Dr. Paul R. Carlier, Dr. Kevin J. Edgar, Dr. Maren Roman, and Dr. S. Richard Turner, my committee members at Virginia Tech, for their constructive comments during my presentations, helpful suggestions on my research, and thorough review of my thesis. I am thanking Dr. Tom Ridgway for the great support during the start of my PhD track. I want to thank Dr. Paul Deck for solving all the problems related to my transfer to VT. I would like to thank both Departments of Chemistry at UC and VT for funding and supporting my research and studies in PhD program. Special thanks to Antons Sizovs, a great chemist and person, for being a true friend to me inside and outside the lab, for invaluable and continuous suggestions on my research, for critical reviews of all my written manuscripts, and advices for my presentations. I am very grateful to Sneha Kelkar for her friendship, encouragement, and collaboration. Thanks to Giovanna Grandinetti and Dr. Nilesh Ingle for their tremendous help with cell culture experiments. Thanks to the former group member, Dr. Vijay Taori, for the friendship and encouragement during his time in the lab and after. Thanks to Dr. Adam Smith for reviewing my manuscripts and support during my job search. Thanks to the former group member Dr. Josh Bryson for the friendship and collaboration. I am thankful to all the current and former the Reineke group members, for their friendship and encouragement during my PhD time. Lastly, I cannot thank enough the whole my family for the invaluable support in everything I do in this life.

Table of Contents

List of Figures

List of Tables

List of Schemes

Chapter 1: Introduction – Dissertation Overview

This dissertation summarizes the results of the projects that I was closely involved in, during my PhD track in Dr. Reineke's research group at the Chemistry Department of the University of Cincinnati and later at the Chemistry Department of Virginia Tech.

Chapter 2 is a brief literature review in the field of non-viral gene delivery and covers the most relevant topics to the thesis work. This chapter gives an overview of the cationic polymers currently developed and used for the delivery of therapeutic nucleic acids, highlighting carbohydrate-oligoamine polycations and, in particular, trehalose-containing systems. The biological properties and applications of these materials are discussed. Mentioned are some of the therapeutics, whose discovery evolved from this concept.

Chapter 3 of this dissertation covers the design, synthesis, and biological characterizations of trehalose-oligoethyleneamine "click" polymers. This polycationic system has been thoroughly studied *in vitro* in neonatal human dermal fibroblasts and rat mesenchymal stem cells and exhibits high potential for stem cell-based and regenerative therapies, outperforming most of the commercially available transfection reagents.

Further development of trehalose-containing "click" polymers toward successful future *in vivo* applications was accomplished by modifying the polymer structures via PEGylation and results of this project are described in **Chapter 4**.

Finally, **Chapter 5** discusses some future directions evolved from the projects described in this thesis. A few concepts and solutions are proposed and some preliminary studies are shown.

The supporting information includes the NMR, IR, and LC-MS characterizations of some of the synthesized compounds and is available in **Appendix A** and **Appendix B**.

Chapter 2: Non-Viral Gene Delivery Vectors

2.1. Introduction

With the Human Genome Project completed[1], gene therapy holds much promise for the treatment and hopefully a cure for the vast majority of diseases and genetic disorders. Thus, the first NIH approved and reported foreign gene transfer trial on humans was performed in 1989 and was based on retroviral-mediated gene transduction to insert a therapeutic gene into tumor-infiltrating lymphocytes (TIL) and subsequent infusion of these lymphocytes into patients with metastatic melanoma.[2] Since 1997, Edelstein *et al.* have been storing the global information on gene therapy clinical trials. Up to June 2010, over 1600 trials were approved, ongoing or completed worldwide (**Figure 2-1**) with 62% of all trials performed in the US alone.[3-5]

Despite big safety concerns with viral vectors, adenoviruses and retroviruses are the most widely used vectors in gene therapy strategies – over 67% of all of the trials are viral vector-based therapies. Naked plasmid DNA (*p*DNA) was used in 18% of trials; among the rest of the trials, lipofection as a non-viral alternative was used in 6% of cases (**Figure 2-2**).

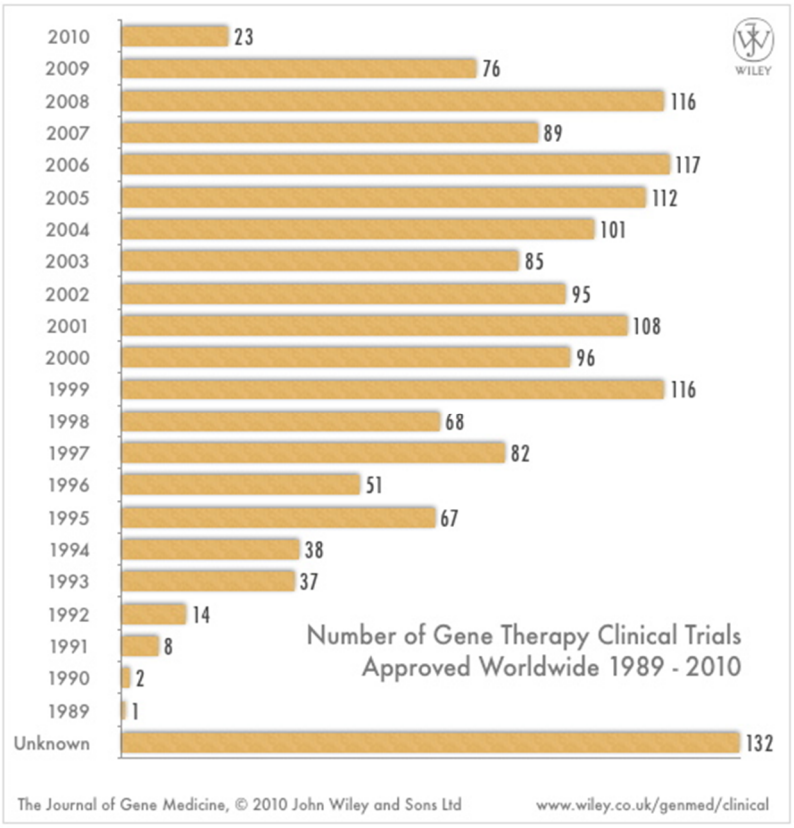

Figure 2-1. Worldwide approved gene therapy trials. (Figure adapted with permission from Ref. [5] Copyright © 2010 John Wiley & Sons, Ltd.)

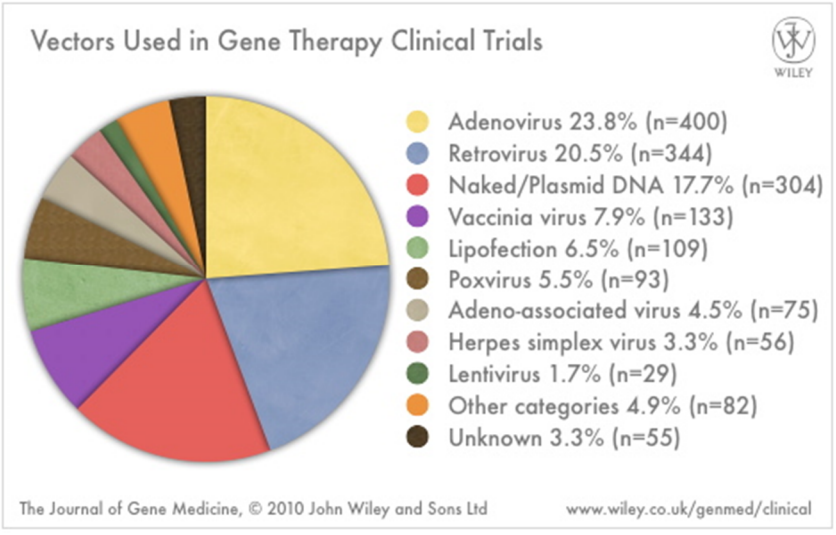

Figure 2-2. Vectors used in gene therapy clinical trials worldwide. (Figure adapted with permission from Ref. [5] Copyright © 2010 John Wiley & Sons, Ltd.)

In 1978, Levine and Levy published the first report on a human clinical trial with the drug Poly-ICLC, describing the polycation-mediated delivery of poly IC (polyinosine-polycytidylic acid – synthetic analog of double stranded RNA) stabilized with low molecular weight poly-L-lysine and carboxymethyl cellulose.[6] This strategy was later taken over by Oncovir, Inc. that is producing Poly-ICLC and its various modifications for cancer treatments under the trade name Hiltonol™.[7]

In April of 2010, Davis *et al*. reported the first human clinical trial involving the systemic administration of siRNA for the treatment of solid cancers (clinical trial registration number NCT00689065 – the first patient was treated in May of 2008).[8,9] In this trial, siRNA was complexed with a cyclodextrin-containing polymer, functionalized with human transferrin as the targeting ligand (functionalization was achieved via the formation of non-covalent β-cyclodextrin inclusion complexes with adamantane-PEG and adamantane-PEG-transferrin) (**Figure 2-3**), and systemically administered to the melanoma patients on days 1, 3, 8, and 10 of a 21-day cycle by a 30-min intravenous infusion (**Figure 2-4**).

The vast increase in studies of polycation- and lipid-mediated nanomedicine technologies improves the understanding of structure-property relationships and leads toward synthetically tailoring macromolecules with multi-task functionalities to improve their specific targeting, transfection efficiency, and toxicity profiles. Macromolecule-based non-viral gene delivery is rapidly expanding and some products have reached Phase 1, Phase 2, and Phase 3 clinical studies (**Table 2-1)**.

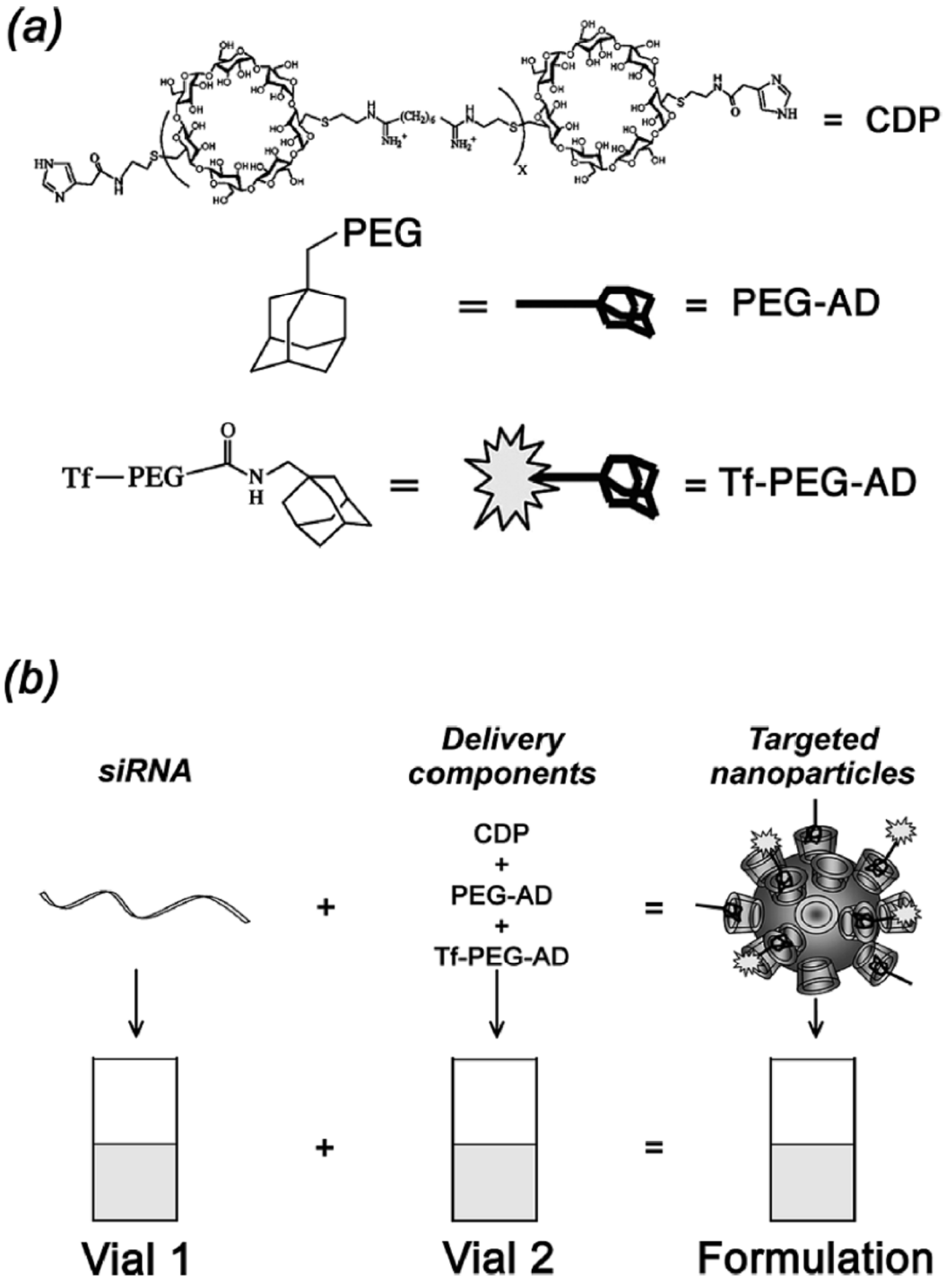

Figure 2-3. Composition of the targeted nanoparticle for siRNA delivery developed by Davis *et al*. a) The components of a delivery vector. b) Clinical formulation of siRNA delivery system (CALAA-01). (Figure adapted with permission from Ref. [9] Copyright © 2009 American Chemical Society.)

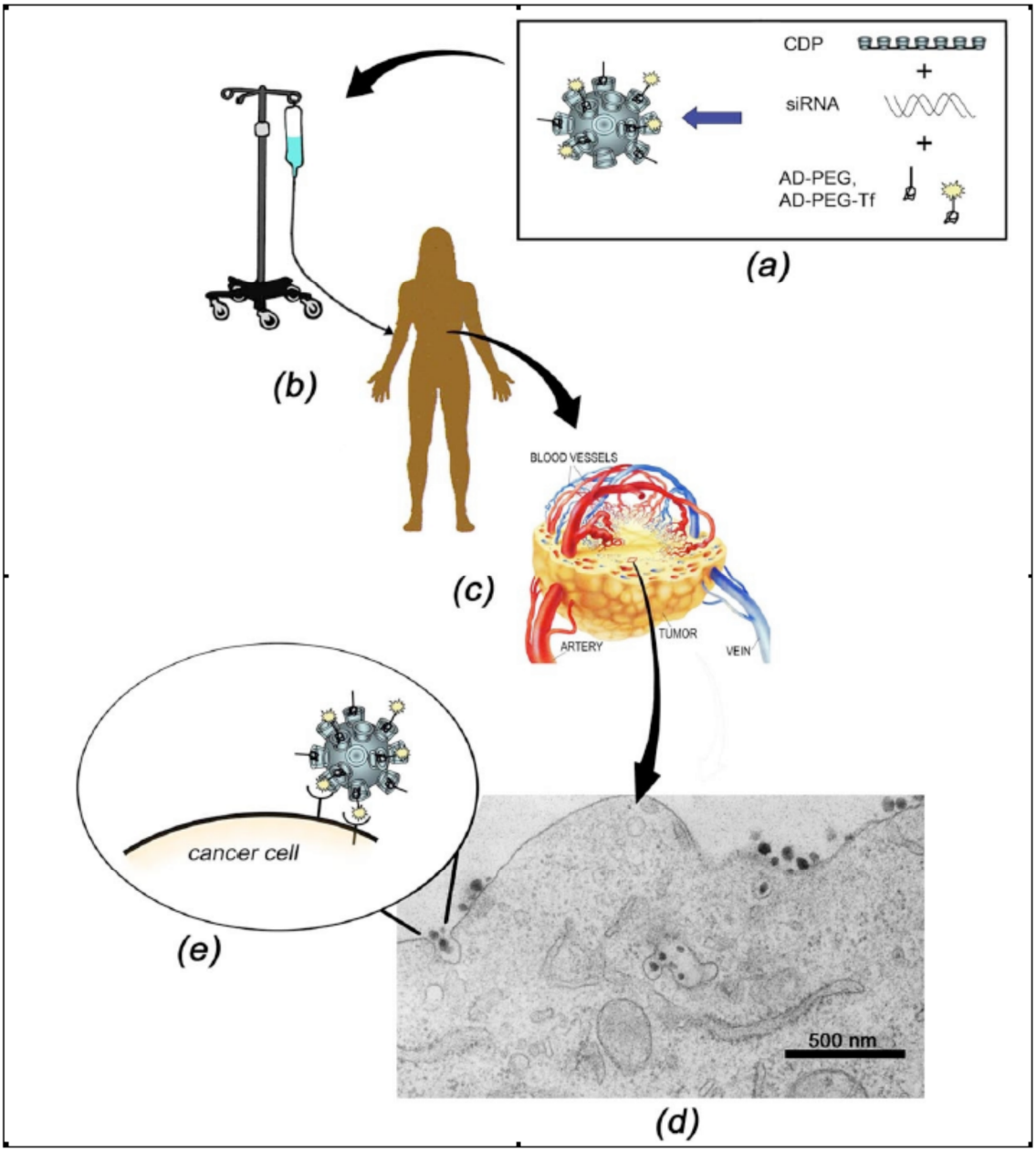

Figure 2-4. Schematic representation of the functions of targeted CALAA-01 during the patient treatment process. a) The formulation of CALAA-01. b) The i.v. infusion of a therapeutic to a patient. c) The representation of a tumor "leaky" vasculature. d) Transmission electron micrograph of CALAA-01 nanoparticles (50 nm in size) entering or inside the cancer cell. e) Interactions of the CALAA-01 nanoparticles with the cell surface that can stimulate cellular entry process. (Figure adapted with permission from Ref. [9] Copyright © 2009 American Chemical Society.)

Table 2-1. Some non-viral nucleic acid transfection agents used in clinical trials. Abbreviations: cyclodextrin (CD), nanoparticle (NP), polyethyleneimine (PEI) polyethyleneglycol (PEG).

SPONSOR	THERAPEUTIC	DRUG/VECTOR	TREATMENT	YEAR	STATUS	REF.
NIH	Poly-ICLC	Polyinosine-polycytidylic acid stabilized with low molecular weight poly-L-lysine and carboxymethyl cellulose	Solid tumors, acute leukemia	1978 (completed)	Phase 1 & 2	[6]
Vical	Allovectin-7®	*p*DNA lipid NPs	Head and neck cancers	2002-2008 (completed)	Phase 2	[10-12]
Vical	Allovectin-7®	*p*DNA-lipid NPs	Metastatic melanoma	2006 (ongoing)	Phase 3	[10-12]
M.D. Anderson Cancer Center/NIH	tgDCC-E1A	*p*DNA-lipid carrier/paclitaxel NPs	Platinum resistant ovarian cancer	2005 (ongoing)	Phase 1 & 2	[10,12]
BioCancell Therapeutics Ltd	BC-819	*p*DNA-PEI NPs	Unresectable pancreatic cancer	2008-2010 (completed)	Phase 1 & 2a	[10,12,13]
BioCancell Therapeutics Ltd	BC-819	*p*DNA-PEI NPs	Bladder cancer	2008 (ongoing)	Phase 2b	[10,12,13]
BioCancell Therapeutics Ltd	BC-819	*p*DNA-PEI NPs	Ovarian cancer	2009 (ongoing)	Phase 1 & 2a	[10,12,13]
Genetic Immunity	DermaVir Patch (LC002)	*p*DNA-PEI/mannose and dextrose NPs	HIV/AIDS vaccine	2008 (ongoing)	Phase 2	[10,12,14]
Calando Pharmaceuticals	CALAA-01	siRNA and CD-based NPs	Solid tumors	2008 (ongoing)	Phase 1	[8,10,15]
Alnylam Pharmaceuticals	ALN-VSP02	siRNA-lipid NPs	Liver solid tumors	2009 (ongoing)	Phase 1	[10,16]
Gynecologic Oncology Group/NCI	EGEN-001	*p*DNA and PEG/PEI/cholesterol lipopolymer NPs	Ovarian and fallopian tube cancers	2010 (ongoing)	Phase 2	[10,12,17]

2.2. Cationic Polymers as Nucleic Acid Delivery Agents

Although, still in its infancy, non-viral gene delivery has tremendous potential over the use of viruses, which have huge safety implications. Sophisticated synthetic modifications of macromolecules can yield "smart" materials – vehicles with multifunctional layers – and ultimately the ideal gene delivery platform with the capabilities for specific targeting, high transfection and gene expression, biodegradability, biocompatibility, non-immunogenicity, producibility in large quantities for low cost and stability for storage.

Described for the first time in 1995 by Bousiff et al.[18], the non-viral gene carrier polyethyleneimine (PEI) has been by far the most commonly used and the best examined polycation for nucleic acid (NA) delivery. According to the reported PEI protonation profile[19], only 11-15% of nitrogens are protonated under physiological conditions (pH 7.4). During the cellular transfection process, PEI/NA complexes traffic from the cytoplasm to other intracellular compartments such as lysosomes and endosomes where the pH drops from 7.4 to 5.5. At this lower pH, the number of protonated nitrogens increases up to 45%, causing PEI to exhibit an extensive "proton sponge" effect that induces the increased influx of protons, counter-ions, and water molecules into the vesicle resulting in its swelling and rapture.[18] Other widely used polycations are polylysine (PLL), chitosan, and poly(β-amino ester)s (**Figure 2-5**).[20]

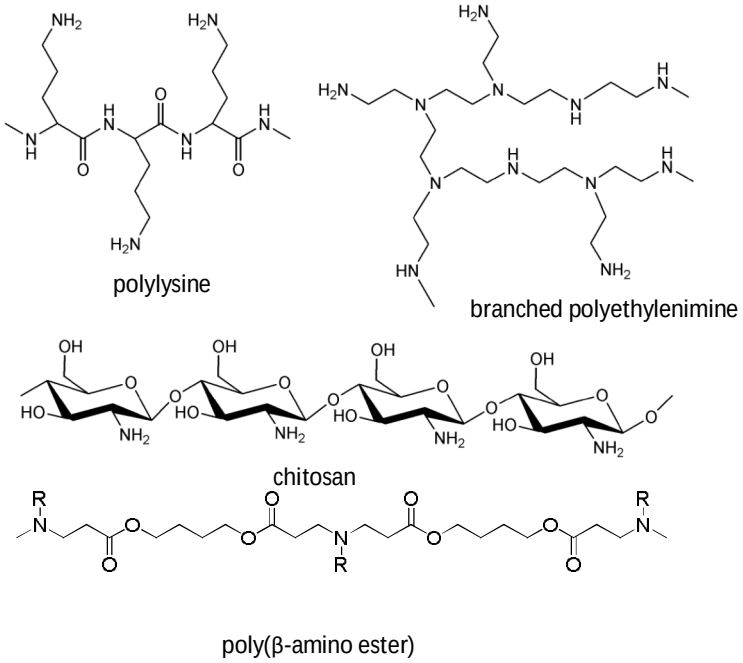

Figure 2-5. Structures of the most known polycations as gene delivery vectors. (Figure adapted with permission from Ref. [20] Copyright © 2003 Springer Berlin/Heidelberg.)

Polycation-NA complexation is mainly due to electrostatic interactions between the positively-charged polymer and negatively-charged phosphates of nucleic acid, although non-electrostatic interactions, such as H-bonding,[21,22] have been suggested to play a role. The mechanism of transfection by these complexes is beyond the scope of this chapter but a brief schematic representation of polyplex formation, endocytosis, endosomal rapture possibly induced by the "proton-sponge" effect and particle release into the cytoplasm is shown in **Figure 2-6**.

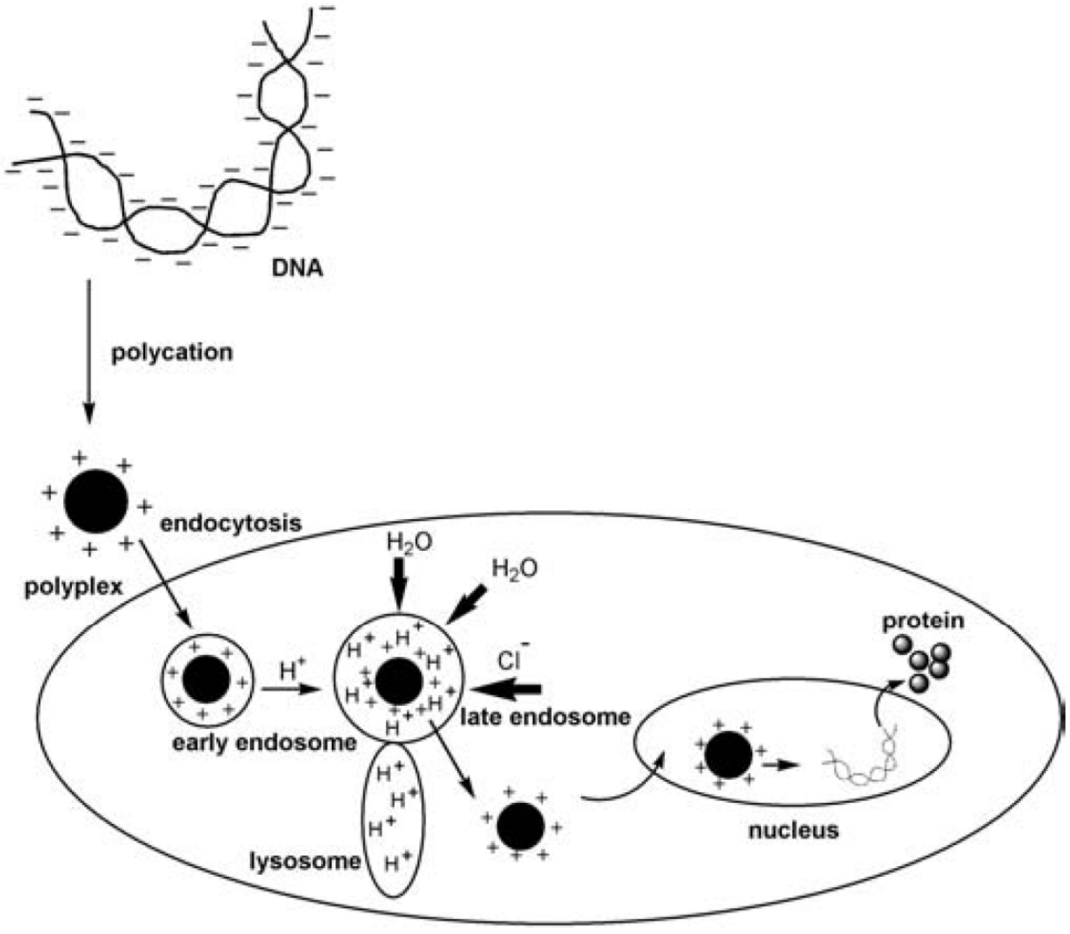

Figure 2-6. Schematic representation of polyplex formation, endocytosis, DNA release, and protein expression. (Figure adapted with permission from Ref. [20] Copyright © 2003 Springer Berlin/Heidelberg.)

The properties of macromolecules can be tuned via synthetic modifications to yield stimuli-responsive nucleic acid delivery vectors. Some examples of these polycationic systems are summarized in **Figure 2-7**. Physical properties of polycation-NA particles (size, zeta potential, the chemical composition of outer layers) can change with changes in the environment and therefore enhance the target-specific drug and gene delivery. These environment-responsive properties can be based on reactions triggered by pH changes[23-28] (for example, the carrier will release the NA cargo if the pH of the environment drops), by changes in the red-ox potential[29] (for example, disulfide bond cleavage in the presence of glutathione), by slight temperature changes that can cause changes in particle size and therefore influence transfection efficiency[30], and also by a magnetic field if the carrier has paramagnetic properties[31].

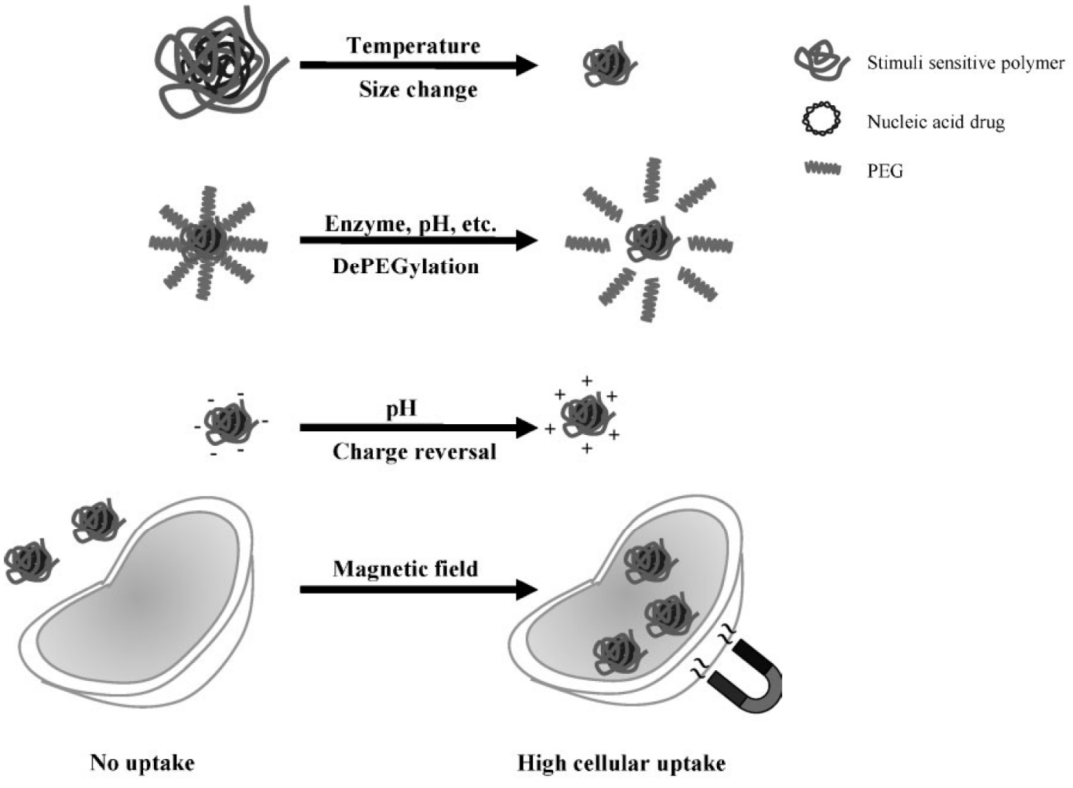

Figure 2-7. Nucleic acid delivery with environment-responsive vectors. (Figure adapted with permission from Ref. [32] Copyright © 2009 WILEY-VCH Verlag.)

2.3. Carbohydrate-Oligoamine Containing Polymers

In nano-medicine applications, polymeric nano-carriers have to perform many different functions to be able to deliver the very delicate therapeutic biomacromolecules to the tissues and cells of interest. Among other properties, discussed in the previous chapter, these materials have to coat nanoparticles with a protective layer that would ensure serum stability and prolonged particle blood circulation time for the purpose of systemic delivery of the drug to the organs of interest. Incorporation of carbohydrates into the structures of polycations has great potential in non-viral gene delivery. Carbohydrates are biocompatible (water soluble, nontoxic) and can be used to shield the nanoparticle surface charge by forming an outer layer of the particle leaving the NA inside its core. For these reasons, chitosan (**Figure 2-5**) has been studied extensively in the field. Other polysaccharides were chemically modified to introduce functionalities that can be protonated in the endosomal pH range. For example, dextran functionalization with different naturally occurring oligoamines (**Figure 2-8)** yielded a potential vector for gene delivery *in vitro*.

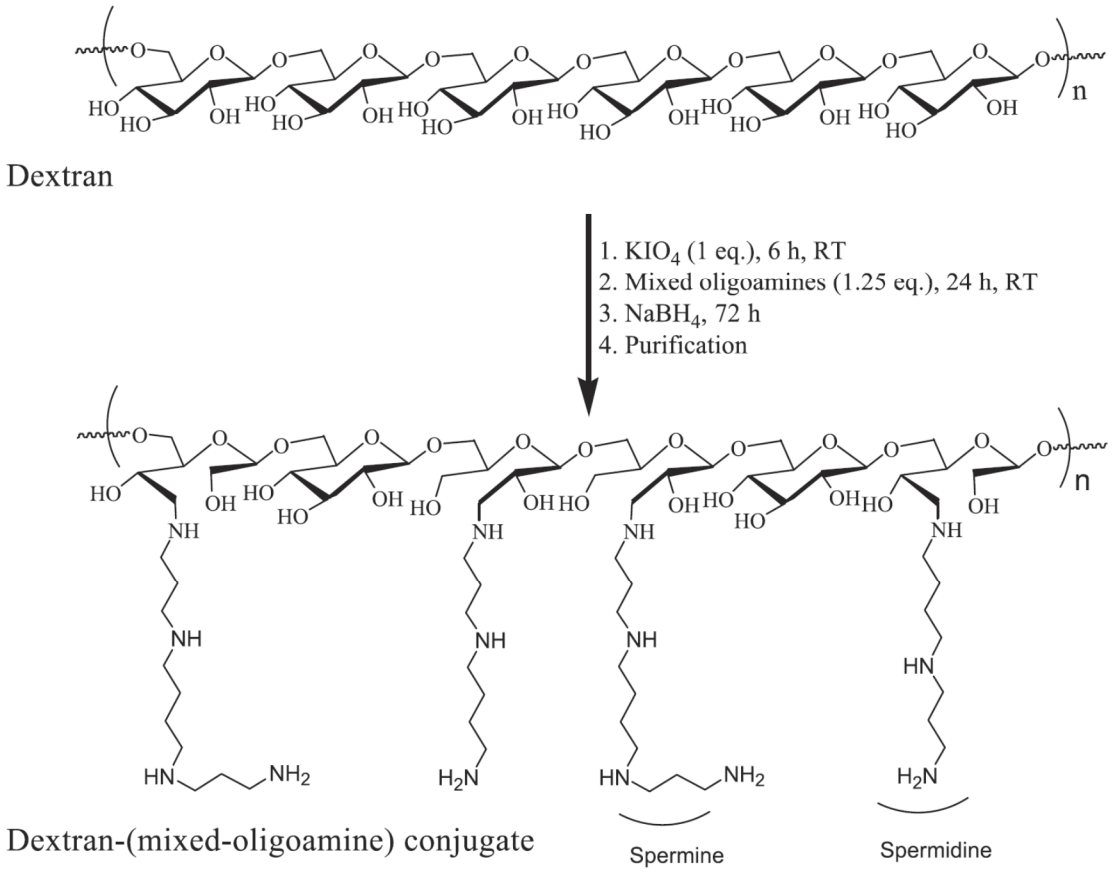

Figure 2-8. Dextran grafting with mixed spermine/spermidine oligoamines. (Figure adapted with permission from Ref. [33] Copyright © 2004 Elsevier B.V.)

Davis and coworkers studied the effect of carbohydrate size and charge center type in carbohydrate containing polycations for gene delivery and created an extensive library of these materials (**Figure 2-9)**.[34,35] Studies of the structure-property relationship led to a discovery of a polycationic system for the first siRNA delivery administered systemically to a human.[8]

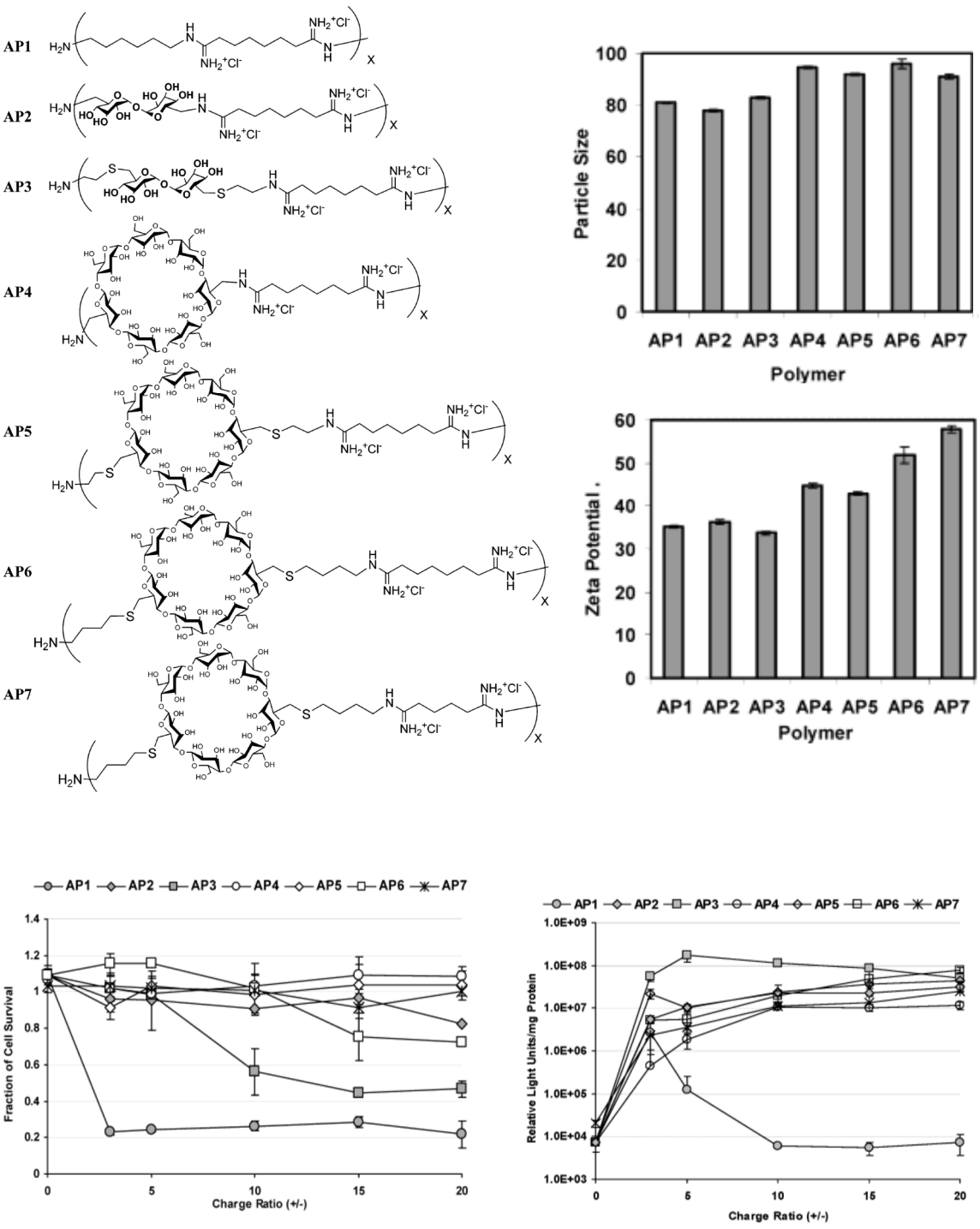

Figure 2-9. Carbohydrate-oligoamine polymers developed in the Davis group. (Figures adapted with permission from Ref. [34] Copyright © 2003 American Chemical Society.)

The Reineke group has developed a vast library of glycopolymers obtained via step-growth polycondensation and step-growth polymerization employing the "click" reaction. The structures of these materials are shown in **Figure 2-10** and some of them are discussed in more details in the following chapters.

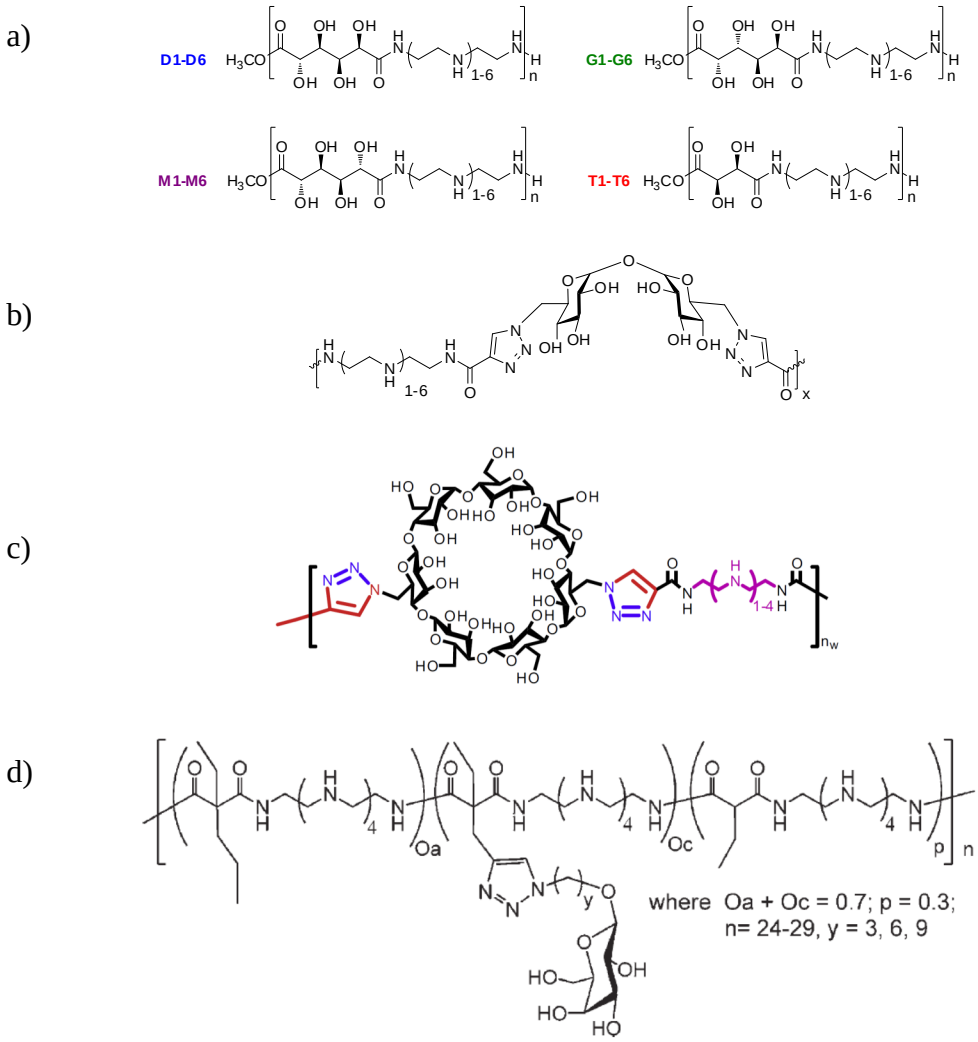

Figure 2-10. Glycopolymers developed in the Reineke group. a) Library of poly(glycoamidoamine)s.[22,36-44] b) Trehalose "click" polymers.[21,45,46] c) β-Cyclodextrin "click" polymers.[47] (Figure adapted with permission from Ref. [47] Copyright © 2009 Elsevier.) d) Galactosylated oligoamine polyamides for hepatocyte-targeted *p*DNA delivery.[48] (Figure adapted with permission from Ref. [48] Copyright © 2010 WILEY-VCH Verlag GmbH & Co. KGaA, Weinheim.)

2.4. Trehalose and Trehalose-Containing Polymers as Biomaterials

α,α-Trehalose is a natural non-reducing disaccharide formed from two glucose units connected through an α,α-1,1-glucosidic bond. It is found in many organisms like plants, fungi, yeast, bacteria, insects, and nematodes; however, its biosynthesis in mammals is not known.[49] Trehalose was discovered in 1832 by H.A.L. Wiggers[50], but in 1859, Marcellin Berthelot reported its isolation from trehala manna[51], a substance made by weevils, and gave it the name "trehalose". Some important physical properties of α,α-trehalose are summarized in **Figure 2-11**.

Melting point	dihydrate	97.0°C
	anhydride	210.5°C
Heat of fusion	dihydrate	57.8 kJ mol^{-1}
	anhydride	53.4 kJ mol^{-1}
Solubility	68.9 g/100 g H_2O at 20°C	
Optical rotation	$[\alpha]_D$ +178°	
Relative sweetness	45% of sucrose	
Digestibility	digested and absorbed by the small intestine	
pH stability of solution	> 99% (pH 3.5-10, at 100°C for 24 h)	
Heat stability of solution	> 99% (at 120°C for 90 min)	

Figure 2-11. Physical properties of α,α-trehalose. (Figure adapted with permission from Ref. [49] Copyright © 2008 by the authors; licensee Molecular Diversity Preservation International, Basel, Switzerland.)

Trehalose plays a very important role in nature. It has the unique property of protecting biological systems against damage by dehydration.[52,53] Trehalose is also a known antioxidant.[54,55] It also prevents the aggregation of proteins,[56] a highly important issue in biotechnological applications. Another property of trehalose, widely known and exploited in industries, is the ability to preserve biological molecules during freeze-drying and lyophilization.[57] Yet the mechanisms for these processes are still under

debate. Some of the existing hypotheses about the topic include the water replacement hypothesis[53], water-layer hypothesis (retention of water at the membrane interface), and mechanical-entrapment hypothesis[58] (the formation of an amorphous sugar glass). Cremer group[59] extensively studied the phenomena of anhydrobiosis at the chemical level and tested seven different carbohydrates (**Figure 2-12**) to understand in detail the mechanism involved in this process.

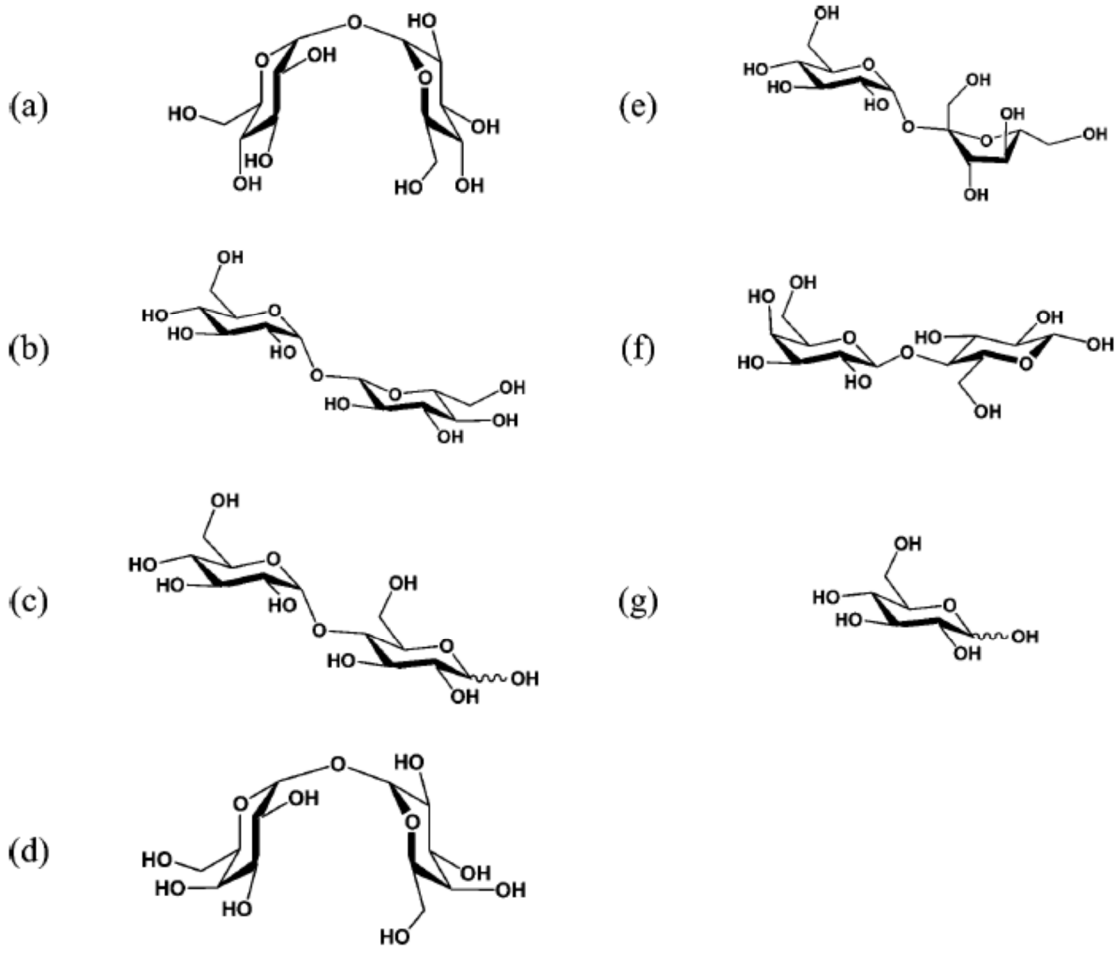

Figure 2-12. Structure of the mono- and disaccharides tested in the anhydrobiosis study by the Cremer group. a) α,α-Trehalose. b) α,*β*-Trehalose. c) Maltose. d) α,α-Galactotrehalose. e) Sucrose. f) Lactose. g) Glucose. (Figure adapted with permission from Ref. [59] Copyright © 2007 American Chemical Society.)

It became clear from their studies that the key to such anhydrobiotic preservation abilities is the α,α-1,1 bond of trehalose (**Figure 2-12a**) as α,α-trehalose had the best performance among other carbohydrates employed in this study. In a supporting experiment, α,α-galactotrehalose (maintaining the same α,α-1,1 linkage) (**Figure 2-12d**) performed similarly to trehalose, but at the same time α,β-trehalose (with an α,β-1,1 linkage) (**Figure 2-12b**) afforded almost no anhydrobiotic protection. It was also interesting to see from their results that maltose (**Figure 2-12c**) was capable of preventing the disruption of lipid bilayers, however upon rehydration, the lipid material lost its mobility, which was an indication that the lipid bilayer was disrupted by air exposure, and this process was not prevented by the presence of maltose. The process of delamination of the membrane lipid-bilayer via dehydration, air-exposure with no lipopreservatives present, and its protection with lipopreservatives is illustrated in **Figure 2-13**.

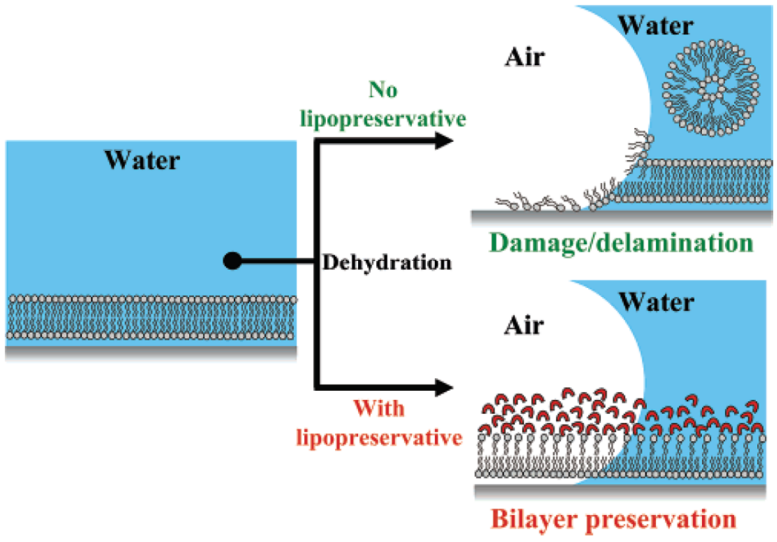

Figure 2-13. The process of delamination of the membrane lipid-bilayer via dehydration and air-exposure with no lipopreservatives present (upper-right corner), and its protection by lipopresevatives such as trehalose (lower-right corner). (Figure adapted with permission from Ref.[59] Copyright © 2007 American Chemical Society.

Control experiments with glycolipids (**Figure 2-14**) revealed that their presence in the membrane does not ensure protection against damage when exposed to drying conditions.

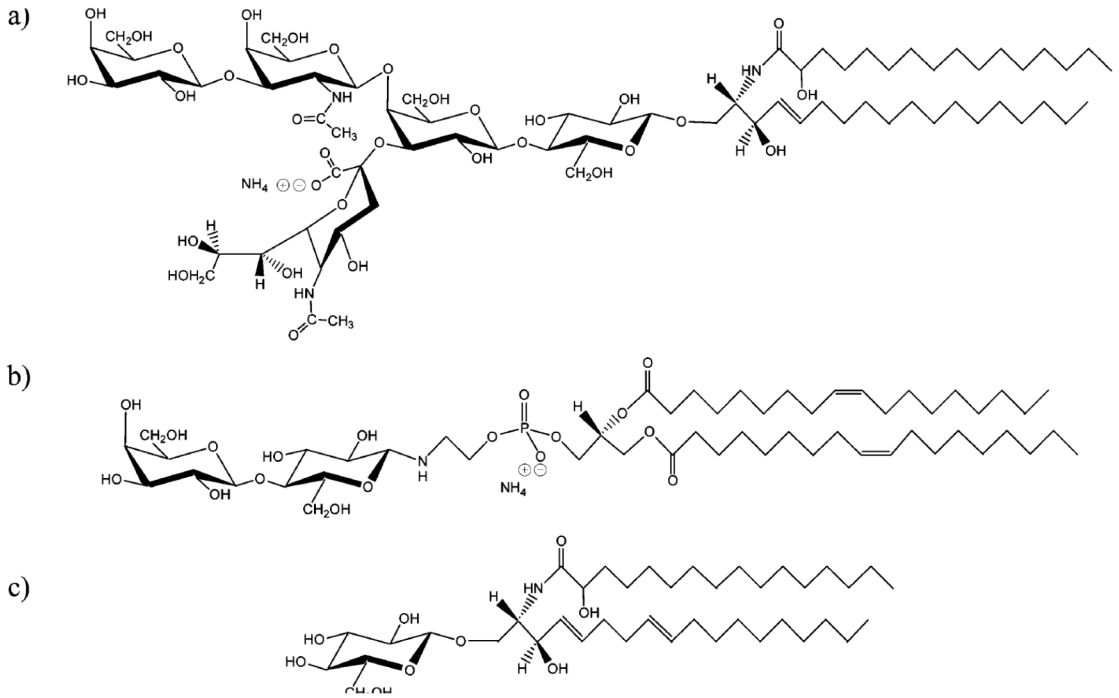

Figure 2-14. Structures of glycolipids used in control experiments by the Cremer group to study the mechanism of anhydrobiosis caused by trehalose. (Figure adapted with permission from Ref. [59] Copyright © 2007 American Chemical Society.)

Despite the unique properties of trehalose observed in organisms, trehalose-containing polymers are not well reported in the literature. In this chapter, only a few examples were found and are shown below. Due to its relatively high chemical and thermal stability in comparison with other carbohydrates and molecular symmetry, the synthesis of a bifunctionalized trehalose monomer for subsequent incorporation into the polymer backbone is straightforward. The two primary hydroxyls are the most reactive, and therefore are usually the first choice for functionalization.

The first trehalose-based polymers were reported in the literature by Kurita *et al*. in 1979 (**Figure 2-15**).[49] Although, in this concept authors assumed that the synthesized

polymers were linear, the possibility of branching (due to the low selectivity between primary and secondary hydroxyls) was not excluded. In 1994, the same group in a continuing effort to produce trehalose linear polymers, utilized a similar polymerization technique, but this time the same series of diisocyanates were polymerized with primary amine-functionalized trehalose to avoid branching (**Figure 2-16**).[60] This series of polymers was susceptible to enzymatic degradation in the presence of trehalase or α-amylase and therefore, at that time, exhibited potential as a novel class of biodegradable synthetic carbohydrate containing polymers.

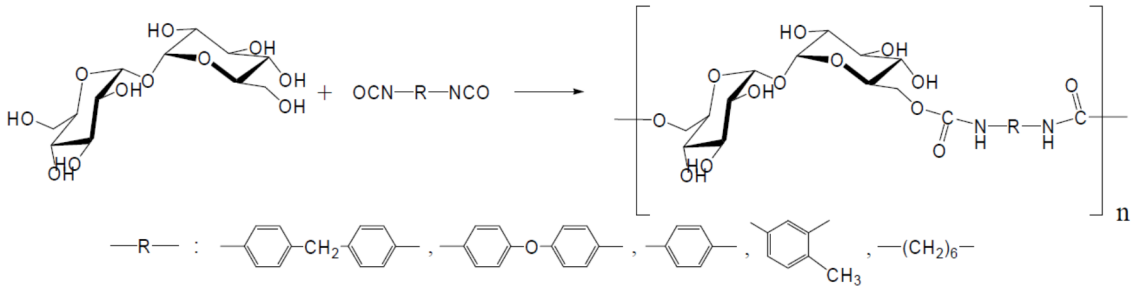

Figure 2-15. The trehalose-containing polyurethanes synthesized by Kurita *et al.* (Figure adapted with permission from Ref. [49] Copyright © 2008 by the authors; licensee Molecular Diversity Preservation International, Basel, Switzerland.)

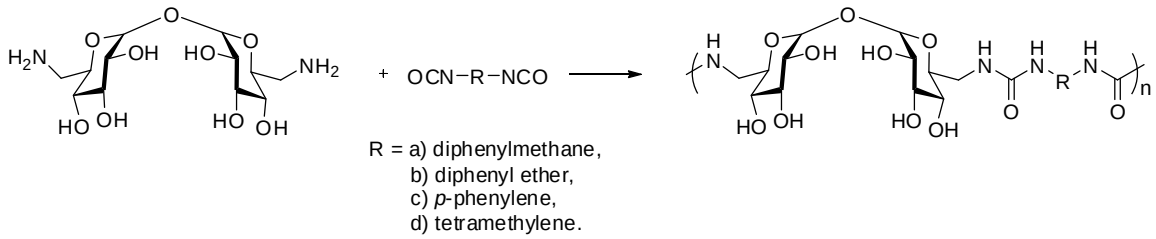

Figure 2-16. The trehalose-containing polyureas synthesized by Kurita *et al.*

Such incorporation of trehalose residues into polyureas showed high material-permeation of both urea and vitamin B_{12}, although, the permeability of these compounds was lower for trehalose-based membranes when compared with cellulose-based membranes, but unlike cellulose, trehalose has an advantage of being more prone to biodegradation. Indeed, the enzymatic hydrolysis, which was monitored based by the change in turbidity of a suspension, showed high biodegradability potential for these trehalose-based materials in the presence of trehalase or α-amylase, indicating their potential in controlled-release drug delivery systems.[60]

In the early 2000s, Teramoto *et al*. reported the synthesis and thermal properties of trehalose-based thermosetting resins containing trehalose and *p*-chloromethylstyrene residues (**Figure 2-17**). By varying the degree of substitution of trehalose hydroxyl groups (between 2 and 4), materials exhibited different physical properties.[61]

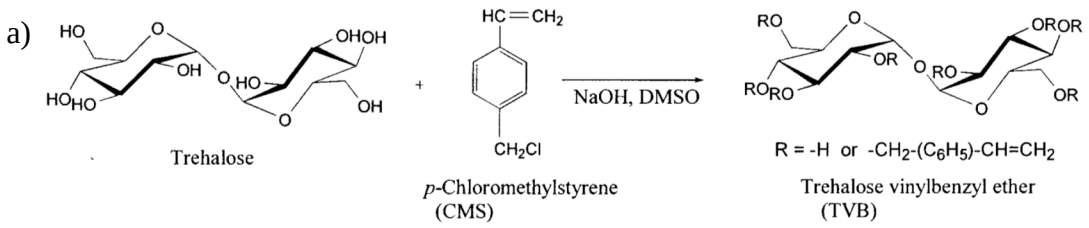

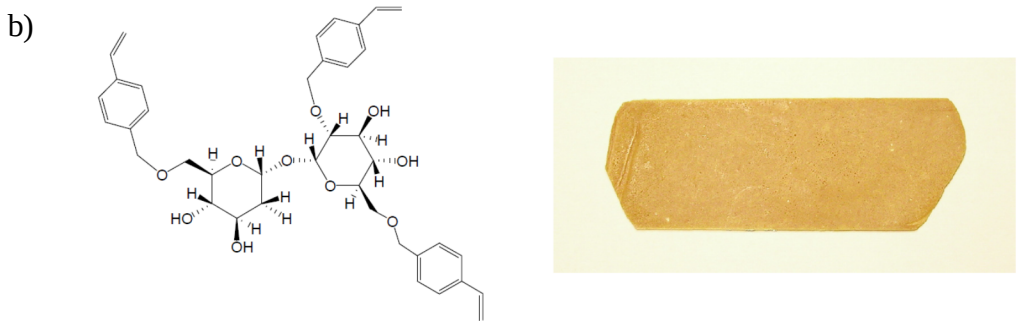

Figure 2-17. a) The synthesis of trehalose vinyl benzyl ether by Teramoto *et* al. b) Structure of trehalose vinylbenzyl ether and photograph of a molded resin. (Figure a) adapted with permission from Ref. [61] Copyright © 2003 Wiley Periodicals, Inc. Figure b) adapted with permission from Ref. [49] Copyright © 2008 by the authors; licensee Molecular Diversity Preservation International, Basel, Switzerland.)

To further advance this technology toward creating efficient coatings for electronics equipment and optical materials, trehalose cinnamoyl esters were synthesized by the same group and subsequently cross-linked via UV irradiation, which resulted in the formation of transparent films (**Figure 2-18**).[62]

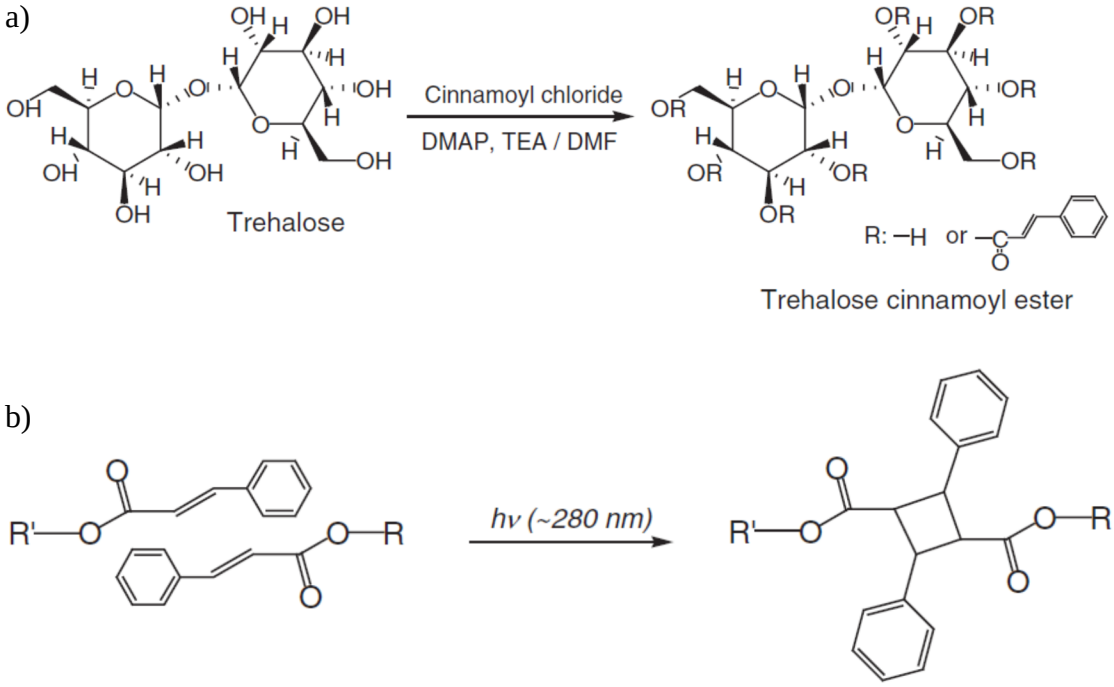

Figure 2-18. a) Structure of trehalose cinnamoyl esters. b) [2+2] cycloaddition reaction of cinnamate groups. (Figure adapted with permission from Ref. [62] Copyright © 2007 John Wiley & Sons, Ltd.)

In 2000, Dordick *et al*. demonstrated enzymatic polymerization of trehalose 6,6'-O-divinyladipate with 1,8-octanediol in a two-step process. The enzyme used in this process – Novozyme-435 – facilitated the synthesis of poly(trehalose-adipate) in an organic solvent, such as acetone, but under aqueous conditions (pH 7) catalyzed the degradation of the polymer by breaking the ester linkages (**Figure 2-19**).[63]

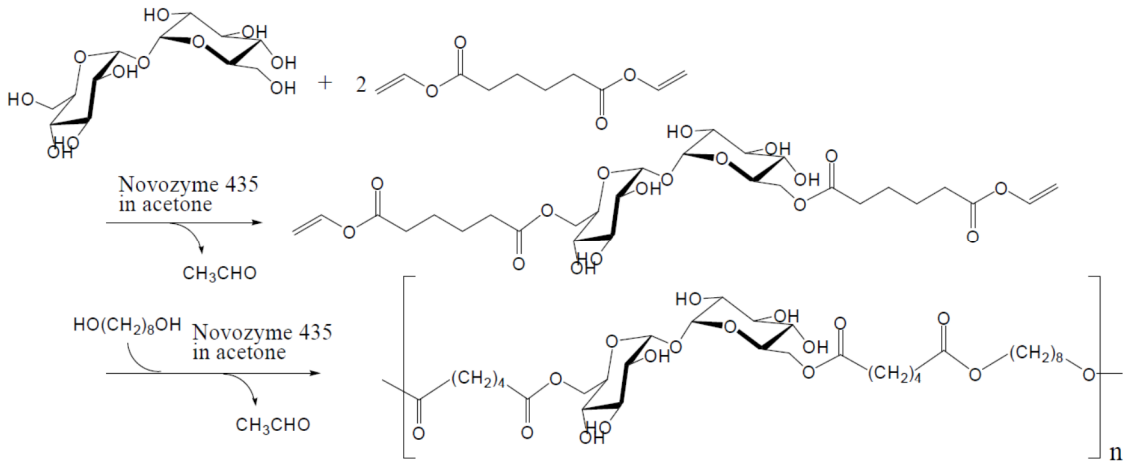

Figure 2-19. Dordick's trehalose-based polyesters synthesized via enzymatic polymerization. (Figure adapted with permission from Ref. [49] Copyright © 2008 by the authors; licensee Molecular Diversity Preservation International, Basel, Switzerland.)

In 1999, Tokiwa's group demonstrated the chemoenzymatic synthesis of polyethylene containing a trehalose moiety in a side chain (for the details see review from Teramoto *et al.*[49]). Similar polymers were also synthesized by Miura and Kobayashi (**Figure 2-20**).[64] Two polymers – α,α-trehalose and α,α-galactotrehalose containing polymers – were obtained in this procedure and compared for their activity against Shiga-toxin-1 (Stx-1), produced by the pathogen *Escherichia coli*. Authors have reported that the α,α-galactotrehalose functionality (α,α-1,1-D-galactopyranosyl-D-glucopyranoside; α,α-1,1-Gal-Glc) has a similar stereochemistry at the α,α-1,1 position to that of the α,α-1,4 linkage in glycobiosyl Gb2 and Gb3 ceramides, which are the ligands of mentioned Shiga toxins. Based on this discovery, polymer containing α,α-galactotrehalose residues, showed the highest and significant inhibition activity against Stx-1 and therefore possesses high biological potential for the treatment of bacterial infections caused by Stx-1 producing bacteria.

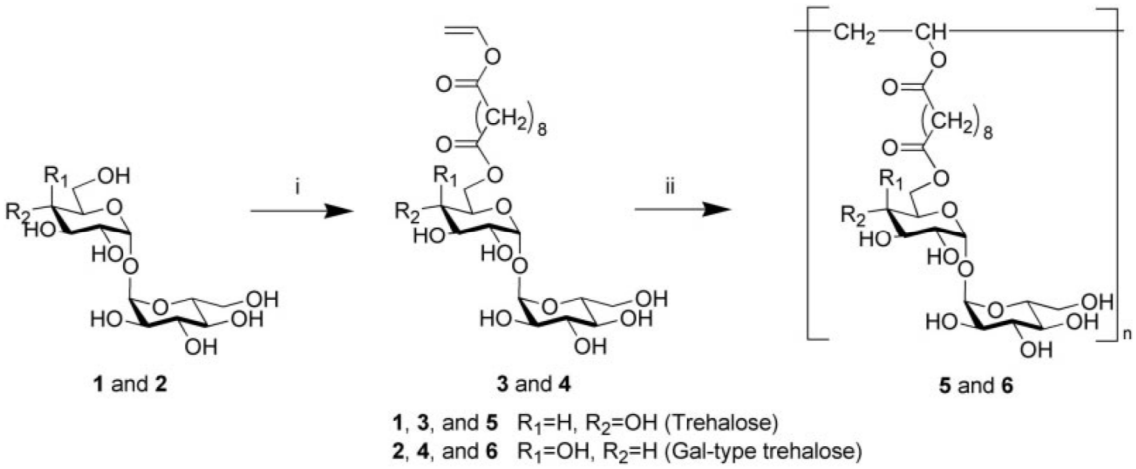

Figure 2-20. Chemoenzymatic synthesis of trehalose functionalized polyethylene. Conditions: (i) divinyl sebacate, pyridine, 60 °C, 72 h, and lipase; (ii) radical initiator (H_2O_2 and L-ascorbic acid) and H_2O/DMSO. (Figure adapted with permission from Ref. [64] Copyright © 2004 Wiley Periodicals, Inc.)

Teramoto and coworkers explored other ways – minimum chemical reaction involving and non-enzymatic – to produce trehalose-containing linear polymers with thermoplastic properties for industrial applications, processing, and recycling. Several examples of their materials and methods are shown in **Figure 2-21** and include polyacetal formation by step-growth polymerization. Trehalose polymer containing dimethylsiloxane unit was prone to form a soft transparent film (**Figure 2-21d**) under specific conditions. This material has a potential for a good use in biotechnologies due to the biocompatability of trehalose and is still under investigation.

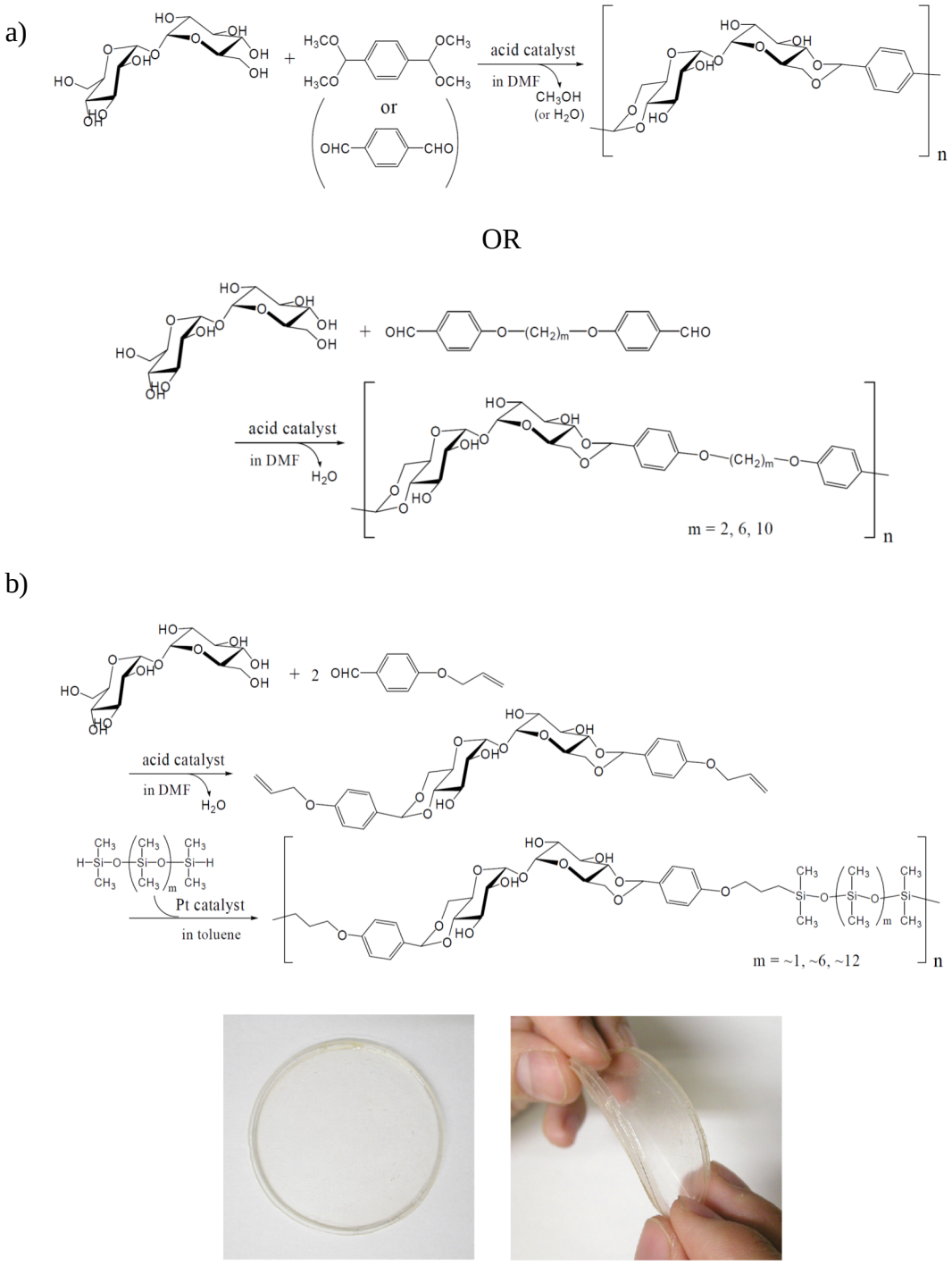

Figure 2-21. a) The synthesis of trehalose-containing polyacetals. (Figure adapted with permission from Ref. [49] Copyright © 2008 by the authors; licensee Molecular Diversity Preservation International, Basel, Switzerland.) b) The synthesis and a film of trehalose-containing silylated polymers. (Figure adapted with permission from Ref. [65] Copyright © 2010 by the authors; licensee Molecular Diversity Preservation International, Basel, Switzerland.)

Another approach yielding similar materials was developed by the same Teramoto research group and employed the Diels-Alder reaction as a tool for the step-growth polymerization, where trehalose was first converted to a difurfurylidene derivative and subsequently polymerized with bismaleimidodiphenylmethane or biamaleimidohexane (**Figure 2-22)**. The polymerization was generally achieved in 24-48 h at 40-70 °C. Both polymers were completely decomposed back into the starting monomers via retro-Diels-Alder reaction after they were heated to 140 °C.[66]

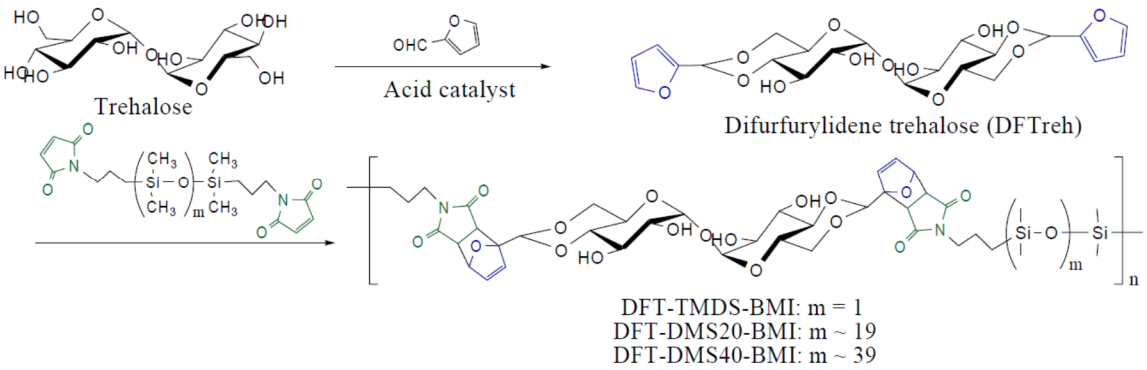

Figure 2-22. The synthesis of trehalose-containing polymers via Diels-Alder reaction. (Figure adapted with permission from Ref. [66] Copyright © 2010 by the authors; licensee Molecular Diversity Preservation International, Basel, Switzerland.)

Inspired by the work of Davis and Reineke, Teramoto *et al.* expanded their trehalose-based polymer research and created polycationic derivatives for DNA-binding applications.[67] Trehalose dibenzylidene acetal was converted to a diepoxide, which was subsequently polymerized with N,N'-dimethyl-1,6-diaminohexane (DMDAH) through the epoxide ring opening polymerization (**Figure 2-23**). Only the thermal properties of the polymers were analyzed (TGA and DSC). However, authors implied that possible biological characterization would be performed in the near future.

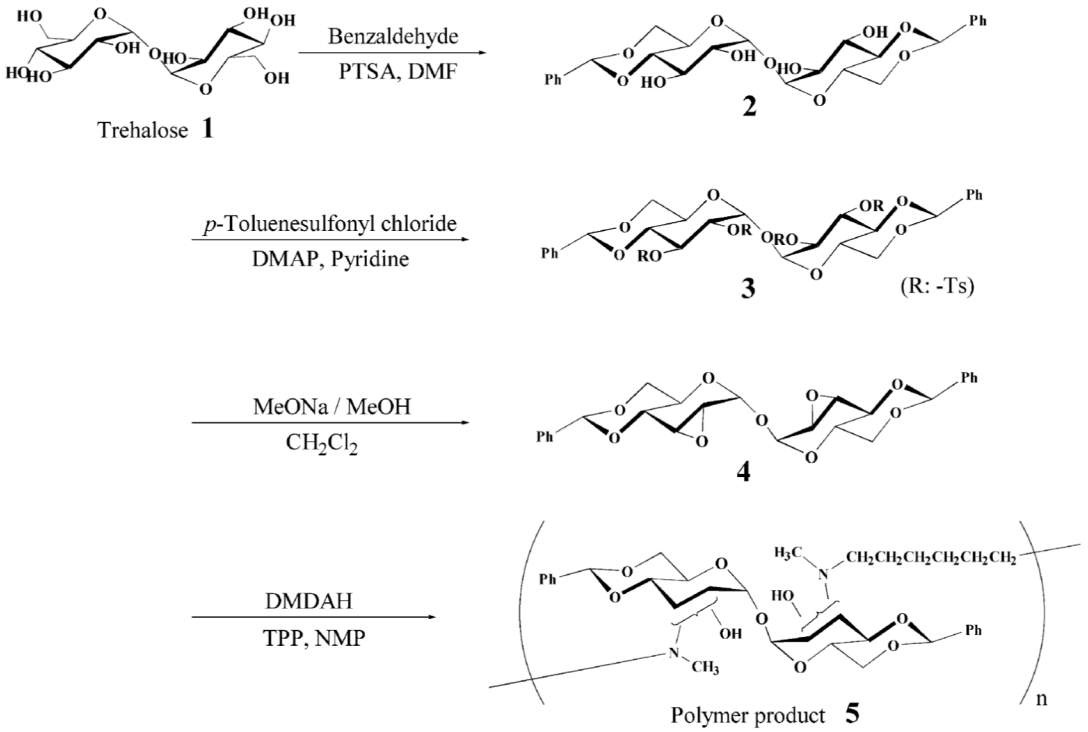

Figure 2-23. The synthesis of trehalose containing polymers via epoxide ring opening polymerization. (Figure adapted with permission from Ref. [67] Copyright © 2004 Elsevier Ltd.)

2.5. PEGylation of Biomaterials

Chapter 4 of this dissertation describes the PEGylatyon of trehalose and oligoethyleneamine-containing polymers. First described in 1977 by Abuchowsky *et al.*[68,69] and approved for clinical trials by FDA for the first time in March of 1990, PEGylation, by far, is one of the most developed and used techniques to enhance the therapeutic potential of drug and gene delivery materials. The advantage of PEG includes low toxicity, good solubility in both aqueous and organic media, high hydration that ensures the increased hydrodynamic volume of the PEGylated materials and water solubility of conjugated molecules, and also PEG can be produced with controlled molecular weights and low polydispersity indexes. In addition PEGylated materials

exhibit increased resistance to antibodies, proteolytic enzymes, and, because of the increase in molecular weight and size of the conjugates, they have longer retention times in the blood and slower renal clearance compared to a non-PEGylated materials.[70] A schematic concept of the formation of the PEG-outer layer and drug encapsulation inside the polymeric micelle is shown in **Figure 2-24**. The main drawback of PEG polymers is their non-biodegradability in addition to easy degradation upon exposure to oxygen.

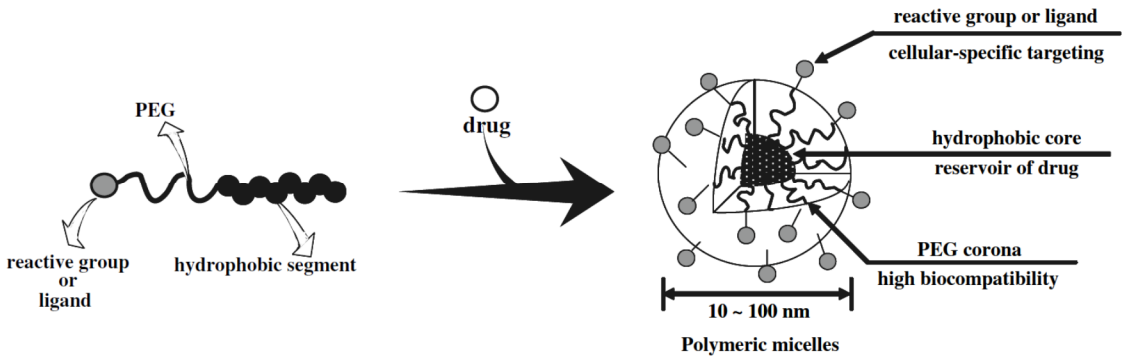

Figure 2-24. The role of PEGylation in self-assembly of micelles. (Figure adapted with permission from Ref. [71] Copyright © 2009 American Association of Pharmaceutical Scientists.)

A few successfully PEGylated drugs are summarized in Figure **2-25**. Among them Adagen® (PEG-bovine adenosine deaminase) is the first FDA approved PEGylated drug. It was developed by Enzon, Inc., the company founded by Abuchowski, who is considered a pioneer in PEGylation research.

Trade name	Generic name	Parent drug	Size of PEG moiety (kDa)	Indication	Year of approval
Adagen®	Pegademase	Adenosine deaminase	5	SCID	1990
Oncaspar®	Pegaspargase	Asparaginase	5	Leukemia	1994
Neulasta®	Pegfilgrastim	G-CSF	20	Neutropenia	2002
PegIntron®	Peginterferon-α-2b	Interferon-α-2b	12	Hepatitis C	2000
Pegasys®	Peginterferon-α-2a	Interferon-α-2a	40	Hepatitis C	2001
Somavert®	Pegvisomant	hGH	5	Acromegaly	2003
Macugen®	Pegaptanib	Anti-VEGF aptamer	40	AMD	2004
Mircera®	PEG-EPO	Erythropoietin	40	Anemia	2007
Cimzia®	Certolizumab pegol	Anti-TNFα Fab′	40	Rheumatoid arthritis and Crohn disease	2008

Figure 2-25. US FDA approved PEGylated proteins or oligonucleotides. (Figure adapted with permission from Ref. [70] Copyright © 2008 Adis Data Information BV.)

2.6. Biological Properties of 1,2,3-Triazoles

Chapter 3 of this thesis summarizes a study involving trehalose-oligoamine polymers that were synthesized via alkyne-azide "click" chemistry and therefore have 1,2,3-triazole functionality. Strategically, this functional group was introduced to the structure of the polycation primarily as an efficient polymerization site; however, the triazole contribution to the formation of *p*DNA-polymer nanoparticle is not excluded. Note that the pKa of a protonated sp^2-hybridized nitrogen atom on a 1,2,3-triazole ring is 1.1 – 1.3[72], thus the neutral triazole will not be protonated at physiological pH. Therefore, this functionality will not contribute to the electrostatic binding with negatively charged nucleic acids; however, it could have a role in H-bonding to nucleic acids. This chapter summarizes a few examples of biological properties of some 1,2,3-triazole-containing small molecules.

Compounds containing 1,2,3-triazole groups are found in the literature as classes with different pharmacological profiles. For example, 1,2,3-triazole analogs were reported as antiplatelet agents[73] (inhibitors for thrombus formation), inhibitors of hemolytic profile of the *Lachesis muta* snake venom[74], and dopamine D2 receptor

ligands[75]. 1,2,3-Triazole derivatives of nor-β-lapachone were investigated as an emerging class of compounds in drug development for Chagas disease.[76] Some 1,2,3-triazole-containing compounds0020 have been found to be active against *Mycobacterium tuberculosis*.[77] Several difluoromethylene 1,2,3-triazoles demonstrated inhibition of growth of the parasite *Leishmania amazonensis* that causes severe skin sores in humans.[78] Triazole derivatives reported by Safonova *et al*. exhibited antiviral properties against FPV influenza virus in FCE cell culture, and one of the compounds showed the ability to inhibit the development of leukemia P-388 in mice.[79] Various saccharidyl-triazole derivatives were tested as inhibitors of a panel of glycosidases.[72]

2.7. References

1. Venter, J. C.; Adams, M. D.; Myers, E. W.; Li, P. W.; Mural, R. J.; Sutton, G. G.; Smith, H. O.; Yandell, M.; Evans, C. A.; Holt, R. A., *et al.* The sequence of the human genome. *Science*, **2001,** *291* (5507), 1304-1351.

2. Rosenberg, S. A.; Aebersold, P.; Cornetta, K.; Kasid, A.; Morgan, R. A.; Moen, R.; Karson, E. M.; Lotze, M. T.; Yang, J. C.; Topalian, S. L., *et al.* Gene Transfer into Humans — Immunotherapy of Patients with Advanced Melanoma, Using Tumor-Infiltrating Lymphocytes Modified by Retroviral Gene Transduction. *New England Journal of Medicine*, **1990,** *323* (9), 570-578.

3. Edelstein, M. L.; Abedi, M. R.; Wixon, J. Gene therapy clinical trials worldwide to 2007 — an update. *The Journal of Gene Medicine*, **2007,** *9* (10), 833-842.

4. Edelstein, M. L.; Abedi, M. R.; Wixon, J.; Edelstein, R. M. Gene therapy clinical trials worldwide 1989-2004 — an overview. *The Journal of Gene Medicine*, **2004,** *6* (6), 597-602.

5. Gene Therapy Clinical Trials Worldwide (provided by the Journal of Gene Medicine). http://www.abedia.com/wiley/index.html (accessed Dec 23, 2010).

6. Levine, A. S.; Levy, H. B. Phase I-II trials of poly IC stabilized with poly-L-lysine. *Cancer treatment reports*, **1978,** *62* (11), 1907-1912.

7. Oncovir, Inc. http://www.oncovir.com/index.html (accessed Jan 7, 2011).

8. Davis, M. E.; Zuckerman, J. E.; Choi, C. H. J.; Seligson, D.; Tolcher, A.; Alabi, C. A.; Yen, Y.; Heidel, J. D.; Ribas, A. Evidence of RNAi in humans from systemically administered siRNA via targeted nanoparticles. *Nature*, **2010,** *464* (7291), 1067-1070.

9. Davis, M. E. The First Targeted Delivery of siRNA in Humans via a Self-Assembling, Cyclodextrin Polymer-Based Nanoparticle: From Concept to Clinic. *Molecular Pharmaceutics*, **2009,** *6* (3), 659-668.

10. Registry of federally and privately supported clinical trials conducted in the United States and around the world. http://clinicaltrials.gov (accessed Dec 22, 2010).

11. Vical. http://www.vical.com (accessed Dec 22, 2010).

12. Mintzer, M. A.; Simanek, E. E. Nonviral Vectors for Gene Delivery. *Chemical Reviews*, **2008,** *109* (2), 259-302.

13. BioCancell Therapeutics Ltd. http://www.biocancell.com (accessed Dec 23, 2010).

14. Genetic Immunity. http://www.geneticimmunity.com/GI0203.html (accessed Dec 23, 2010).

15. Calando Pharmaceuticals. http://www.calandopharma.com (accessed Dec 22, 2010).

16. Semple, S. C.; Akinc, A.; Chen, J.; Sandhu, A. P.; Mui, B. L.; Cho, C. K.; Sah, D. W. Y.; Stebbing, D.; Crosley, E. J.; Yaworski, E., *et al.* Rational design of cationic lipids for siRNA delivery. *Nat Biotech*, **2010,** *28* (2), 172-176.

17. National Cancer Institute. http://www.cancer.gov/clinicaltrials/GOG-0170Q (accessed Dec 23, 2010).

18. Boussif, O.; Lezoualc'h, F.; Zanta, M. A.; Mergny, M. D.; Scherman, D.; Demeneix, B.; Behr, J. P. A versatile vector for gene and oligonucleotide transfer into cells in culture and in vivo: polyethylenimine. *Proceedings of the National Academy of Sciences of the United States of America*, **1995,** *92* (16), 7297-7301.

19. Suh, J.; Paik, H. J.; Hwang, B. K. Ionization of Poly(ethylenimine) and Poly(allylamine) at Various pH's. *Bioorganic Chemistry*, **1994,** *22* (3), 318-327.

20. Thomas, M.; Klibanov, A. M. Non-viral gene therapy: polycation-mediated DNA delivery. *Applied Microbiology and Biotechnology*, **2003,** *62* (1), 27-34.

21. Prevette, L. E.; Lynch, M. L.; Kizjakina, K.; Reineke, T. M. Correlation of amine number and pDNA binding mechanism for trehalose-based polycations. *Langmuir*, **2008,** *24* (15), 8090-8101.

22. Prevette, L. E.; Kodger, T. E.; Reineke, T. M.; Lynch, M. L. Deciphering the role of hydrogen bonding in enhancing pDNA-Polycation interactions. *Langmuir*, **2007,** *23* (19), 9773-9784.

23. Jorge, A. F.; Dias, R. S.; Pereira, J. C.; Pais, A. A. C. C. DNA Condensation by pH-Responsive Polycations. *Biomacromolecules*, **2010,** *11* (9), 2399-2406.

24. Knorr, V.; Allmendinger, L.; Walker, G. F.; Paintner, F. F.; Wagner, E. An Acetal-Based PEGylation Reagent for pH-Sensitive Shielding of DNA Polyplexes. *Bioconjugate Chem*, **2007,** *18* (4), 1218-1225.

25. Xu, S.; Krämer, M.; Haag, R. pH-Responsive dendritic core-shell architectures as amphiphilic nanocarriers for polar drugs. *Journal of Drug Targeting*, **2006,** *14* (6), 367-374.

26. Kim, Y. H.; Park, J. H.; Lee, M.; Kim, Y.-H.; Park, T. G.; Kim, S. W. Polyethylenimine with acid-labile linkages as a biodegradable gene carrier. *Journal of Controlled Release*, **2005,** *103* (1), 209-219.

27. Kanazawa, H.; Higuchi, M.; Yamamoto, K. Synthesis and Chemical Degradation of Thermostable Polyamide with Imine Bond for Chemical Recycling. *Macromolecules*, **2005,** *39* (1), 138-144.

28. Bae, Y.; Nishiyama, N.; Fukushima, S.; Koyama, H.; Yasuhiro, M.; Kataoka, K. Preparation and Biological Characterization of Polymeric Micelle Drug Carriers with Intracellular pH-Triggered Drug Release Property: Tumor Permeability, Controlled Subcellular Drug Distribution, and Enhanced in Vivo Antitumor Efficacy. *Bioconjugate Chem*, **2004,** *16* (1), 122-130.

29. Defang, O.; Shah, N.; Hong, Z.; Smith, S. C.; Parekh, H. S. Reducible Disulfide-Based Non-Viral Gene Delivery Systems. *Mini Reviews in Medicinal Chemistry*, **2009,** *9* (10), 1242-1250.

30. Zintchenko, A.; Ogris, M.; Wagner, E. Temperature Dependent Gene Expression Induced by PNIPAM-Based Copolymers: Potential of Hyperthermia in Gene Transfer. *Bioconjugate Chem*, **2006,** *17* (3), 766-772.

31. Chorny, M.; Polyak, B.; Alferiev, I. S.; Walsh, K.; Friedman, G.; Levy, R. J. Magnetically driven plasmid DNA delivery with biodegradable polymeric nanoparticles. *The FASEB Journal*, **2007,** *21* (10), 2510-2519.

32. Mok, H.; Park, T. G. Functional polymers for targeted delivery of nucleic acid drugs. *Macromolecular Bioscience*, **2009,** *9* (8), 731-743.

33. Azzam, T.; Eliyahu, H.; Makovitzki, A.; Linial, M.; Domb, A. J. Hydrophobized dextran-spermine conjugate as potential vector for in vitro gene transfection. *Journal of Controlled Release*, **2004,** *96* (2), 309-323.

34. Reineke, T. M.; Davis, M. E. Structural effects of carbohydrate-containing polycations on gene delivery. 1. Carbohydrate size and its distance from charge centers. *Bioconjugate Chem*, **2002,** *14* (1), 247-254.

35. Reineke, T. M.; Davis, M. E. Structural Effects of Carbohydrate-Containing Polycations on Gene Delivery. 2. Charge Center Type. *Bioconjugate Chem*, **2002,** *14* (1), 255-261.

36. McLendon, P. M.; Fichter, K. M.; Reineke, T. M. Poly(glycoamidoamine) Vehicles Promote pDNA Uptake through Multiple Routes and Efficient Gene Expression via Caveolae-Mediated Endocytosis. *Molecular Pharmaceutics*, **2010,** *7* (3), 738-750.

37. McLendon, P. M.; Buckwalter, D. J.; Davis, E. M.; Reineke, T. M. Interaction of Poly(glycoamidoamine) DNA Delivery Vehicles with Cell-Surface Glycosaminoglycans Leads to Polyplex Internalization in a Manner Not Solely Dependent on Charge. *Molecular Pharmaceutics*, **2010,** *7* (5), 1757-1768.

38. Liu, Y.; Reineke, T. M. Degradation of Poly(glycoamidoamine) DNA Delivery Vehicles: Polyamide Hydrolysis at Physiological Conditions Promotes DNA Release. *Biomacromolecules*, **2010,** *11* (2), 316-325.

39. Lee, C. C.; Liu, Y.; Reineke, T. M. General structure-activity relationship for poly(glycoamidoamine)s: The effect of amine density on cytotoxicity and DNA delivery efficiency. *Bioconjugate Chem*, **2008,** *19* (2), 428-440.

40. Liu, Y. M.; Reineke, T. M. Poly(glycoamidoamine)s for gene delivery. Structural effects on cellular internalization, buffering capacity, and gene expression. *Bioconjugate Chem*, **2007,** *18* (1), 19-30.

41. Liu, Y. M.; Wenning, L.; Lynch, M.; Reineke, T. M. Gene delivery with novel poly(1-tartaramidoamine)s. *Acs Sym Ser*, **2006,** *923*, 217-227.

42. Liu, Y. M.; Reineke, T. M. Poly(glycoamidoamine)s for gene delivery: Stability of polyplexes and efficacy with cardiomyoblast cells. *Bioconjugate Chem*, **2006,** *17* (1), 101-108.

43. Liu, Y. M.; Reineke, T. M. Hydroxyl stereochemistry and amine number within poly(glycoamidoamine)s affect intracellular DNA delivery. *J Am Chem Soc*, **2005,** *127* (9), 3004-3015.

44. Liu, Y. M.; Wenning, L.; Lynch, M.; Reineke, T. M. New poly(D-glucaramidoamine)s induce DNA nanoparticle formation and efficient gene delivery into mammalian cells. *J Am Chem Soc,* **2004,** *126* (24), 7422-7423.

45. Srinivasachari, S.; Liu, Y.; Prevette, L. E.; Reineke, T. M. Effects of trehalose click polymer length on pDNA complex stability and delivery efficacy. *Biomaterials*, **2007,** *28* (18), 2885-2898.

46. Srinivasachari, S.; Liu, Y.; Zhang, G.; Prevette, L.; Reineke, T. M. Trehalose click polymers inhibit nanoparticle aggregation and promote pDNA delivery in serum. *J Am Chem Soc,* **2006,** *128* (25), 8176-8184.

47. Srinivasachari, S.; Reineke, T. M. Versatile supramolecular pDNA vehicles via "click polymerization" of beta-cyclodextrin with oligoethyleneamines. *Biomaterials*, **2009,** *30* (5), 928-938.

48. Lee, C. C.; Grandinetti, G.; McLendon, P. M.; Reineke, T. M. A Polycation Scaffold Presenting Tunable “Click” Sites: Conjugation to Carbohydrate Ligands and Examination of Hepatocyte-Targeted pDNA Delivery. *Macromolecular Bioscience*, **2010,** *10* (6), 585-598.

49. Teramoto, N.; Sachinvala, N.; Shibata, M. Trehalose and Trehalose-based Polymers for Environmentally Benign, Biocompatible and Bioactive Materials. *Molecules*, **2008,** *13* (8), 1773-1816.

50. Wiggers, H. A. L. Untersuchung über das Mutterkorn, Secale cornutum. *Annalen der Pharmacie*, **1832,** *1* (2), 129-182.

51. Tillequin, F. [Trehala, a meeting point between zoology, botany, chemistry, and biochemistry]. *Rev Hist Pharm (Paris)*, **2009,** *57* (362), 163-72.

52. Di Gregorio, G. M.; Ferraris, P.; Mariani, P. Wetting properties of dioleoyl-phosphatidyl-choline bilayers in the presence of trehalose: an X-ray diffraction study. *Chemistry and Physics of Lipids*, **2010,** *163* (6), 601-606.

53. Clegg, J. S.; Seitz, P.; Seitz, W.; Hazlewood, C. F. Cellular responses to extreme water loss: The water-replacement hypothesis. *Cryobiology*, **1982,** *19* (3), 306-316.

54. Luo, Y.; Li, W.-M.; Wang, W. Trehalose: Protector of antioxidant enzymes or reactive oxygen species scavenger under heat stress? *Environmental and Experimental Botany*, **2008,** *63* (1-3), 378-384.

55. Benaroudj, N.; Lee, D. H.; Goldberg, A. L. Trehalose Accumulation during Cellular Stress Protects Cells and Cellular Proteins from Damage by Oxygen Radicals. *J Biol Chem*, **2001,** *276* (26), 24261-24267.

56. Barreca, D.; Laganà, G.; Ficarra, S.; Tellone, E.; Leuzzi, U.; Magazù, S.; Galtieri, A.; Bellocco, E. Anti-aggregation properties of trehalose on heat-induced secondary structure and conformation changes of bovine serum albumin. *Biophysical Chemistry*, **2010,** *147* (3), 146-152.

57. Magazù, S.; Villari, V.; Faraone, A.; Maisano, G.; Heenan, R. K.; King, S. α,α-Trehalose-Water Solutions VI. A View of the Structural and Dynamical Properties of OβG Micelles in the Presence of Trehalose. *The Journal of Physical Chemistry B*, **2002,** *106* (27), 6954-6960.

58. Hagen, S.; Hofrichter, J.; Eaton, W. Protein reaction kinetics in a room-temperature glass. *Science*, **1995,** *269* (5226), 959-962.

59. Albertorio, F.; Chapa, V. A.; Chen, X.; Diaz, A. J.; Cremer, P. S. The α,α-(1→1) Linkage of Trehalose Is Key to Anhydrobiotic Preservation. *J Am Chem Soc*, **2007,** *129* (34), 10567-10574.

60. Kurita, K.; Masuda, N.; Aibe, S.; Murakami, K.; Ishii, S.; Nishimura, S.-I. Synthetic Carbohydrate Polymers Containing Trehalose Residues in the Main Chain: Preparation and Characteristic Properties. *Macromolecules*, **1994,** *27* (26), 7544-7549.

61. Teramoto, N.; Shibata, M. Trehalose-based thermosetting resins. I. Synthesis and thermal properties of trehalose vinylbenzyl ether. *Journal of Applied Polymer Science*, **2004,** *91* (1), 46-51.

62. Teramoto, N.; Shibata, M. Synthesis and photocuring of cinnamoyl trehalose esters. *Polymers for Advanced Technologies*, **2007,** *18* (12), 971-977.

63. Park, O.-J.; Kim, D.-Y.; Dordick, J. S. Enzyme-catalyzed synthesis of sugar-containing monomers and linear polymers. *Biotechnology and Bioengineering*, **2000,** *70* (2), 208-216.

64. Miura, Y.; Wada, N.; Nishida, Y.; Mori, H.; Kobayashi, K. Chemoenzymatic synthesis of glycoconjugate polymers starting from nonreducing disaccharides. *Journal of Polymer Science Part A: Polymer Chemistry*, **2004,** *42* (18), 4598-4606.

65. Teramoto, N.; Unosawa, M.; Matsushima, S.; Shibata, M. Synthesis and Properties of Thermoplastic Alternating Copolymers Containing Trehalose and Siloxane Units by Hydrosilylation Reaction. *Polym. J*, **2007,** *39* (9), 975-981.

66. Teramoto, N.; Niwa, M.; Shibata, M. Synthesis and Properties of Trehalose-Based Flexible Polymers Prepared from Difurfurylidene Trehalose and Maleimide-Terminated Oligo(dimethylsiloxane) by Diels-Alder Reactions. *Materials*, **2010,** *3* (1), 369-385.

67. Teramoto, N.; Abe, Y.; Enomoto, A.; Watanabe, D.; Shibata, M. Novel synthetic route of a trehalose-based linear polymer by ring opening of two epoxy groups with aliphatic diamine. *Carbohydrate Polymers*, **2005,** *59* (2), 217-224.

68. Abuchowski, A.; van Es, T.; Palczuk, N. C.; Davis, F. F. Alteration of immunological properties of bovine serum albumin by covalent attachment of polyethylene glycol. *J Biol Chem*, **1977,** *252* (11), 3578-3581.

69. Abuchowski, A.; McCoy, J. R.; Palczuk, N. C.; van Es, T.; Davis, F. F. Effect of covalent attachment of polyethylene glycol on immunogenicity and circulating life of bovine liver catalase. *J Biol Chem*, **1977,** *252* (11), 3582-3586.

70. Veronese, F. M.; Mero, A. The Impact of PEGylation on Biological Therapies. *BioDrugs*, **2008,** *22* (5), 315-329.

71. Oishi, M.; Nagasaki, Y. Block Copolymer Synthesis for Nanoscale Drug and Gene Delivery. In *Nanotechnology in Drug Delivery*, Villiers, M. M.; Aramwit, P.; Kwon, G. S., Eds. Springer New York: 2009; pp 35-67.

72. Périon, R.; Ferrières, V.; Isabel García-Moreno, M.; Ortiz Mellet, C.; Duval, R.; García Fernández, J. M.; Plusquellec, D. 1,2,3-Triazoles and related glycoconjugates as new glycosidase inhibitors. *Tetrahedron*, **2005,** *61* (38), 9118-9128.

73. Cunha, A. C.; Figueiredo, J. M.; Tributino, J. L. M.; Miranda, A. L. P.; Castro, H. C.; Zingali, R. B.; Fraga, C. A. M.; de Souza, M. C. B. V.; Ferreira, V. F.; Barreiro, E. J. Antiplatelet properties of novel N-substituted-phenyl-1,2,3-triazole-4-acylhydrazone derivatives. *Bioorganic & Medicinal Chemistry*, **2003,** *11* (9), 2051-2059.

74. Campos, V. R.; Abreu, P. A.; Castro, H. C.; Rodrigues, C. R.; Jordão, A. K.; Ferreira, V. F.; de Souza, M. C. B. V.; Santos, F. d. C.; Moura, L. A.; Domingos, T. S., *et al.* Synthesis, biological, and theoretical evaluations of new 1,2,3-triazoles against the hemolytic profile of the Lachesis muta snake venom. *Bioorganic & Medicinal Chemistry*, **2009,** *17* (21), 7429-7434.

75. Menegatti, R.; Cunha, A. C.; Ferreira, V. F.; Perreira, E. F. R.; El-Nabawi, A.; Eldefrawi, A. T.; Albuquerque, E. X.; Neves, G.; Rates, S. M. K.; Fraga, C. A. M., *et al.* Design, synthesis and pharmacological profile of novel dopamine D2 receptor ligands. *Bioorganic & Medicinal Chemistry*, **2003,** *11* (22), 4807-4813.

76. da Silva Jr, E. N.; Menna-Barreto, R. F. S.; Pinto, M. d. C. F. R.; Silva, R. S. F.; Teixeira, D. V.; de Souza, M. C. B. V.; De Simone, C. A.; De Castro, S. L.; Ferreira, V. F.; Pinto, A. V. Naphthoquinoidal [1,2,3]-triazole, a new structural moiety active against Trypanosoma cruzi. *European Journal of Medicinal Chemistry*, **2008,** *43* (8), 1774-1780.

77. Gallardo, H.; Conte, G.; Bryk, F.; Lourenço, M. C. S.; Costa, M. S.; Ferreira, V. F. Synthesis and evaluation of 1-alkyl-4-phenyl-[1,2,3]-triazole derivatives as antimycobacterial agent. *Journal of the Brazilian Chemical Society*, **2007,** *18*, 1285-1291.

78. Ferreira, S. B.; Costa, M. S.; Boechat, N.; Bezerra, R. J. S.; Genestra, M. S.; Canto-Cavalheiro, M. M.; Kover, W. B.; Ferreira, V. F. Synthesis and evaluation of new difluoromethyl azoles as antileishmanial agents. *European Journal of Medicinal Chemistry*, **2007,** *42* (11-12), 1388-1395.

79. Safonova, T. S.; Nemeryuk, M. P.; Likhovidova, M. M.; Sedov, A. L.; Grineva, N. A.; Keremov, M. A.; Solov'eva, N. P.; Anisimova, O. S.; Sokolova, A. S. Synthesis and Biological Properties of Arylthio-1,2,3-Triazole Derivatives. *Pharmaceutical Chemistry Journal*, **2003,** *37* (6), 298-305.

Chapter 3: Trehalose-Oligoethyleneimine Linear "Click" Copolymers as Potent In Vitro Gene Delivery Agents for Stem Cell- and Regenerative Therapies*

*Chapter adopted from: Kizjakina K.; Bryson J.M.; Grandinetti G., and Reineke T.M. *in preparation for submission.*

3.1. Abstract

Trehalose-containing "click" polymers have previously demonstrated efficient *p*DNA delivery and transgene expression in the presence of serum proteins. Herein, we study the structure-property relationships within the series of trehalose-oligoethyleneamine linear "click" copolymers in which the number of secondary amines within the polymer repeat unit is varied (from 4 to 6, **Tr4**, **Tr5**, and **Tr6**, respectively) and determine the optimal *p*DNA delivery conditions in both human primary cell types and progenitor cells in the presence of serum. The three glycopolymers bind to *p*DNA at an N/P ratio of 2 (based on gel electrophoresis shift assay) and form stable complexes with a diameter of 60-80 nm in nuclease-free water and of 300-350 nm at a multitude of N/P ratios tested in DMEM medium supplemented with 10% FBS. For genetic engineering of primary cells for immunological and genetic therapies, cells must be reliably transfected *ex vivo* under optimal culture conditions, such as in the presence of serum proteins and antibiotics, to insure robust cell health and minimal contamination. To demonstrate this feasibility with trehalose-containing "click" polymers, two primary cell types were used for full transfection evaluation in comparison to common commercially available transfection reagent controls. Neonatal human dermal fibroblasts (HDFn) and

rat mesenchymal stem cells (RMSC) were evaluated for expression of both luciferase and green fluorescent protein (GFP) transgenic reporters, using a variety of methods to quantify total gene expression, percent population expression, and cytotoxicity. Among these structures, **Tr4** showed the greatest transfection efficiency in both cell lines tested. All three structures outperformed most of the commercially available transfection reagents, which may be a significant contribution to future regenerative and stem cell based therapies.

3.2. Introduction

With the mapping of the entire human genome having been completed,[1] nucleic acids have the potential to yield customized therapies for a broad array of the most devastating human diseases. However, the delivery of nucleic acids *in vivo* and *ex vivo* to therapeutically-relevant cells remains the major hurdle towards realizing the full utility of this powerful therapeutic tool. Nucleic acids are bulky, charged macromolecules that are unstable in the presence of nucleases, thus vehicles are required to compact them into nanosized particles, protect them from degradation, carry them through cellular membranes, and release them at the desired locations within target cells. This has been demonstrated with both viruses[2,3] and chemical reagent-based methods relying on calcium phosphate,[4,5] lipids,[6-8] and macromolecules.[9-12] Chemical materials that fulfill these duties but interfere minimally with native cellular function and viability are continually refined and improved to offer tailored methods for nucleic acid administration; however, all delivery methods developed thus far have limitations in either delivery efficiency or toxicity. At the forefront of nucleic acid delivery are carbohydrate-oligoamine copolymers, which demonstrate a high propensity towards

nucleic acid delivery while exhibiting low toxicity and high stability in endogenous conditions.[13-15] Indeed, polycationic carbohydrate-based synthetic polymers were recently used by Davis and coworkers for the first demonstration of systemic delivery of siRNA and the demonstration of RNAi in human subjects, a major milestone in nucleic acid-based therapeutics.[16]

To continue to advance the field of nucleic acid therapeutics, vehicles must be designed that can deliver nucleic acids both *in vivo* and *ex vivo* under a wide variety of conditions, including in the presence of serum proteins and antibiotics. This is a major limitation for many commercially-available transfection reagents formulated with both lipids and polymers.[17] Compatibility with serum and antibiotics is especially important to researchers performing *ex vivo* genetic engineering of therapeutic cells, as these conditions permit cells being transfected to exhibit optimal growth, behave as they would in native environments, and remain free of bacterial contamination. These factors are essential for the success of cell-based therapies after cell reintroduction or engineered tissue implantation has occurred. Major cells of interest to the community include a wide variety of immunological,[18-21] progenitor,[22-24] and structural tissue-based cells.[25,26] We have developed a new series of trehalose-oligoethyleneamine copolymers and demonstrated their ability to transfect neonatal human dermal fibroblasts (HDFn), which are of high therapeutic importance for their ability to be induced into pluripotent stem (iPS) cells.[27] In addition, these polymers have efficiently transfected primary rat mesenchymal stem cells (RMSCs) in serum-containing medium, which demonstrates the ability of this new series of macromolecules to transfect progenitor-type cells.

Herein, we further expand the library of trehalose containing oligoamine "click" copolymers[28-30] by increasing the number of secondary amines within the polymer backbone to 5 and 6. We also demonstrate that an integrated trehalose moiety contributes to particle stabilization in serum, making this a highly versatile transfection reagent. Polymers were synthesized in similar degrees of polymerization via step-growth Cu(I)-catalyzed azide-alkyne cycloaddition polymerization, resulting in a series of trehalose-containing copolymers with a range of numbers of secondary amines (from 4 to 6 per repeat unit) within the polymer backbone. These glycopolymers were tested for *p*DNA binding, cytotoxicity, cellular uptake, and transfection efficiency *in vitro* in primary and progenitor cells. This work contributes to our continuing efforts to design better nucleic acid carriers based upon structure-bioactivity relationships, in order to enable therapies aimed at important current clinical cellular therapeutic targets.

3.3. Experimental Procedures

3.3.1. General. All reagents and solvents used in the synthesis, if not specified otherwise, were obtained from Sigma-Aldrich (St. Louis, MO) or Fisher Scientific Co. (Pittsburgh, PA). All reagents were used without further purification. Methanol, dichloromethane, and dimethylformamide (DMF) were purified with MBRAUN MB SPS solvent purification system. Compounds **6a** and **6b**, partially-Boc-protected tetraethylenepentamine and pentaethylenehexamine, respectively, were synthesized through a previously-published procedure.[29,30] All the reactions were monitored to completion by thin layer chromatography (TLC) with ninhydrin staining for oligoamines and p-anisaldehyde staining for visualizing oligosaccharides along with UV light when possible. Ultrapure water was used in synthesis and dialysis. The dialysis membranes

were manufactured by Spectrum Laboratories, Inc. (Rancho Dominguez, CA). The liquid chromatography-mass spectra (LC-MS) were obtained with an Agilent system with a time-of-flight (TOF) analyzer coupled to a Thermo Electron TSQ-LC/MS ESI mass spectrometer. IR spectra were measured with a Perkin Elmer Spectrum One FT-IR spectrometer. ^{1}H and ^{13}C-NMR were recorded on a 400MR Varian-400 Hz spectrometer. The ^{1}H NMR data are reported as follows: chemical shift (δ ppm), multiplicity, J coupling constant (Hz), and peak integration. Either $CHCl_3$ (7.27 ppm) or HOD (4.79 ppm) was used as an internal reference.

Cell culture media and supplements were obtained from Gibco/Invitrogen (Carlsbad, CA). JetPEI solution was purchased from Polyplus Transfection™ (New York, NY). RMSC and HDFn cells were purchased from Invitrogen (Carlsbad, CA).

3.3.2. Synthesis of the Trehalose Monomer.

*2,3,4,2',3',4'-Hexa-O-acetyl-6,6'-diiodo-6,6'-dideoxy-D-trehalose (**2**).* Trehalose **1** (10.0 g, 29.2 mmol) was dissolved in anhydrous dimethylformamide (DMF) (300 mL) and cooled to 0 ºC. Triphenylphosphine (48.9 g, 186 mmol) and then iodine (38.2 g, 150 mmol) were added to that mixture, which was allowed to stir at 0 ºC for 10 min, after which the temperature was raised to 80 ºC and the reaction mixture was stirred for additional 3 h. The reaction mixture was concentrated under reduced pressure, cooled to 0 ºC and ice-cold water (500 mL) was added under vigorous stirring to precipitate the triphenylphosphine oxide side product, which was removed via filtration. The remaining solution was evaporated under reduced pressure to yield a brown solid. This crude material was dried *in vacuo*, then dissolved in anhydrous pyridine (200 mL) and acetic anhydride was added (100 mL). The reaction mixture was stirred at room temperature

under N_2 for 24 h. Then the mixture was concentrated via rotary evaporation and poured on ice (500 g) under vigorous stirring. Off-white precipitates were isolated by filtration, air dried and recrystallized from ethanol to yield the final product, 2,3,4,2',3',4'-hexa-O-acetyl-6,6'-diiodo-6,6'-dideoxy-D-trehalose, as a white crystalline solid. Yield after recrystallization: 11.2 g (47%). ^{1}H-NMR ($CDCl_3$): δ = 2.02 (s, 6H, CO*CH*$_3$), 2.07 (s, 6H, CO*CH*$_3$), 2.15 (s, 6H, CO*CH*$_3$), 3.07 (dd, J = 2.3, 8.6 Hz, 2H, H−6), 3.23 (dd, J = 2.3, 11.0 Hz, 2H, H−6), 3.95 (td, J = 2.4, 9.5 Hz, 2H, H−5), 4.90 (dd, J = 9.2 Hz, 2H, H−4), 5.20 (dd, J = 3.9, 10.2 Hz, 2H, H−2), 5.42 (d, J = 3.9 Hz, 2H, H−1), 5.48 (dd, J = 9.2, 10.2 Hz, 2H, H−3). ^{13}C-NMR ($CDCl_3$): δ = 2.61 (C–6), 20.79 (*CH*$_3$CO), 20.85 (*CH*$_3$CO), 21.35 (*CH*$_3$CO), 69.45 (C–2), 69.91 (C–3), 70.12 (C–5), 72.50 (C–4), 91.94 (C–1), 169.58 (CH_3*CO*), 169.72 (CH_3*CO*), 170.05 (CH_3*CO*). LC-ESI-MS (*m/z*): Theoretical $(M+H)^+$ $C_{24}H_{33}I_2O_{15}$ = 814.99; Found = 814.85; Theoretical $(M+NH_4)^+$ $C_{24}H_{36}I_2NO_{15}$ = 832.02; Found = 831.87.

*2,3,4,2',3',4'-Hexa-O-acetyl-6,6'-diazido-6,6'-dideoxy-D-trehalose (**3**).* To a solution of **2** (11.0 g, 13.5 mmol) dissolved in anhydrous DMF (100 mL), sodium azide (5.3 g, 81.5 mmol) was added. The heterogeneous mixture was then heated, while stirring, to 80 ºC and allowed to react for 24 h. The reaction mixture was then cooled, concentrated under reduced pressure and titrated with ice cold water (200 mL) to precipitate the crude product, which was filtered and dried *in vacuo* to yield 7.8 g (90%) of pure acetylated title product **3**. ^{1}H-NMR ($CDCl_3$): δ = 2.03 (s, 6H, CO*CH*$_3$), 2.07 (s, 6H, CO*CH*$_3$), 2.13 (s, 6H, CO*CH*$_3$), 3.18 (dd, J = 2.5, 13.3 Hz, 2H, H−6), 3.37 (dd, J = 7.3, 13.3 Hz, 2H, H−6), 4.10 (ddd, J = 2.5, 7.3, 10.0 Hz, 2H, H−5), 5.00 (dd, J = 9.3, 10.2 Hz, 2H, H−4), 5.09 (dd, J = 3.9, 10.3 Hz, 2H, H−2), 5.33 (d, J = 3.9 Hz, 2H, H−1), 5.48

(dd, J = 9.3, 10.3 Hz, 2H, H−3). ^{13}C-NMR ($CDCl_3$): δ = 20.60 ($\underline{CH_3}CO$), 50.95 (C–6), 69.63 (C–3), 69.68 (C–4), 69.79 (C–2), 69.88 (C–5), 92.97 (C–1), 169.57 ($CH_3\underline{CO}$), 169.60 ($CH_3\underline{CO}$), 169.92 ($CH_3\underline{CO}$). FT-IR: (cm^{-1}) 2961, 2097, 1745, 1436, 1368, 1289, 1212. LC-ESI-MS (*m/z*): Theoretical $(M+H)^+$ $C_{24}H_{33}N_6O_{15}$ = 645.20; Found = 645.06. Theoretical $(M+NH_4)^+$ $C_{24}H_{36}N_7O_{15}$ = 662.23; Found = 662.09.

3.3.3. Synthesis of the Oligoethyleneamine Monomers.

*N^1,N^5-bis(2-ethylphthalimido)-N^1,N^2,N^3,N^4,N^5-penta(tert-butoxycarbonyl)-tetraethylenepentamine (***7a***)*. N^2,N^3,N^4-tri(*tert*-butoxycarbonyl)-tetraethylenepentamine[30] **6a** (4.0 g, 8.2 mmol) was dissolved in anhydrous dichloromethane (100 mL) under nitrogen atmosphere and cooled to 0 ºC. With stirring, a solution of phthalimidoacetaldehyde[31] (3.8 g, 21 mmol) in dichloromethane (10 mL) was added slowly through a syringe to the solution of partially-protected oligoamine. The resulting solution turned from colorless to slightly yellowish, indicating formation of imine bond. The reaction mixture was stirred at 0 ºC for an additional 30 min, and subsequently concentrated into an oil, which was re-dissolved in anhydrous methanol (100 mL). Sodium triacetoxyborohydride (4.2 g, 20 mmol) was added to the reaction flask and the resulting heterogeneous mixture was stirred for 1 h at 0 ºC, then overnight at room temperature. The mixture was washed with saturated sodium bicarbonate solution (2 × 100 mL) to neutralize the residual sodium triacetoxyborohydride, and then washed with distilled water (2 × 100 mL). The washed organic layer was retrieved, dried with sodium sulfate, filtered, and concentrated to yield a yellowish oil. This crude product was re-dissolved in dichloromethane, and Boc-anhydride (3.9 g, 18 mmol) was added to this solution. The reaction was stirred for 6 h at room temperature, after which the solution

was concentrated to a viscous oil, which was purified by flash chromatography (ethyl acetate/hexane, 1/1 (v/v)). Fractions containing the product were isolated and concentrated under reduced pressure to yield a colorless oil, which, after stirring with cold diethyl ether, yielded a white amorphous solid. Yield: 3.9 g (46%). ^{1}H-NMR ($CDCl_3$): δ= 1.43-1.45 (m, 45H, ($\underline{CH_3}$)$_3$CO), 3.23-3.38 (m, 20H, CH_2), 3.45-3.53 (m, 2H, CH_2), 3.78-3.87 (m, 2H, CH_2), 7.65-7.86 (m, 8H, arom.). LC-ESI-MS (*m/z*): Theoretical $(M+H)^+$ $C_{53}H_{78}N_7O_{14}$ = 1036.56; Found = 1036.64. Theoretical $(M+Na)^+$ $C_{53}H_{77}N_7NaO_{14}$ = 1058.54; Found = 1058.61.

*N^1,N^6-bis(2-ethylphthalimido)-N^1,N^2,N^3,N^4,N^5,N^6-hexa(tert-butoxycarbonyl)-pentaethylenehexamine (***7b***).* The compound was synthesized with the procedure described for the synthesis of **7a** except *N^2,N^3,N^4,N^5-tetra(tert-butoxycarbonyl)-pentaethylenehexamine* **6b** (4.2 g, 6.6 mmol) was used in place of **6a** with the other reagents in corresponding molar ratios. Yield: 3.1 g (40%). ^{1}H-NMR ($CDCl_3$): δ = 1.43-1.46 (m, 54H, ($\underline{CH_3}$)$_3$CO), 3.22-3.37 (m, 24H, CH_2), 3.42-3.55 (m, 2H, CH_2), 3.79-3.87 (m, 2H, CH_2), 7.66-7.87 (m, 8H, arom.). LC-ESI-MS (*m/z*): Theoretical $(M+H)^+$ $C_{60}H_{91}N_8O_{16}$ = 1179.65; Found = 1179.71. Theoretical $(M+Na)^+$ $C_{60}H_{90}N_8NaO_{16}$ = 1201.64; Found = 1201.70.

*N^2,N^3,N^4,N^5,N^6-penta(tert-butoxycarbonyl)-hexaethyleneheptamine (***8a***).* Compound **7a** (1.5 g, 1.4 mmol) was dissolved in methanol (20 mL) and reacted with hydrazine monohydrate (1 mL, d=1.032 g/mL, 21 mmol) under reflux conditions for 4 h. The progression of the reaction was monitored by TLC (dichloromethane/methanol/ammonia hydroxide, 100/10/1 (v/v/v)). Upon completion, the reaction mixture was cooled, causing the formation of a white precipitate, the side

product 2,3-dihydrophthalazine-1,4-dione. The reaction mixture was concentrated under reduced pressure to yield a white amorphous solid, which was dissolved in dichloromethane (30 mL) and washed with 4 M NH_4OH solution (2 × 20 mL) and then with water (2 × 20 mL). The washed organic layer was collected, dried with sodium sulfate, filtered, and concentrated under reduced pressure to yield a colorless oil, which formed a white amorphous solid following the addition of 5 mL of diethyl ether and cooling for 1 h at -24 ºC. The crude solid was recrystallized from methyl *tert*-butyl ether (MTBE). Yield: 0.9 g (82%). ^{1}H-NMR ($CDCl_3$): δ = 1.45 (s, 45H, ($\underline{CH_3}$)$_3$CO), 2.81 (t, 4H, $\underline{CH_2}NH_2$), 3.31 (q, 20H, $\underline{CH_2}$NBoc). LC-ESI-MS (*m/z*): Theoretical $(M+H)^+$ $C_{37}H_{74}N_7O_{10}$ = 776.55; Found = 776.55.

*N^2,N^3,N^4,N^5,N^6,N^7-hexa(tert-butoxycarbonyl)-heptaethyleneoctamine (***8b***).* The compound was synthesized according to the procedure described for the synthesis of **8a** where, instead of **7a**, **7b** (1.2 g, 1.0 mmol) was used with the other reagents in corresponding molar ratios. Yield: 0.8 g (93%). ^{1}H-NMR ($CDCl_3$): δ = 1.45 (s, 54H, ($\underline{CH_3}$)$_3$CO), 2.79-2.84 (m, 4H, $\underline{CH_2}NH_2$), 3.22-3.37 (m, 24H, $\underline{CH_2}$NBoc). LC-ESI-MS (*m/z*): Theoretical $(M+H)^+$ $C_{44}H_{87}N_8O_{12}$ = 919.64; Found = 919.64.

*N^1,N^5-bis(2-ethylpropynamido)-N^1,N^2,N^3,N^4,N^5-penta(tert-butoxycarbonyl)-tetraethylenepentamine (***9a***).* A solution of N,N'-dicyclohexylcarbodiimide (DCC) (1.6 g, 7.9 mmol) in anhydrous dichloromethane (20 mL) was cooled to 0 ºC under N_2(g). A solution of propiolic acid (0.6 g, 8.6 mmol) in dichloromethane (3 mL) was then added dropwise through a syringe. The resulting heterogeneous mixture was stirred at 0 ºC for additional 30 min, then a solution of diamine **8a** (1.4 g, 1.8 mmol) in dichloromethane (5 mL) was added dropwise through a syringe. The mixture was stirred for 1 h at 0 ºC and

then overnight at room temperature. The insoluble side product, 1,3-dicyclohexylurea, was filtered from the reaction mixture. The remaining filtrate was concentrated under reduced pressure to yield a brown oil, which was purified via flash chromatography (ethyl acetate/chloroform, 2/1 (v/v)). The fractions with the desired product were combined and concentrated under reduced pressure to yield an off-white amorphous solid, which was recrystallized in ethyl acetate to yield the title product **9a**. Yield: 0.9 g (57%). ^{1}H-NMR ($CDCl_3$): δ = 1.44-1.47 (m, 45H, ($\underline{CH_3}$)$_3$CO), 2.71-2.76 (bs, 2H, C≡$\underline{CH}$), 3.25-3.46 (m, 24H, CH_2). FT-IR: 3294, 3210, 2973, 2926, 2101, 1675, 1660, 1519, 1471, 1418, 1362, 1235, 1155. LC-ESI-MS (*m/z*): Theoretical $(M+H)^+$ $C_{43}H_{74}N_7O_{12}$ = 880.54; Found = 880.48. Theoretical $(M+Na)^+$ $C_{43}H_{73}N_7NaO_{12}$ = 902.52; Found = 902.44.

*N^1,N^6-bis(2-ethylpropynamido)-N^1,N^2,N^3,N^4,N^5,N^6-hexa(tert-butoxycarbonyl) pentaethylenehexamine (***9b***).* This compound was obtained following a similar procedure as the one reported above for **9a**, with **8b** (2.0 g, 2.2 mmol) used as a starting material. Yield: 1.3 g (58%). ^{1}H-NMR ($CDCl_3$): δ = 1.44-1.47 (m, 54H, ($\underline{CH_3}$)$_3$CO), 2.72-2.76 (bs, 2H, C≡$\underline{CH}$), 3.25-3.46 (m, 28H, $\underline{CH_2}$). FT-IR: 3216, 2975, 2932, 2104, 1682, 1658, 1537, 1471, 1415, 1365, 1244, 1158. LC-ESI-MS (*m/z*): Theoretical $(M+H)^+$ $C_{24}H_{33}N_6O_{15}$ = 1023.63; Found = 1023.55. Theoretical $(M+Na)^+$ $C_{24}H_{36}N_7O_{15}$ = 1045.62; Found = 1045.53.

3.3.4. Synthesis of Tr4-Tr6 Polymers.

General procedure for the polymerization. The diazido trehalose monomer **3** (0.15-0.60 mmol), the equivalent molar amount of alkyne terminated oligoethyleneamines **9**, **9a** or **9b**, and *tert*-butanol (1-2 mL) were mixed in a 5 mL vial and cooled to 0 ºC. To the cooled, stirred reaction mixture, 1 M copper sulfate (0.2 eq)

and 1 M sodium ascorbate (0.4 eq) aqueous solutions were added, after which water was added to a 1/1 (v/v) total ratio of *tert*-butanol/water. The mixture was heated to 50 ºC and vigorously stirred at that temperature for 2 h. The reaction was terminated by cooling the heterogeneous mixture with an ice bath. After cooling, the reaction mixture separated into a viscous yellow oily layer and a blue aqueous supernatant. The copper-containing supernatant was removed and the remaining viscous oily residue was dissolved in 1 mL of DMSO and precipitated by adding 4 M NH_4OH (2 mL) solution. Precipitates were recovered via centrifugation, after which a fresh portion of 4 M NH_4OH solution was added to the precipitant and the centrifugation was repeated. This cycle was repeated until no blue color was visually detectable in the NH_4OH supernatant, indicating that copper (II) was removed from the "click" polymer product. The off-white precipitate was washed with water (2 × 2 mL) in a similar manner described for NH_4OH and the resulting precipitates dried *in vacuo* and carried to the deprotection steps.

General Procedure for the Deprotection of Acetyl and Boc. The hydroxyl-protecting acetyl groups were removed from each of the polymers by dissolving each polymer from the polymerization step in 2 mL of sodium methoxide solution in dry methanol (0.05 g/mL). This solution was then stirred overnight at room temperature, dialyzed against methanol with 1000 MWCO membrane to remove NaOMe, and then dried under vacuum. The resulting deacetylated polymer was dissolved in 1 mL of a solution of 4 M HCl in dioxane and stirred at room temperature for 4 h to remove the Boc protecting groups. The HCl/dioxane was removed under vacuum yielding a solid product which was re-dissolved in ultrapure water and purified via dialysis with 3500 MWCO membrane against ultrapure H_2O for 48 h (water changes: 3 × 4 L; at 8, 24, and 36

hours). The final deprotected polymers (**10**, **10a**, and **10b**) were lyophilized to dryness to yield a white fluffy solid.

Tr4. *Poly[(trehalose-ditriazolamido)pentaethylenetetraamine] (**10**).* Yield in 3 steps: 105 mg, (51%). ^{1}H-NMR (D_2O): δ = 3.11-3.28 (m, 18H), 3.47-3.52 (m, 2H), 3.75 (t, J = 5.7 Hz, 4H), 3.84 (t, J = 9.4 Hz, 2H), 4.19 (t, J = 7.8 Hz, 2H), proton signals overlapping with HOD peak, 8.49 (s, 2H). FT-IR: (cm^{-1}) 3235, 2921, 1654, 1577, 1510, 1435, 1346, 1246.

Tr5. *Poly[(trehalose-ditriazolamido)hexaaethylenepentaamine] (**10a**).* Yield in 3 steps: 156 mg, (61%). ^{1}H-NMR (D_2O): δ = 3.01-3.05 (m, 8H), 3.19-3.27 (m, 10H), 3.36 (t, J = 5.4 Hz, 4H), 3.48 (dd, J = 3.6, 10.0 Hz, 4H), 3.78-3.84 (m, 6H), 4.18 (t, J = 8.0 Hz, 2H), proton signals overlapping with HOD peak, 8.49 (s, 2H). FT-IR: (cm^{-1}) 3280, 1651, 1575, 1512, 1435, 1372, 1244.

Tr6. *Poly[(trehalose-ditriazolamido)heptaethylenehexaamine] (**10b**).* Yield in 3 steps: 96 mg, (79%). ^{1}H-NMR (D_2O): δ = 2.88-3.64 (m, 26H), 3.65-4.11 (m, 8H), 4.12-4.23 (m, 2H), proton signals overlapping with HOD peak, 8.51 (s, 2H). FT-IR: (cm^{-1}) 3270, 2920, 2842, 1646, 1572, 1509, 1453, 1433, 1365, 1244.

3.3.5. Polymer and Polyplex Characterization. *Gel Permeation Chromatography (GPC).* The resulting **Tr4** (**10**), **Tr5** (**10a**), **Tr6** (**10b**) "click" polymers were characterized by aqueous GPC utilizing an eluent of 1 wt% acetic acid/0.1 M $NaSO_4$ (aq) at a flow rate of 0.3 mL/min at 25 ºC with an injection volume of 100 μL, Eprogen, Inc. CATSEC columns (100, 300, and 1000 Å), Waters 2489 UV/vis detector (λ = 274 nm), Wyatt Optilab rex refractometer (λ = 658 nm), and Wyatt DAWN Heleos-II

multiangle laser light scattering (MALLS) detector (λ = 662 nm). See Supporting Information for GPC chromatograms.

Gel Electrophoresis Shift Assays. The ability of the polymers **Tr4**, **Tr5,** and **Tr6** to bind *p*DNA was measured by gel electrophoresis at 65 V. Agarose gel (0.6%, w/v) containing ethidium bromide (0.06%, w/v) was prepared in TAE buffer (40 mM Tris-acetate, 1 mM EDTA). Each polymer was dissolved in nuclease-free water (Gibco, Carlsbad, CA). Plasmid DNA (10 μL, 0.075 μg/μL) was mixed with the same volume of polymer solution at N/P ratios between 0 and 20 (N = moles of secondary amine groups on polymer backbone; P = moles of phosphate groups on the *p*DNA) and incubated for 45 min at room temperature before addition of loading buffer (2 μL of Blue Juice, Invitrogen, Carlsbad, CA). An aliquot (10 μL) of each sample was loaded into the well of the gel. A stable polymer-*p*DNA complex is shown by the lack of the migration of the *p*DNA in the electrophoretic field.

Dynamic Light Scattering and Zeta Potential Measurements. Polyplex sizes and zeta potentials were measured on a Zetasizer (Nano ZS) dynamic light scattering instrument (Malvern Instruments, Malvern UK). The instrument employs a 4.0 mW He-Ne laser operating at 633 nm with a 173° scattering angle. The polyplexes were formed at five different N/P ratios in triplicate (20, 10, 7, 5, and 3) by adding an aqueous solution of a polymer (150 μL) to an aqueous solution of *p*DNA (pCMVβ) (150 μL, 0.075 μg/mL), gently mixing with a pipette tip, and incubating at room temperature for 45 min. Prior to the measurement, polyplex solutions were diluted either with nuclease-free water (700 μL) or DMEM supplemented with 10% FBS (700 μL). The particle diameter was analyzed based on the particle distribution by both volume and intensity (the readings

were very close) for the measurements performed in water, and particle distribution by intensity only was used when measuring particle size in DMEM (two large extra peaks at around 10 and 40 nm are always present and correspond to the serum proteins). Zeta potentials were measured with the same polyplex solutions in nuclease-free water only.

Luciferase and BCA Potein Assay. Prior to transfection, either primary neonatal human dermal fibroblast cells (HDFn, Invitrogen, Carlsbad, CA) or rat mesenchymal stem cells (RMSC, Invitrogen, Carlsbad, CA) were plated on 24-well plates at a density of 100,000 cells per well, with approximately 70% confluency. HDFn cells were incubated in Medium 106, supplemented with 2% FBS, hydrocortisone (1 μg/mL), human epidermal growth factor (1 ng/mL), basic fibroblast growth factor (3 ng/mL), and heparin (10 μg/mL), for 24 h at 37 ºC in a 5% CO_2 environment. RMSC were incubated in Mesanpro RS medium (Invitrogen) supplemented with 2% FBS. For both cell lines, medium was changed 30 minutes prior to transfection. Stock solutions at N/P 20 for each polymer were prepared and diluted to lower N/P ratios (10, 7) so that equal volume of polymer solution (V = 13.33 μL) and *p*DNA ([*p*DNA] = 0.075 mg/mL, V_t = 13.33 μL) could be combined to form the polyplex solution for each well (total *p*DNA per well = 1 μg). Positive controls - Lipofectamine™ 2000 (Invitrogen, Carlsbad, CA), Lipofectamine™ LTX with Plus™ (Invitrogen, Carlsbad, CA), jetPEI™ (Polyplus Transfection™, New York, NY), and Glycofect™ (Techulon Inc., Blacksburg, VA) - were formulated with *p*DNA based upon their recommended protocols. Solutions of transfection reagent-*p*DNA (gWiz-Luciferase, Aldevron, Fargo, ND) complexes for each N/P were added in triplicate to the corresponding wells. Plates were swirled to ensure homogenous solution formation and incubated for 4 h, after which more medium (500

μL) was added to each well. Cells were incubated for additional 20 h, followed by a medium change and 24 h of additional incubation time (48 h total). Medium was removed from wells and cells were lysed in 100 μL Cell Lysis Buffer (Promega, Madison, WI). Cell lysates were deposited on 96-well plates and analyzed for luciferase activity and total protein concentration. Protein concentration was analyzed relative to controls to determine cell viability.

MTT Assay. Cells were prepared and transfected using the same methodology as reported above under the luciferase and Lowry assays. However, at the 47 h time point, medium was removed from each well and replaced with medium containing 3-(4,5-dimethylthiazol-2-yl)-2,5-diphenyltetrazolium bromide (MTT, [MTT] = 0.5 mg/mL). Cells were incubated for an additional 1 h then washed with PBS and lysed in 250 μL DMSO. Sample cell lysates were analyzed via absorbance vs. negative control lysate absorbance to determine cell viability.

GFP Analysis via Flow Cytometry. Cells were plated and polyplexes were formed by the same methods reported above with a plasmid encoding enhanced green florescent protein (EGFP-C1). Transfection and medium change conditions are consistent with those reported above; however, cells were only subjected to complexes at a single charge ratio, N/P=20. After 48 h, cells were trypsinized, washed with PBS twice, and suspended in 500 μL of PBS. Flow cytometry analysis of each sample provided mean fluorescence intensity as well as the percentage of cells positive for EGFP.

GFP Analysis via Microscopy. Cells were plated and polyplexes were formed by the same methods described for Section 4.5. After transfecting cells for 48 h, each well was washed twice with PBS buffer and treated with 4% *para*-formaldehyde solution in

PBS. After 20 min, each well was washed with PBS. Each well was then imaged with a Nikon TE2000U widefield microscope equipped with a GFP excitation/emission filter set and liquid-cooled CCD camera. Wells were imaged with consistent exposure time and normalized to control backgrounds.

3.4. Results and Discussion

Herein, we present a series of trehalose-oligoethyleneamine linear copolymers containing a varying number of secondary amines within the polymer backbone that demonstrate the propensity to enable highly efficient transfection of therapeutically-relevant primary cells. This work expands upon the characterization of structure-property relationships in carbohydrate-containing copolymers previously reported by our group.[28-30] Furthermore, this work is intended to demonstrate reagent-based solutions for primary tissue transfections in the presence of serum and antibiotics, an area where commercially-available transfection reagents fall short. Accomplishing this goal would enable *ex vivo* cellular engineering to be carried out more efficiently, with better cellular viability, and free from bacterial contamination, all critical constraints in translating engineered cellular therapies to the clinic.

Previously, Reineke et al. have designed and synthesized trehalose-oligoethyleneamine copolymers containing 1 to 4 secondary amines that have shown promising plasmid DNA (*p*DNA) transfection results for HeLa and H9c2 cell lines in the presence of serum proteins.[29,30,32-37] Upon electrostatic complexation of the polycations and *p*DNA in aqueous media, nanosized particles were formed, and their sizes and zeta-potentials were characterized via dynamic light scattering (DLS). In general, trehalose-oligoethyleneamine polymers efficiently bind *p*DNA at low nitrogen to phosphate (N/P)

ratios forming nanoparticles of 60-100 nm diameter in water and 300-400 nm diameter in serum medium, demonstrate cellular uptake and transfection in HeLa and H9c2 cell lines, and appear to be relatively non-toxic. Polymers comprised of trehalose moieties and four secondary amines in the repeat unit showed the greatest promise in *p*DNA delivery *in vitro*. In order to find out the optimal length of the oligoethyleneamine for the polymer repeat unit to achieve the highest transfection efficiency with low toxicity, we needed to further expand these polymer series. We synthesized two new polymers — containing 5 and 6 ethyleneamine units, respectively — along with the trehalose moiety in the polymer backbone and studied whether further increase of amine density will concomitantly influence the transfection efficiency and toxicity profiles.

Trehalose-oligoethyleneamine copolymers were synthesized via step-growth Cu(I)-catalyzed "click" chemistry in order to examine how the amine density within a polymer backbone influences the efficiency of *p*DNA delivery to sensitive primary cell types. Our previous studies indicate that increasing density of protonatable secondary amines (from 1-4 per repeat unit) within a polymer backbone of a series of glycopolymers, the poly(glycoamidoamine)s,[33,35-37] resulted in significant increase in transfection efficiency, without any significant reduction in cellular viability. However, with a further increase in secondary amines (5 and 6), gene expression plateaued and cytotoxicity increased.[32] Transfection efficiency and serum stability within trehalose copolymer series also seems to increase as the number of secondary amines within the polymer repeat unit increases.

Synthesis and Characterization of Polymers. Trehalose diazido monomer was synthesized by utilizing a slight modification from the previously-published method[30] as

shown in **Scheme 3-1**. We first exchanged both primary hydroxyls with iodo groups by triphenylphosphine-mediated substitution as described in a previously-published procedure[38] and all secondary hydroxyl groups were acetylated with acetic anhydride in pyridine to yield compound **2**, which was purified by recrystallization from ethanol. (In the case of incomplete iodine substitution, monoiodotrehalose, along with the peracetylated trehalose as side products, can be removed from the product mixture via column chromatography with a mixture of 5% diethyl ether in dichloromethane as eluent). Purified compound **2** was then converted to **3** via substitution of iodines with azido groups in a similar manner to previously reported methods.[39,40]

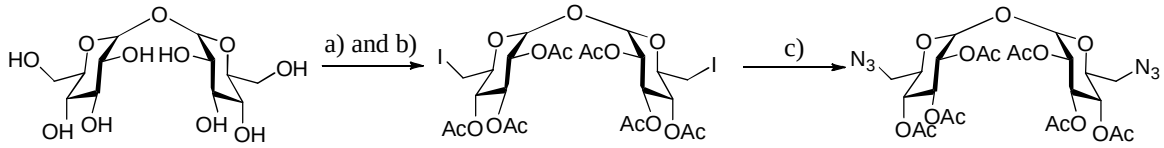

1 **2** **3**

Scheme 3-1. Synthesis of trehalose monomer. Conditions: a) Ph_3P, I_2, DMF, 80 ºC, 3 h; b) Ac_2O:Py (1:2), 24 h, RT, c) NaN_3, DMF, 80 ºC, 24 h.

In order to synthesize trehalose copolymers with additional amine units, higher-order oligoamine precursors had to be synthesized, leading to the creation of alkyne-functionalized oligoethyleneamines with 5 and 6 secondary amines, as shown in **Scheme 3-2**. Briefly, primary amines of either tetraethylenepentamine or pentaethylenehexamine were selectively protected with trifluoroacetyl groups, followed by tert-butoxycarbonyl (Boc) protection of the secondary amines, and subsequent deprotection of triflouroacetyl groups in basic conditions, thus liberating the primary amine end groups and obtaining compounds **6a** and **6b** as we reported before.[30] The additional amines were introduced to the molecule via reductive amination, in reaction of **6a** and **6b** with

phthalimidoacetaldehyde **5**[31] and subsequently using sodium triacetoxyborohydride as a mild reducing agent to convert formed imine bonds to the amines following a slightly modified procedure from Abdel-Magid *et al.*[41] Newly-formed secondary amines were then protected with Boc groups to yield **7a** and **7b**. Phthalimido groups were subsequently removed in reaction with hydrazine, yielding terminal diamines **8a** and **8b**. Alkyne functionalities were further introduced via DCC coupling of the primary amines of **8a** and **8b** with propiolic acid. In general, synthesis of these protected oligoamines is quite challenging because of multiple synthetic steps, low yields at each step and tedious purification, as is common with amines. The detailed scheme of all the routes employed for the synthesis of these oligoethyleneamines is available in **Appendix B**.

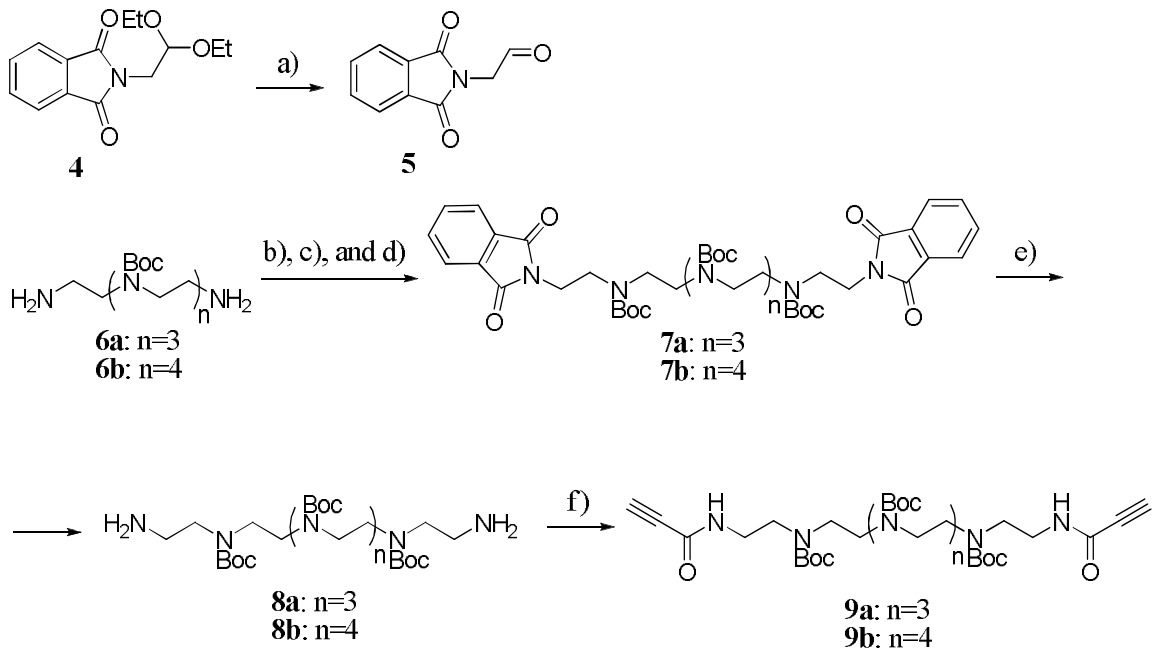

Scheme 3-2. Synthesis of oligoethyleneamine monomers. Conditions: a) TFA, DCM, 12 h, 0 °C→RT;[31] b) **5**, DCM, 0 °C→RT, 30 min; c) $Na(OAc)_3BH$, MeOH, 12 h, RT; d) Boc_2O, MeOH, 6 h, RT; e) $N_2H_4 \cdot H_2O$, MeOH, 3 h, reflux; f) DCC+propiolic acid, DCM, 0 °C→RT, 12 h.

Polymerization was carried out in a *tert*-butanol:water mixture (1:1) in the presence of Cu(I), which was generated *in situ* via Cu(II) sulfate reduction with sodium ascorbate. This highly-reported "click" procedure[42-44] yielded polymers with protected secondary amines and hydroxyls to avoid chelating of copper. Upon completion of the polymerization reactions, copper was removed via multiple washes of the protected polymers with aqueous NH_4OH. Protecting groups were subsequently deprotected with sodium methoxide in methanol and 4 M HCl in dioxane, as described in **Scheme 3-3**. The final materials were dialyzed against water to narrow their respective polydispersity indexes, which are intrinsically larger in step-growth based polymerization procedures.

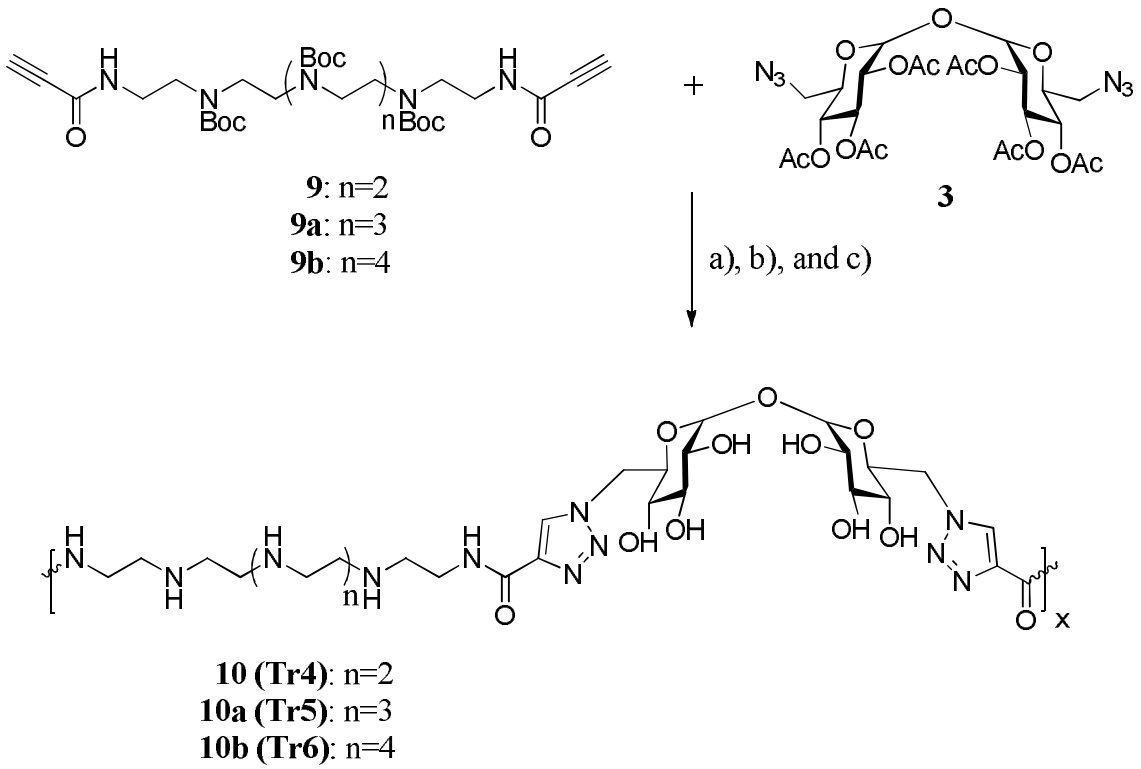

Scheme 3-3. Synthesis of **Tr4-Tr6** polymers. Conditions: a) $CuSO_4$ (0.2 eq), sodium ascorbate (0.4 eq), *t*BuOH/H_2O (1/1), 50 ºC, 2 h; b) 0.1 g/mL NaOMe in MeOH, RT, 12 h; c) 4 M HCl in dioxane RT, 4 h.

The conditions of polymerization established previously[29] lead to a library of polymers with similar degrees of polymerization. This permits valid comparison within the **Tr4-Tr6** series. The weight-average molecular weight and degree of polymerization for each of the purified polymers, along with their respective polydispersity indexes, were determined by gel permeation chromatography analysis (**Figure 3-1)** and results are summarized in **Table 3-1**. Polymer structures were also characterized and confirmed with ^{1}H-NMR and IR (see **Appendix A**).

Table 3-1. Characterizations of **Tr4-Tr6** polymers: weight average molecular weight ($\mathbf{M_w}$), polydispersity ($\mathbf{M_w/M_n}$), and degree of polymerization ($\mathbf{DP_w}$) obtained from GPC analysis and the *N*/*P* ratios of polymer-*p*DNA binding and charge neutralization (**N/P**) obtained from gel electrophoresis assay.

Polymer	**M_w (kDa)**	**M_w/M_n**	**DP_w**	**N/P**
Tr4	24.5	1.4	33	2
Tr5	23.0	1.1	30	2
Tr6	25.9	1.1	32	2

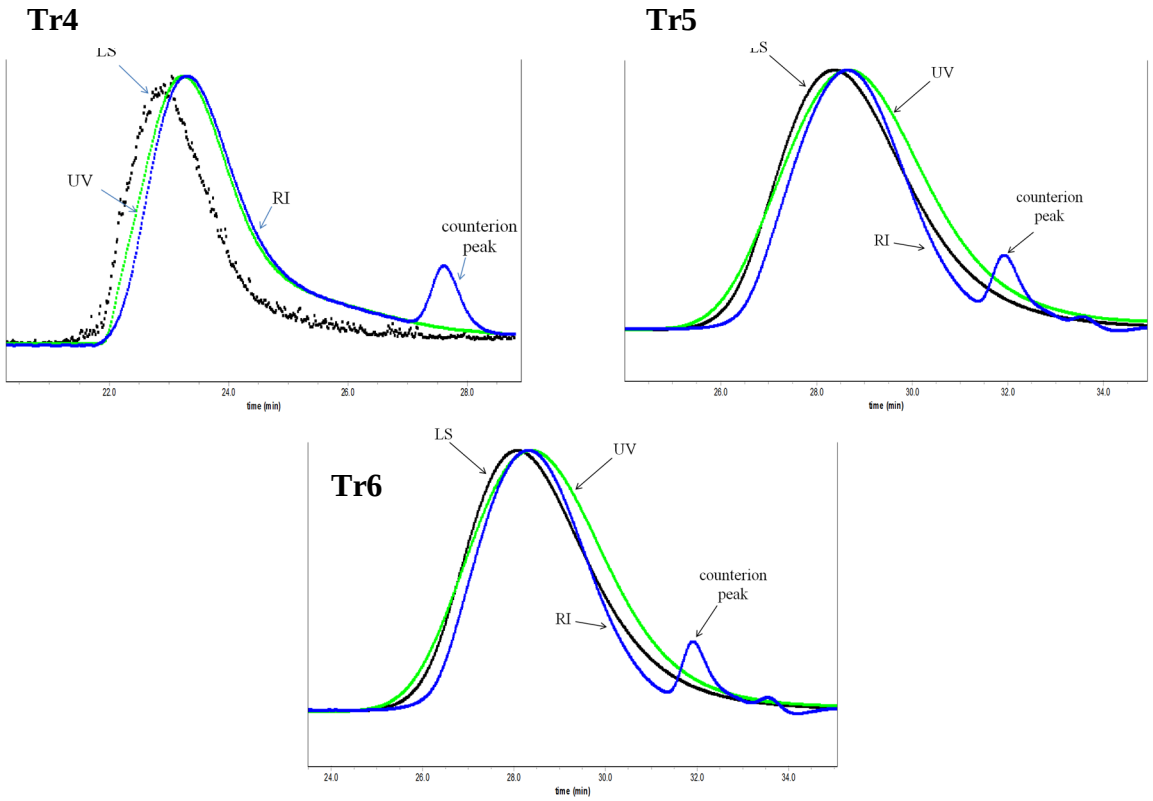

Figure 3-1. GPC chromatograms for **Tr4-Tr6** polymers.

Polymer-*p*DNA Binding, Particle Size, and Zeta Potential. Gel electrophoresis shift assays revealed that all the polymers (**Tr4**, **Tr5**, and **Tr6**) were able to inhibit *p*DNA migration in the electrophoretic field at a very low N/P ratio of 2 (**Figure 3-2**). Indeed, all three polymers formed stable nanoparticles (polyplexes) with *p*DNA in nuclease-free water at an N/P ratio of ≥3 as confirmed with dynamic light scattering (DLS) experiments. This data indicates that polyplex sizes are in a size range of 60-80 nm with the zeta potential increasing in correlation with polyplex N/P ratio increase (**Figure 3-3**). After diluting the polyplex solution in medium supplemented with 10% FBS, the particles increase in size over time indicating polyplex aggregation with serum proteins is occurring and, thus, some formulations of the **Tr4-Tr6** series (particularly N/P

3 and 5) are not ideal for serum transfections. For higher N/P ratios, increased particle stability in the presence of serum proteins is observed based on the small particle size increase after 4 h in serum solution. It is also worth mentioning that, at N/P ratios above 20, we started to notice multimodal peak distributions in DLS analysis, which suggests that at these high ratios polyplex sizes are not monodisperse and unbound trehalose polymer is likely present in the solution. Based on these observations, N/P ratios of 7, 10, and 20 were chosen for further cell culture experiments.

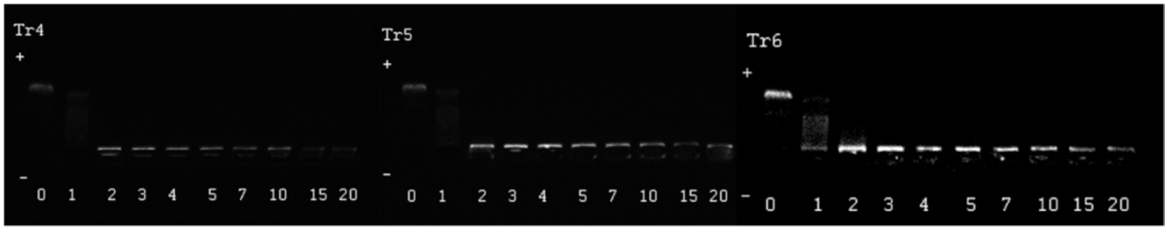

Figure 3-2. Gel binding for **Tr4-Tr6** polymers.

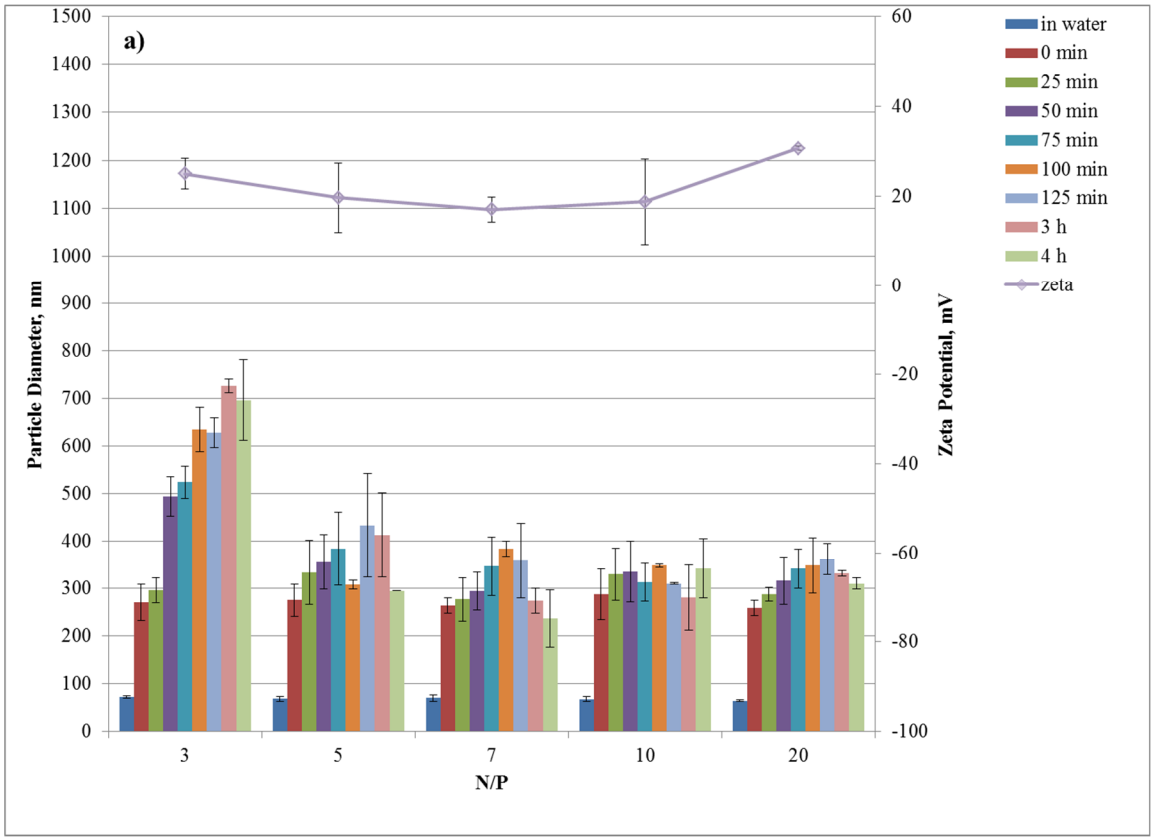
a)
Particle Diameter, nm
Zeta Potential, mV
N/P
in water
0 min
25 min
50 min
75 min
100 min
125 min
3 h
4 h
zeta

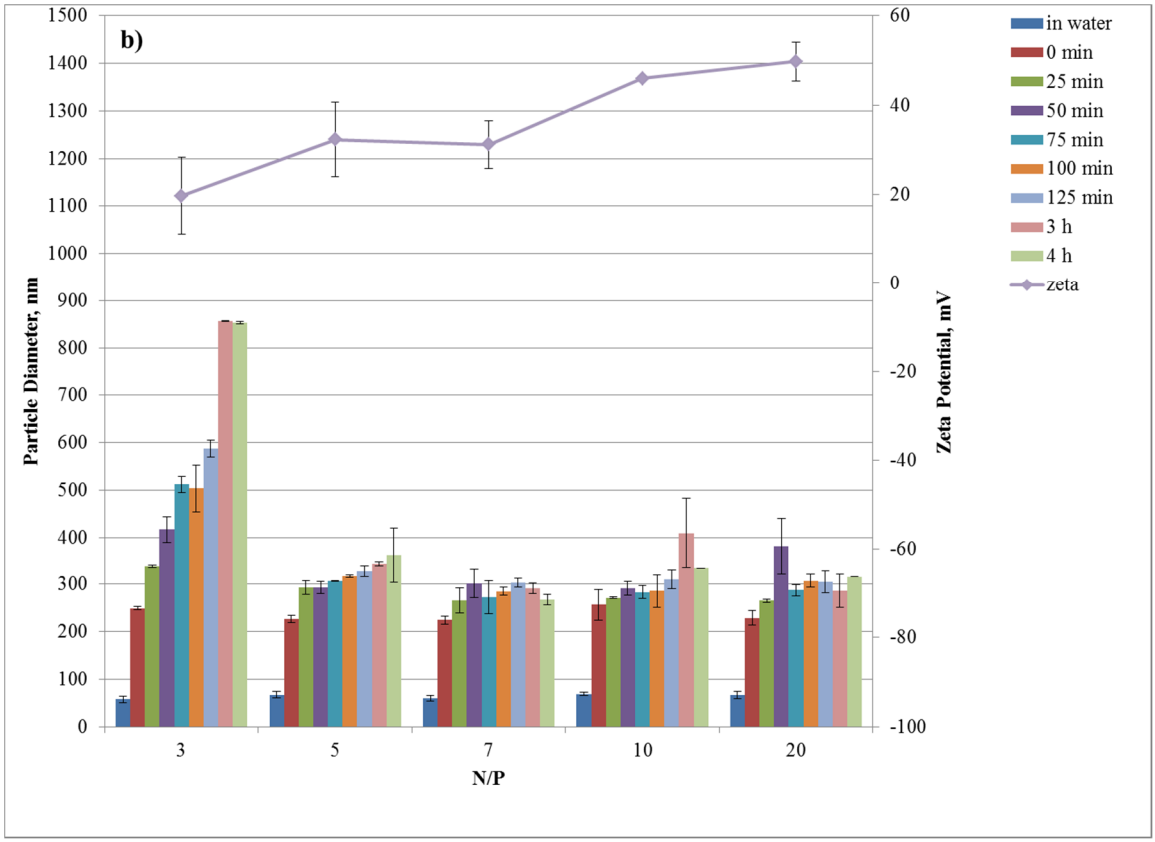
b)
Particle Diameter, nm
Zeta Potential, mV
N/P
in water
0 min
25 min
50 min
75 min
100 min
125 min
3 h
4 h
zeta

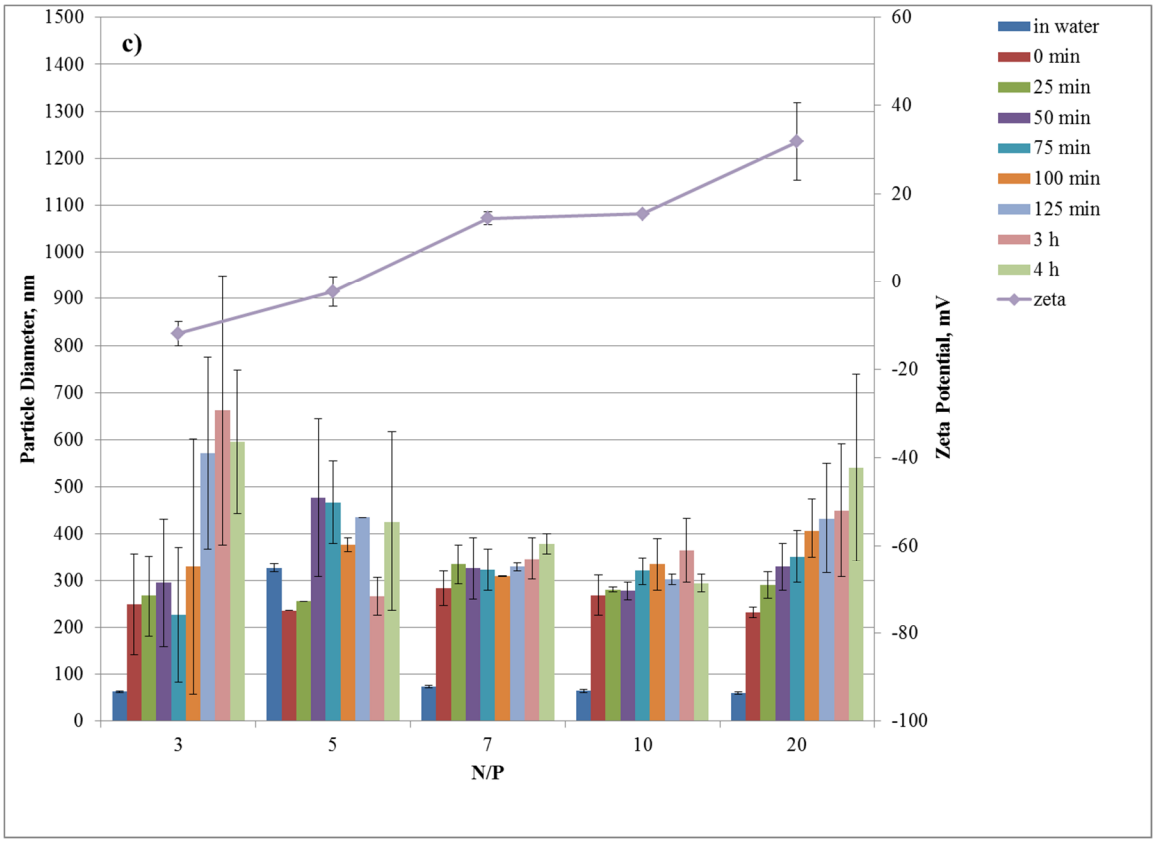

Figure 3-3. Zeta potential in water and particle diameter in water and serum containing media for corresponding polyplex formulations at N/P 3, 5, 7, 10, and 20. Polyplexes were incubated at RT for 45 min prior to dilution with water (followed by immediate DLS and zeta potential measurements) or with DMEM (followed by DLS measurements in time intervals from 0 min after dilution to 4 h). a) **Tr4**. b) **Tr5**. c) **Tr6**.

Cellular Delivery and Toxicity Studies. Transfection efficiency and cytotoxicity were measured in two therapeutically-relevant cell types — implantable cells used in regenerative therapies, human dermal fibroblasts (HDFn), and progenitor-type cells, rat mesenchymal stem cells (RMSC). Transfection efficiency was determined with both luciferase reporter gene expression assay and GFP detection via flow cytometry and fluorescence microscopy. The primary cell lines were transfected with reporter gene plasmids formulated with **Tr4**, **Tr5**, or **Tr6** polymers, at N/P ratios of 7, 10, and 20. At 48 h post-transfection, luciferase activity was measured in cell lysates with a

luminometer plate reader and reported as relative light units (RLU) and relative light units per milligram of protein (RLU/mg). The results were compared with commercially available transfection reagent positive controls: Lipofectamine™ 2000, Lipofectamine™ LTX with Plus™, jetPEI™, and Glycofect™ Transfection Reagent. In HDFn cells (**Figure 3-4a**), **Tr4** and **Tr5** polymers showed similar transfection efficiency at N/P 20 and 10, but, at N/P 7, **Tr5** transfected more efficiently than **Tr4**. **Tr6** generally showed lower transfection efficiency than either **Tr4** or **Tr5**; this is likely an artifact imparted by relying on N/P ratio formulation as opposed to weight/weight formulation, as a lower molar amount of **Tr6** polymer is used at similar N/P ratios compared with **Tr4** and **Tr5**. All three polymers showed higher transgene expression than jetPEI™, though jetPEI™ transfection was carried out at a lower N/P ratio (at N/P 5) per manufacturer's recommendations. Glycofect™ gives very high total gene expression; however, the protocol for use of Glycofect™ mandates transfection to be carried out in serum-free conditions for the first four hours. In RMSCs (**Figure 3-4b**) we saw a similar trend within the trehalose polymer series and we were encouraged to see extremely high efficacy for **Tr4**, indicating that this polymer may be an effective tool for new cellular therapies. In general, in both primary cell types, **Tr4** mediated the highest transgene expression, followed by **Tr5**; **Tr6** showed the poorest transfection efficiency. Again, this is likely attributable to the decrease in molar amount of polymer used as the degree of secondary amine quantity increases.

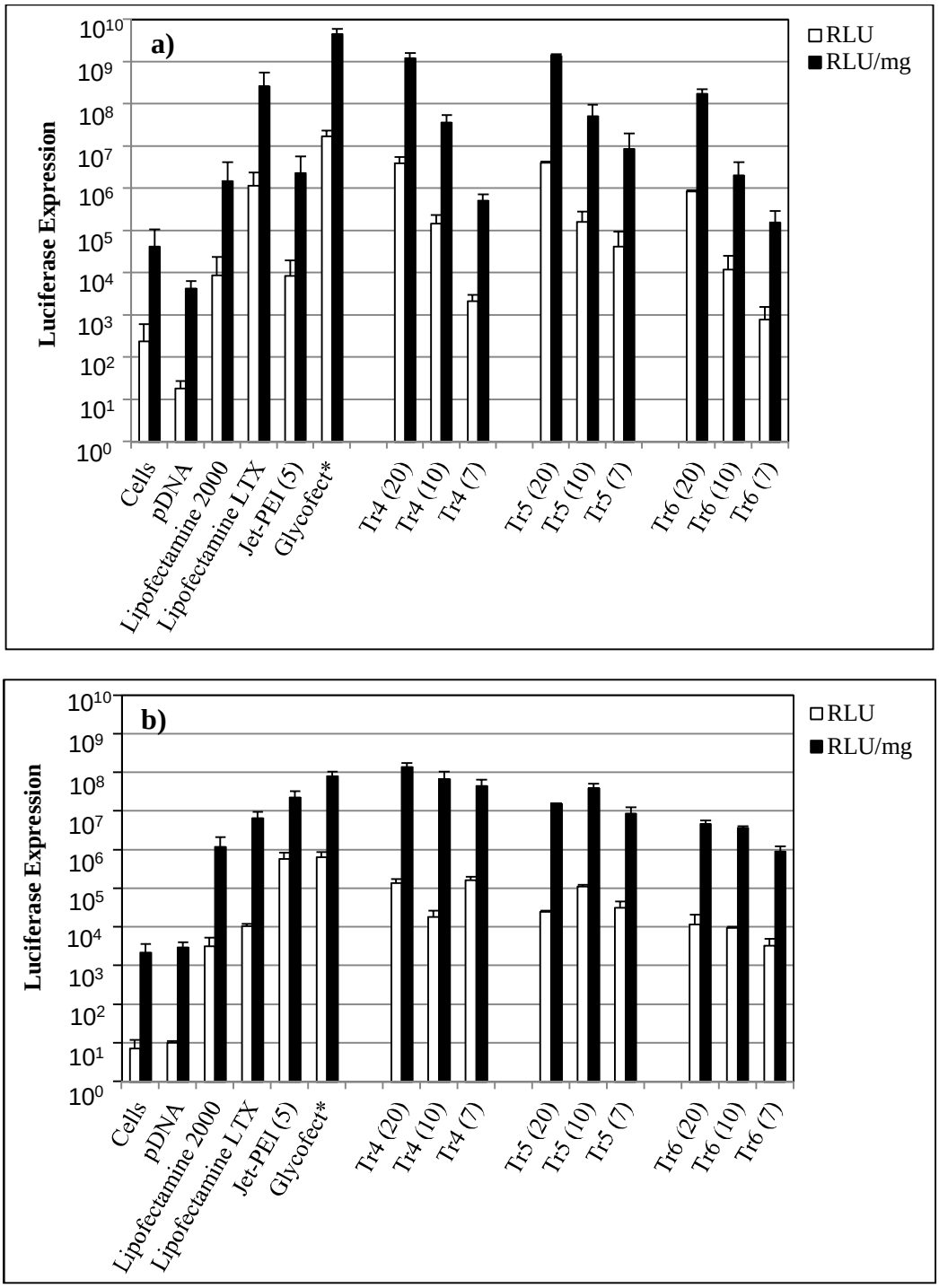

Figure 3-4. Luciferase gene expression observed with polyplexes formed with *p*DNA and **Tr4-Tr6** series at N/P 7, 10, and 20. Positive controls (Lipofectamine™ 2000, Lipofectamine™ LTX, jetPEI™ at N/P 5, and Glycofect™) were formulated with *p*DNA based upon their recommended protocols. The gene expression values are shown as relative light units (RLU) and as relative light units per milligram of protein (RLU/mg). The data are reported as the mean ± standard of deviation of three replicates. a) HDFn. b) RMSC. The experiment was performed by Joshua M. Bryson.

To gain information about cell viability under luciferase transfection conditions, both MTT and BCA protein assays were performed in parallel. Both assays indicate similar toxicity profiles within the **Tr4-Tr6** polymer series. Increased toxicity was observed for the entire polymer series, at N/P 20, in both cell lines (below 60% survival for **Tr4** and **Tr5**) (**Figure 3-5**). **Tr6** polymer appeared to be less toxic at N/P 20, which again can be explained by the lower molar ratio of this higher-order polymer. Nevertheless, at N/P 7 all the polymers were relatively non-toxic to the tested cell lines with the cellular survival at 80% and above, which is a crucial property the transfection reagent should have and is still lacking in several commercially available products.

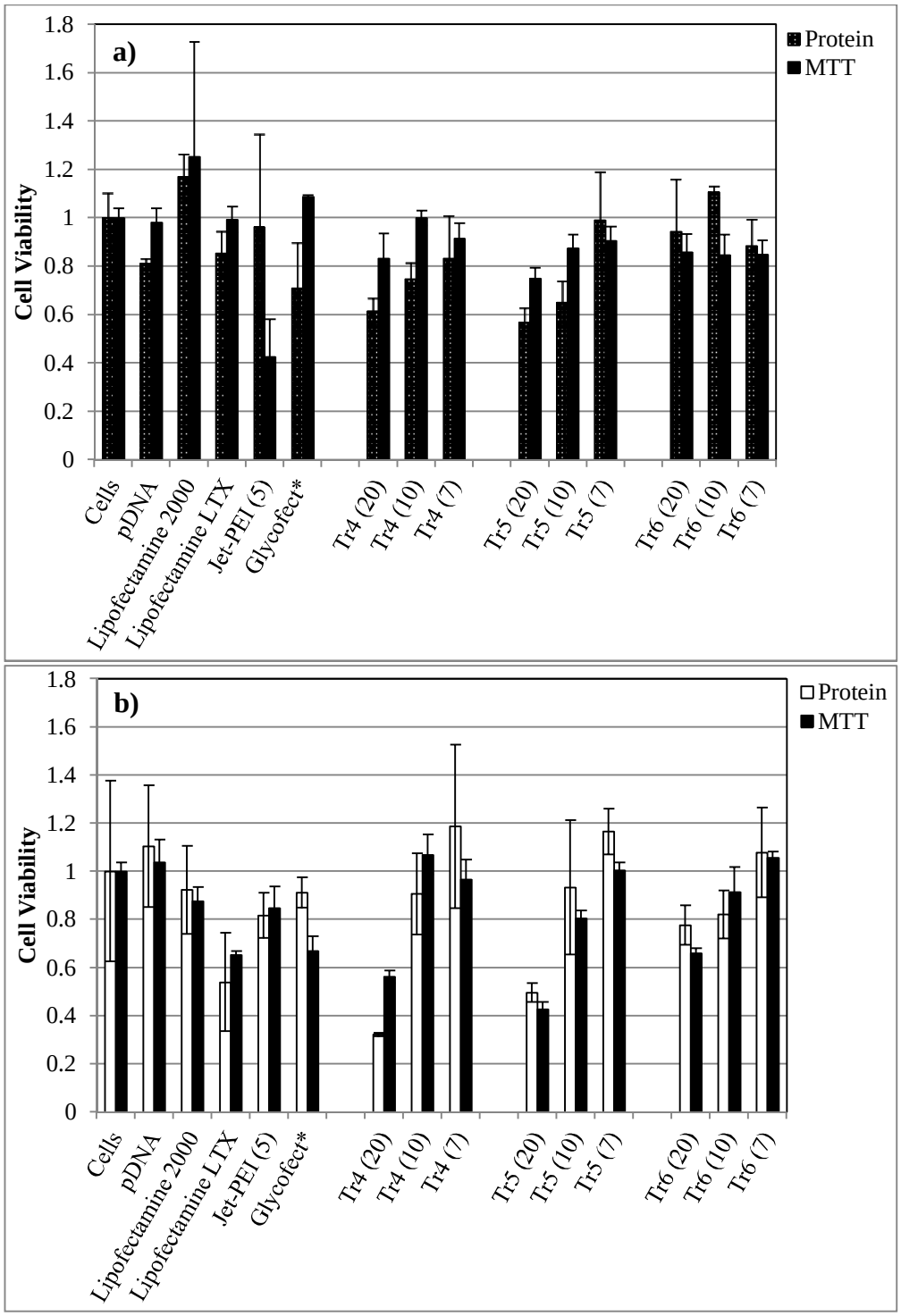

Figure 3-5. MTT and BCA protein assays for **Tr4-Tr6** series. Polyplexes were formed with *p*DNA and **Tr4-Tr6** series at N/P 7, 10, and 20. Positive controls (Lipofectamine™ 2000, Lipofectamine™ LTX, jetPEI™ at N/P 5, and Glycofect™) were formulated with *p*DNA based upon their recommended protocols. The data are reported as the mean ± standard of deviation of three replicates. a) HDFn. b) RMSC. The experiment was performed by Joshua M. Bryson.

To quantify transfection efficiency on a per-cell basis, cells were transfected with a plasmid encoding enhanced green florescent protein (EGFP) under the same conditions used in the cellular assays described above. After 48 h, flow cytometry analysis was performed and reported as the percentage of cells positive for EGFP. In general, **Tr4** showed the greatest GFP transgene expression per cell (**Figure 3-5**) (16% in HDFn and 20% in RMSC) among the series of trehalose polymers. **Tr4** also showed significantly higher gene expression on a per cell basis compared with all of the positive controls. In fact, the only standard that elicited significant gene expression in HDFn cells was Glycofect™ with 12% positive for EGFP expression. In RMSCs, all EGFP expression was quite low; however, the trehalose series showed high transgene expression relative to the other controls. Fluorescence microscopy (**Figure 3-6**) further demonstrates the trends observed in the FACS experiments. We observed detectable numbers of EGFP-positive cells via fluorescence microscopy upon transfection with each of the commercially-available transfection reagents. While this may appear to contradict the FACS results, we believe it is the result of differences in the procedures employed for these two methods, including selection of only live cells for assessment of EGFP expression via FACS. This selectivity is not achievable with the fluorescence microscopy method that we utilized.

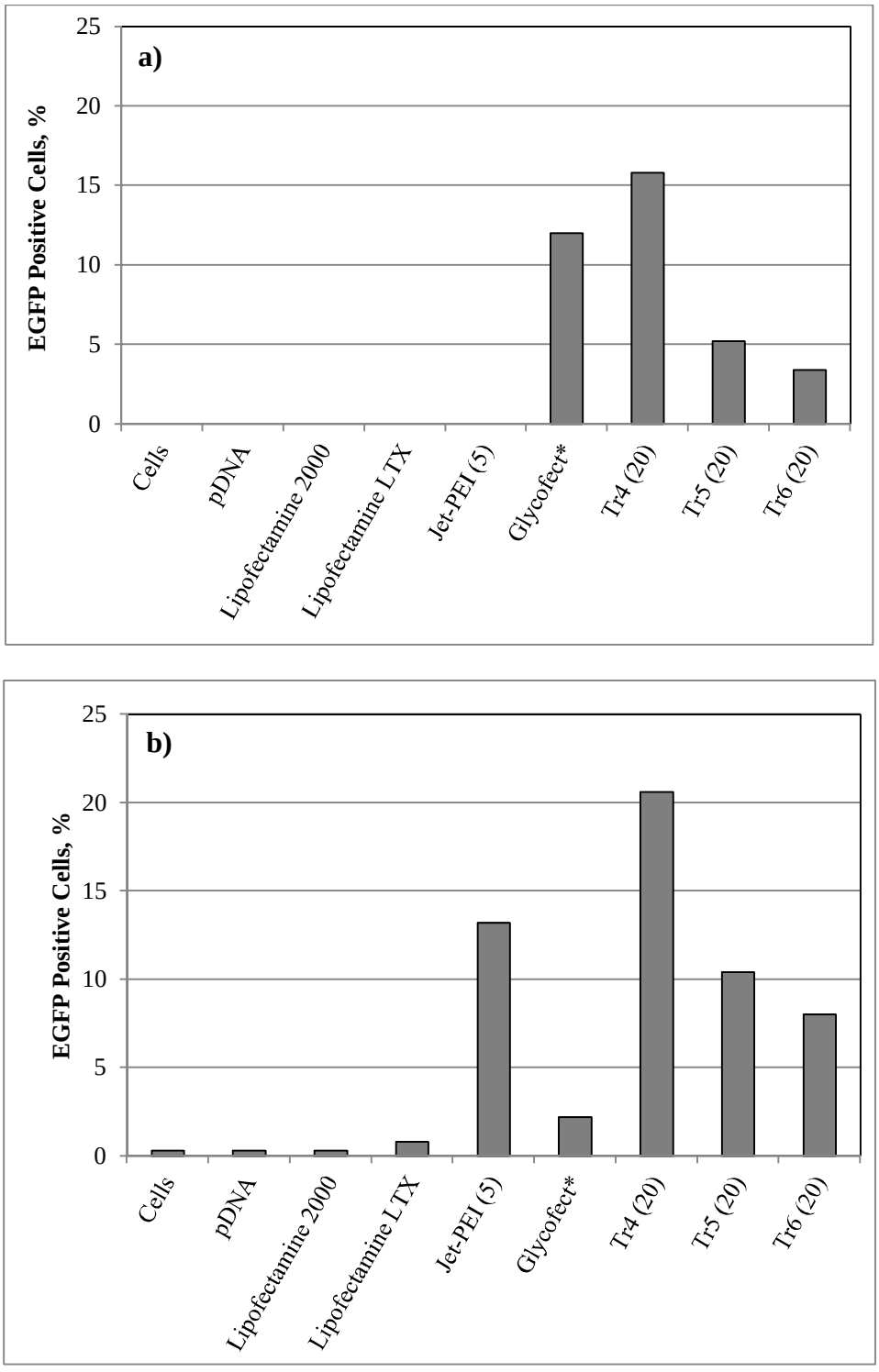

Figure 3-6. EGFP expression observed via flow cytometry with polyplexes formed with *p*DNA and **Tr4-Tr6** series at N/P 20. Positive controls (Lipofectamine™ 2000, Lipofectamine™ LTX, jetPEI™ at N/P 5, and Glycofect™) were formulated with *p*DNA based upon their recommended protocols. The data is shown is % of EGFP positive cells. (a) HDFn. (b) RMSC. The experiment was performed by Joshua M. Bryson.

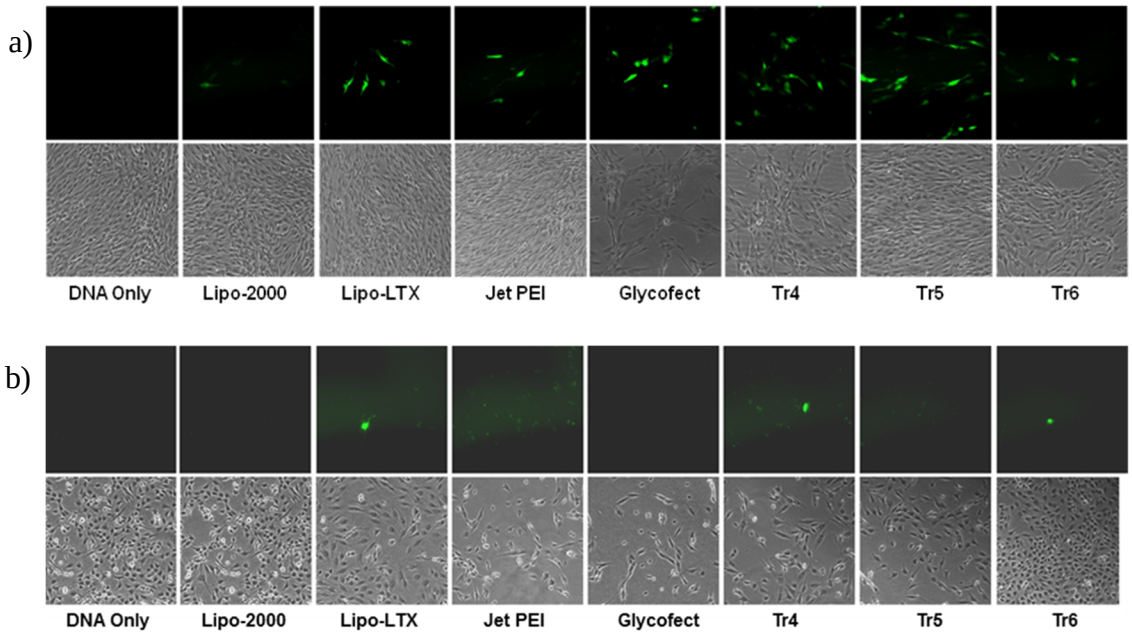

Figure 3-7. EGFP expression observed via fluorescence microscopy with polyplexes formed with *p*DNA and **Tr4-Tr6** series at N/P 20. Positive controls (Lipofectamine™ 2000, Lipofectamine™ LTX, jetPEI™ at N/P 5, and Glycofect™) were formulated with *p*DNA based upon their recommended protocols. a) HDFn. b) RMSC. The experiment was performed by Joshua M. Bryson.

3.5. Conclusions

Ultimately, transfection solutions need to be developed for gene transfer to sensitive cells in robust cell culture environments; such materials would further enable regenerative medical procedures based on *ex vivo* engineered cells. In an attempt to achieve this goal, trehalose-oligoethyleneamine "click" copolymers were designed and synthesized to demonstrate the high binding affinity and delivery efficiency associated with an incorporated short polyethyleneamine (PEI) unit coupled with the biocompatibility and serum stability provided by the trehalose unit. We have demonstrated that higher order trehalose-based polymers, with an increased number of secondary amines (4-6 per repeat unit), show promise for transfection of primary

neonatal human dermal fibroblasts and rat mesenchymal stem cells in conditions requiring the presence of serum. **Tr4** showed the most promising results for delivering *p*DNA and mitigating transgene expression of reporters in these primary cells. Indeed, future therapies may rely on polymers derived from this structure.

3.6. Acknowledgements

The author acknowledges funding of this project provided by NSF and Virginia Tech. We also thank Dr. Mehdi Ashraf-Khorassani for performing LC-ESI-MS for small molecules, as well as Dr. Larry Sallans and Dr. Stephen Macha, both of University of Cincinnati Mass Spectrometry Facility, for valuable discussions in MS analysis of oligoamines. We thank Dr. Jeremy Heidel for reviewing the chapter.

3.7. References

1. Venter, J. C.; Adams, M. D.; Myers, E. W.; Li, P. W.; Mural, R. J.; Sutton, G. G.; Smith, H. O.; Yandell, M.; Evans, C. A.; Holt, R. A., *et al.* The sequence of the human genome. *Science*, **2001,** *291* (5507), 1304-1351.

2. Schaffer, D. V.; Koerber, J. T.; Lim, K.-i. Molecular engineering of viral gene delivery vehicles. *Annual Review of Biomedical Engineering*, **2008,** *10* (1), 169-194.

3. Alvarez-Breckenridge, C.; Kaur, B.; Chiocca, E. A. Pharmacologic and chemical adjuvants in tumor virotherapy. *Chemical Reviews*, **2009,** *109* (7), 3125-3140.

4. Kovtun, A.; Heumann, R.; Epple, M. Calcium phosphate nanoparticles for the transfection of cells. *Bio-Medical Materials & Engineering*, **2009,** *19* (2/3), 241-247.

5. Epple, M.; Ganesan, K.; Heumann, R.; Klesing, J.; Kovtun, A.; Neumann, S.; Sokolova, V. Application of calcium phosphate nanoparticles in biomedicine. *Journal of Materials Chemistry*, **2010,** *20* (1), 18-23.

6. Bhattacharya, S.; Bajaj, A. Advances in gene delivery through molecular design of cationic lipids. *Chemical Communications*, **2009,** *31*, 4632-4656.

7. Rao, N.; Gopal, V. Cell biological and biophysical aspects of lipid-mediated gene delivery. *Bioscience Reports*, **2006,** *26* (4), 301-324.

8. Tros de Ilarduya, C.; Sun, Y.; Düzgünes, N. Gene delivery by lipoplexes and polyplexes. *European Journal of Pharmaceutical Sciences*, **2010,** *40* (3), 159-170.

9. Ortiz Mellet, C.; Benito, J.; García Fernández, J. Preorganized, macromolecular, gene-delivery systems. *Chemistry – A European Journal*, **2010,** *16* (23), 6728-6742.

10. Parekh, H. S. The advance of dendrimers - a versatile targeting platform for gene/drug delivery. *Current Pharmaceutical Design*, **2007,** *13* (27), 2837-2850.

11. Pietersz, G. A.; Choon-Kit, T.; Apostolopoulos, V. Structure and design of polycationic carriers for gene delivery. *Mini Reviews in Medicinal Chemistry*, **2006,** *6* (12), 1285-1298.

12. Mok, H.; Park, T. G. Functional polymers for targeted delivery of nucleic acid drugs. *Macromolecular Bioscience*, **2009,** *9* (8), 731-743.

13. Reineke, T. M. Poly(glycoamidoamine)s: cationic glycopolymers for DNA delivery. *Journal of Polymer Science Part A: Polymer Chemistry*, **2006,** *44* (24), 6895-6908.

14. Davis, M. E.; Pun, S. H.; Bellocq, N. C.; Reineke, T. M.; Popielarski, S. R.; Mishra, S.; Heidel, J. D. Self-assembling nucleic acid delivery vehicles via linear, water-soluble, cyclodextrin-containing polymers. *Curr Med Chem*, **2004,** *11* (2), 179-197.

15. Sizovs, A.; McLendon, P. M.; Srinivasachari, S.; Reineke, T. M. Carbohydrate Polymers for Nonviral Nucleic Acid Delivery. *Topics in Current Chemistry*, **2010**, 1-60.

16. Davis, M. E.; Zuckerman, J. E.; Choi, C. H. J.; Seligson, D.; Tolcher, A.; Alabi, C. A.; Yen, Y.; Heidel, J. D.; Ribas, A. Evidence of RNAi in humans from systemically administered siRNA via targeted nanoparticles. *Nature*, **2010,** *464* (7291), 1067-1070.

17. See protocols for Lipo 2k and LTX.

18. Higano, C. S.; Schellhammer, P. F.; Small, E. J.; Burch, P. A.; Nemunaitis, J.; Yuh, L.; Provost, N.; Frohlich, M. W. Integrated data from 2 randomized, double-blind, placebo-controlled, phase 3 trials of active cellular immunotherapy with sipuleucel-T in advanced prostate cancer. *Cancer*, **2009,** *115* (16), 3670-3679.

19. Lipscomb, M. F.; Masten, B. J. Dendritic cells: immune regulators in health and disease. *Physiol. Rev.*, **2002,** *82* (1), 97-130.

20. Syme, R.; Glück, S. Generation of dendritic cells: role of cytokines and potential clinical applications. *Transfusion and Apheresis Science*, **2001,** *24* (2), 117-124.

21. Fong, L.; Engleman, E. G. Dendritic cells in cancer immunotherapy. *Annual Review of Immunology*, **2000,** *18* (1), 245.

22. McNeish, J. Embryonic stem cells in drug discovery. *Nature Reviews Drug Discovery*, **2004,** *3* (1), 70-80.

23. Charge, S. B. P.; Rudnicki, M. A. Cellular and molecular regulation of muscle regeneration. *Physiol. Rev.*, **2004,** *84* (1), 209-238.

24. Grewal, S. I. S.; Moazed, D. Heterochromatin and epigenetic control of gene expression. *Science*, **2003,** *301* (5634), 798-802.

25. Rafii, S.; Lyden, D. Therapeutic stem and progenitor cell transplantation for organ vascularization and regeneration. *Nature Medicine*, **2003,** *9* (6), 702.

26. Lechler, R.; Ng, W. F.; Steinman, R. M. Dendritic cells in transplantation - friend or foe? *Immunity*, **2001,** *14* (4), 357-368.

27. Wernig, M.; Meissner, A.; Foreman, R.; Brambrink, T.; Manching, K.; Hochedlinger, K.; Bernstein, B. E.; Jaenisch, R. In vitro reprogramming of fibroblasts into a pluripotent ES-cell-like state. *Nature*, **2007,** *448* (7151), 318-324.

28. Prevette, L. E.; Lynch, M. L.; Kizjakina, K.; Reineke, T. M. Correlation of amine number and pDNA binding mechanism for trehalose-based polycations. *Langmuir*, **2008,** *24* (15), 8090-8101.

29. Srinivasachari, S.; Liu, Y.; Prevette, L. E.; Reineke, T. M. Effects of trehalose click polymer length on pDNA complex stability and delivery efficacy. *Biomaterials*, **2007,** *28* (18), 2885-2898.

30. Srinivasachari, S.; Liu, Y.; Zhang, G.; Prevette, L.; Reineke, T. M. Trehalose click polymers inhibit nanoparticle aggregation and promote pDNA delivery in serum. *J Am Chem Soc*, **2006,** *128* (25), 8176-8184.

31. Veale, E. B.; O'Brien, J. E.; McCabe, T.; Gunnlaugsson, T. The synthesis, N-alkylation and epimerisation study of a phthaloyl derived thiazolidine. *Tetrahedron*, **2008,** *64* (28), 6794-6800.

32. Lee, C. C.; Liu, Y.; Reineke, T. M. General structure-activity relationship for poly(glycoamidoamine)s: The effect of amine density on cytotoxicity and DNA delivery efficiency. *Bioconjugate Chem*, **2008,** *19* (2), 428-440.

33. Liu, Y. M.; Reineke, T. M. Hydroxyl stereochemistry and amine number within poly(glycoamidoamine)s affect intracellular DNA delivery. *J Am Chem Soc*, **2005,** *127* (9), 3004-3015.

34. Liu, Y. M.; Reineke, T. M. Poly(glycoamidoamine)s for gene delivery: Stability of polyplexes and efficacy with cardiomyoblast cells. *Bioconjugate Chem*, **2006,** *17* (1), 101-108.

35. Liu, Y. M.; Reineke, T. M. Poly(glycoamidoamine)s for gene delivery. Structural effects on cellular internalization, buffering capacity, and gene expression. *Bioconjugate Chem*, **2007,** *18* (1), 19-30.

36. Liu, Y. M.; Wenning, L.; Lynch, M.; Reineke, T. M. New poly(D-glucaramidoamine)s induce DNA nanoparticle formation and efficient gene delivery into mammalian cells. *J Am Chem Soc*, **2004,** *126* (24), 7422-7423.

37. Liu, Y. M.; Wenning, L.; Lynch, M.; Reineke, T. M. Gene delivery with novel poly(1-tartaramidoamine)s. *Acs Sym Ser*, **2006,** *923*, 217-227.

38. García Fernández, J.; Ortiz Mellet, C.; Jiménez Blanco, J.; Fuentes Mota, J.; Gadelle, A.; Coste-Sarguet, A.; Defaye, J. Isothiocyanates and cyclic thiocarbamates of [alpha], [alpha]'-trehalose, sucrose, and cyclomaltooligosaccharides. *Carbohydrate Research*, **1995,** *268* (1), 57-71.

39. Menger, F. M.; Mbadugha, B. N. A. Gemini surfactants with a disaccharide spacer. *J Am Chem Soc*, **2001,** *123* (5), 875-885.

40. Reineke, T. M.; Davis, M. E. Structural effects of carbohydrate-containing polycations on gene delivery. 1. Carbohydrate size and its distance from charge centers. *Bioconjugate Chem*, **2002,** *14* (1), 247-254.

41. Abdel-Magid, A. F.; Carson, K. G.; Harris, B. D.; Maryanoff, C. A.; Shah, R. D. Reductive amination of aldehydes and ketones with sodium triacetoxyborohydride. Studies on direct and indirect reductive amination procedures. *The Journal of Organic Chemistry*, **1996,** *61* (11), 3849-3862.

42. Qin, A.; Lam, J. W. Y.; Tang, B. Z. Click Polymerization: Progresses, Challenges, and Opportunities. *Macromolecules*, **2010,** *43* (21), 8693-8702.

43. Golas, P. L.; Matyjaszewski, K. Marrying click chemistry with polymerization: expanding the scope of polymeric materials. *Chemical Society Reviews*, **2010,** *39* (4), 1338-1354.

44. Finn, M. G.; Fokin, V. V. Click chemistry: function follows form. *Chemical Society Reviews*, **2010,** *39* (4), 1231-1232.

Chapter 4: Controlled PEGylation of Trehalose-Oligoethyleneamine "Click" Copolymers for Increased Serum Stability and Prolonged Blood Circulation Time

4.1. Abstract

Trehalose-oligoethyleneamine "click" polymers described in **Chapter 3** exhibit *p*DNA binding affinity, transfection efficiency, and *p*DNA uptake and EGFP expression in HDFn and RMS cell lines under serum-containing conditions. These polymers have high promise for regenerative and stem cell based therapies. Among the three investigated structures, **Tr4** appeared to be the most promising candidate – it had the best biological properties and, in addition, the synthesis of **Tr4** was the least complicated. In an effort to achieve even better performance of **Tr4** for nucleic acid delivery, PEGylated analogs of the polymer were synthesized and tested for toxicity and cellular transfection, in both HDFn and RMSC. In addition, **Tr4** was synthesized with a greater degree of polymerization, to see whether the molecular weight affects the transfection profile. The results revealed that the increase in molecular weight of **Tr4** polymer did have significant impact on transfection efficiency as a significant increase in EGFP expression was noticed. The PEGylation of **Tr4** did not significantly change the *in vitro* transfection profiles as compared to the non-PEGylated analogs. However, *in vivo* studies are necessary to evaluate the full biological potential of these materials.

4.2. Introduction

The library of trehalose-oligoethyleneamine "click" polymers[1] is further expanded by designing and synthesizing the PEGylated analogs of **Tr4**. The PEG (5 kDa) moiety was selectively incorporated at both ends of the linear trehalose-containing polycation. With this modification, the resulting structure becomes an A-B-A block copolymer where A (PEG) is a neutral block and does not contribute to the electrostatic binding with negatively charged phosphates of nucleic acids unlike the polycationic B block (**Tr4**) (**Figure 4-1**). We hypothesized that the **Tr4** block bound to the *p*DNA is the core of the polyplex, while PEG is displayed on the outer layer of the particle, therefore partially shielding the positive surface charge and increasing the hydrodynamic radius. This would provide additional protection against aggregation with serum proteins and other undesired interactions with the components of physiological systems. In addition, PEG functionalities can be used in the future as linkers for the incorporation of other functionalities, like targeting ligands, MRI contrast agents, and radiotracers for the development of multifunctional systems for both gene delivery and imaging.[2-4]

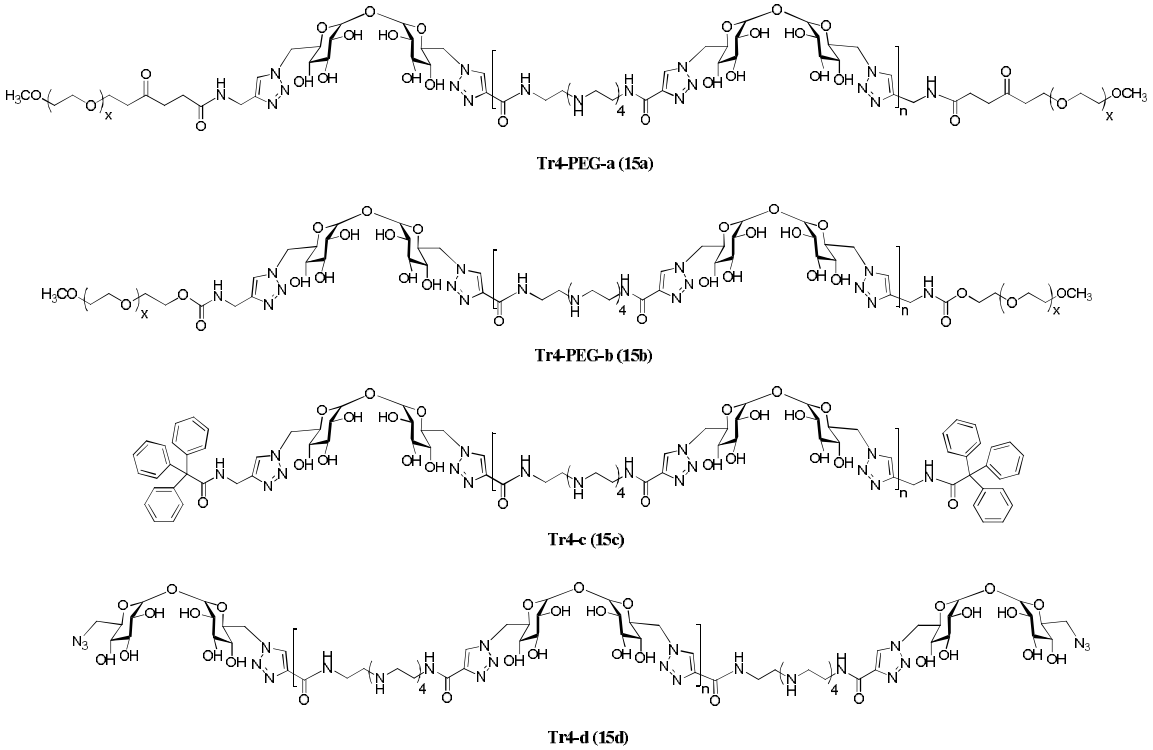

Figure 4-1. Structures of end-capped **Tr4** polymers.

4.3. Experimental Procedures

4.3.1. General. All reagents and solvents used in the synthesis, if not specified otherwise, were obtained from Sigma-Aldrich (St. Louis, MO) or Fisher Scientific Co. (Pittsburgh, PA) and used without further purification. PEGs were obtained from NOF America Corporation. Methanol, dichloromethane, and dimethylformamide were purified with MBRAUN MB SPS solvent purification system. All the reactions were monitored to completion using thin layer chromatography (TLC) with ninhydrin staining for oligoamines and p-anisaldehyde staining for visualizing oligosaccharides along with UV light when possible. Ultrapure water was used in synthesis and dialysis. The dialysis membranes were manufactured by Spectrum Laboratories, Inc. (Rancho Dominguez,

CA). The liquid chromatography-mass spectra (LC-MS) were obtained with an Agilent system with a time-of-flight (TOF) analyzer coupled to a Thermo Electron TSQ-LC/MS ESI mass spectrometer. ^{1}H and ^{13}C-NMR were recorded on a 400MR Varian-400 Hz spectrometer. The ^{1}H-NMR data are reported as follows: chemical shift (δ ppm), multiplicity, J coupling constant (Hz), and peak integration. Either $CHCl_3$ (7.27 ppm) or HOD (4.79 ppm) were used as an internal reference.

Cell culture media and supplements were obtained from Gibco/Invitrogen (Carlsbad, CA). JetPEI solution was purchased from Polyplus Transfection™ (New York, NY). RMSC and HDFn cells were purchased from Invitrogen (Carlsbad, CA).

4.3.2. Synthesis of end-groups for Tr4a-Tr4d polymers. *mPEG-CO-CH_2CH_2-CO-NH-CH_2C≡CH (***12a***)*. To a solution of *m*PEG-NHS (**11a**) (1.00 g) in 7 mL of chloroform, propargylamine (0.30 g) dissolved in 3 mL of chloroform was added. The resulting mixture was stirred at room temperature for 44 h. After that, solvent was evaporated and a the yellowish oily residue was redissolved in methanol (10 mL), transported to a 1000 MWCO membrane and dialyzed against methanol (1 L) for 24 h (water changes: 3 × 1 L; at 2, 5, and 22 h). The dialyzed compound was concentrated and the resulting oily residue was precipitated by adding cold diethyl ether (5 mL). The white amorphous precipitate was filtered and dried under vacuum to yield solid alkyne-terminated *methoxy*-PEG **12a**. Yield: 0.80 g (80%). ^{1}H-NMR ($CDCl_3$): δ = 2.20 (t, J = 2.6 Hz, 1H, C≡*CH*), 2.46 (t, J = 6.8 Hz, 2H), 2.67 (t, J = 6.8 Hz, 2H), 3.34 (s, 3H, O*CH_3*), 3.43 (m, 4H,), 3.61 (m, 364H, O–*CH_2CH_2*–O), 3.78 (m, 4H), 4.00 (dd, J = 2.6, 5.3, 2H), 4.21 (m, 2H).

*mPEG-O-CO-NH-CH_2C≡CH (***12b***).* The compound was synthesized as described in the procedure above for **11b**, except 0.50 g of *m*PEG-NHS **12a** (dissolved in 5 mL of chloroform) and 0.06 g of propargylamine was used and the reaction was stopped at 24 h. Yield: 0.40 g (80%). ^{1}H-NMR ($CDCl_3$): δ = 2.24 (t, J = 2.5 Hz, 1H, C≡*CH*), 3.38 (s, 3H, O*CH_3*), 3.46 (m, 4H), 3.64 (m, 364H, O–*CH_2CH_2*–O), 3.82 (m, 4H), 3.96 (m, 2H), 4.24 (m, 2H).

*2,2,2-Triphenyl-N-(prop-2-yn-1-yl)acetamide (***14***).* A solution of 2,2,2-triphenylacetic acid (5.00 g, 17.3 mmol) in anhydrous dichloromethane (20 mL) was cooled to 0 °C. The solution of DCC in 20 mL of anhydrous dichloromethane was added dropwise and the reaction mixture was stirred at 0 °C for 1 h. Then propargylamine (0.87 g, 15.7 mmol) solution in 10 mL of anhydrous methylene chloride was added to the reaction mixture and it was stirred for an additional hour at 0 °C, then at room temperature overnight. The insoluble white precipitate that formed in the course of the reaction was filtered and the filtrate evaporated to yield a slightly off-white solid, which was subjected to flash chromatography (ethyl acetate/hexane:1/1). The fraction with the R_f = 0.4 was isolated to obtain the title product, 2,2,2-triphenyl-N-(prop-2-yn-1-yl)acetamide (**14**). Yield: 2.81 g (50%). ^{1}H-NMR ($CDCl_3$): δ = 2.18 (t, J = 2.6 Hz, 1H, C≡*CH*), 4.12 (dd, J = 2.6, 5.3, 2H, NH*CH_2*), 5.94 (bs, 1H, NH), 7.21-7.36 (m, 15H, arom.). ^{13}C-NMR ($CDCl_3$): δ = 29.97, 67.62, 71.53, 71.93, 127.05, 127.48, 127.89, 128.33, 130.44, 130.85, 143.21, 173.25. LC-ESI-MS (*m/z*): Theoretical $(M+H)^+$ $C_{23}H_{20}NO$ = 326.15; Found = 326.04. Theoretical $(M+NH_4)^+$ $C_{23}H_{23}N_2O$ = 343.18; Found = 343.06.

3.3.3. Synthesis of Tr4-PEGa, Tr4-PEGb, Tr4-c, and Tr4-d Polymers.

General procedure for the polymerization. The diazido trehalose monomer **3**, the equivalent molar amount of alkyne terminated oligoethyleneamine **9**, and *tert*-butanol were mixed in a 10 mL vial and cooled to 0 ºC. To the cooled, stirred reaction mixture, 1 M copper sulfate (0.2 eq) and 1 M sodium ascorbate (0.4 eq) aqueous solutions were added, after which water was added to a 1/1 (v/v) total ratio of *tert*-butanol/water (the concentration of each of the monomers should be about 5_{wt}% in the mixture). The mixture was heated to 50 ºC and vigorously stirred at that temperature for 1 h. Then additional 0.2 eq of trehalose monomer **3** was added to the mixture to end-cap the formed polymer product, and it was stirred for 1 h at the same temperature. The reaction was terminated by cooling the heterogeneous mixture with an ice bath. After cooling, the reaction mixture separated into a viscous yellow oily layer and a blue aqueous supernatant. The copper-containing supernatant was removed and the remaining viscous oily residue was dissolved in 1 mL of DMSO and precipitated by adding 4 M NH_4OH (2 mL) solution. Precipitates were recovered via centrifugation, after which a fresh portion of 4 M NH_4OH solution was added to the precipitant and the centrifugation was repeated. This cycle was repeated until no blue color was visually detectable in the NH_4OH supernatant, indicating that copper (II) was removed from the "click" polymer product. The off-white precipitate was washed with water (2 × 2 mL) in a similar manner described for NH_4OH and the resulting precipitates dried *in vacuo* and carried to the deprotection steps.

*General Procedure for the End-Capping of **Tr4**.* The batch of the fully protected **Tr4** polymer from the previous step was separated in 4 parts: A, B, C, and D. Parts A and

be were further functionalized with PEG groups resulting in the protected polymers **15a** and **15b**, part C was end-capped with the 2,2,2-triphenyl-N-(prop-2-yn-1-yl)acetamide (**14**) and resulted in protected **15c**. Part D was carried on to the deprotection steps without further modifications.

*General Procedure for the PEGylation of **Tr4***. Parts A and B were each mixed with the corresponding PEG agent (**Tr4**:PEG/100:25 wt.%) and *tert*-butanol/water mixture following the same procedure as described for the polymerization of the **Tr4** polymer. Copper(II) sulfate (1 M, 0.3 eq) and sodium ascorbate (1 M, 0.6 eq) were added to the reaction mixture and it was stirred overnight at 70 °C. After the completion of the reaction the product was isolated the same way as described in the procedure for the polymerization of **Tr4**. The solid product was redissolved in methanol, transported to a 1000 MWCO membrane and dialyzed against methanol (1 L) for 12 h (methanol was changed after 6 h). A small amount of **Tr4** (part C) was also end-capped with the triphenylacetamide **14** in a similar manner to yield protected **15c**.

General Procedure for the Deprotection of Acetyl and Boc. The deprotection of the acetyl and Boc groups was achieved by the same method as described in **Chapter 3**.

Tr4-PEG-a. *mPEG-Tr4-mPEG (**15a**).* Yield: 120 mg, (53%). ^{1}H-NMR (D_2O): δ = 2.94-3.08 (m, 14H), 3.23 (t, 2H), 3.45-3.60 (m, 6H), 3.74 (s, 3H), 3.81 (t, 2H), 4.16 (t, 2H), proton signals overlapping with HOD peak, 8.41 and 8.44 (2 s, 2H).

Tr4-PEG-b. *mPEG-Tr4-mPEG (**15b**).* Yield: 98 mg, (46%). ^{1}H-NMR (D_2O): δ = 2.79-2.93 (m, 14H), 3.08 (t, 2H), 3.32-3.60 (m, 6H), 3.74 (s, 3H), 3.81 (t, 2H), 4.16 (t, 2H), proton signals overlapping with HOD peak, 8.41 and 8.44 (2 s, 2H).

Tr4-c. *Tr4 terminated with triphenylacetamides***.** ***(*****15c*****)***. Yield: 19 mg, (48%). ^{1}H-NMR (D_2O): δ = 2.94-3.08 (m, 14H), 3.23 (t, 2H), 3.45-3.60 (m, 6H), 3.74 (s, 3H), 3.82 (t, 2H), 4.18 (t, 2H), proton signals overlapping with HOD peak, 8.44 and 8.47 (2 s, 2H).

Tr4-d. *Tr4 terminated with trehalose azide***.** ***(*****15d*****)***. Yield: 97 mg, (63%). ^{1}H-NMR (D_2O): δ = 2.87-3.00 (m, 14H), 3.23 (t, 2H), 3.44-3.61 (m, 8H), 3.82 (t, 2H), 4.16 (t, 2H), proton signals overlapping with HOD peak, 8.44 (s, 2H).

4.3.4. Polymer and Polyplex Characterization. *GPC, gel electrophoresis shift assays, DLS and zeta potential measurements, luciferase and Lowry assay, MTT assay, GFP analysis via flow cytometry, GFP analysis via microscopy.* The procedures for these experiments were performed as described in **Chapter 3** of this dissertation.

4.4. Results and Discussion

Polymer Synthesis and Characterization. The 5 kDa NHS-activated mPEG molecules **11a** and **11b** were functionalized with alkyne end-group by reaction with an excess of propargylamine, therefore preparing the "click" chemistry-ready conjugation site (**Scheme 4-1**). To remove the excess of propargylamine, the products were dialyzed against methanol, resulting in a slight loss of material and reducing the yield to 80%. The molecular weight of the compounds was analyzed with GPC and MALDI (**Figure 4-2 and Table 4-1**). GPC analysis also proved the absence of mPEG showing just one peak on a chromatogram (corresponding to **15a** or **15b** respectively), thus indicating that all residual mPEG was removed from the reaction mixture via dialysis. PEGylated **Tr4** polymer **15a** contains an amide bond, another polymer **15b** – a less stable carbamate bond between the PEG and **Tr4** moieties. Different linkages between the PEG and **Tr4** blocks were chosen to see whether this slight modification would have any impact on

biological properties of the polymers. In addition, non-PEGylated **Tr4** (**15d**), is end-capped with trehalose functionality, and a small amount of this material was further end-capped with the triphenylacetamide group to yield **15c** for number average molecular weight determination using ^{1}H-NMR by comparing the integration of phenyl groups with any individual sugar peak or a triazole peak integration. The synthesis of the triphenylacetamide end-group is shown in **Scheme 4-2**.

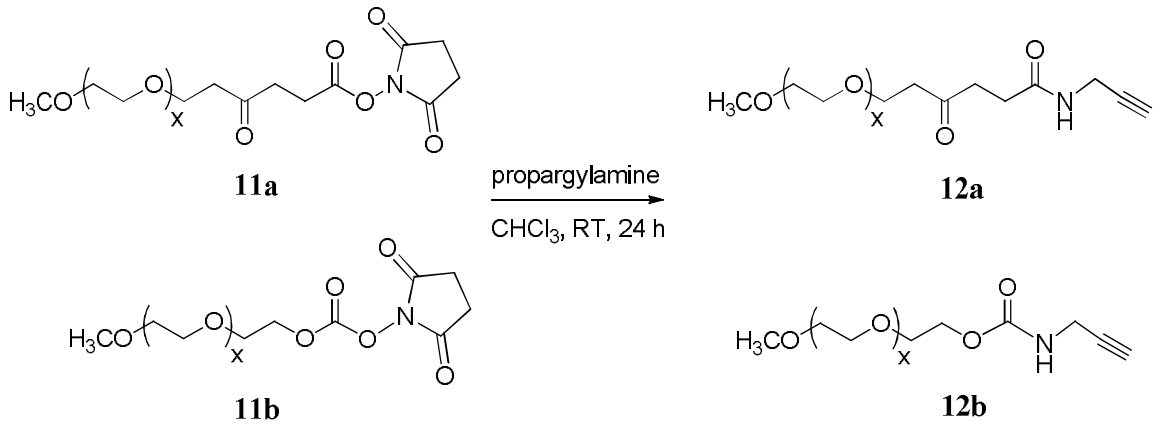

11a **12a** **11b** **12b**

Scheme 4-1. Synthesis of PEGs for end-capping of **Tr4** to yield **15a** and **15b**.

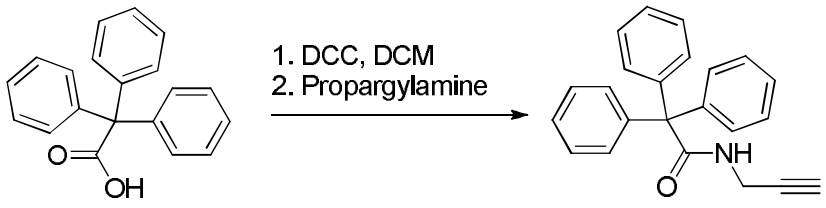

13 **14**

Scheme 4-2. Synthesis of triphenyl-N-(propargyl)acetamide for end-capping of **15d** to yield **15c**.

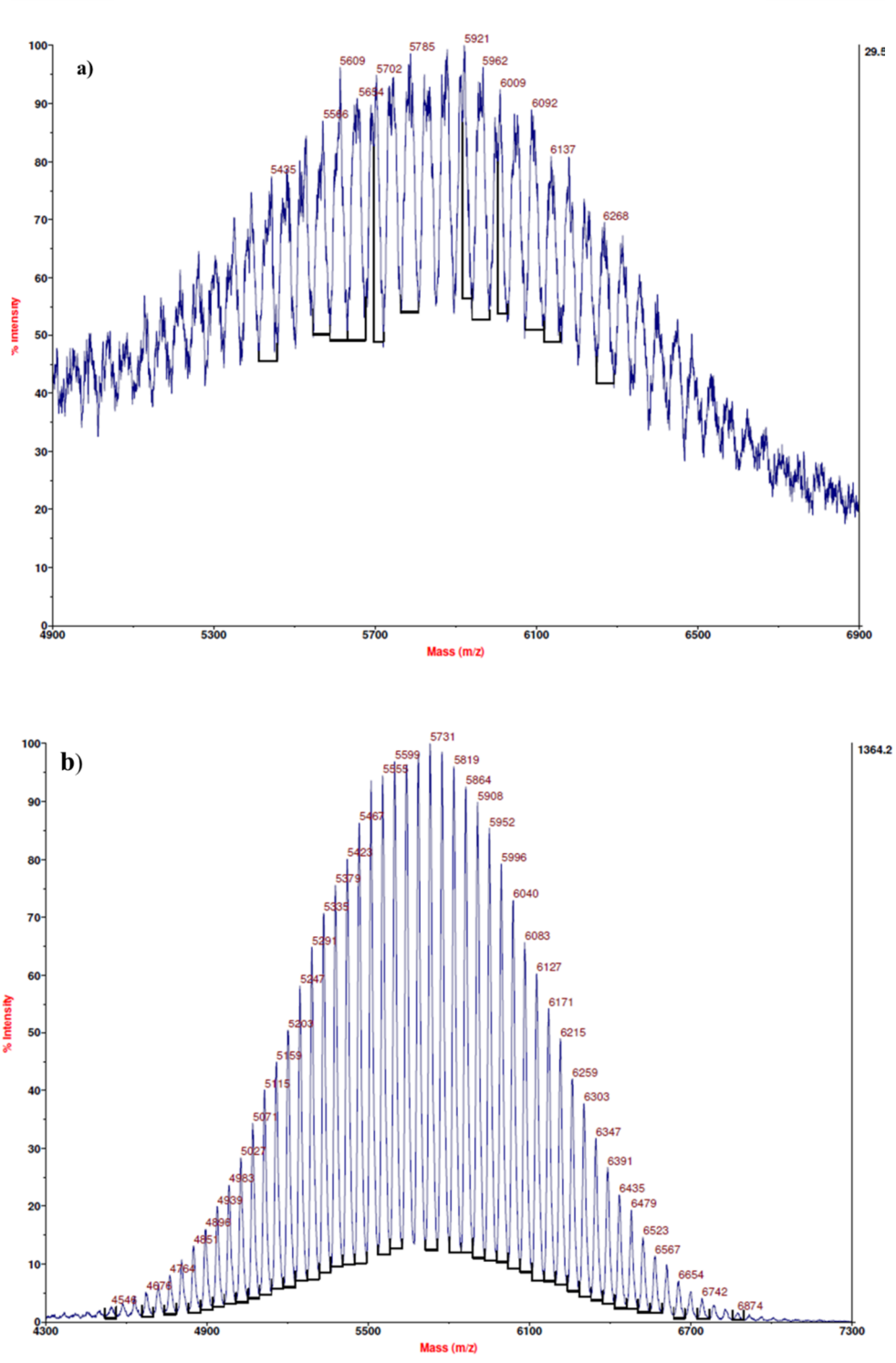

Figure 4-2. MALDI of the PEG-alkynes. a) **12a** (MW = 5921 Da). b) **12b** (MW = 5731 Da).

GPC analysis of the final polymers (**15a-15d**) revealed the molecular weight of the polymers and therefore the loading of the PEG functionality per polymer molecule was calculated. These results are summarized in **Table 4-1**. The PEGylated **Tr4** polymers each contained about 10_{wt}% of the incorporated PEG functionality, and all the materials were based on **Tr4** with the degree of polymerization of 100. The measured polydispersities are common for step-growth polymerization.

Table 4-1. The molecular weights, polydispersity (M_w/M_n), percentage of PEG loading in **Tr4a-Tr4d** polymers, and degree of polymerization of the **Tr4** block measured by GPC. (The molecular weight of PEG in **15a** and **15b** was rounded to 5 kDa. Polymers **15c** and **15d** have no PEG in their structures.)

Polymer	M_w, kDa	M_n, kDa	M_w/M_n (Tr4-PEG)	$\%_w$Tr4	$\%_w$PEG	$\%_n$Tr4	$\%_n$PEG	DP_w (Tr4)	DP_n (Tr4)
15a	103.6	58.3	1.78	90%	10%	83%	17%	128	66
15b	95.7	81.6	1.17	90%	10%	88%	12%	118	98
15c	77.8	64.7	1.20	100%	0%	100%	0%	107	89
15d	72.1	65.4	1.10	100%	0%	100%	0%	99	90

Polymer-*p*DNA Binding, Particle Size, and Zeta Potential. The PEGylation of the **Tr4** did not affect both the polymer-*p*DNA binding affinity (**Figure 4-3**) and the particle size that was measured by DLS (**Figure 4-4**).

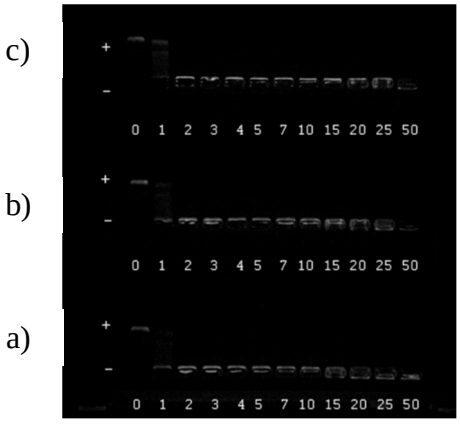

Figure 4-3. The agarose gel binding for the **15a-15c** polymers. a) **15a**. b) **15b**. c) **15c**.

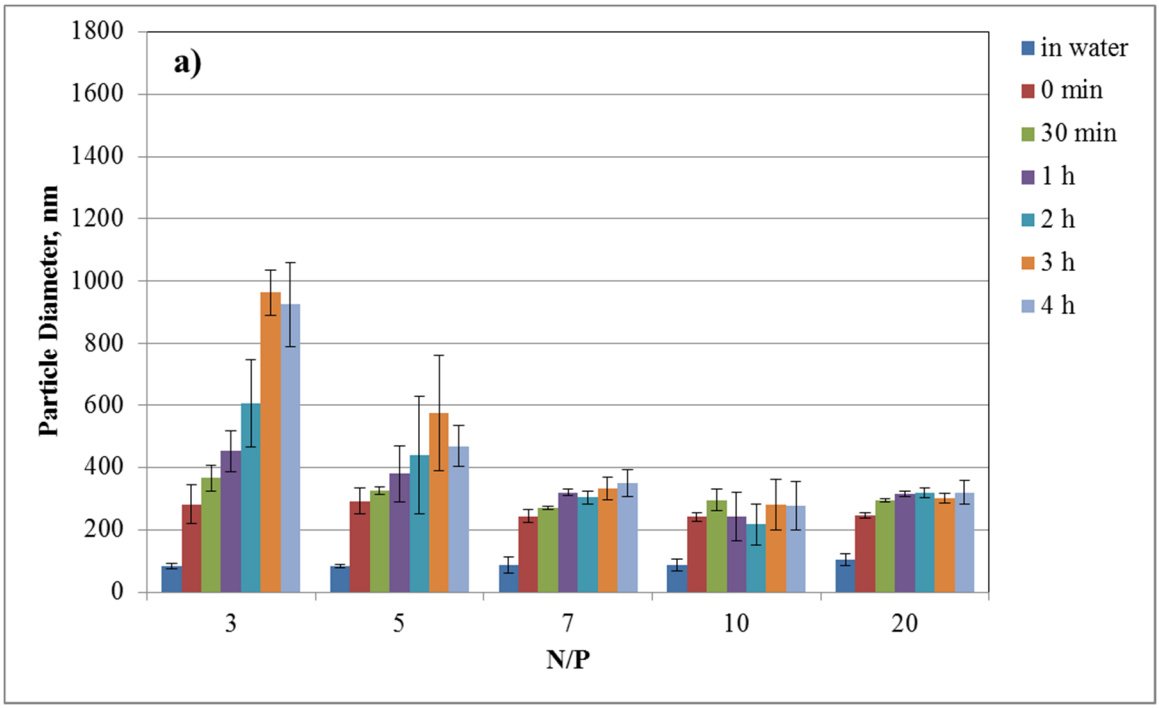
a)
Particle Diameter, nm
1800
1600
1400
1200
1000
800
600
400
200
0
3
5
7
10
20
N/P
in water
0 min
30 min
1 h
2 h
3 h
4 h

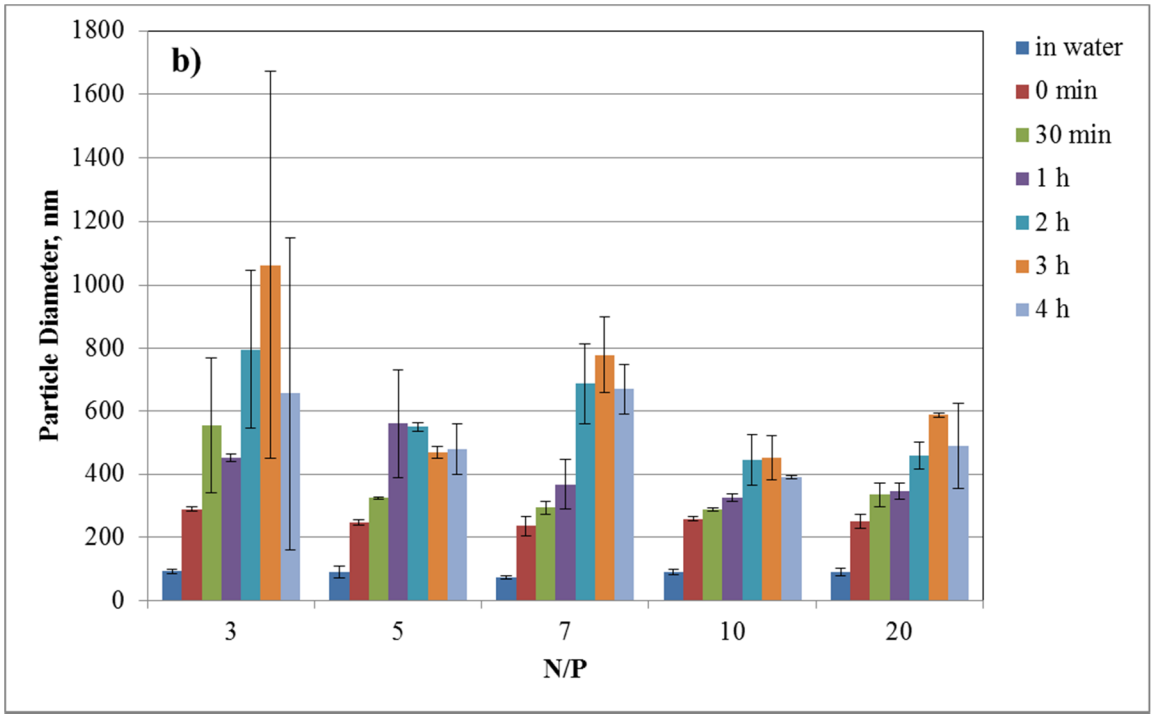
b)
Particle Diameter, nm
1800
1600
1400
1200
1000
800
600
400
200
0
3
5
7
10
20
N/P
in water
0 min
30 min
1 h
2 h
3 h
4 h

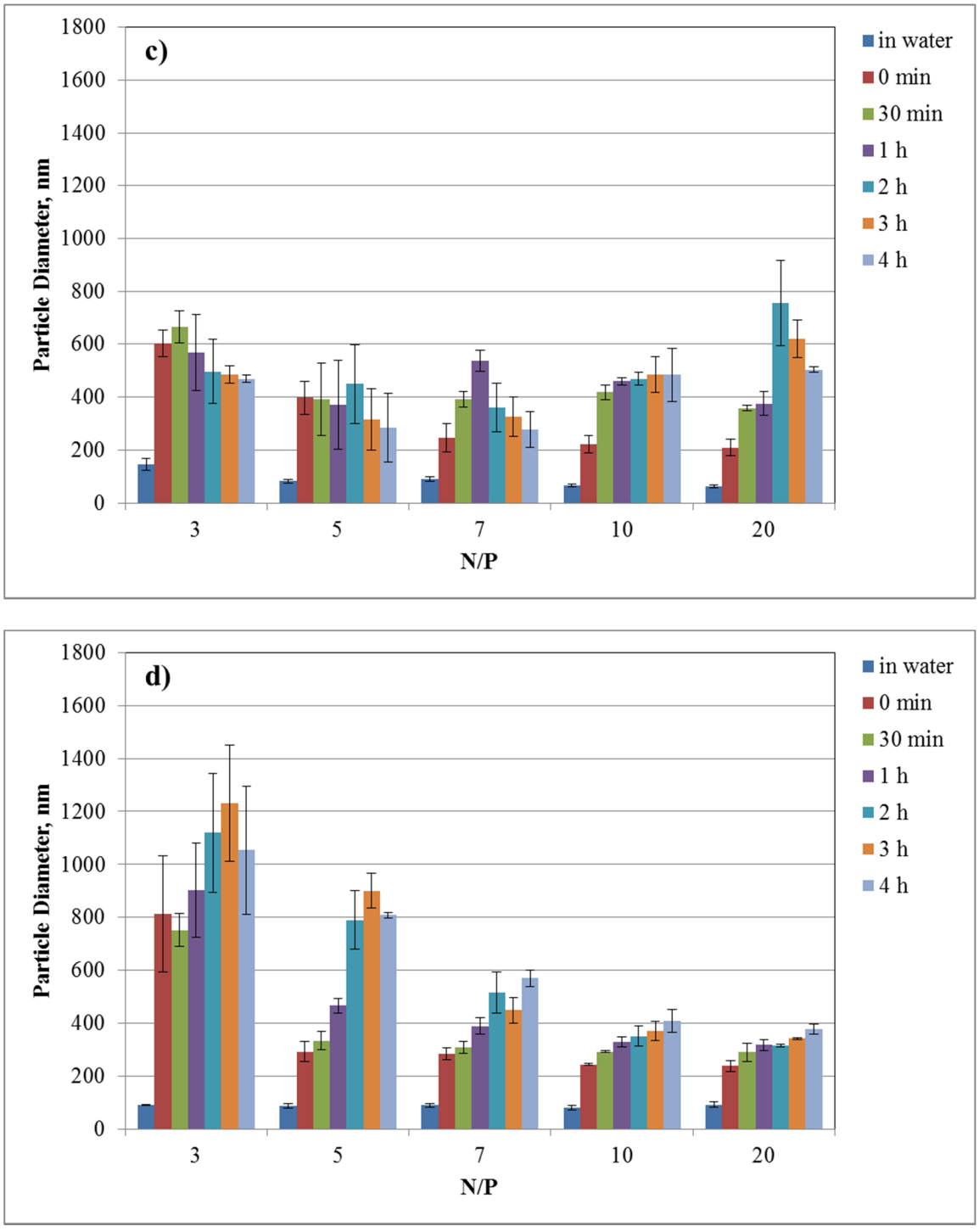

Figure 4-4. Particle size in water and serum containing media for corresponding polyplex formulations at N/P 3, 5, 7, 10, and 20. Polyplexes were incubated at RT for 45 min prior to dilution with water (followed by immediate DLS measurements) or with DMEM (followed by DLS measurements in time intervals from 0 min after dilution to 4 h). a) **15a**. b) **15b**. c) **15c**. d) **15d**.

Cellular Delivery and Toxicity Studies.

Transfection efficiency and cytotoxicity were measured in two therapeutically-relevant cell types — implantable cells used in regenerative therapies, human dermal fibroblasts (HDFn), and progenitor-type cells, rat mesenchymal stem cells (RMSC). Transfection efficiency was determined with both luciferase reporter gene expression assays, EGFP detection via flow cytometry, and fluorescence microscopy. Cellular toxicity was measured via MTT and protein assays. All cell culture experiments were performed in the same manner as described in **Chapter 3**. Results revealed that in the HDFn cell line, transfection (gene expression) was noticed only at N/P ratio of 20 without causing toxicity effect. In RMSC all three tested N/P ratios (7, 10, and 20) exhibited good transfection efficiency; however a slightly higher toxicity profile (cell survival 60%) was noticed (**Figure 4-5** and **Figure 4-6**). No visible difference on transfection efficiency was seen in PEGylated vs. non-PEGylated polymers. However, significant increase in EGFP expression in rat mesenchymal stem cells was noticed in flowcytometry experiments with **15a-15d** polymers with comparing to **Tr4-Tr6** series discussed in **Chapter 3** (**Figure 4-7**). This could be explained with the increase in molecular weight of the Tr4 polymer (DP around 30 in **Tr4-Tr6** series vs. DP around 100 in **15a-15d** analogs). EGFP expression was also observed in RMSC via fluorescence microscopy with polyplexes formed with *p*DNA. Note that the differences in the procedures employed for these two methods, including selection of only live cells for assessment of EGFP expression via FACS result in slightly contradicting results.

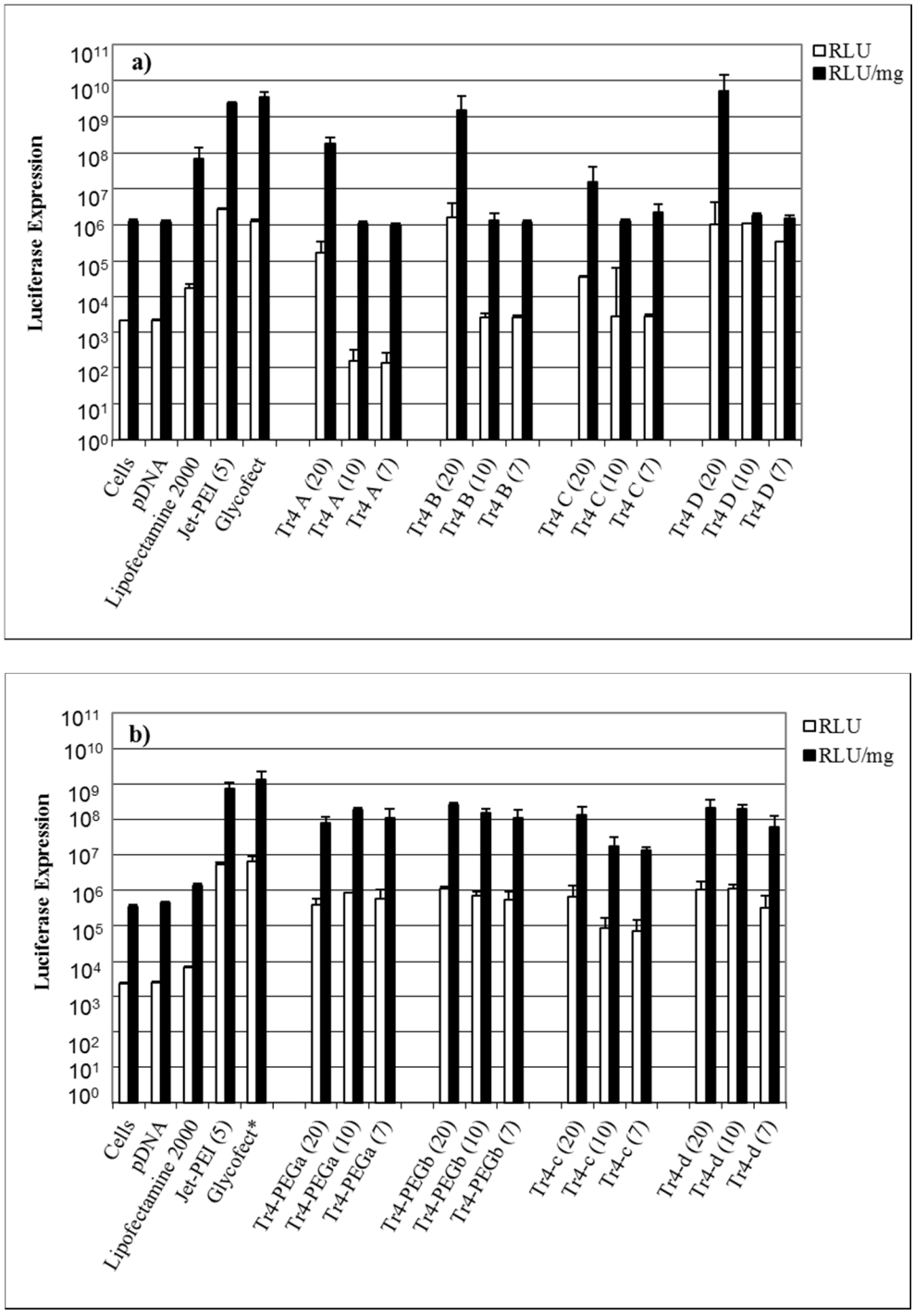

Figure 4-5. Luciferase assays for **Tr4a-Tr4d** (**15a-15d**) series. Polyplexes were formed with *p*DNA and **Tr4a-Tr4d** series at N/P 7, 10, and 20. Positive controls (Lipofectamine™ 2000, Lipofectamine™ LTX, jetPEI™ at N/P 5, and Glycofect™) were formulated with *p*DNA based upon their recommended protocols. The data are reported as the mean ± standard of deviation of three replicates. a) HDFn. b) RMSC. The experiment was performed by Giovanna Grandinetti.

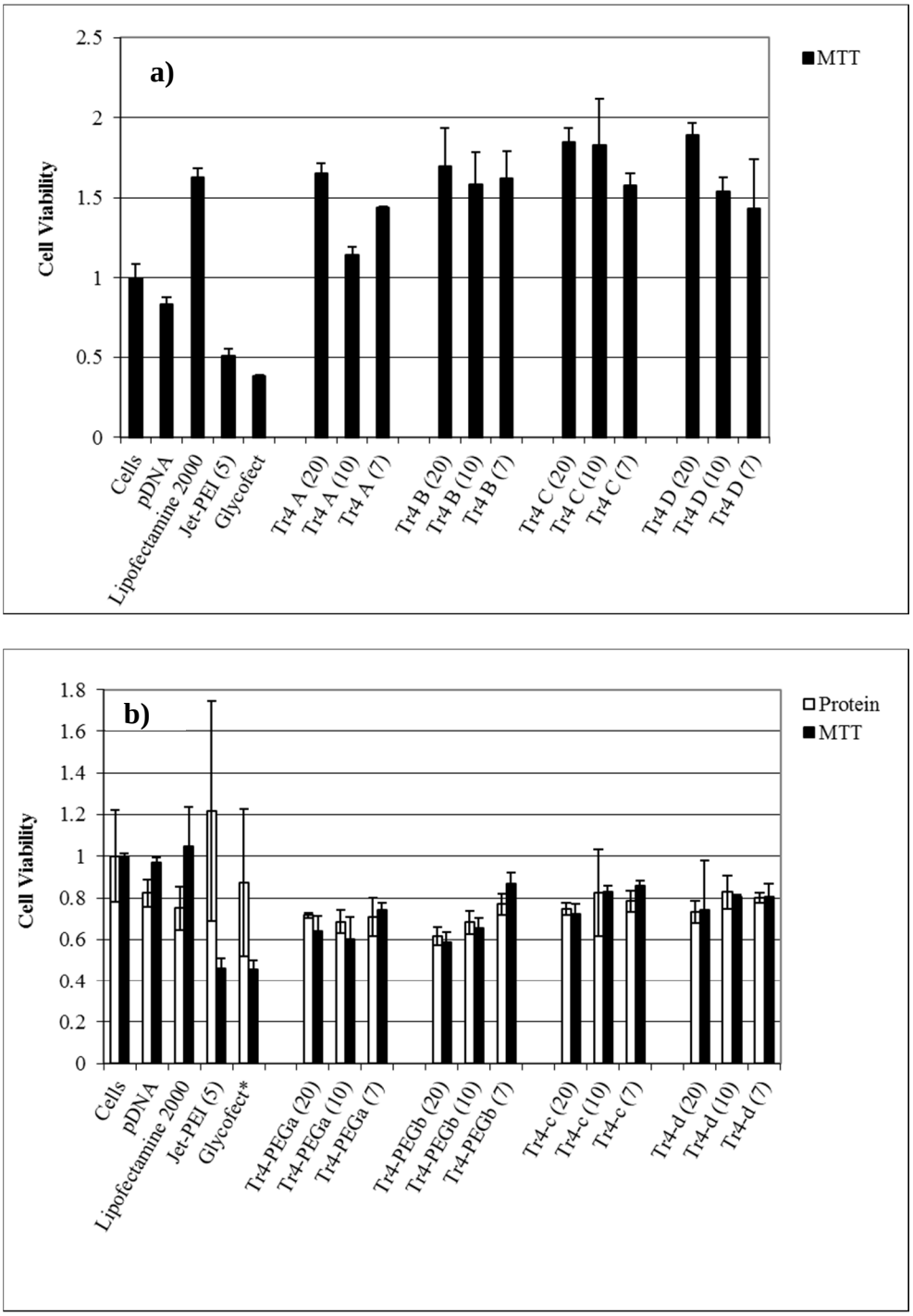

Figure 4-6. MTT and BCA protein assays for **Tr4a-Tr4d** (**15a-15d**) series. Polyplexes were formed with *p*DNA and **Tr4a-Tr4d** series at N/P 7, 10, and 20. Positive controls (Lipofectamine™ 2000, Lipofectamine™ LTX, jetPEI™ at N/P 5, and Glycofect™) were formulated with *p*DNA based upon their recommended protocols. The data are reported as the mean ± standard of deviation of three replicates. a) HDFn. b) RMSC. The experiment was performed by Giovanna Grandinetti.

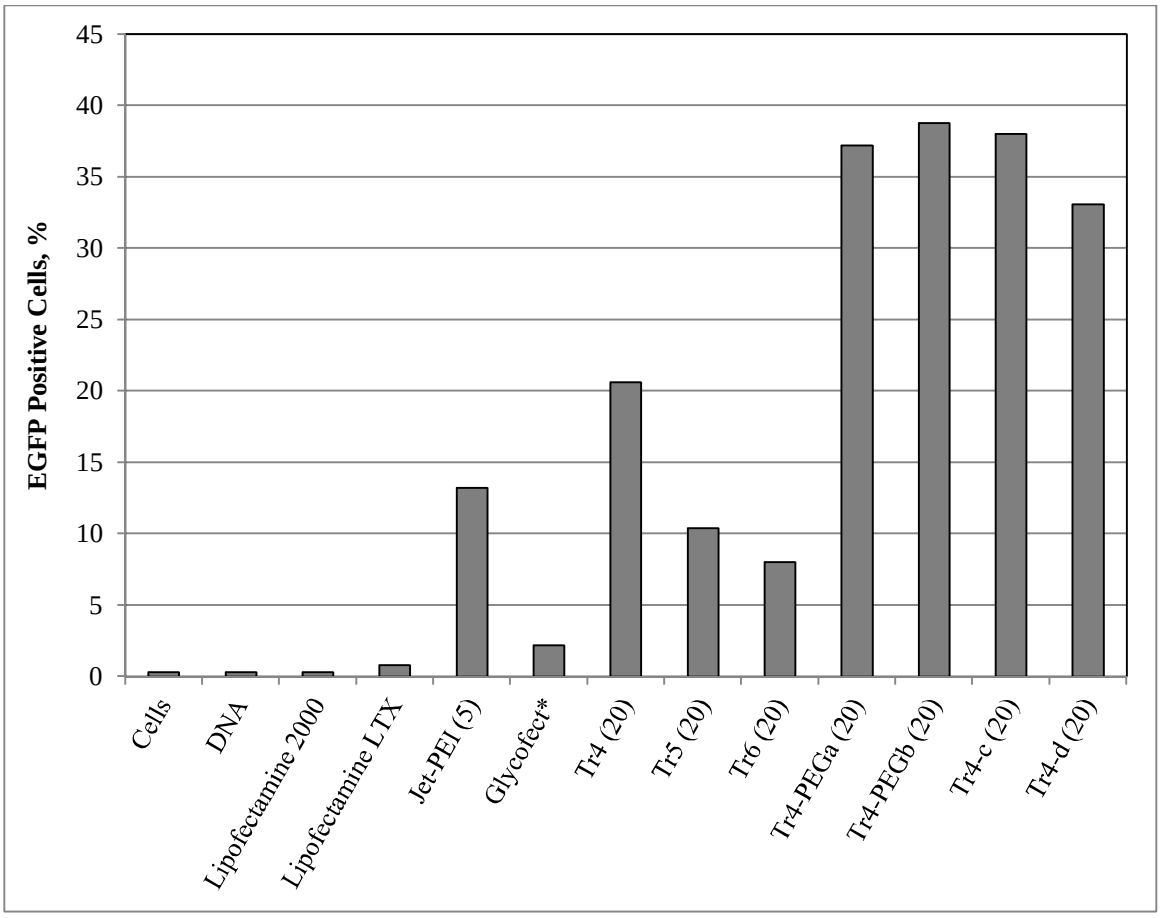

Figure 4-7. EGFP expression in RMSC observed via flow cytometry with polyplexes formed with *p*DNA and **Tr4a-Tr4d** (**15a-15d**) series at N/P 20. Results are compared with **Tr4-Tr5** EGFP expression (**Figure 3-5b**). Positive controls (Lipofectamine™ 2000, Lipofectamine™ LTX, jetPEI™ at N/P 5, and Glycofect™) were formulated with *p*DNA based upon their recommended protocols. The data is shown is % of EGFP positive cells. The experiment was performed by Joshua M. Bryson and Giovanna Grandinetti.

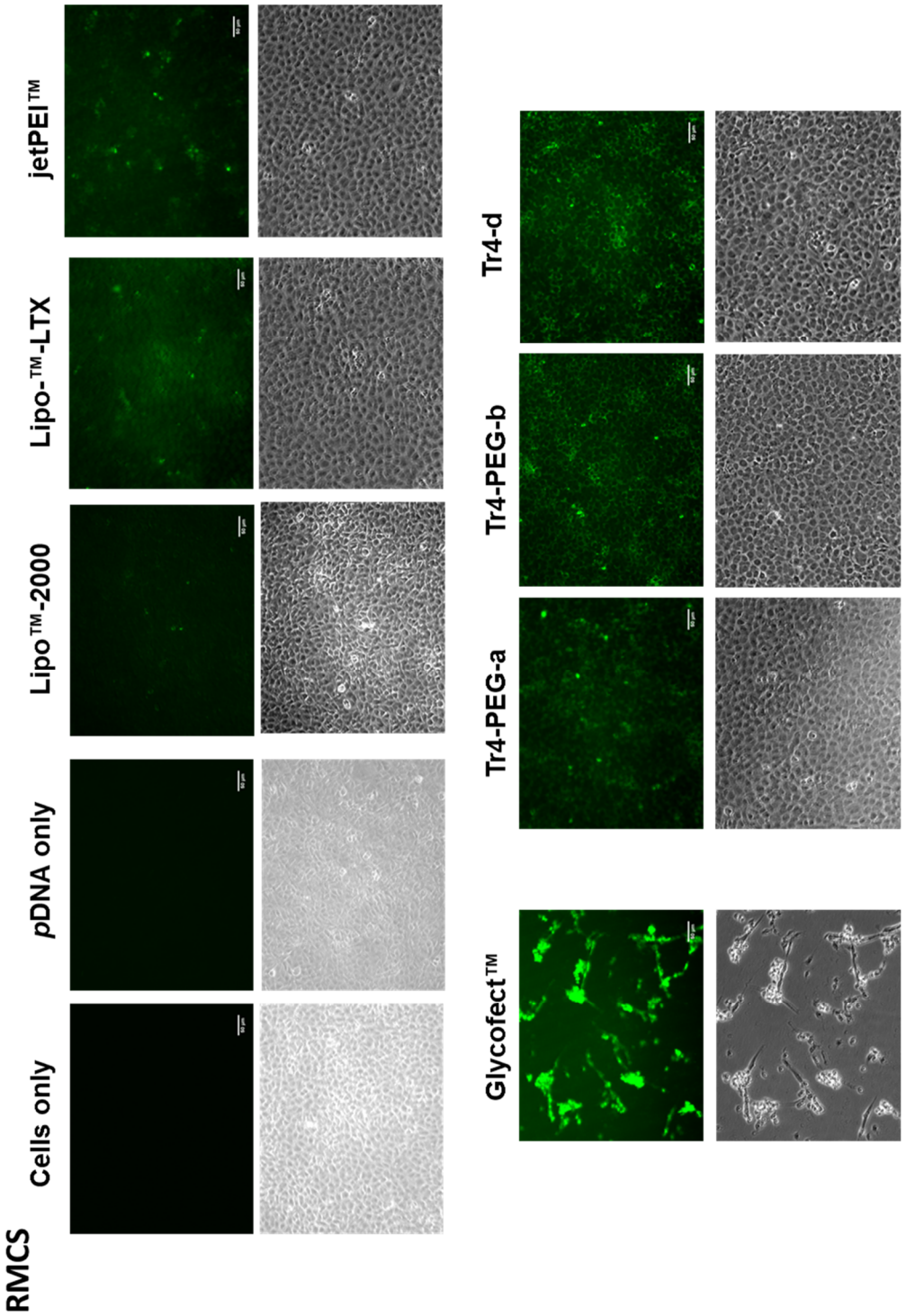

Figure 4-8. EGFP expression observed in RMSC via fluorescence microscopy with polyplexes formed with *p*DNA and **15a, 15b, and 15d** series at N/P 20. Positive controls (Lipofectamine™ 2000, Lipofectamine™ LTX, jetPEI™ at N/P 5, and Glycofect™) were formulated with *p*DNA based upon their recommended protocols. Scale bar is 50 µm. The experiment was performed by Giovanna Grandinetti.

4.5. Conclusions

In vitro characterizations of PEGylated and unmodified **Tr4** and *p*DNA complexes provided only limited conclusions about the effect of PEGylation on *in vivo* transfection. Although, there is no significant difference in transfection profiles within this series of modified **Tr4** polymers, there is a possibility that PEGylated and non-PEGylated trehalose-polycations can have different cellular internalization and intracellular trafficking mechanisms. In support of this hypothesis, similar cases were discussed in the literature before.[5] Further experiments need to be performed in order to better examine the effect of PEGylation of trehalose-oligoethyleneamine "click" polymers. However, the results of the *in vitro* characterizations described here, suggest that both modified and unmodified **Tr4** polymers have a great promise for stem-cell based and regenerative therapies. In addition, PEG-functionality can be further modified to yield polyplexes, with incorporated targeting ligands, MRI agents, or radiotracers toward the development of multifunctional "smart" vehicles for successful gene delivery treatment and diagnostic applications.

4.6. Acknowledgements

The authors would like to acknowledge Giovanna Grandinetti and Dr. Joshua M. Bryson for performing cell culture experiments. The work was supported by the NSF and Virginia Tech funding.

4.7. References

1. *Chapter 3 of this thesis.*

2. Davis, M. E. The First Targeted Delivery of siRNA in Humans via a Self-Assembling, Cyclodextrin Polymer-Based Nanoparticle: From Concept to Clinic. *Molecular Pharmaceutics*, **2009,** *6* (3), 659-668.

3. Kojima, H.; Mukai, Y.; Yoshikawa, M.; Kamei, K.; Yoshikawa, T.; Morita, M.; Inubushi, T.; Yamamoto, T. A.; Yoshioka, Y.; Okada, N., *et al.* Simple PEG Conjugation of SPIO via an Au−S Bond Improves Its Tumor Targeting Potency as a Novel MR Tumor Imaging Agent. *Bioconjugate Chem*, **2010,** *21* (6), 1026-1031.

4. Jiang, Y.-Y.; Liu, C.; Hong, M.-H.; Zhu, S.-J.; Pei, Y.-Y. Tumor Cell Targeting of Transferrin−PEG−TNF-α Conjugate via a Receptor-Mediated Delivery System: Design, Synthesis, and Biological Evaluation. *Bioconjugate Chem*, **2006,** *18* (1), 41-49.

5. Mishra, S.; Webster, P.; Davis, M. E. PEGylation significantly affects cellular uptake and intracellular trafficking of non-viral gene delivery particles. *European Journal of Cell Biology*, **2004,** *83* (3), 97-111.

Chapter 5: Suggested Future Work: Degradable Maltose-Oligoethyleneimine "Click" Copolymers for Nucleic Acid Delivery

5.1. Introduction

Polycation-based gene delivery research in the Reineke group is oriented towards the discovery and development of a high performance vector for the delivery of therapeutic nucleic acids. To achieve this goal a series of glycopolymers were designed and synthesized (**Figure 2-10**, **Chapter 2**). The structure-property relationships are being established by studying the effects of the variation of several parameters in the polymer structures, namely, stereochemistry and molecular weight of the carbohydrate moiety, the number of secondary amines, and degree of polymerization of a polymer on a bioactivity. In addition, dendritic structures are being compared to polymers.[1] Among the investigated materials by the Reineke group thus far, the trehalose-oligoethyleneamine "click" polymers have high potential for *in vivo* applications. They are relatively non-toxic, have satisfactory cellular uptake and transfection efficiency, can help prevent polyplexes from aggregating in serum, and can be easily modified with other functionalities selectively at the polymer ends, allowing incorporation of imaging agents, PEG groups, and targeting agents for targeted delivery and diagnostics. Enzymatic degradation of trehalose is mentioned in **Chapter 2**; however, trehalose polymers do not easily degrade in aqueous media (pH 5.5 and 7.4 for 24 h) (**Appendix B**). By substituting the trehalose moiety with maltose, we can investigate how the disaccharide affects both

the delivery and toxicity profile. Maltose differs from trehalose in that it is linked via a α,α-1,4 glycosidic bond (**Figure 5-1**), which affords a degradable linkage. In addition, because of such a difference in stereochemistry, maltose is prone to degradation in acidic conditions, which potentially would yield biodegradable analogs of trehalose "click" polymers. This project has been started and will be continued in the future with a colleague, Sneha Kelkar, a current PhD student in the Reineke group. The efforts toward the synthesis of these new materials, and preliminary characterizations are described.

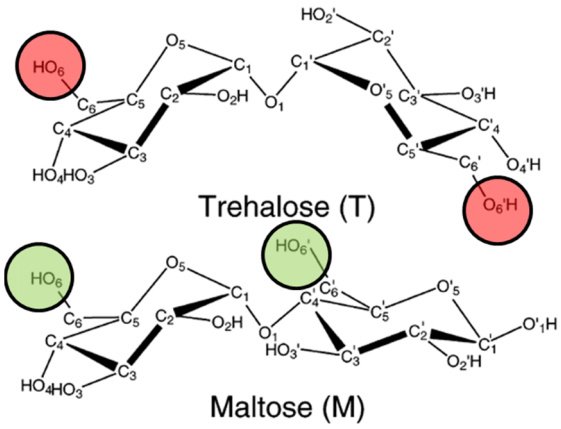

.
Figure 5-1. The stereochemistry of trehalose vs. maltose. Figure adapted with permission from Ref.[2] Copyright © 2005 American Chemical Society.

5.2. Experimental Procedures and Preliminary Results

Since **Tr4** polymer exhibited the best biological properties among the series of trehalose "click" polymers, for preliminary studies we have chosen to prepare its maltose analog containing four secondary amines. The synthesis of **Malt4** polymer is described in **Scheme 5-1**. The oligoamine monomer **9** was synthesized following the procedure described in **Chapter 3**. The maltose monomer **16** was synthesized in a one-pot reaction

from maltose following the previously published procedure.[3] The 1D and 2D NMR spectra of **16** are included in **Appendix A**.

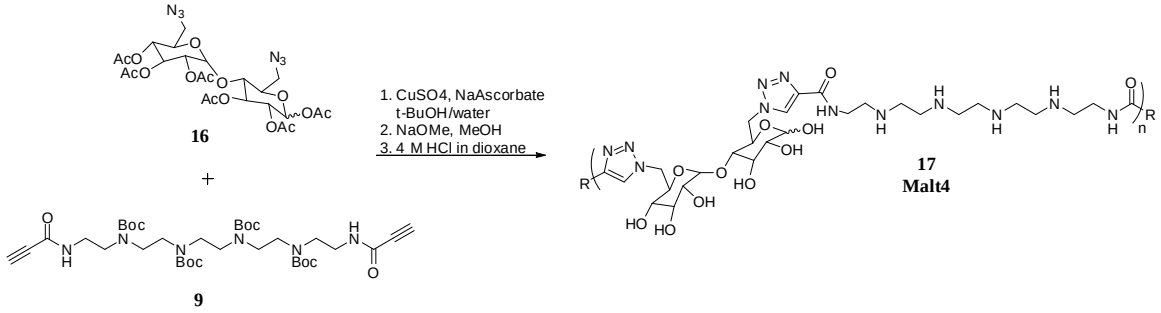

Scheme 5-1. The synthesis of **Malt4** polymer. Conditions: **16**:**9** – 1 eq:1 eq; copper(II) sulfate:sodium ascorbate – 0.2 eq:0.4 eq; 60 °C; 16 h. Yield: 13%.

Due to the high susceptibility of maltose to acidic hydrolysis (and methanolysis), the deprotection step should be carried out very carefully (in nitrogen and acid free atmosphere), to avoid the degradation of the polymer. The development of GPC conditions for MW characterizations is still in progress.

The preliminary *p*DNA-**Malt4** agarose gel binding experiments revealed a drastic difference in comparison to **Tr4**. Unlike trehalose polymers that usually already inhibit the electrophoretic mobility of polymer-pDNA nanoparticle at N/P (nitrogen to phosphate) ratio of 2 (**Figure 3-2**, **Chapter 3**), the maltose polymer showed the binding between N/P 10-15 (**Figure 5-2**).

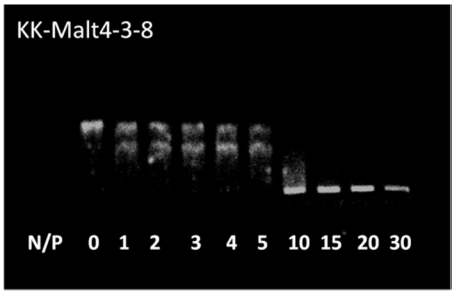

Figure 5-2. Agarose gel binding for **Malt4**.

To understand the possible degradation mechanism of a maltose "click" polymer, a small-molecular model compound needs to be synthesized and the process of degradation can be studied via ^{1}H-NMR experiments. The proposed, partially completed synthesis of the model compound is shown in **Scheme 5-2**.

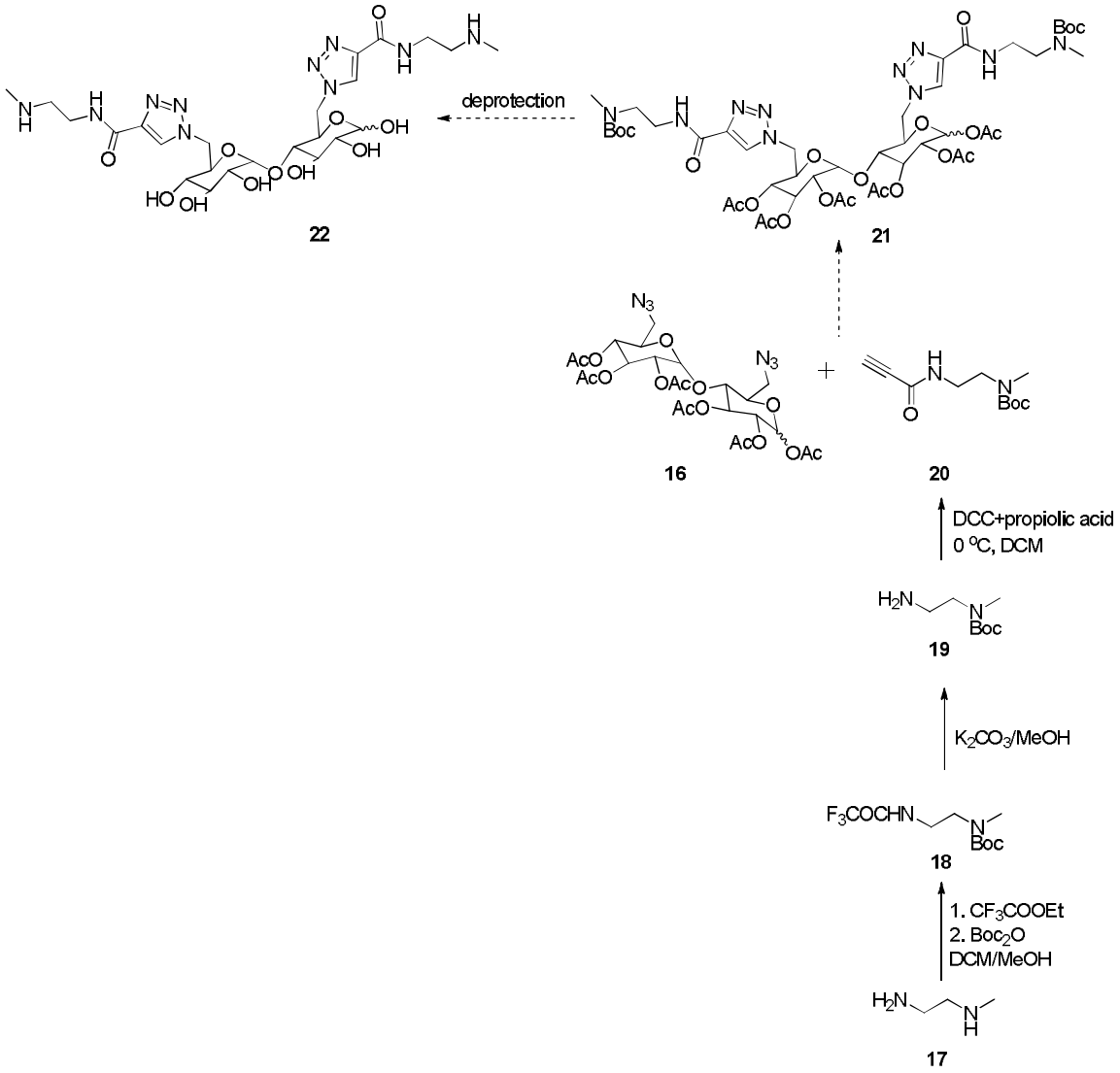

Scheme 5-2. The proposed and partially completed synthesis of the maltose model structure for the degradation studies.

The understanding of the kinetics of the degradation of the proposed maltose-containing model will yield a better insight into the conditions of the synthesis of the

polymers, and their degradation in aqueous media (of various pH levels) can be studied by GPC. In addition, biological characterizations of these polymers could be performed and compared with trehalose analogs.

5.3. References

1. Srinivasachari, S.; Fichter, K. M.; Reineke, T. M. Polycationic β-Cyclodextrin "Click Clusters": Monodisperse and Versatile Scaffolds for Nucleic Acid Delivery. *J Am Chem Soc,* **2008,** *130* (14), 4618-4627.

2. Lerbret, A.; Bordat, P.; Affouard, F.; Descamps, M.; Migliardo, F. How Homogeneous Are the Trehalose, Maltose, and Sucrose Water Solutions? An Insight from Molecular Dynamics Simulations. *The Journal of Physical Chemistry B,* **2005,** *109* (21), 11046-11057.

3. Gouin, S. G.; Kovensky, J. Direct azidation of unprotected carbohydrates with PPh3/CBr4/NaN3. Modulation of the degree of substitution. *Tetrahedron Letters,* **2007,** *48* (16), 2875-2879.

Appendix A: Important NMR and Mass Spectra

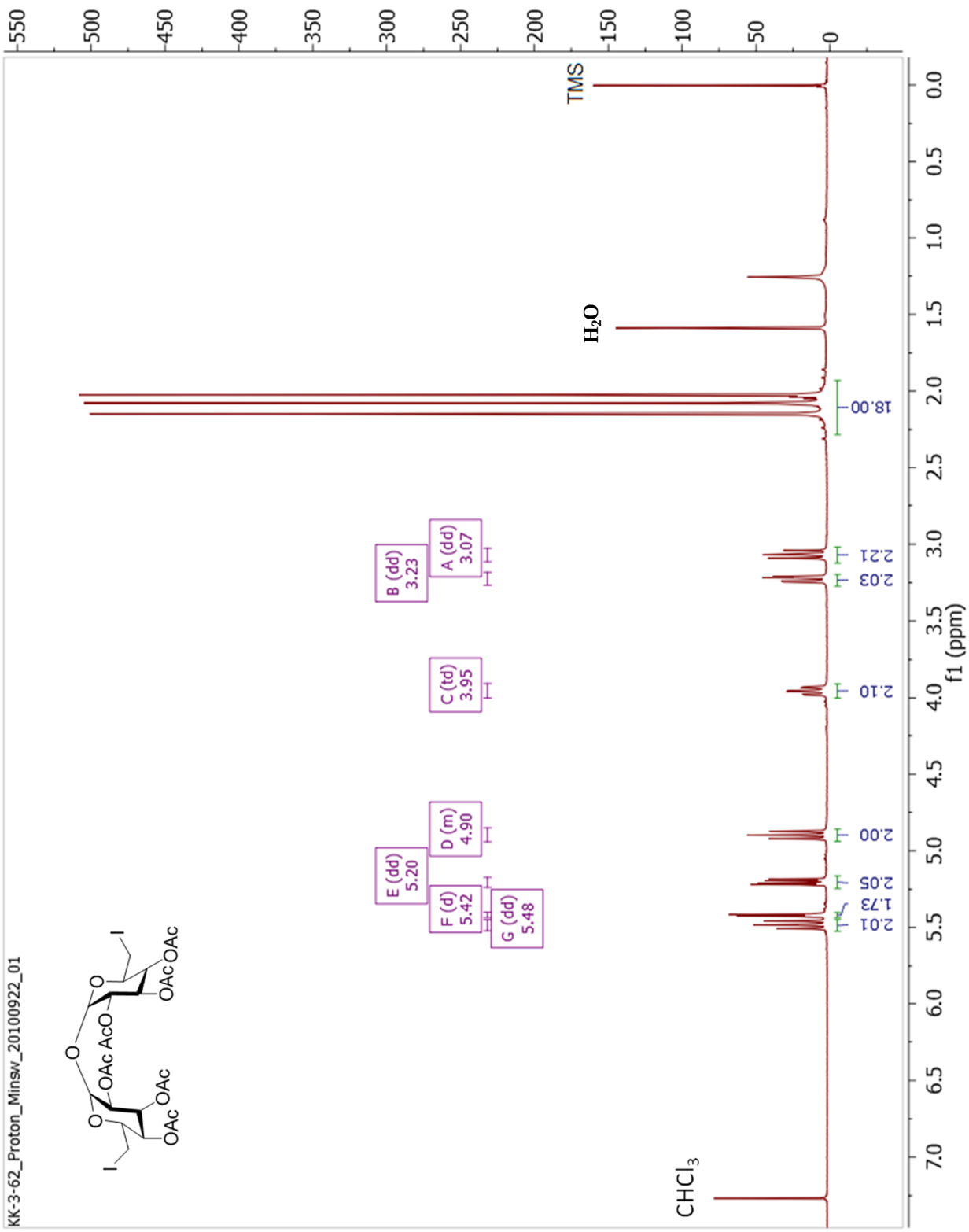
KK-3-62_Proton_Minsw_20100922_01
TMS
H_2O
$CHCl_3$
A (dd) 3.07
B (dd) 3.23
C (td) 3.95
D (m) 4.90
E (dd) 5.20
F (d) 5.42
G (dd) 5.48
18.00
2.21
2.03
2.10
2.00
2.05
1.73
2.01
f1 (ppm)

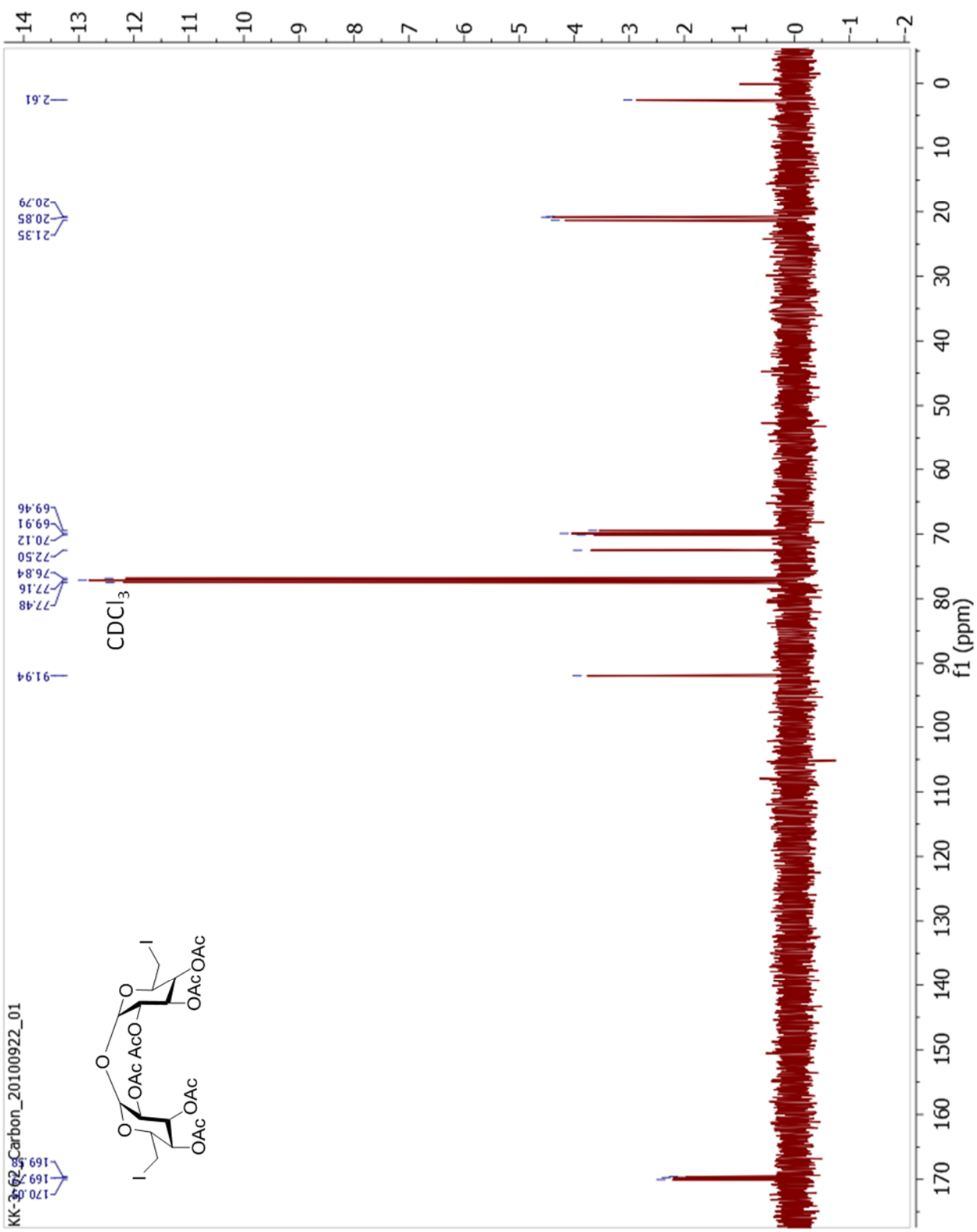
KK-3-62_Carbon_20100922_01
CDCl3
f1 (ppm)
OAc
AcO
I

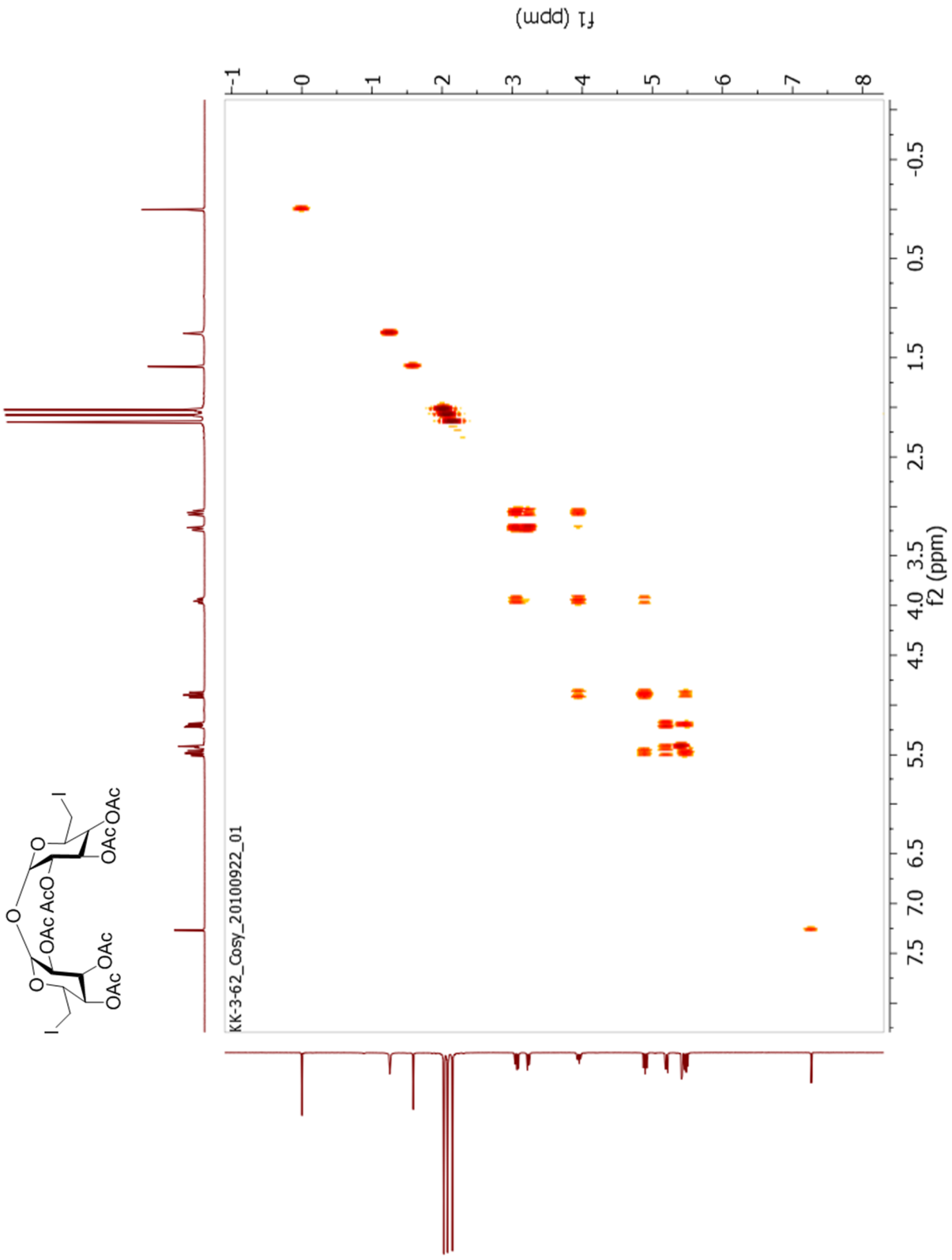
f1 (ppm)
-1
0
1
2
3
4
5
6
7
8
KK-3-62_Cosy_20100922_01
7.5
7.0
6.5
5.5
4.5
4.0
3.5
2.5
1.5
0.5
-0.5
f2 (ppm)
O
OAc
AcO
OAc
OAc
OAc
OAc
I
I

KK-3-62_Cosy_20100922_01
f1 (ppm)
f2 (ppm)
OAc
AcO
I

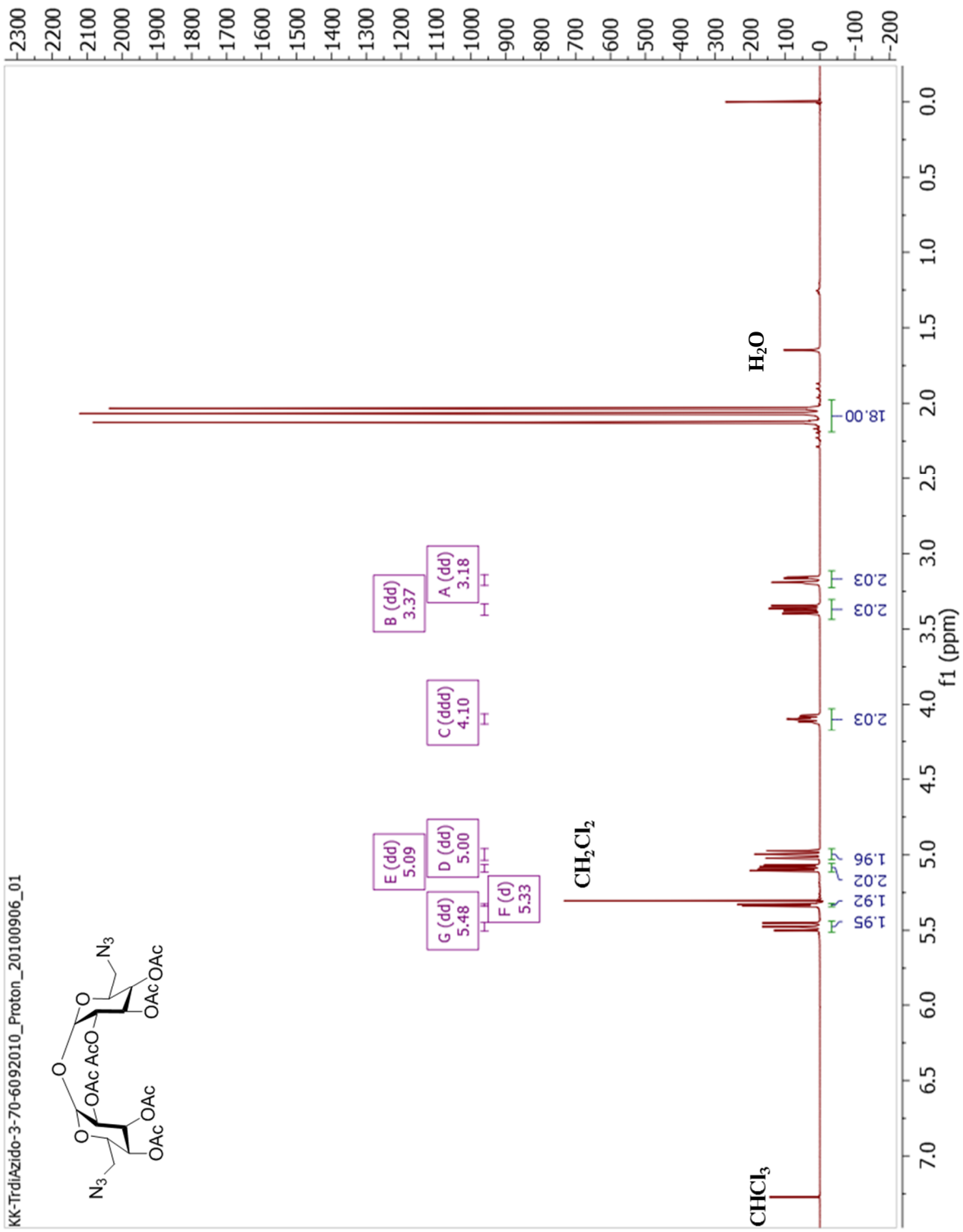
KK-TrdiAzido-3-70-6092010_Proton_20100906_01
OAc AcO
OAc OAc
OAc OAc
N3
N3
O
O
O
A (dd) 3.18
B (dd) 3.37
C (ddd) 4.10
D (dd) 5.00
E (dd) 5.09
F (d) 5.33
G (dd) 5.48
CH2Cl2
H2O
CHCl3
18.00
2.03
2.03
2.03
1.96
2.02
1.92
1.95
f1 (ppm)

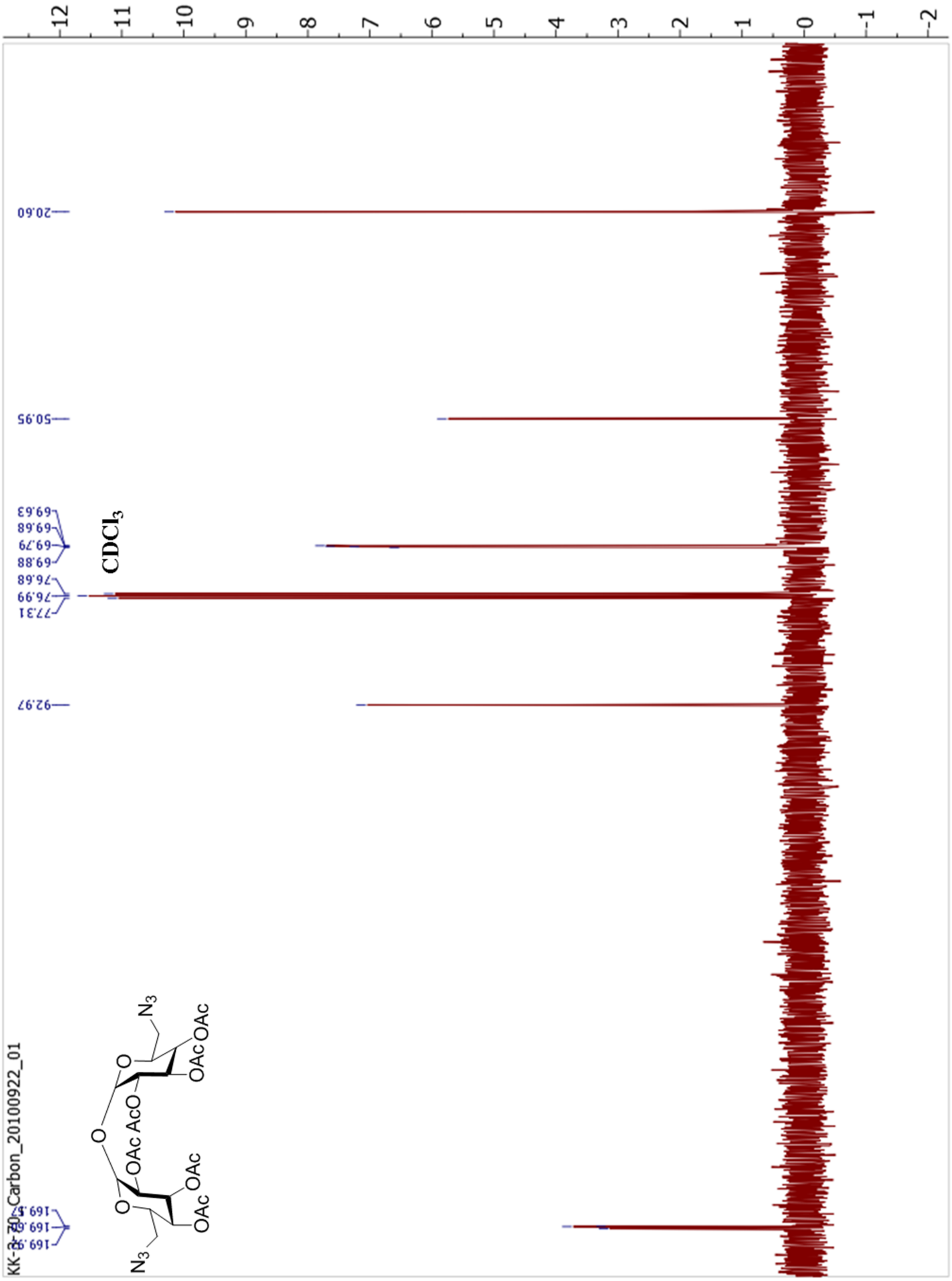
KK-3-70_Carbon_20100922_01
CDCl3
20.60
50.95
69.63
69.68
69.79
69.88
76.68
76.99
77.31
92.97
f1 (ppm)

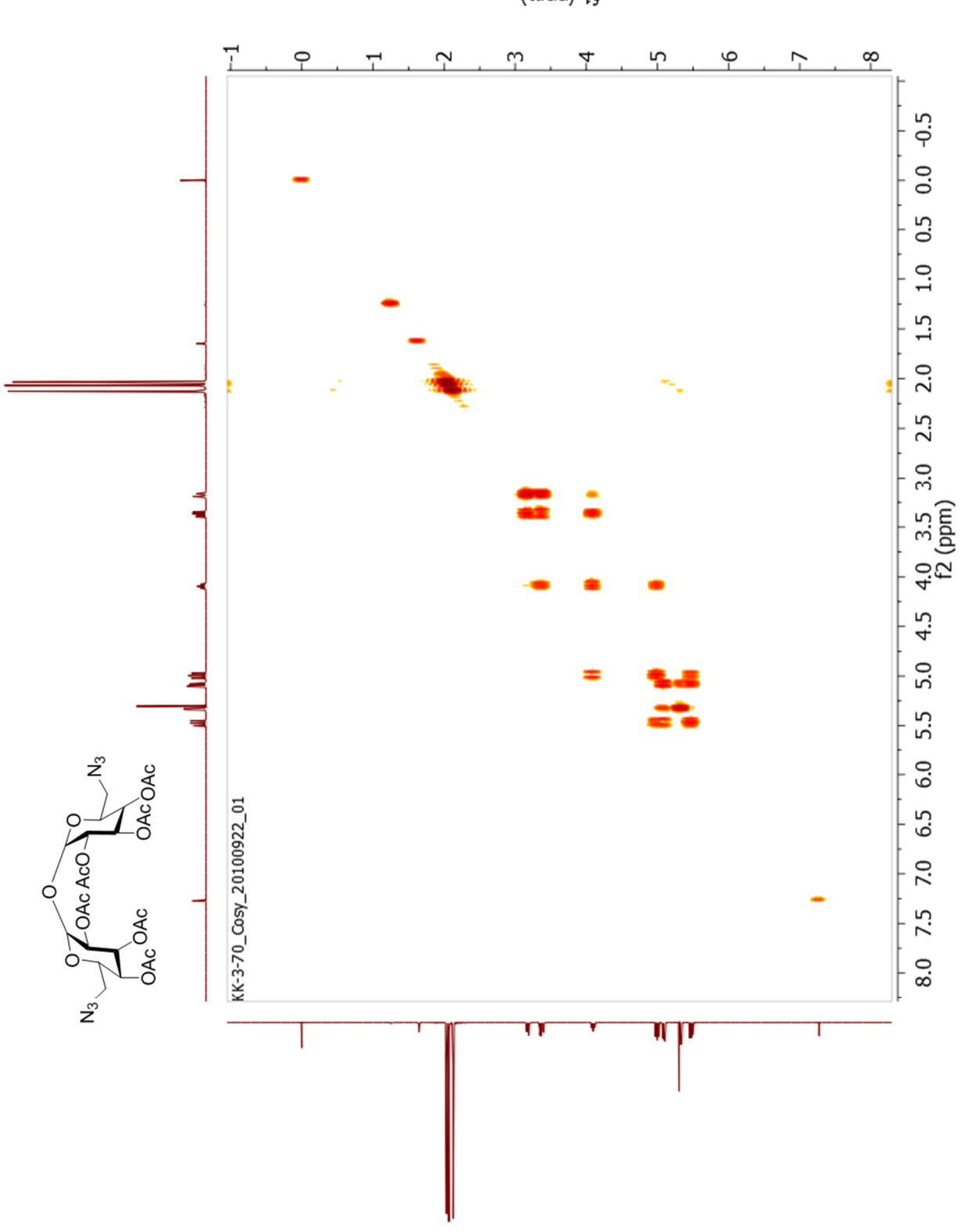
f1 (ppm)
f2 (ppm)
KK-3-70_Cosy_20100922_01
N3
OAc
AcO
O

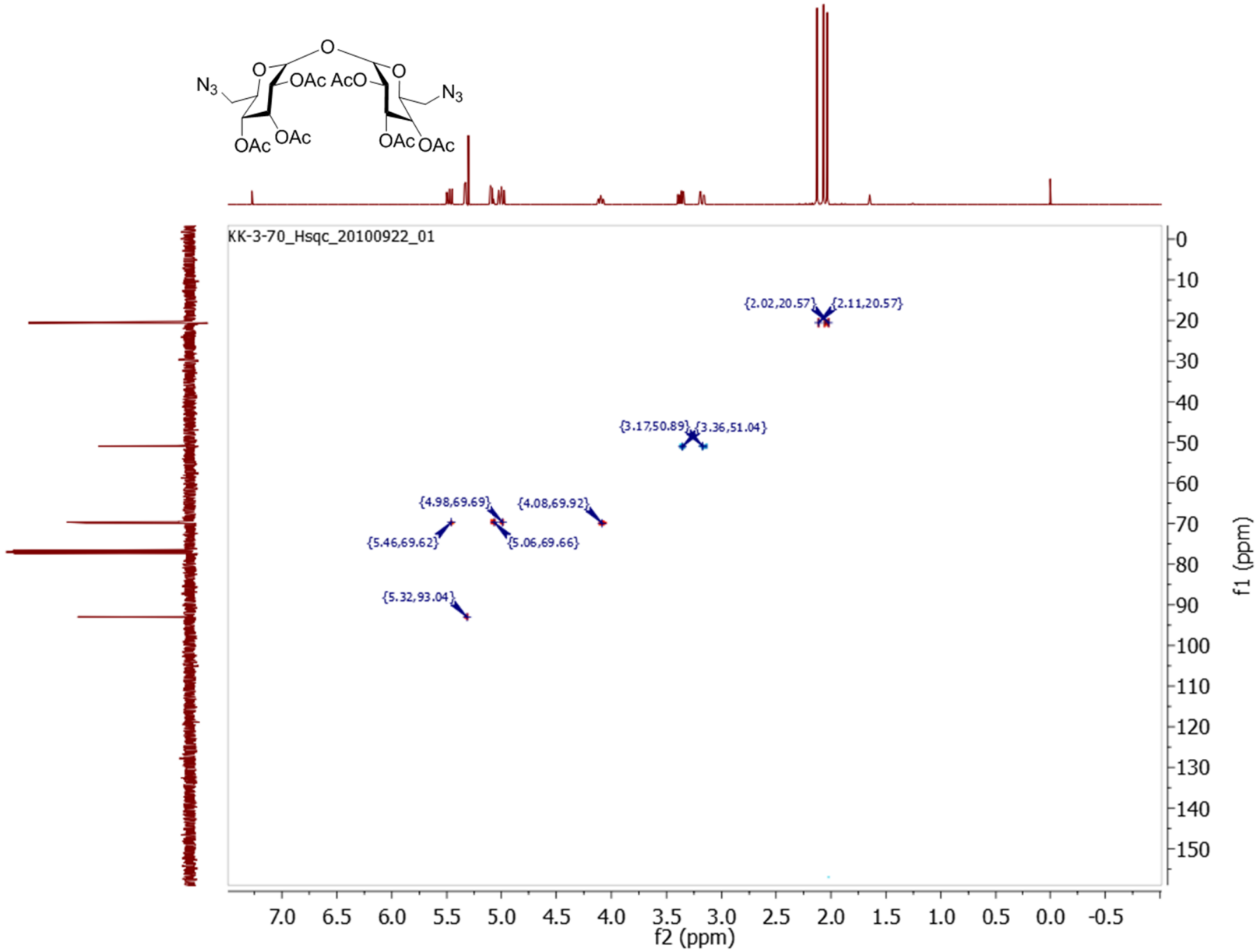
KK-3-70_Hsqc_20100922_01
{2.02,20.57}
{2.11,20.57}
{3.17,50.89}
{3.36,51.04}
{4.98,69.69}
{4.08,69.92}
{5.46,69.62}
{5.06,69.66}
{5.32,93.04}
f2 (ppm)
f1 (ppm)

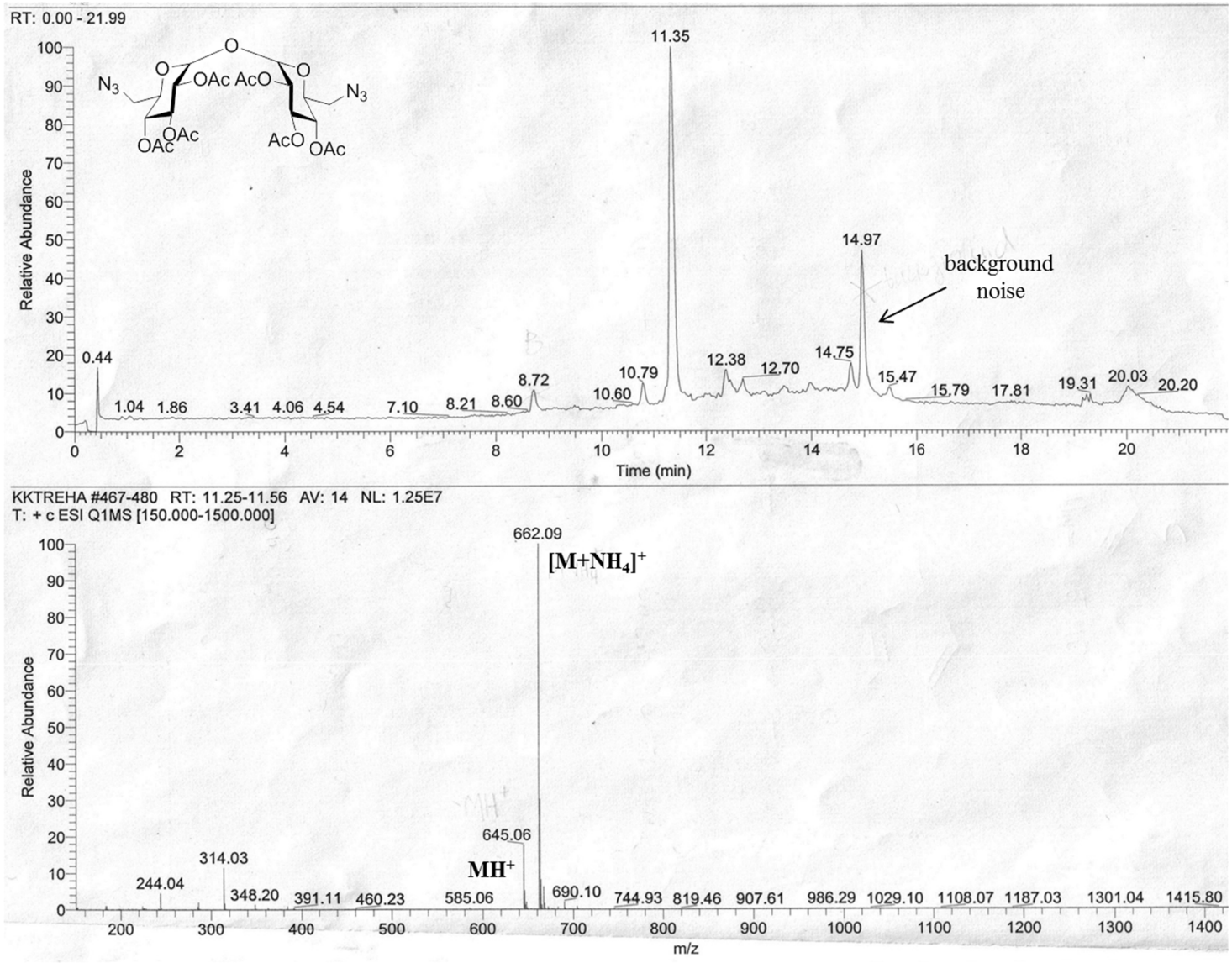
RT: 0.00 - 21.99
Relative Abundance
Time (min)
11.35
14.97
background
noise
0.44
1.04
1.86
3.41
4.06
4.54
7.10
8.21
8.60
8.72
10.60
10.79
12.38
12.70
14.75
15.47
15.79
17.81
19.31
20.03
20.20
KKTREHA #467-480 RT: 11.25-11.56 AV: 14 NL: 1.25E7
T: + c ESI Q1MS [150.000-1500.000]
662.09
[M+NH4]+
645.06
MH+
314.03
244.04
348.20
391.11
460.23
585.06
690.10
744.93
819.46
907.61
986.29
1029.10
1108.07
1187.03
1301.04
1415.80
m/z

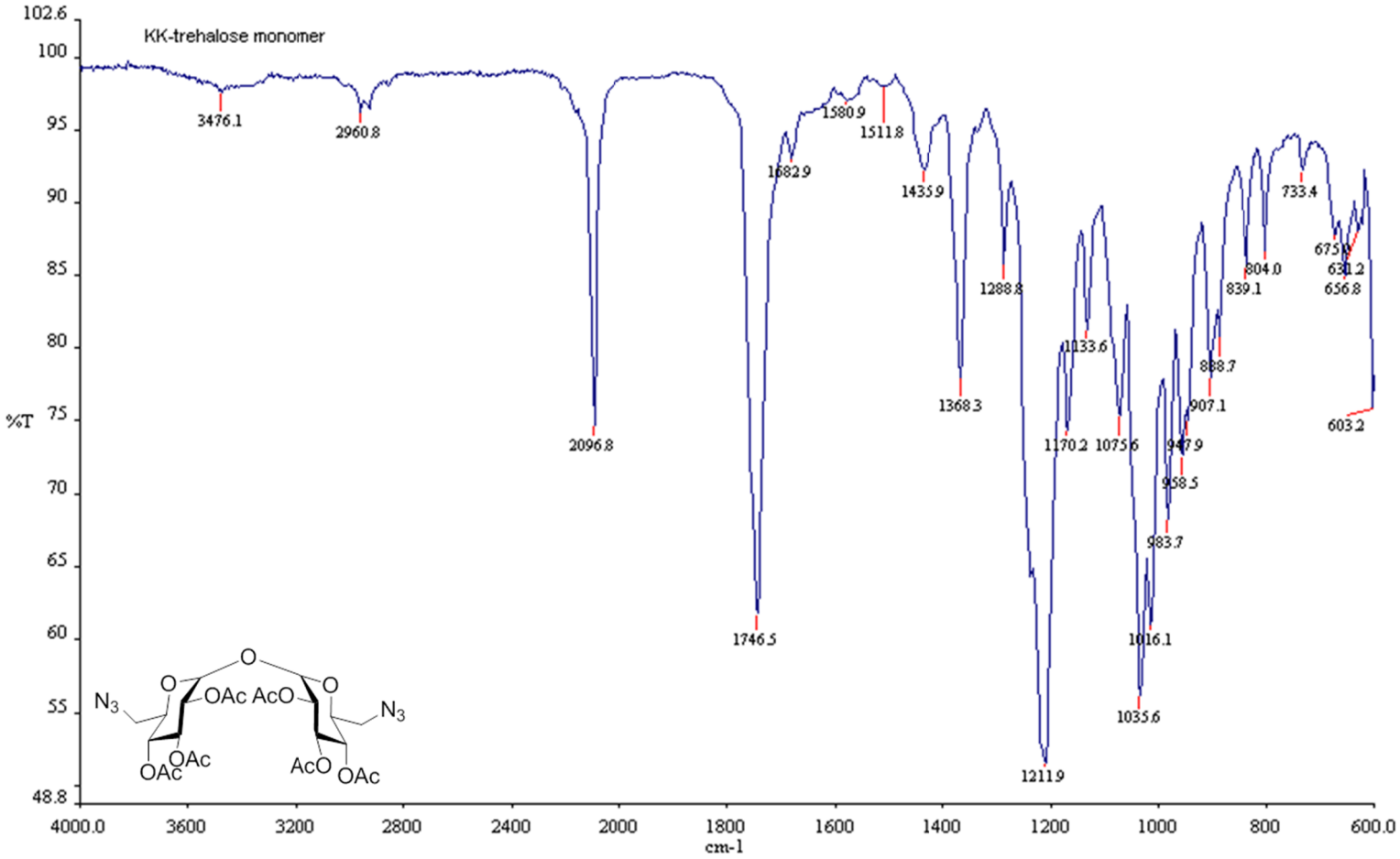
KK-trehalose monomer
%T
cm-1
3476.1
2960.8
2096.8
1746.5
1682.9
1580.9
1511.8
1435.9
1368.3
1288.8
1211.9
1170.2
1133.6
1075.6
1035.6
1016.1
983.7
958.5
947.9
907.1
888.7
839.1
804.0
733.4
675.9
656.8
603.2
102.6
100
95
90
85
80
75
70
65
60
55
48.8
4000.0
3600
3200
2800
2400
2000
1800
1600
1400
1200
1000
800
600.0
N3
OAc
AcO
O

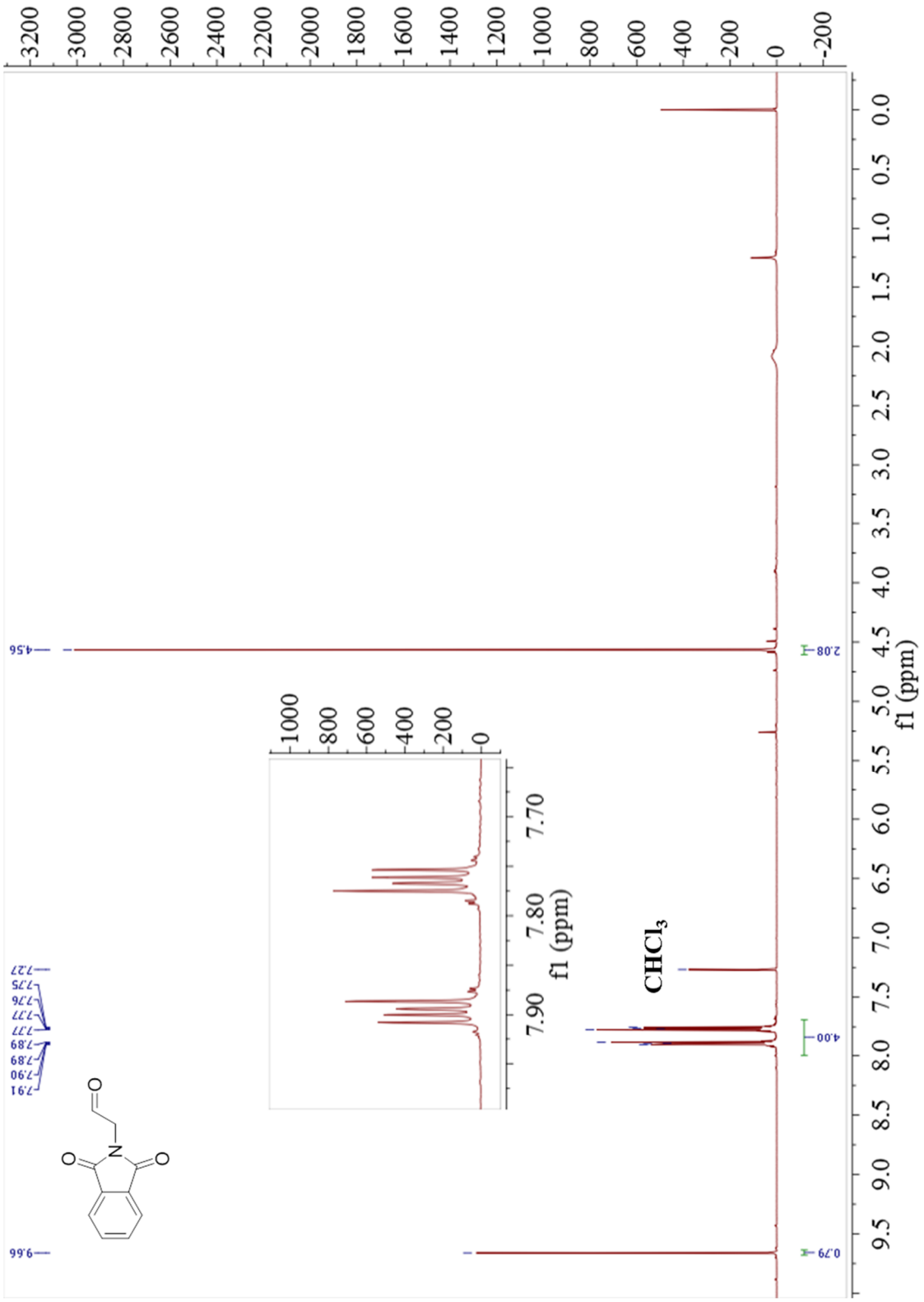
9.66
7.91
7.90
7.89
7.89
7.77
7.77
7.76
7.75
7.27
4.56
0.79
4.00
2.08
CHCl3
f1 (ppm)
7.90
7.80
7.70
f1 (ppm)

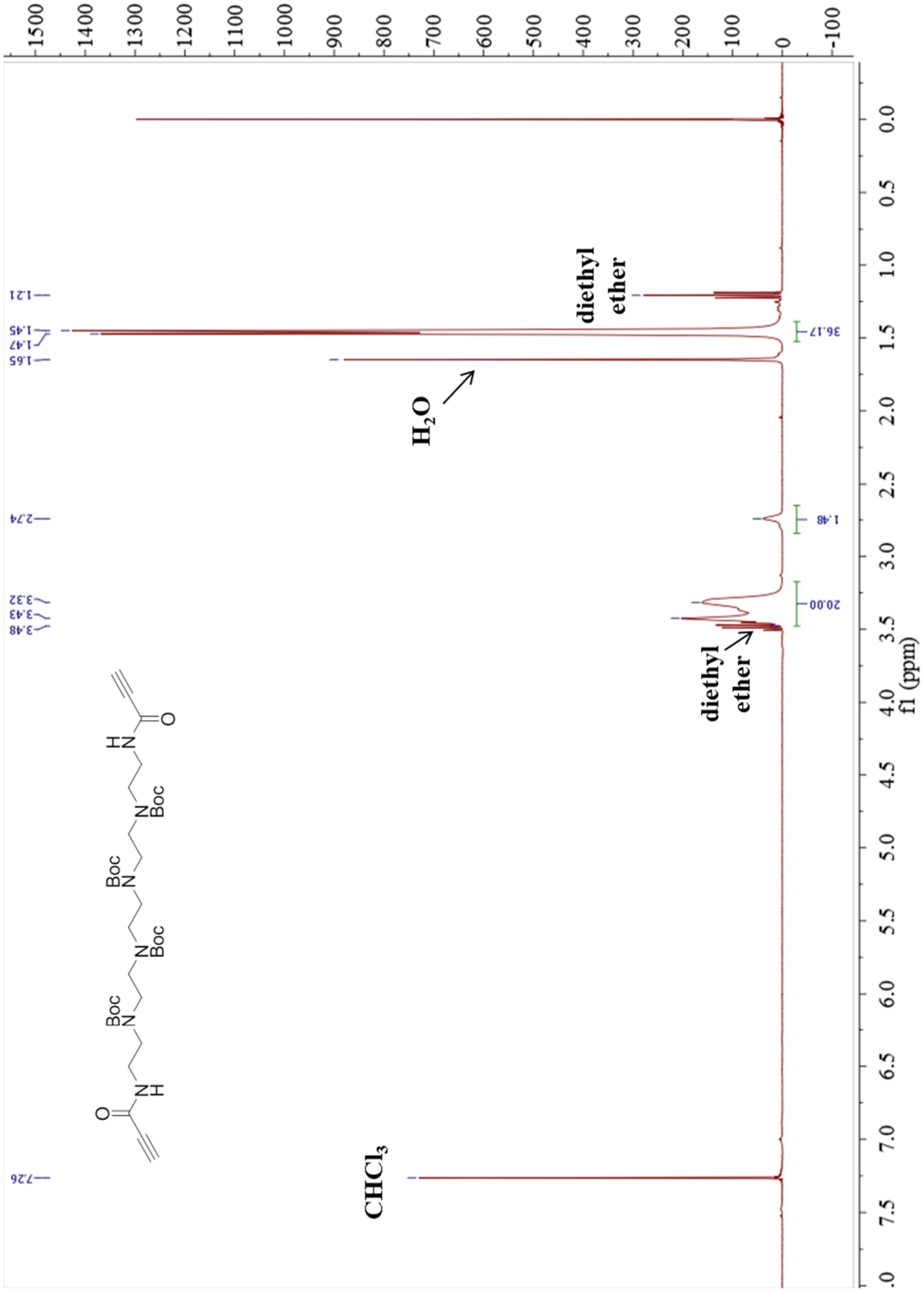
diethyl ether
H_2O
diethyl ether
$CHCl_3$
f1 (ppm)

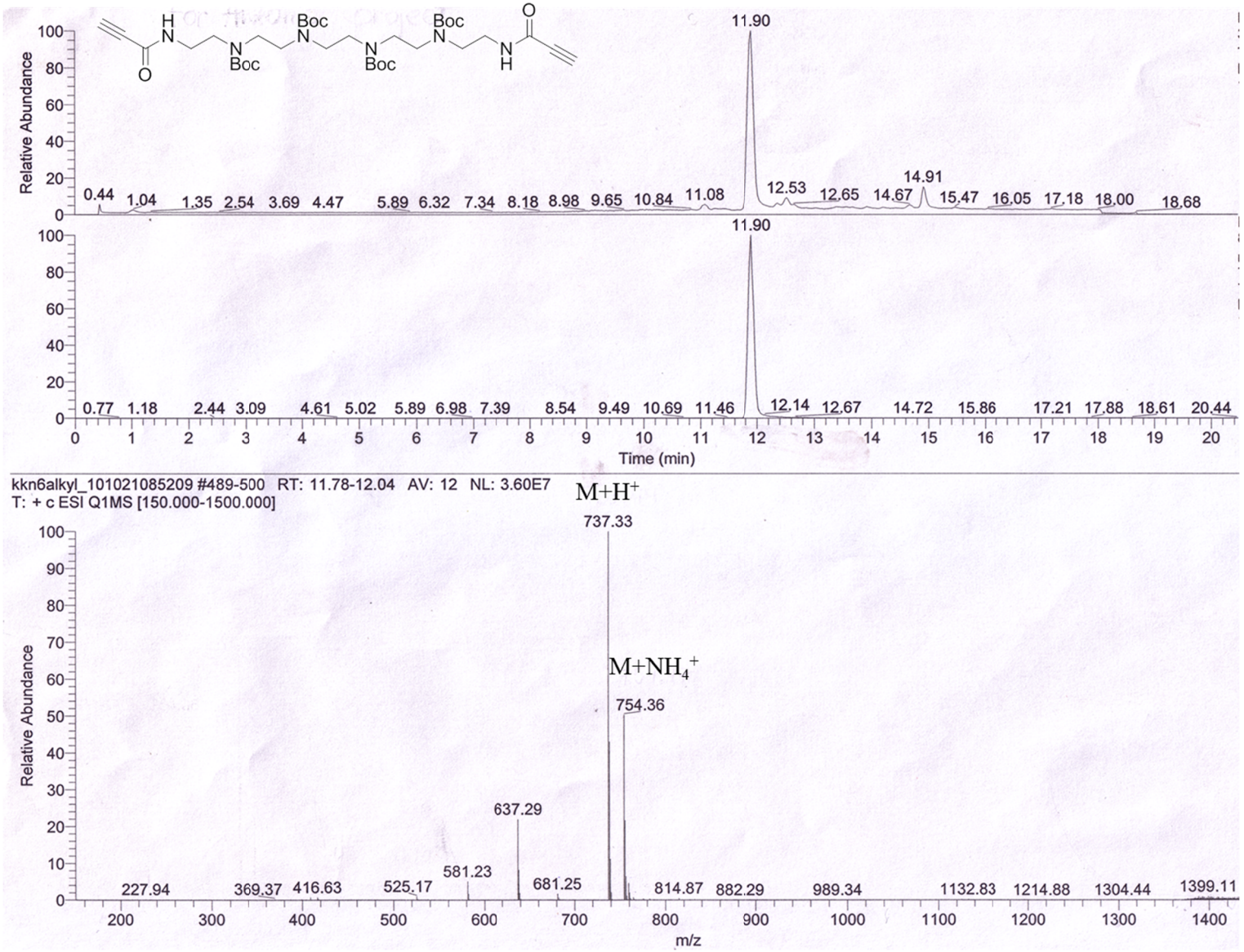
Relative Abundance
Time (min)
11.90
0.44 1.04 1.35 2.54 3.69 4.47 5.89 6.32 7.34 8.18 8.98 9.65 10.84 11.08 12.53 12.65 14.67 14.91 15.47 16.05 17.18 18.00 18.68
0.77 1.18 2.44 3.09 4.61 5.02 5.89 6.98 7.39 8.54 9.49 10.69 11.46 12.14 12.67 14.72 15.86 17.21 17.88 18.61 20.44
kkn6alkyl_101021085209 #489-500 RT: 11.78-12.04 AV: 12 NL: 3.60E7
T: + c ESI Q1MS [150.000-1500.000]
M+H+
737.33
M+NH4+
754.36
637.29
581.23
227.94 369.37 416.63 525.17 681.25 814.87 882.29 989.34 1132.83 1214.88 1304.44 1399.11
m/z

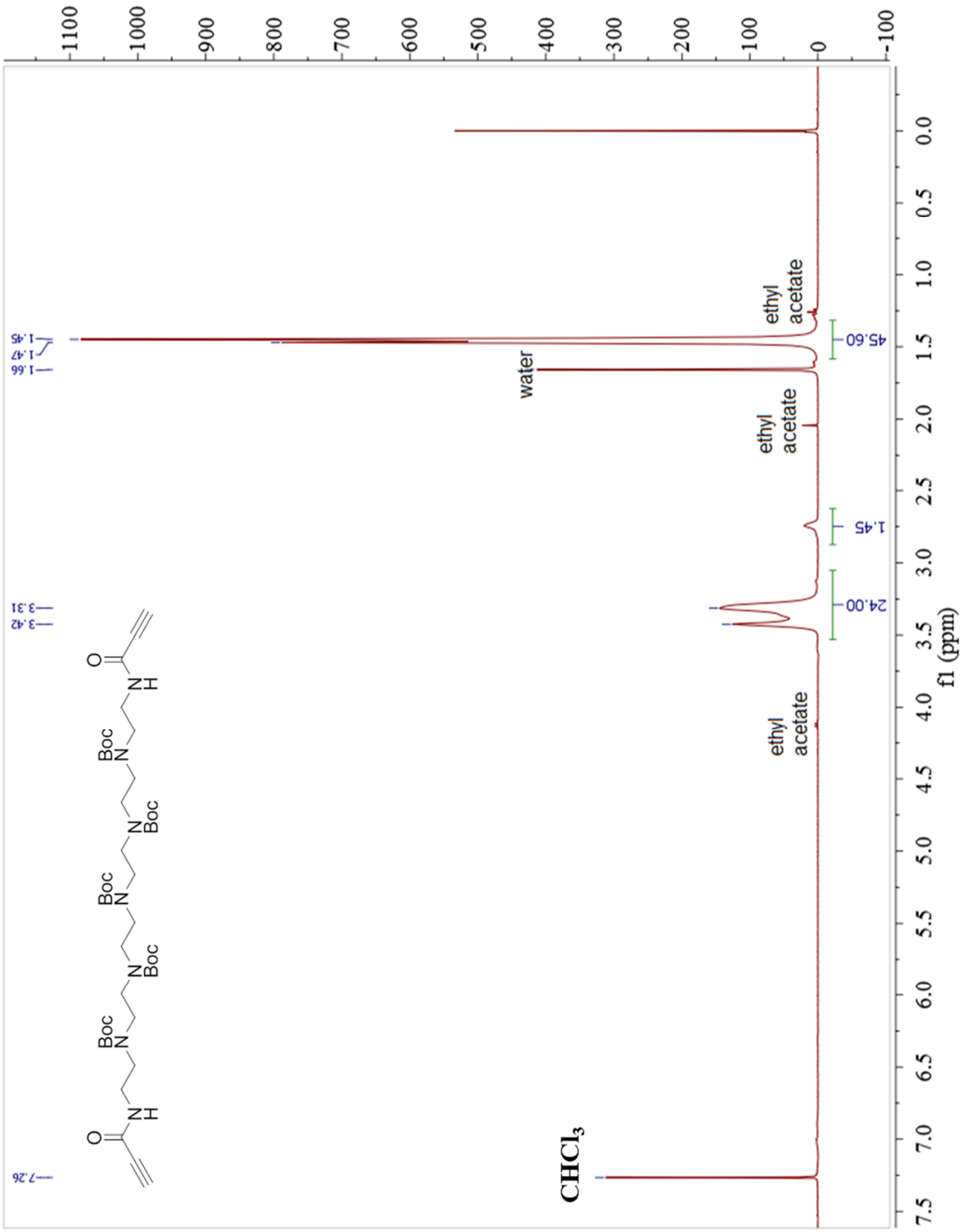
7.26
3.42
3.31
1.66
1.47
1.45
CHCl3
water
ethyl acetate
ethyl acetate
ethyl acetate
45.60
1.45
24.00
f1 (ppm)
Boc
N
H
O

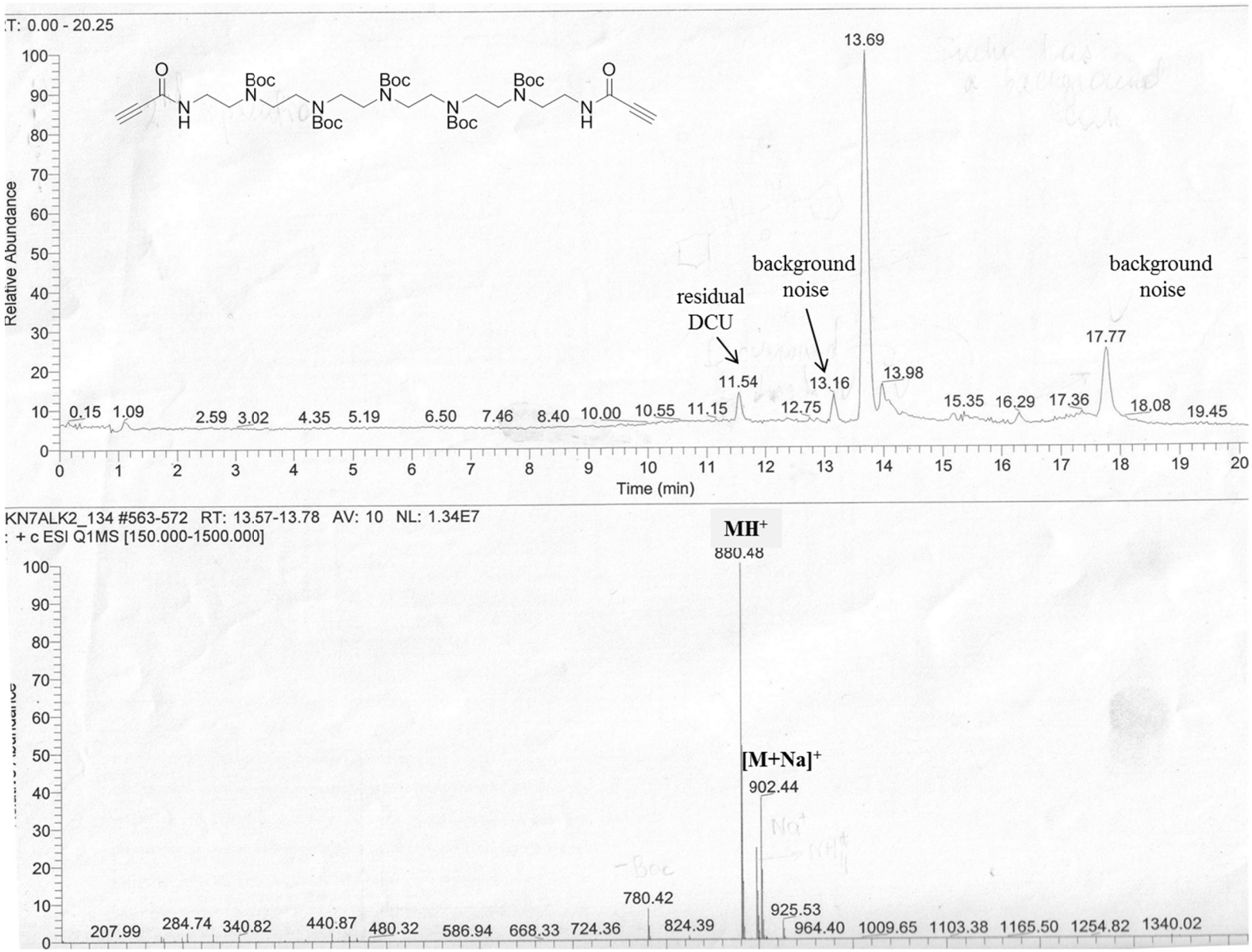
T: 0.00 - 20.25
Relative Abundance
Time (min)
residual DCU
background noise
background noise
13.69
11.54
13.16
13.98
17.77
KN7ALK2_134 #563-572 RT: 13.57-13.78 AV: 10 NL: 1.34E7
+ c ESI Q1MS [150.000-1500.000]
MH+
880.48
[M+Na]+
902.44
780.42
925.53

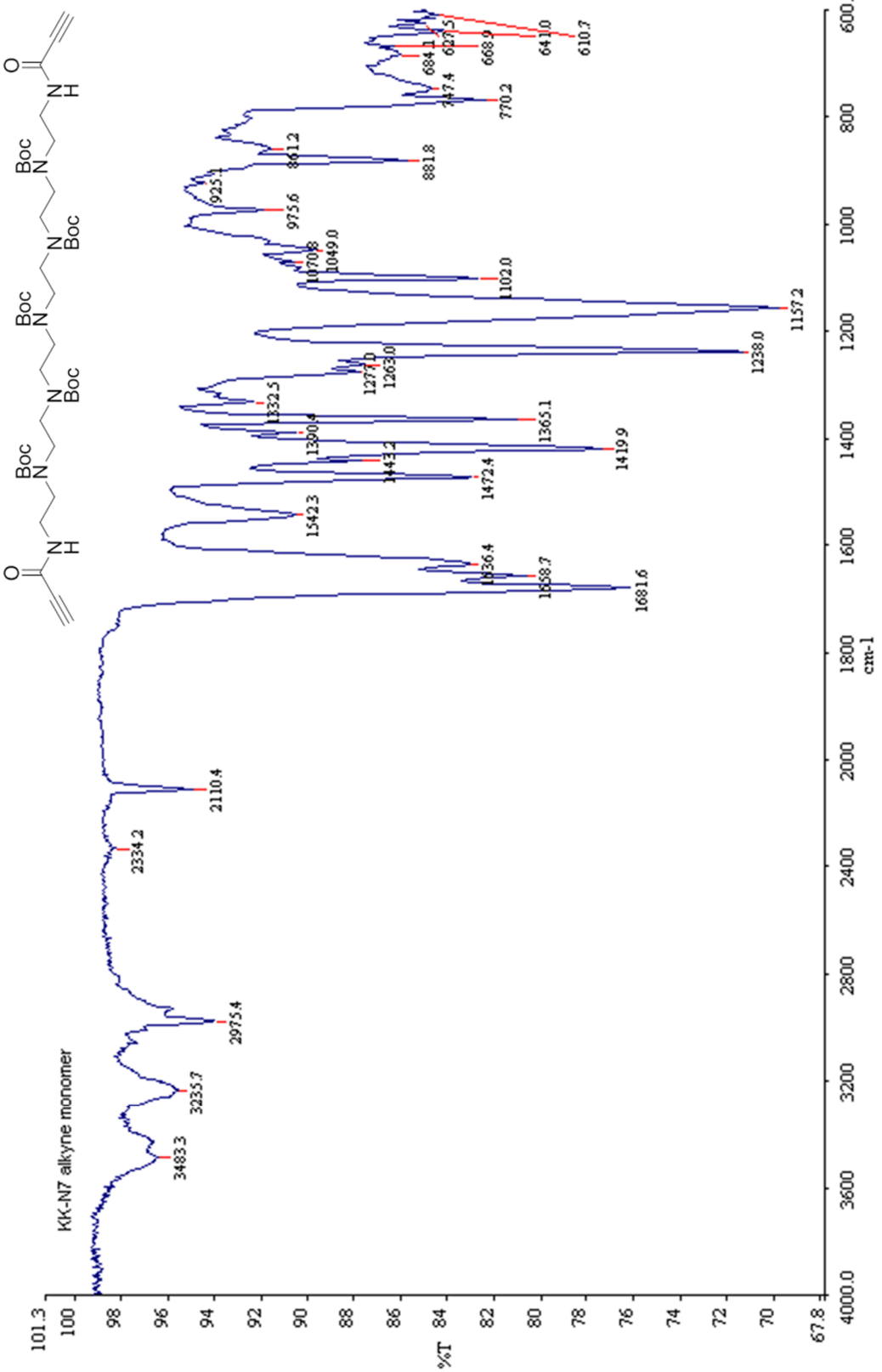
KK-N7 alkyne monomer
%T
cm-1
101.3
100
98
96
94
92
90
88
86
84
82
80
78
76
74
72
70
67.8
4000.0
3600
3200
2800
2400
2000
1800
1600
1400
1200
1000
800
600.0
3483.3
3335.7
2975.4
2334.2
2110.4
1681.6
1658.7
1636.4
1542.3
1472.4
1443.2
1419.9
1390.4
1365.1
1332.5
1277.0
1263.0
1238.0
1157.2
1102.0
1070.8
1049.0
975.6
925.4
881.8
861.2
770.2
747.4
684.1
627.5
668.9
641.0
610.7
Boc
N
H
O

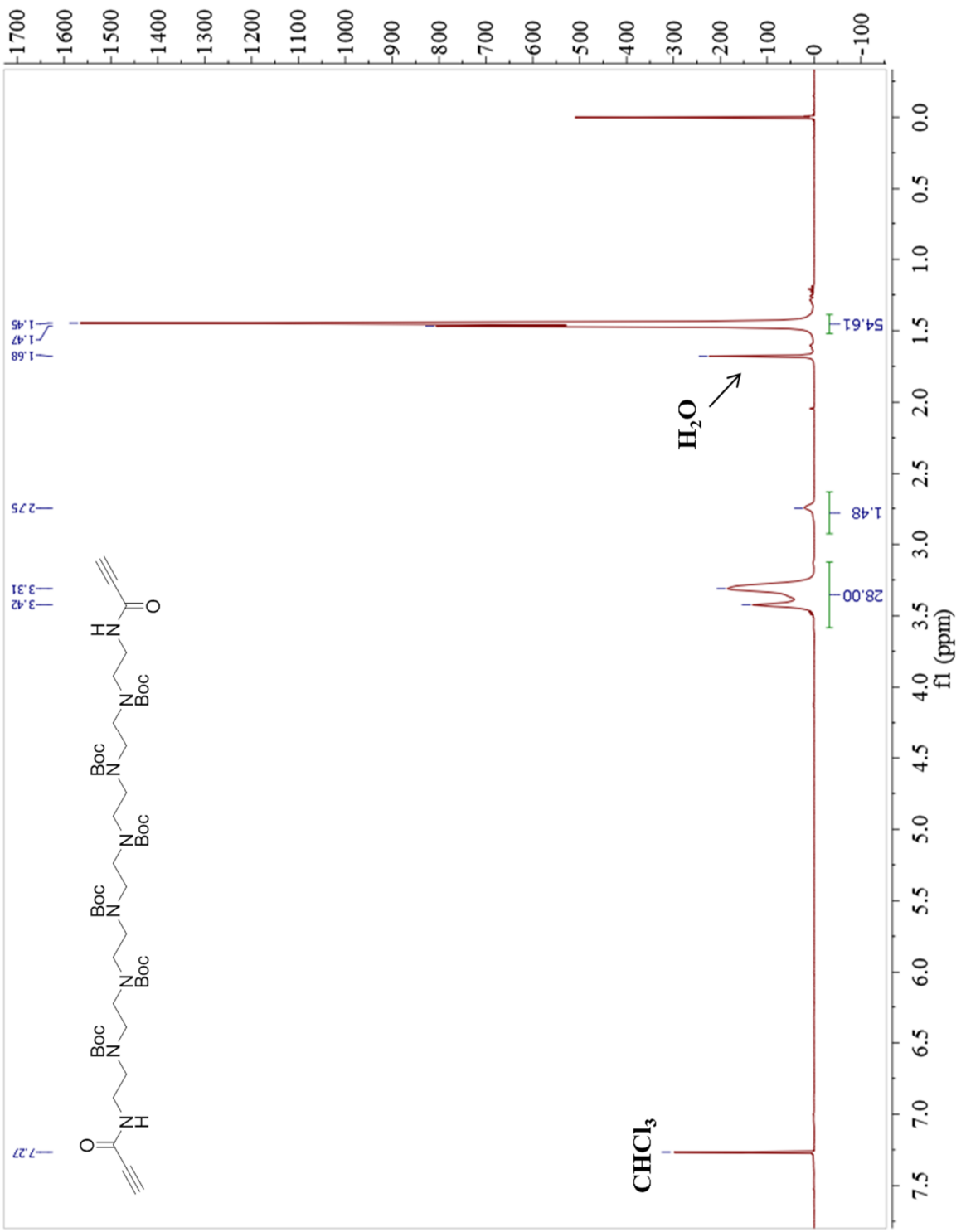
7.27
3.42
3.31
2.75
1.68
1.47
1.45
CHCl3
H2O
28.00
1.48
54.61
f1 (ppm)

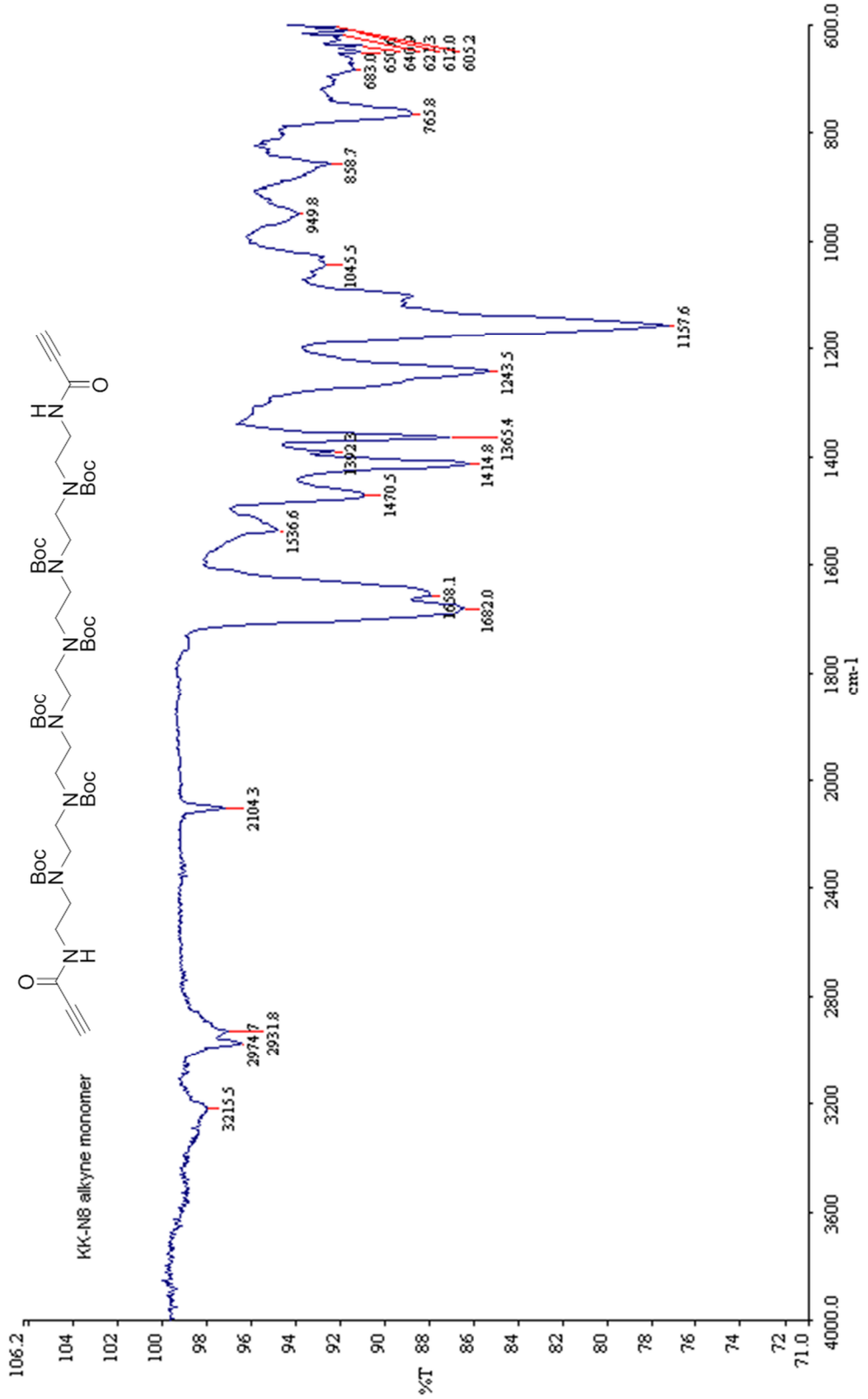
KK-N8 alkyne monomer
Boc
N
H
O
%T
cm-1
106.2
104
102
100
98
96
94
92
90
88
86
84
82
80
78
76
74
72
71.0
4000.0
3600
3200
2800
2400
2000
1800
1600
1400
1200
1000
800
600.0
3215.5
2974.7
2931.8
2104.3
1682.0
1658.1
1536.6
1470.5
1414.8
1365.4
1243.5
1157.6
1045.5
949.8
858.7
765.8
683.0
650.6
640.9
627.3
617.0
605.2

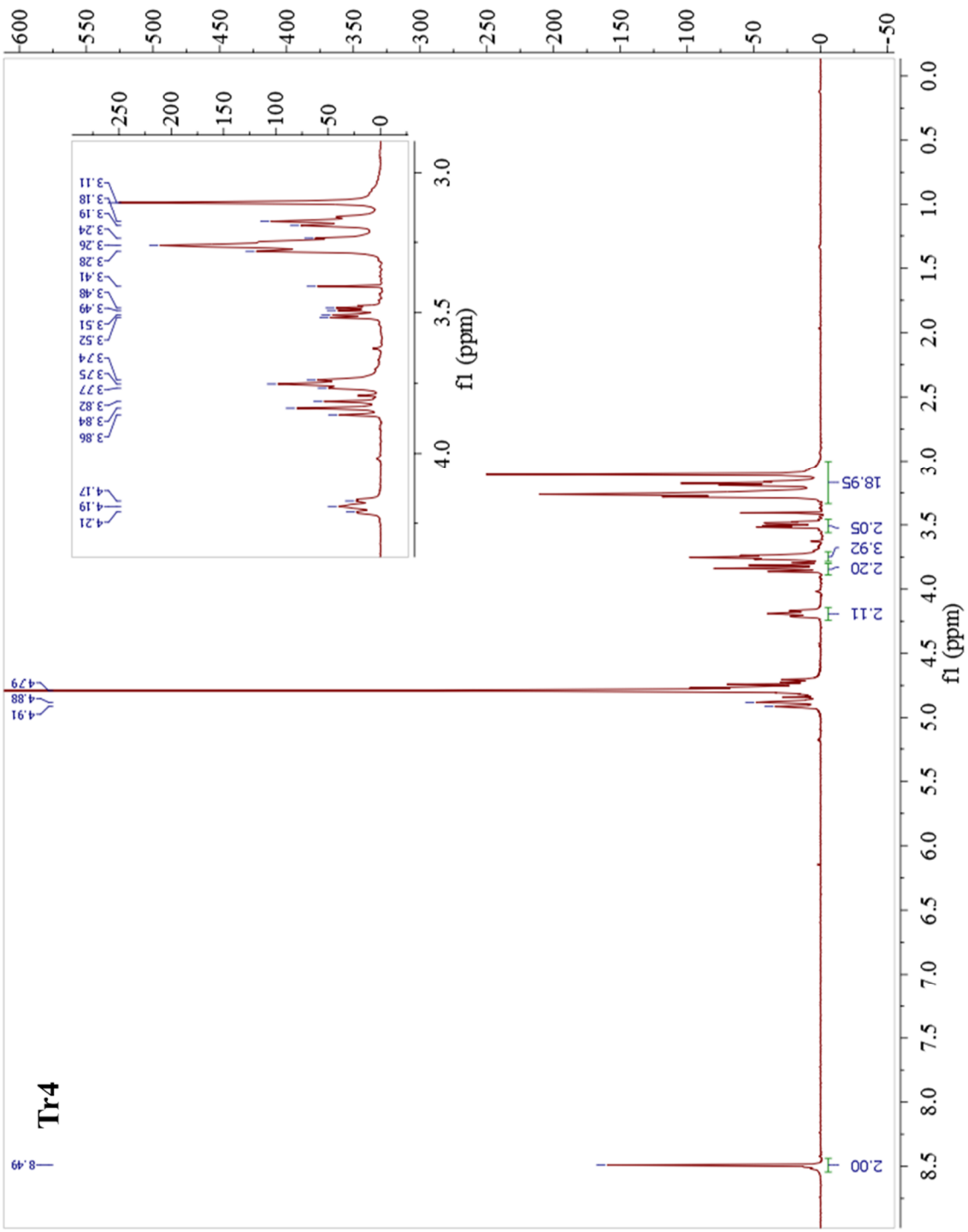
Tr4
f1 (ppm)
f1 (ppm)
8.49
4.91
4.88
4.79
4.21
4.19
4.17
3.86
3.84
3.82
3.77
3.75
3.74
3.52
3.51
3.49
3.48
3.41
3.28
3.26
3.24
3.19
3.18
3.11
2.00
18.95
2.05
3.92
2.20
2.11

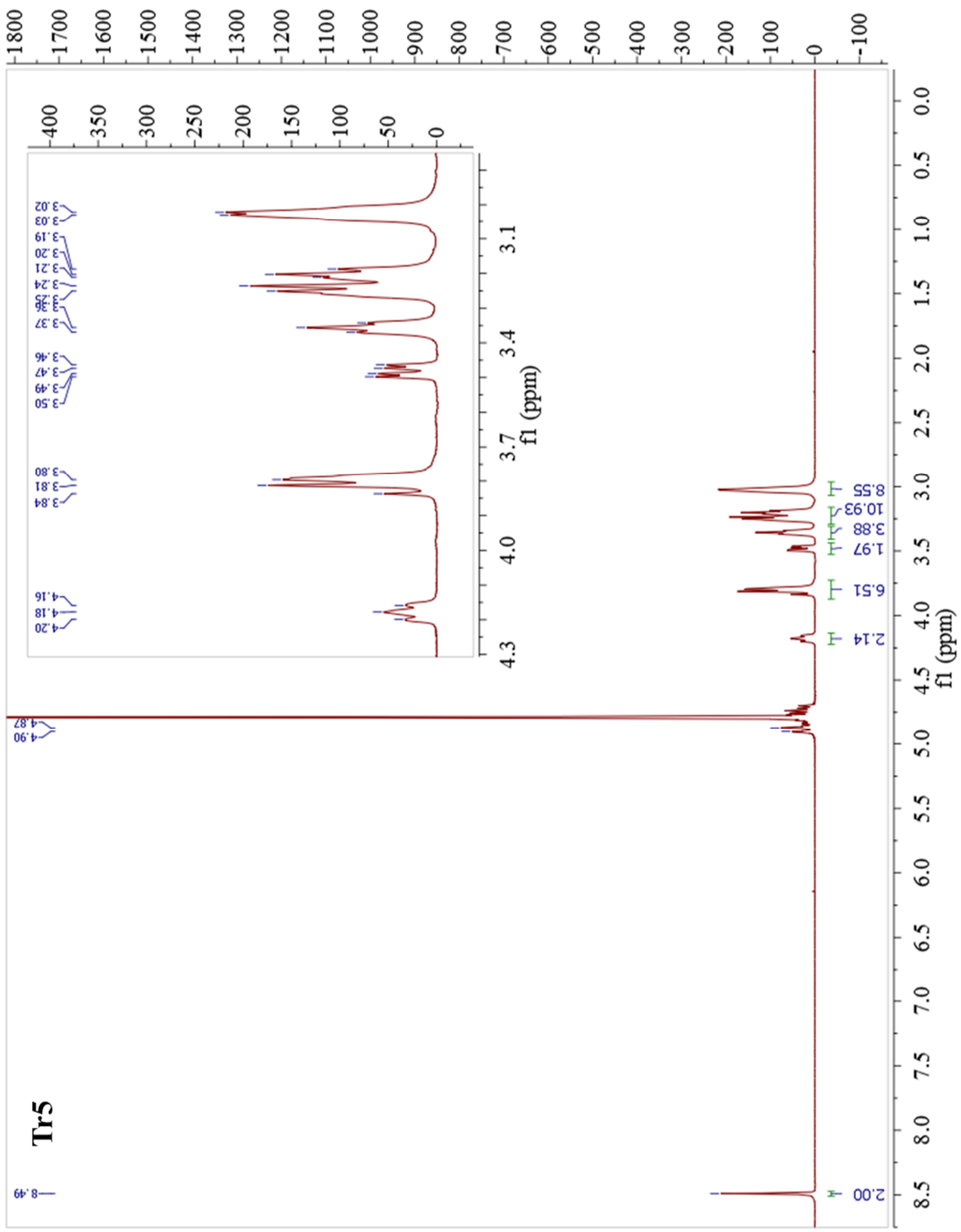
Tr5
f1 (ppm)
f1 (ppm)
8.49
4.90
4.87
4.20
4.18
4.16
3.84
3.81
3.80
3.50
3.49
3.47
3.46
3.37
3.36
3.24
3.21
3.20
3.19
3.03
3.02
2.00
2.14
6.51
1.97
3.88
10.93
8.55

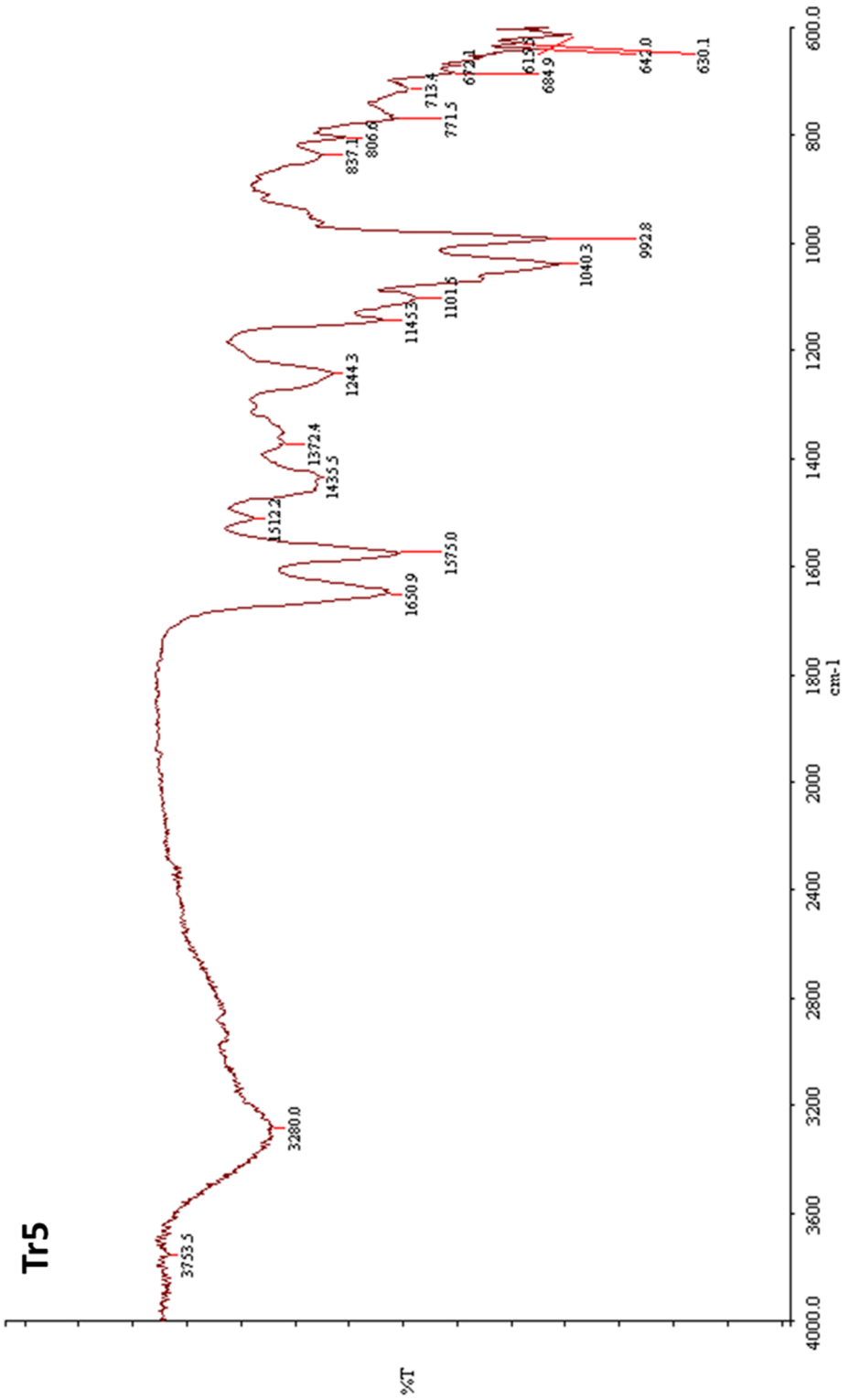
Tr5
%T
cm-1
4000.0
3600
3200
2800
2400
2000
1800
1600
1400
1200
1000
800
600.0
3753.5
3280.0
1650.9
1575.0
1512.2
1435.5
1372.4
1244.3
1145.3
1101.5
1040.3
992.8
837.1
806.6
771.5
713.4
684.9
642.0
630.1

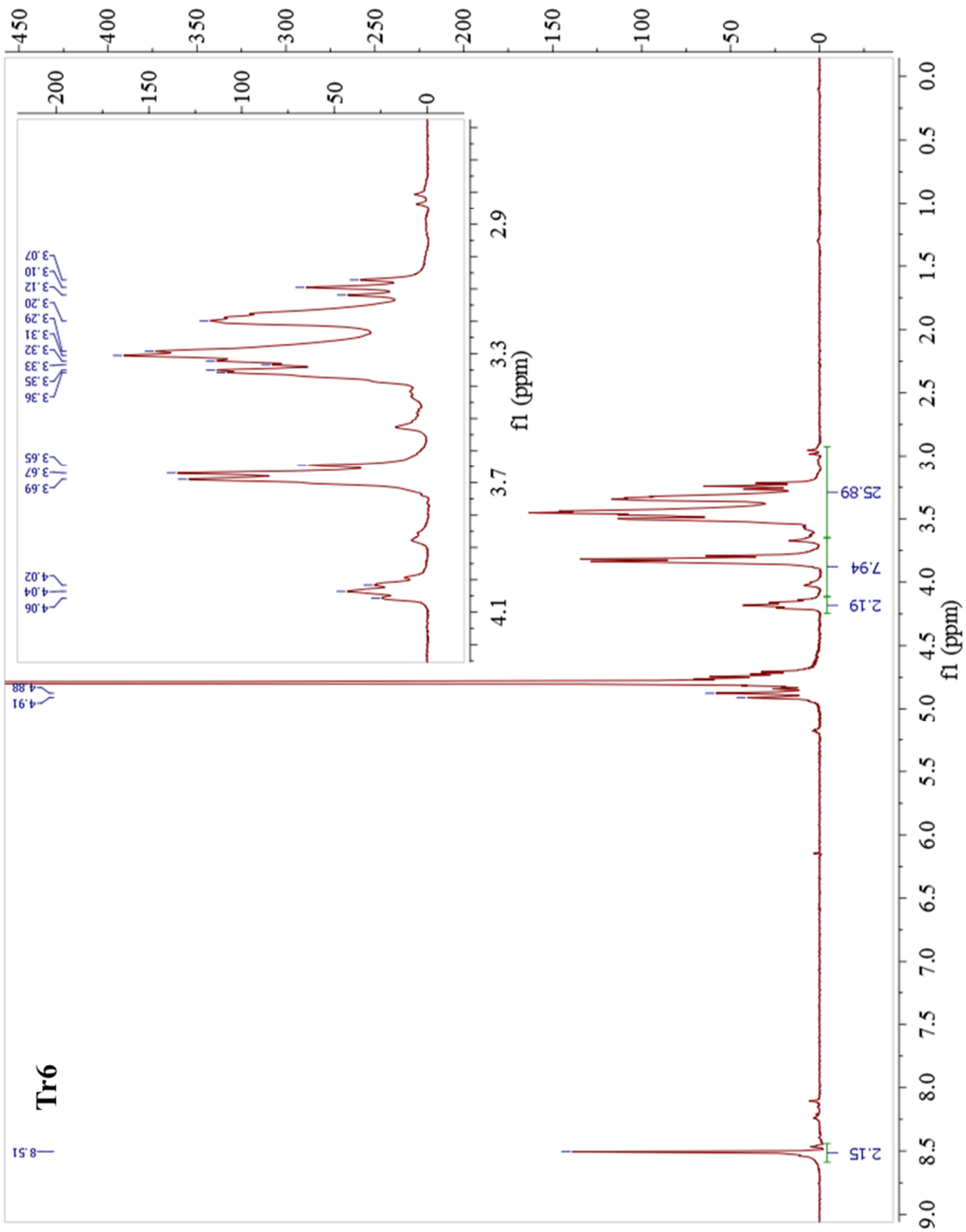
Tr6
8.51
4.91
4.88
4.06
4.04
4.02
3.69
3.67
3.65
3.36
3.35
3.33
3.32
3.31
3.29
3.20
3.12
3.10
3.07
2.15
2.19
7.94
25.89
f1 (ppm)

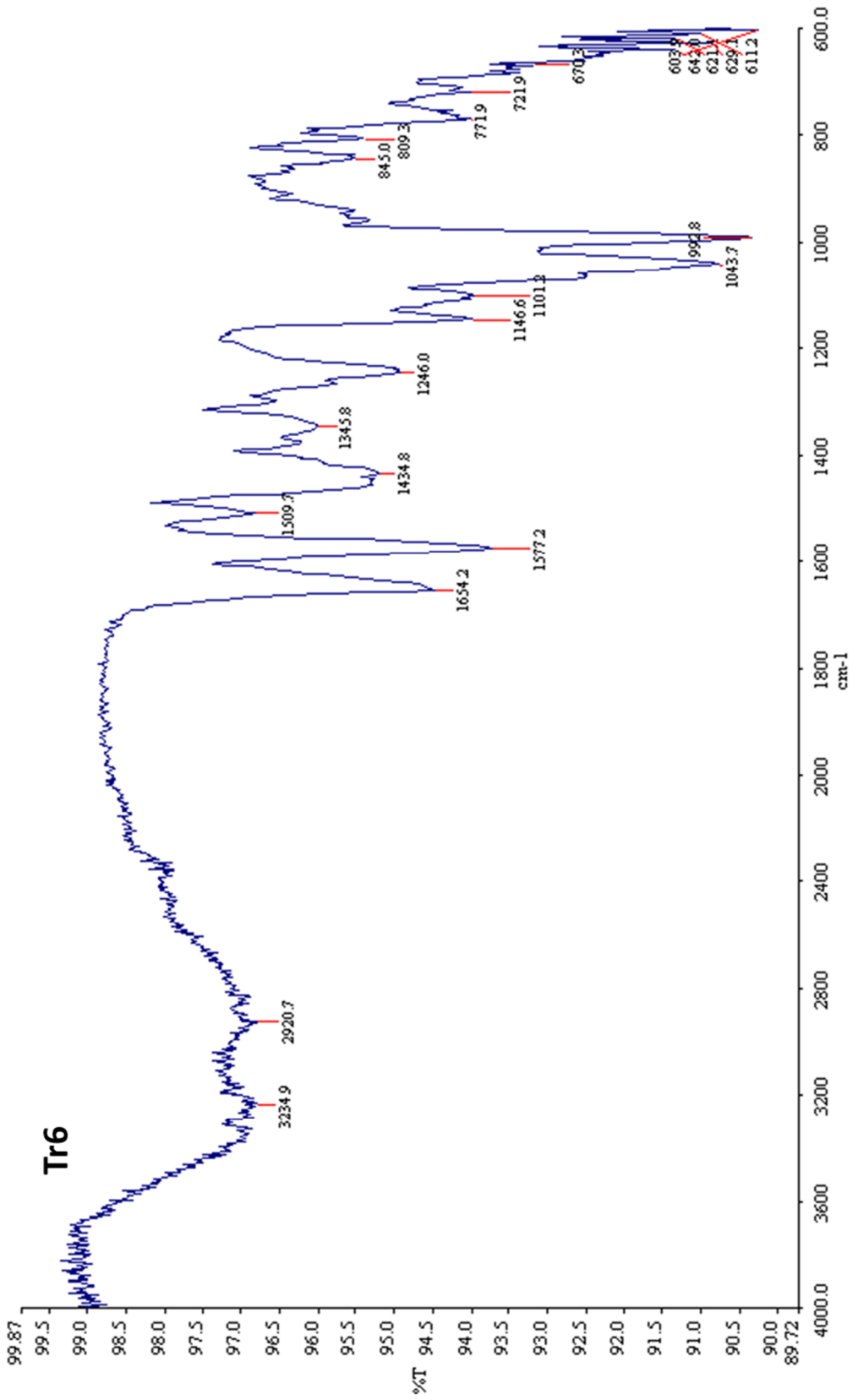
Tr6
%T
cm-1
99.87
89.72
4000.0
600.0
3234.9
2920.7
1654.2
1577.2
1509.7
1434.8
1345.8
1246.0
1146.6
1101.2
1043.7
999.8
845.0
809.3
771.9
721.9
670.3
611.2

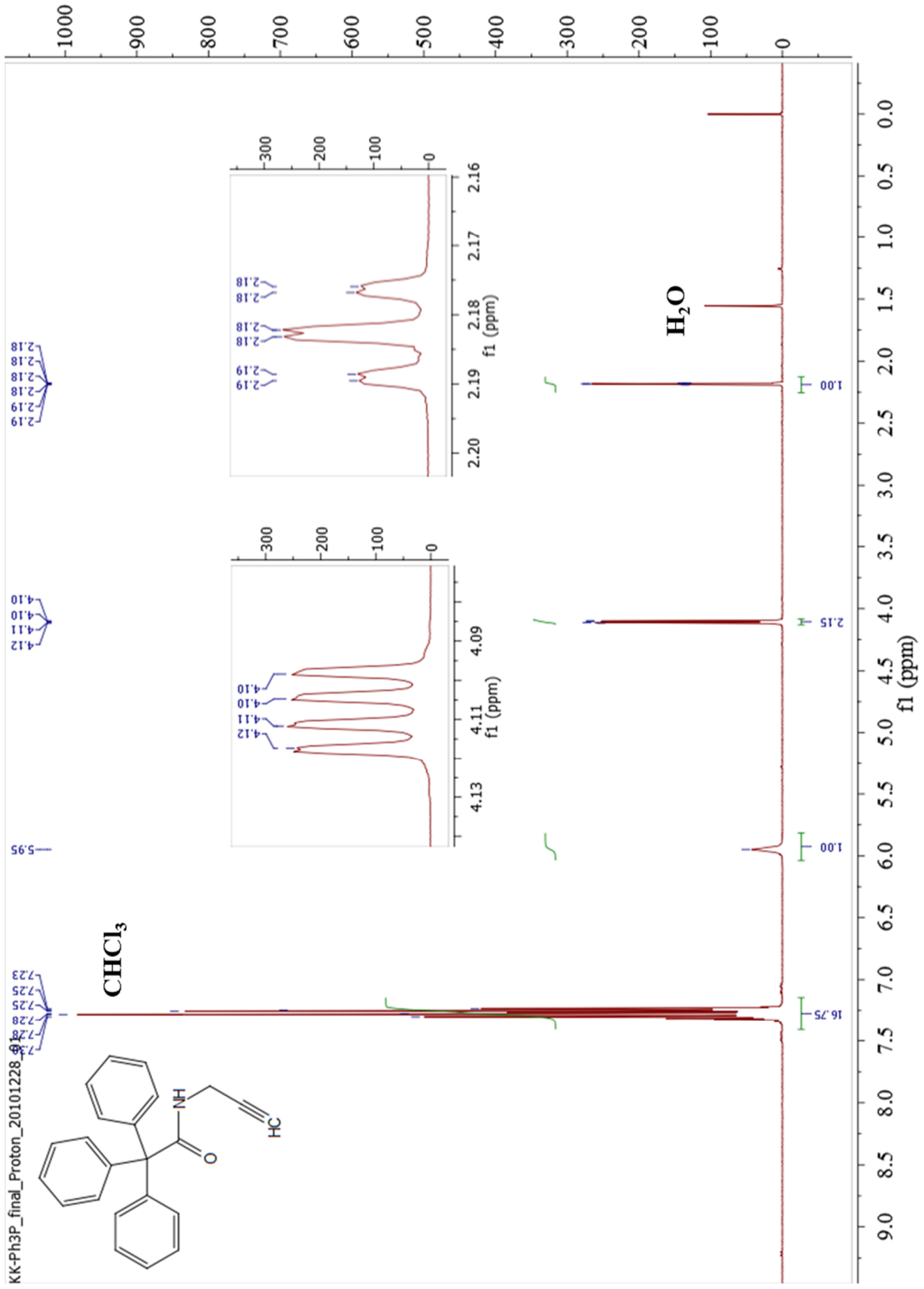
KK-Ph3P_final_Proton_20101228_01
CHCl3
H2O
NH
O
HC
f1 (ppm)

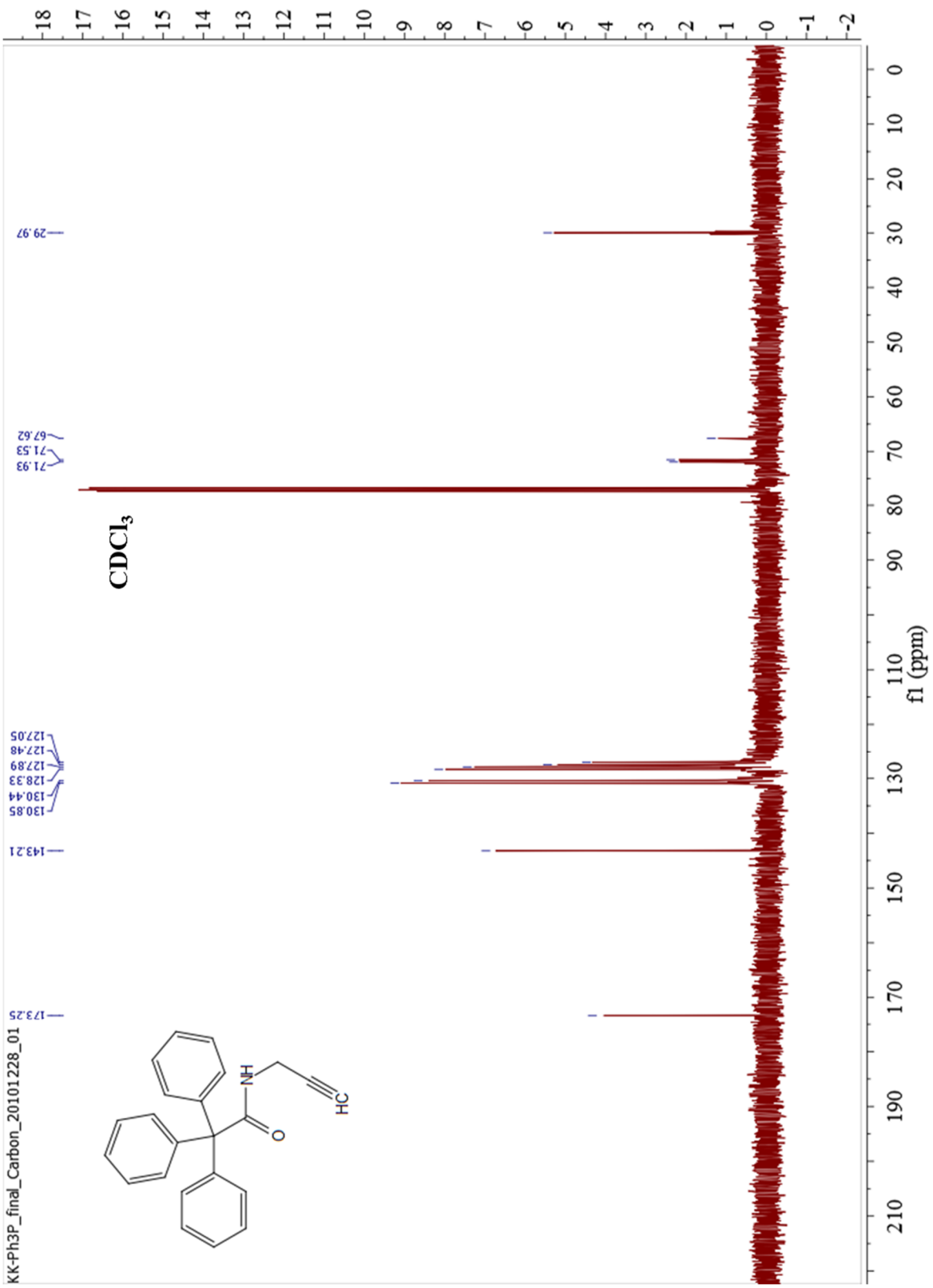
KK-Ph3P_final_Carbon_20101228_01
173.25
143.21
130.85
130.44
128.33
127.89
127.48
127.05
71.93
71.53
67.62
29.97
CDCl3
NH
O
HC
f1 (ppm)

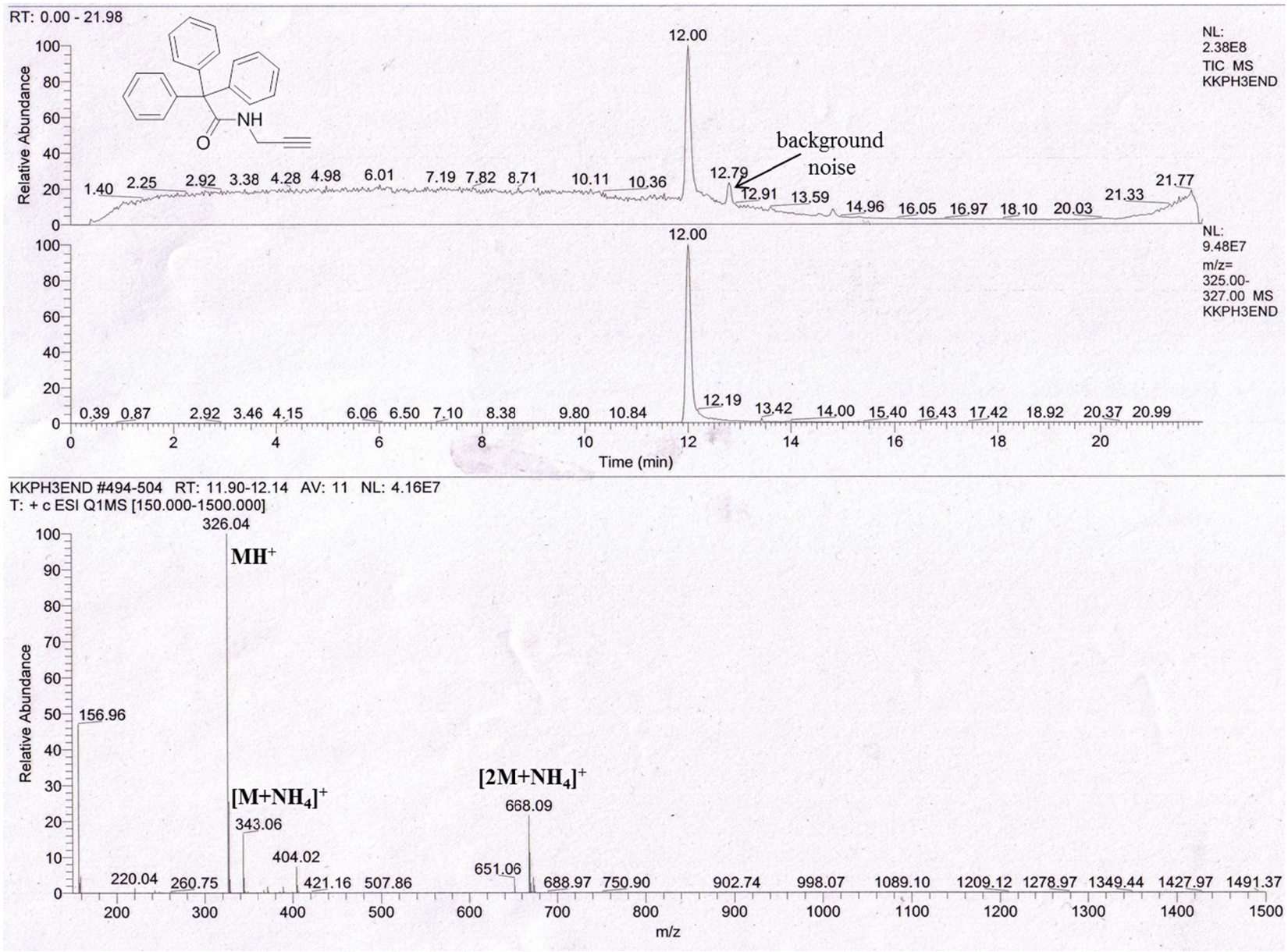
RT: 0.00 - 21.98
Relative Abundance
12.00
NL:
2.38E8
TIC MS
KKPH3END
background
noise
1.40 2.25 2.92 3.38 4.28 4.98 6.01 7.19 7.82 8.71 10.11 10.36 12.79 12.91 13.59 14.96 16.05 16.97 18.10 20.03 21.33 21.77
NL:
9.48E7
m/z=
325.00-
327.00 MS
KKPH3END
0.39 0.87 2.92 3.46 4.15 6.06 6.50 7.10 8.38 9.80 10.84 12.19 13.42 14.00 15.40 16.43 17.42 18.92 20.37 20.99
Time (min)
KKPH3END #494-504 RT: 11.90-12.14 AV: 11 NL: 4.16E7
T: + c ESI Q1MS [150.000-1500.000]
326.04
MH+
156.96
[M+NH4]+
343.06
404.02
220.04 260.75 421.16 507.86
[2M+NH4]+
668.09
651.06
688.97 750.90 902.74 998.07 1089.10 1209.12 1278.97 1349.44 1427.97 1491.37
m/z

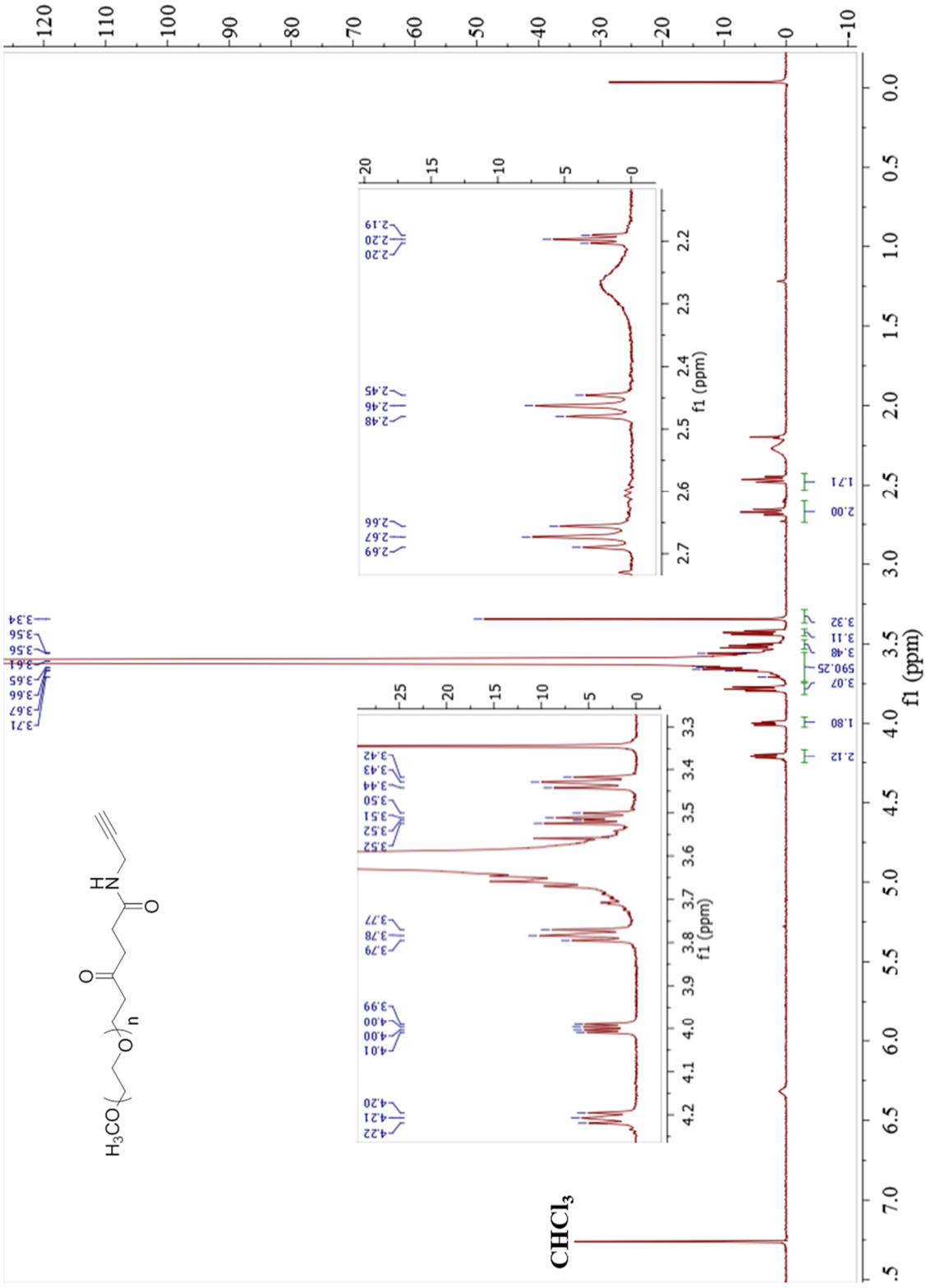
CHCl3
H3CO
O
n
O
O
H
N
f1 (ppm)

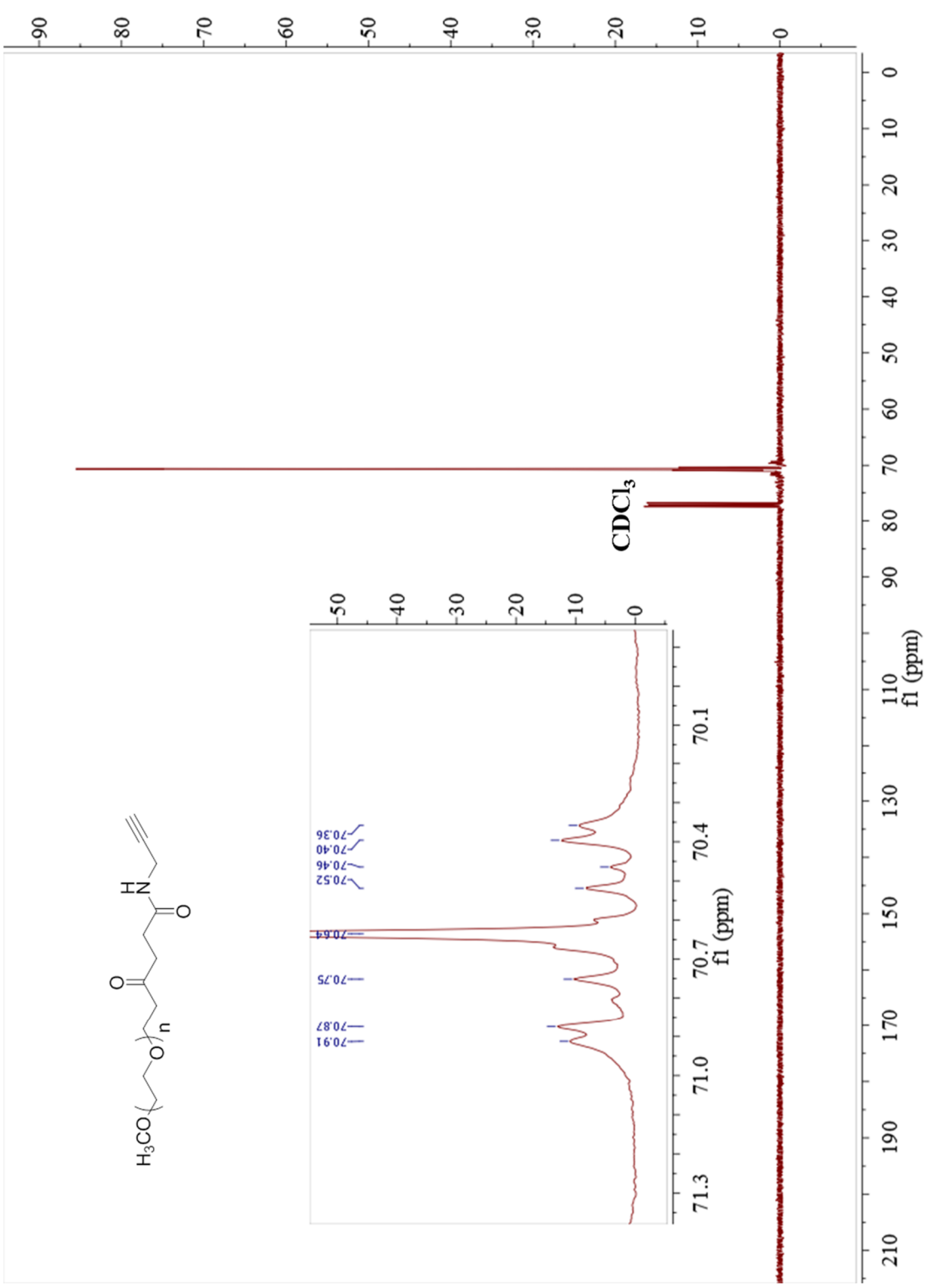
CDCl3
f1 (ppm)
70.64
70.75
70.87
70.91
70.52
70.46
70.40
70.36
H3CO
O
n
H
N
O
O

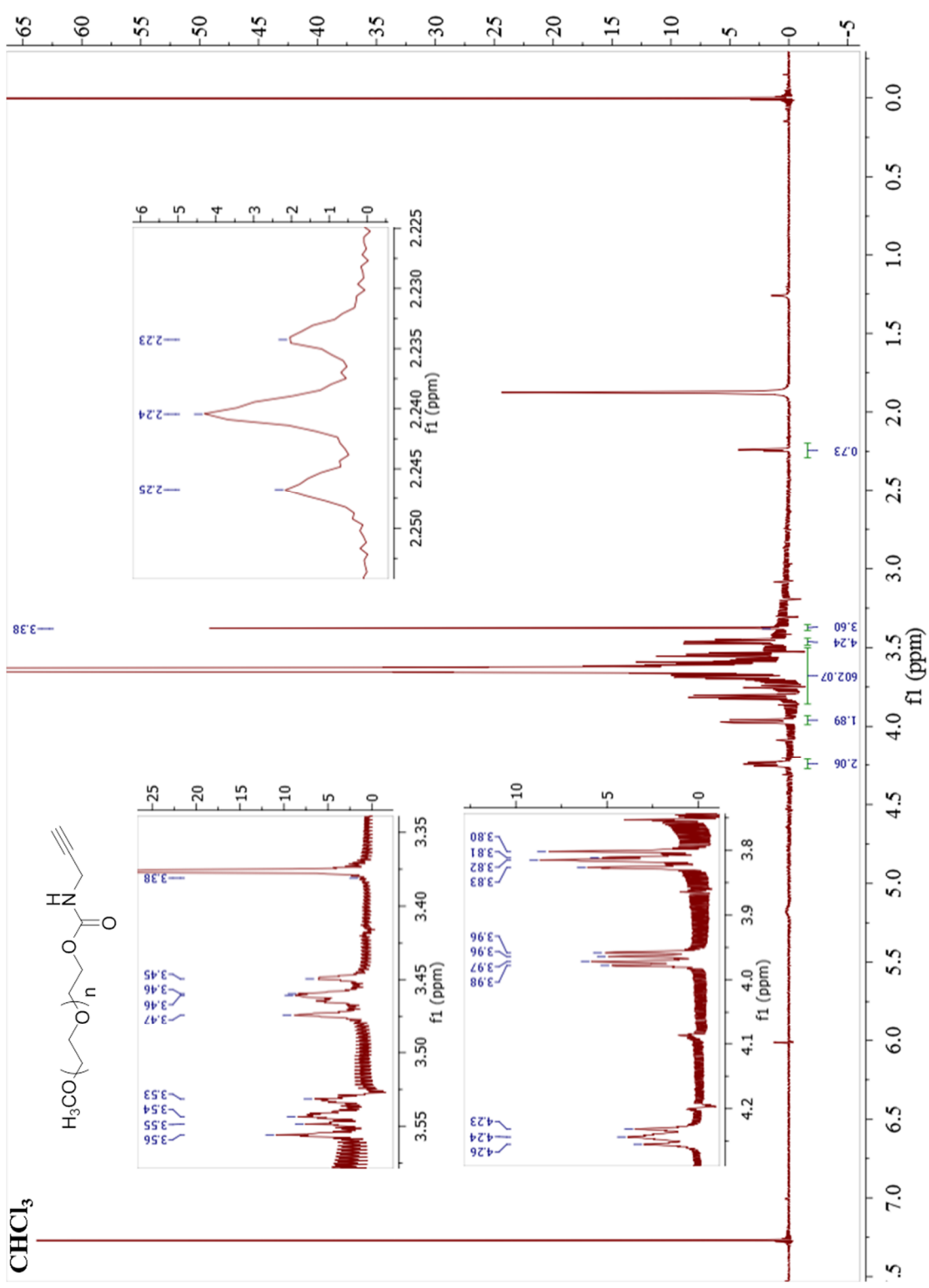
CHCl3
H3CO
n
f1 (ppm)

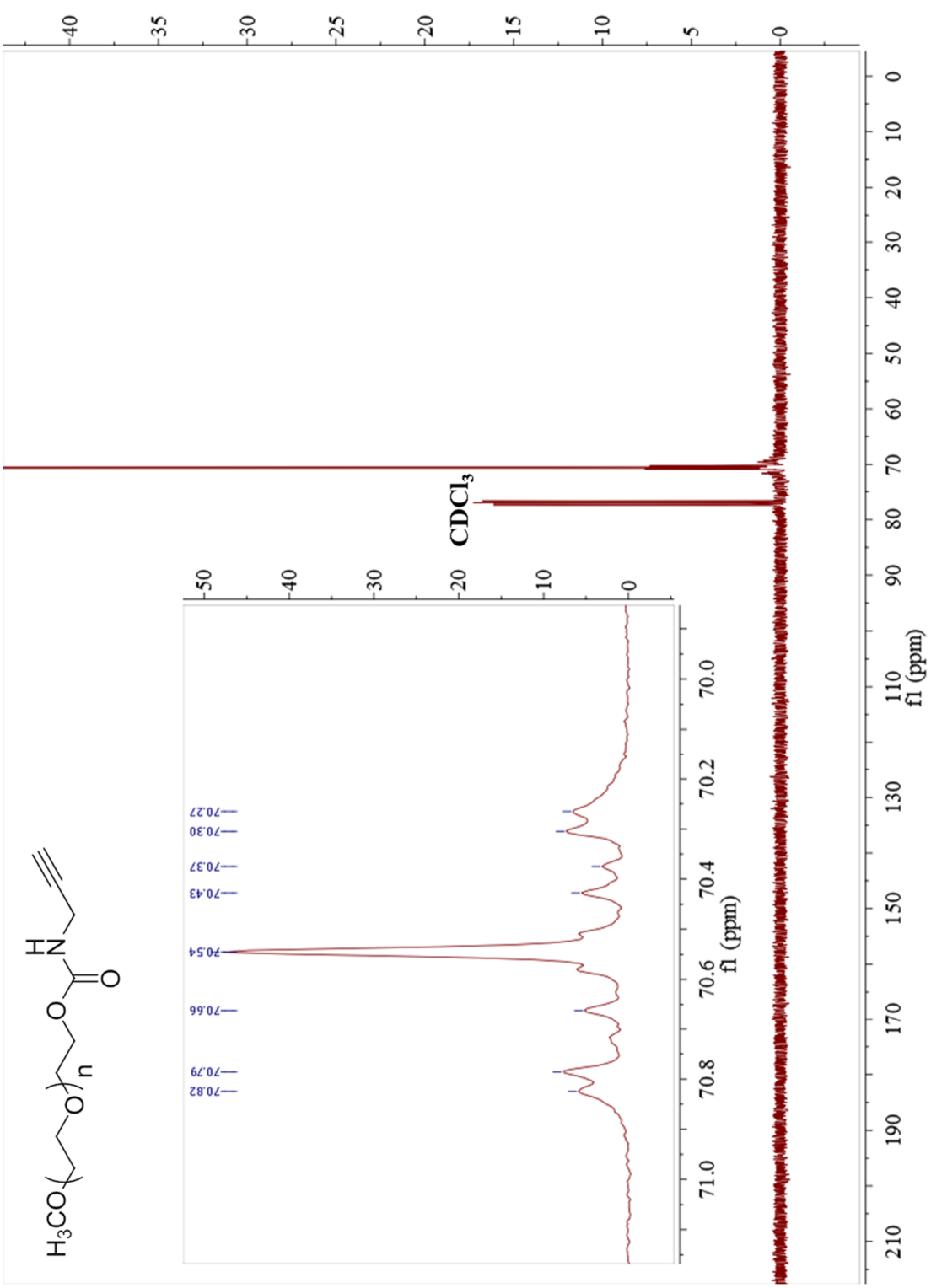
H3CO
O
n
O
O
H
N
O
CDCl3
70.82
70.79
70.66
70.54
70.43
70.37
70.30
70.27
f1 (ppm)
f1 (ppm)

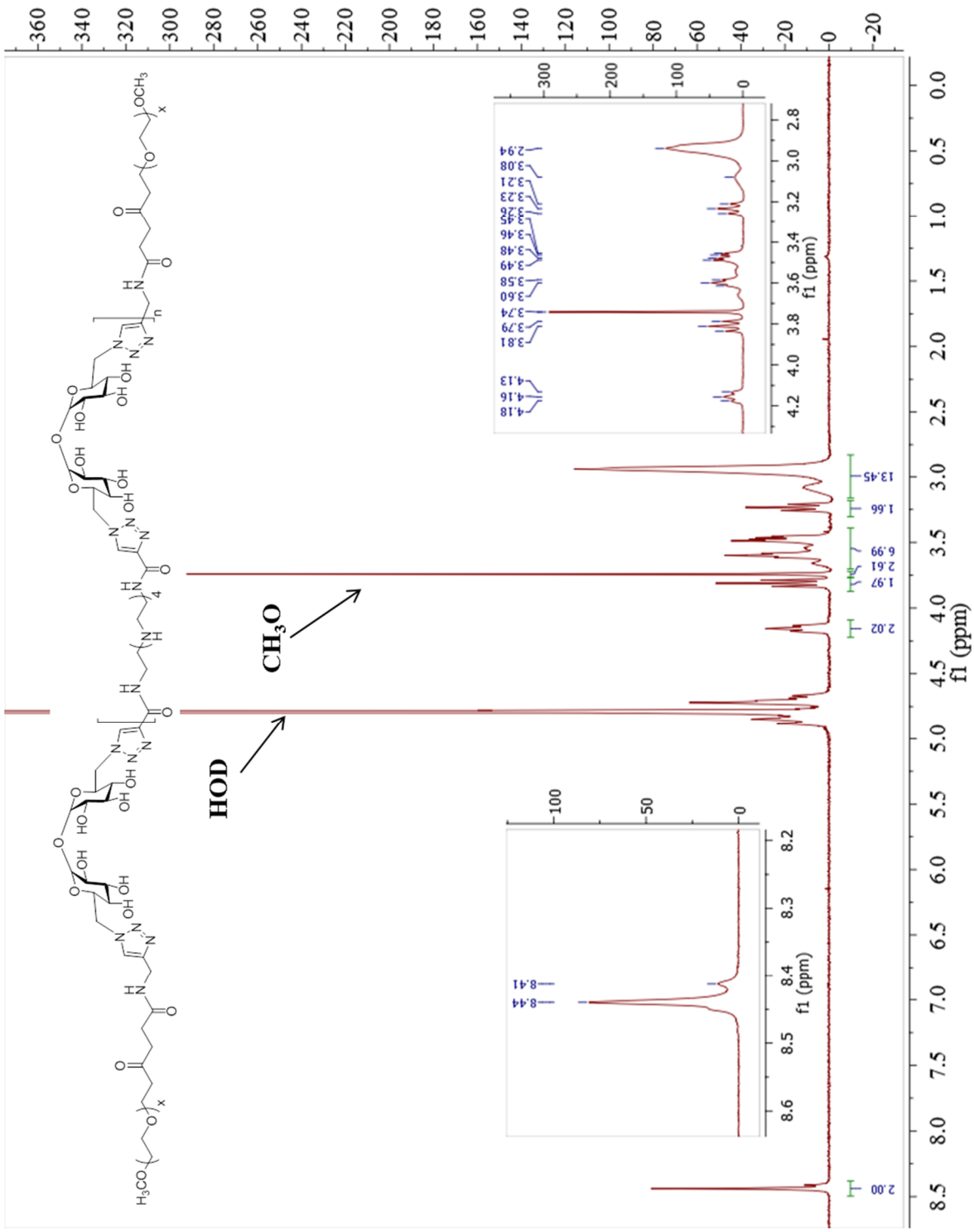
HOD
CH3O
f1 (ppm)

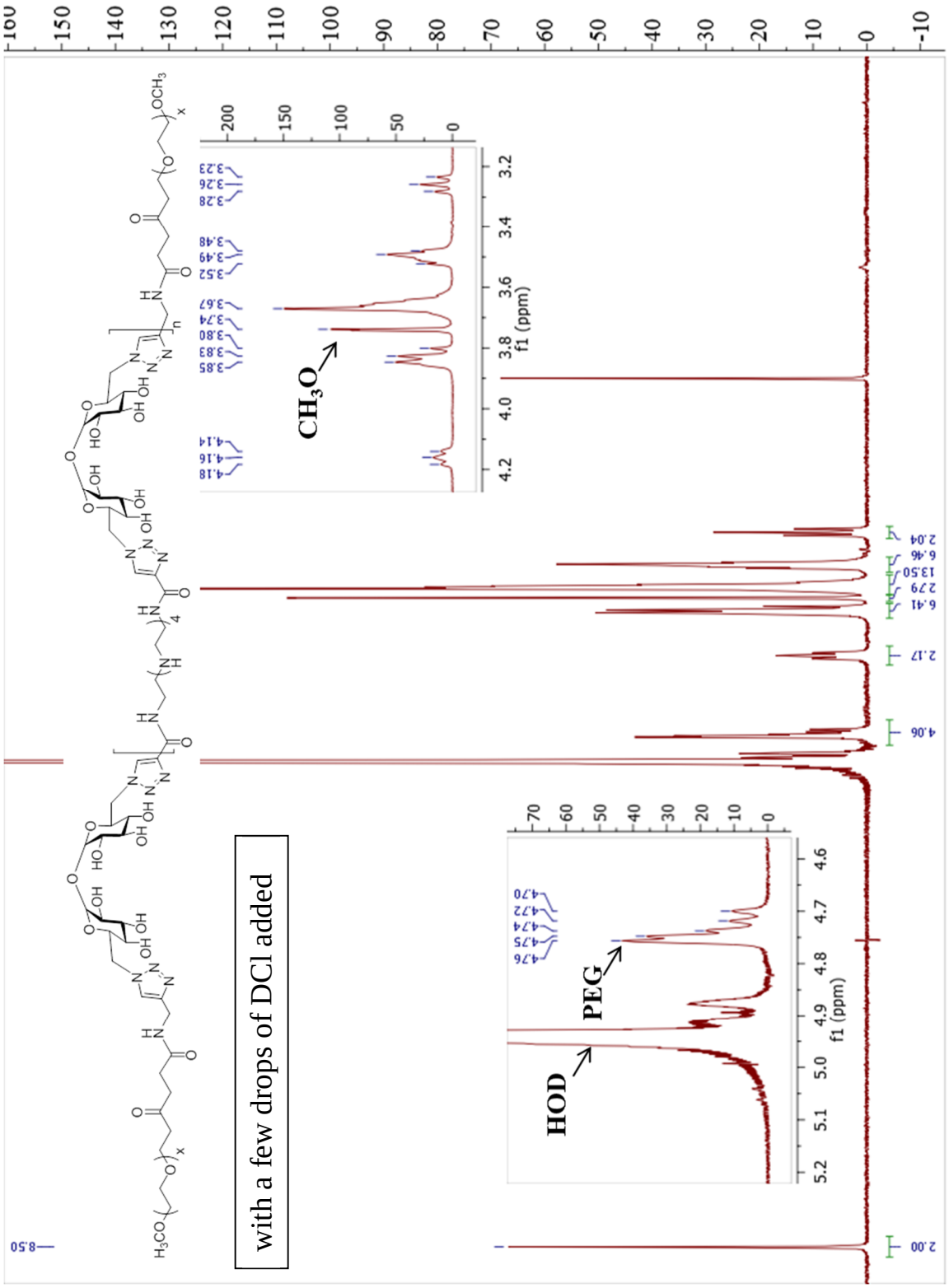
with a few drops of DCl added
HOD
PEG
CH_3O
f1 (ppm)

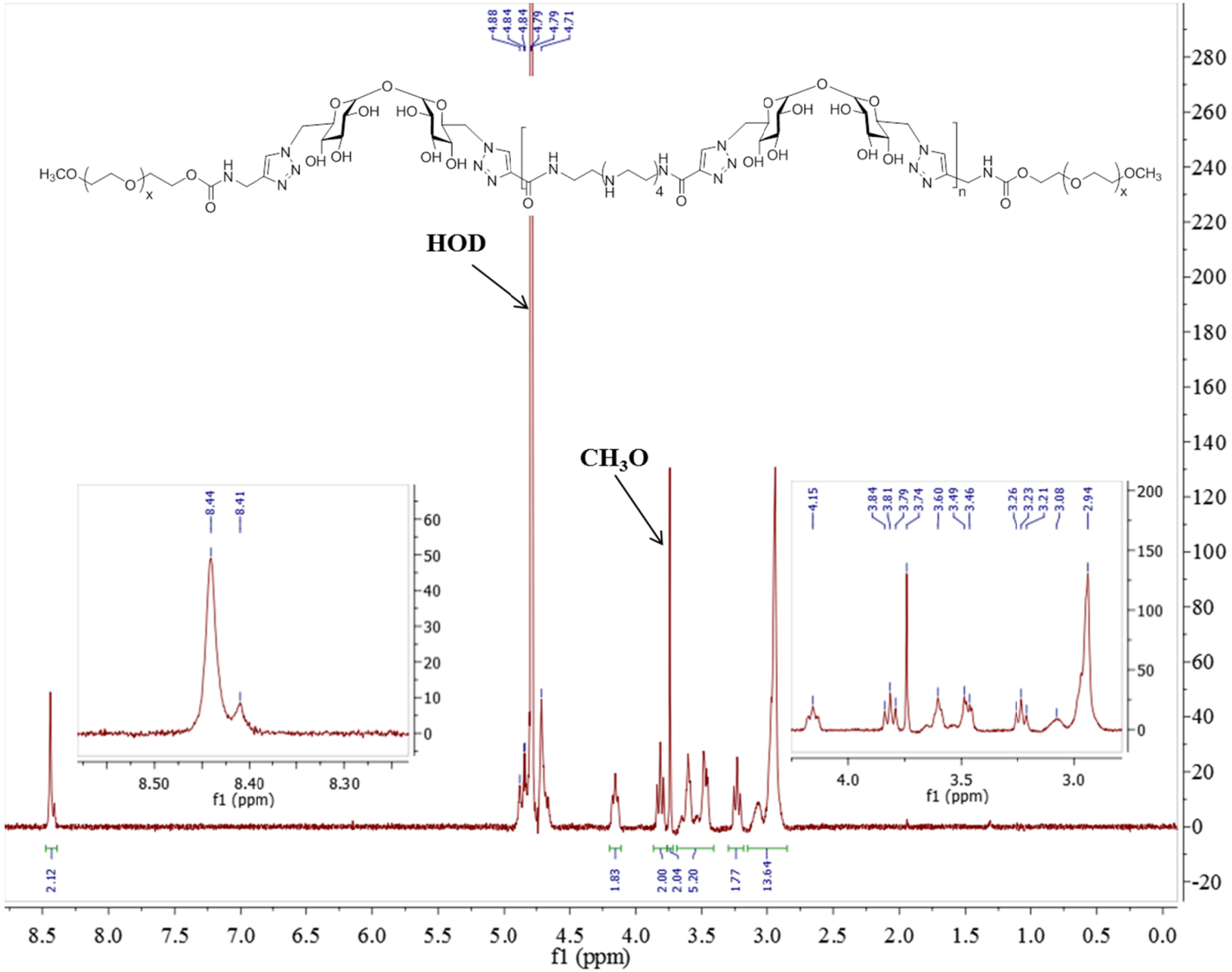
HOD
CH3O
f1 (ppm)

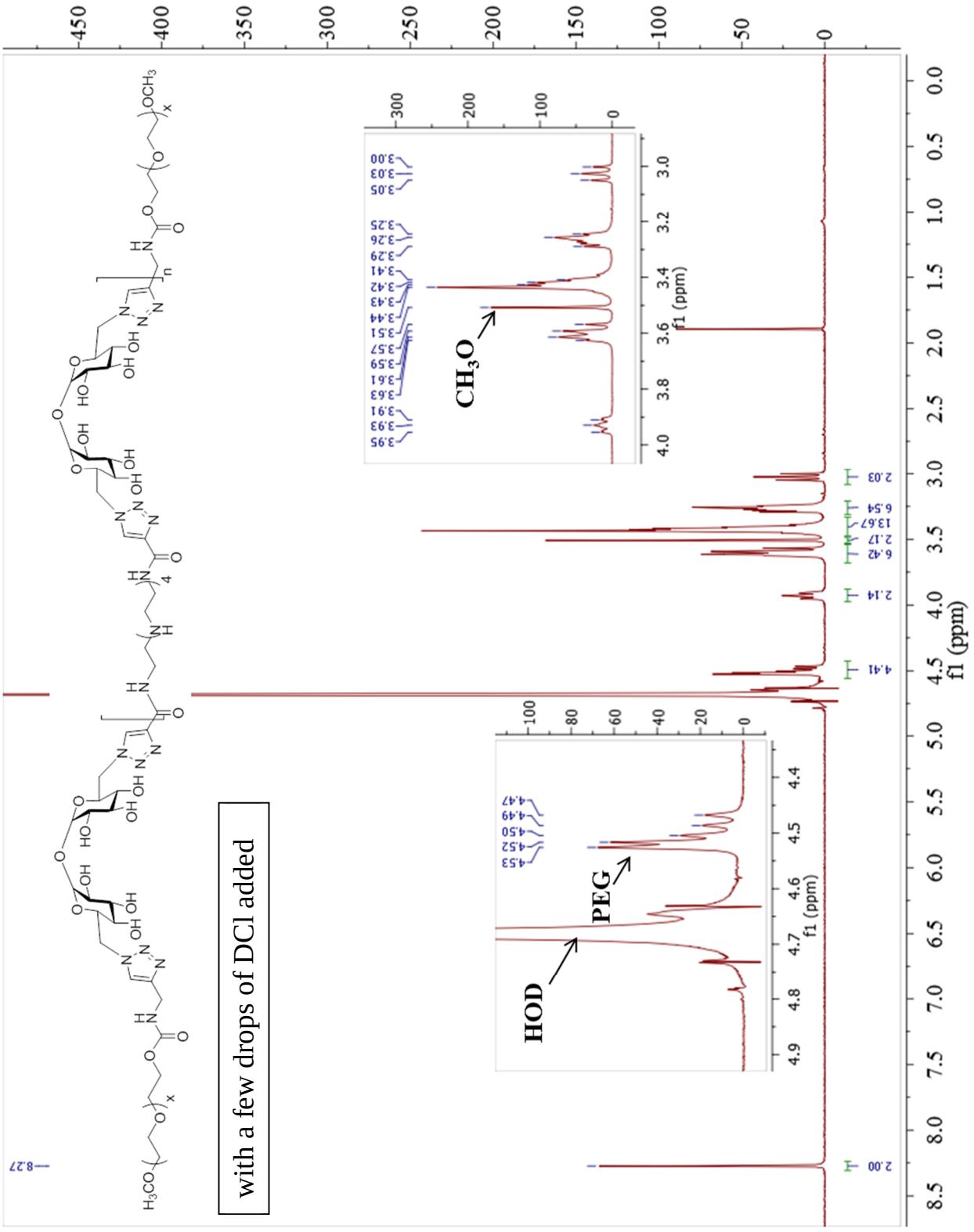
with a few drops of DCl added
HOD
PEG
CH_3O
f1 (ppm)

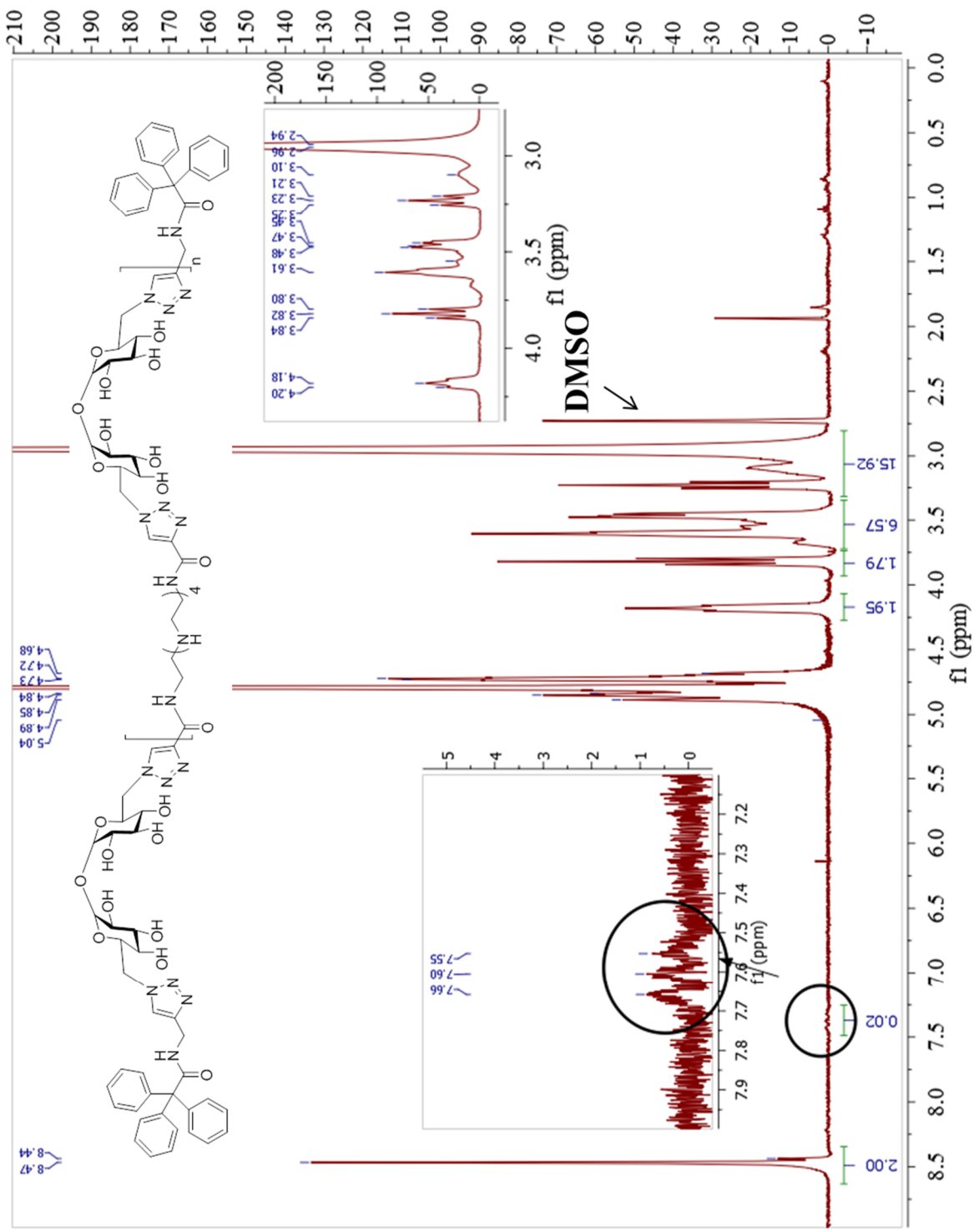
DMSO
f1 (ppm)
2.00
0.02
1.95
1.79
6.57
15.92

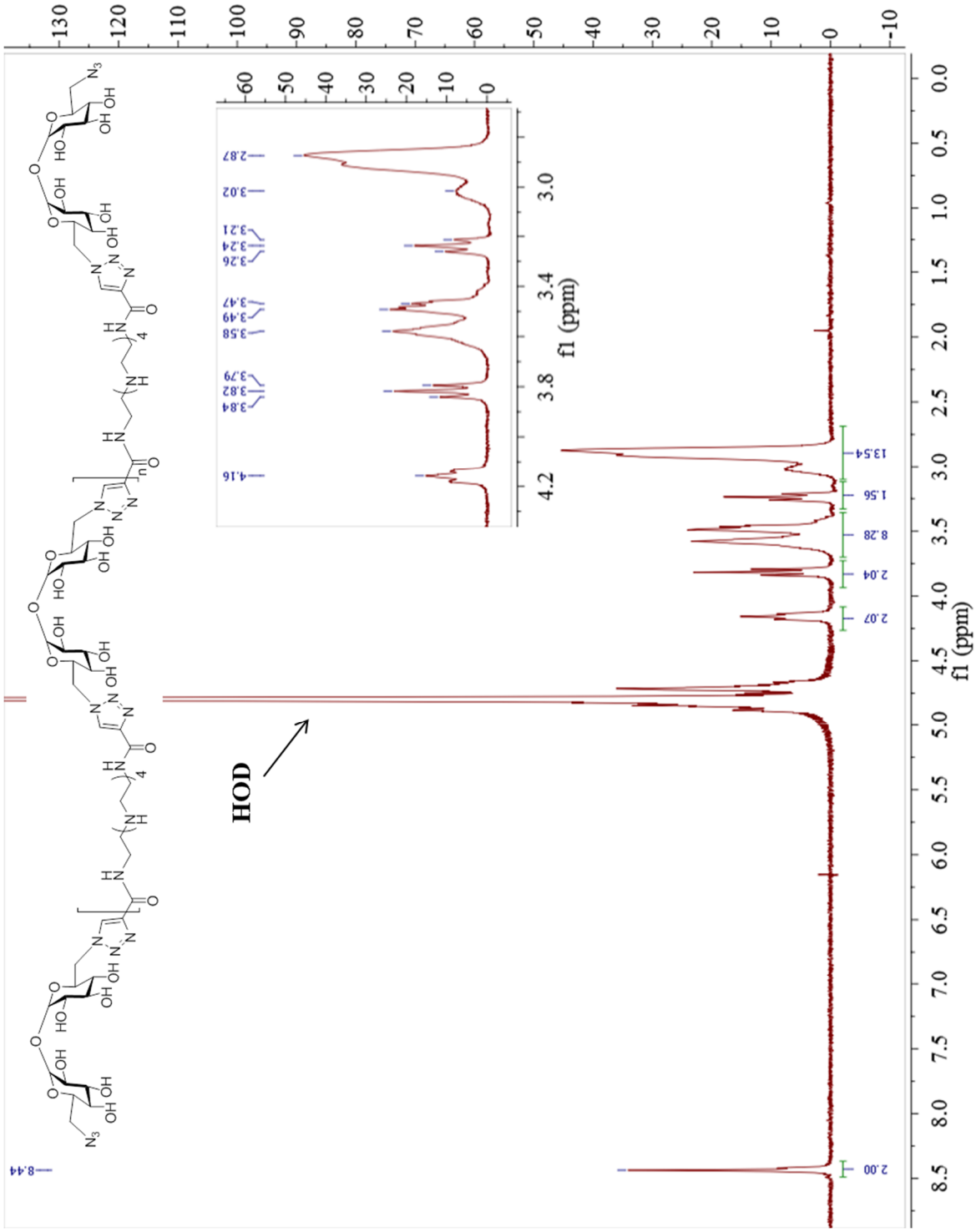
HOD
f1 (ppm)
f1 (ppm)

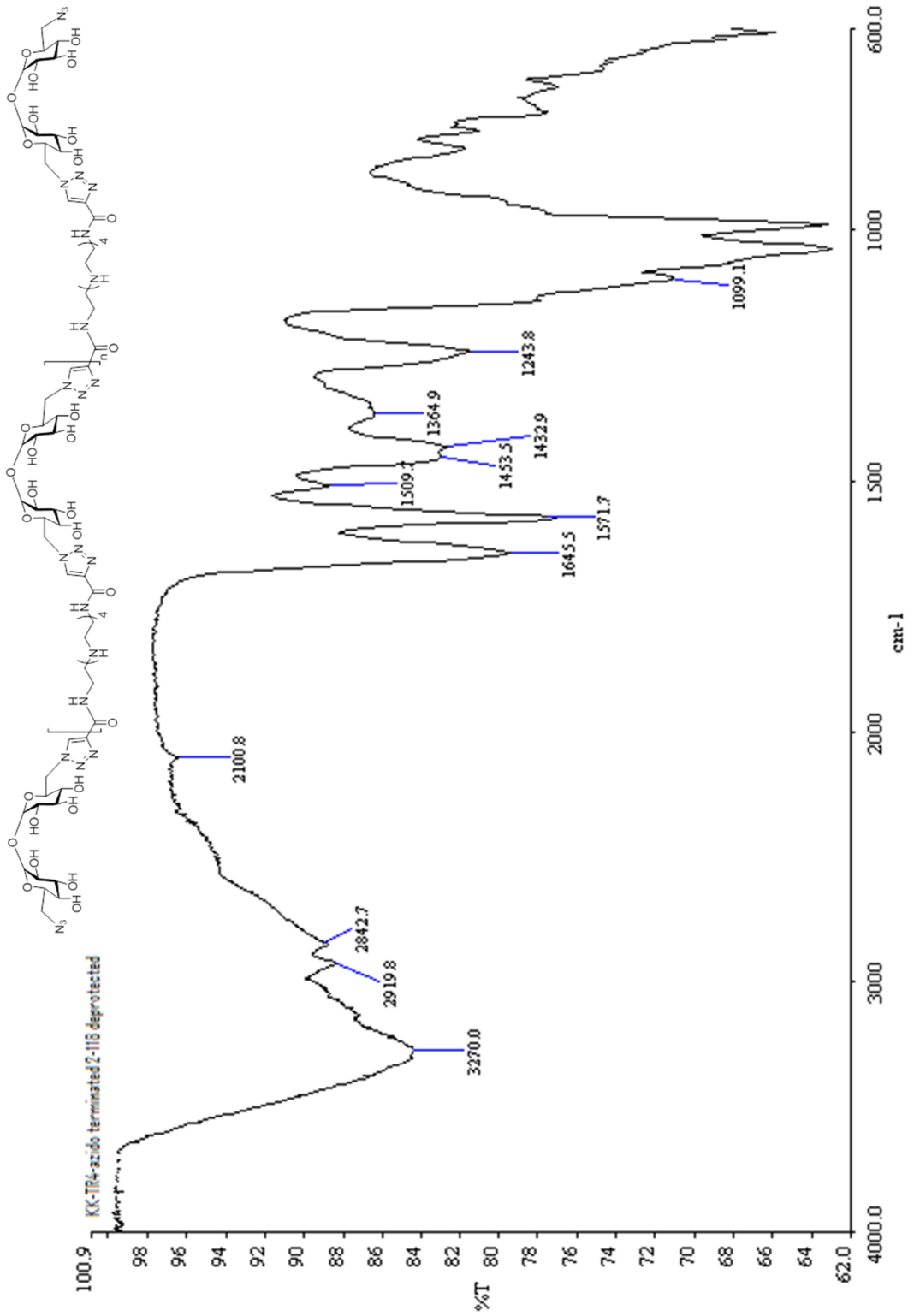
KK-TR4-azido terminated f2-118 deprotected
100.9
98
96
94
92
90
88
86
84
82
80
78
76
74
72
70
68
66
64
62.0
%T
4000.0
3000
2000
1500
1000
600.0
cm-1
3370.0
2919.8
2842.7
2100.8
1645.5
1571.7
1509.1
1453.5
1432.9
1364.9
1243.8
1099.1

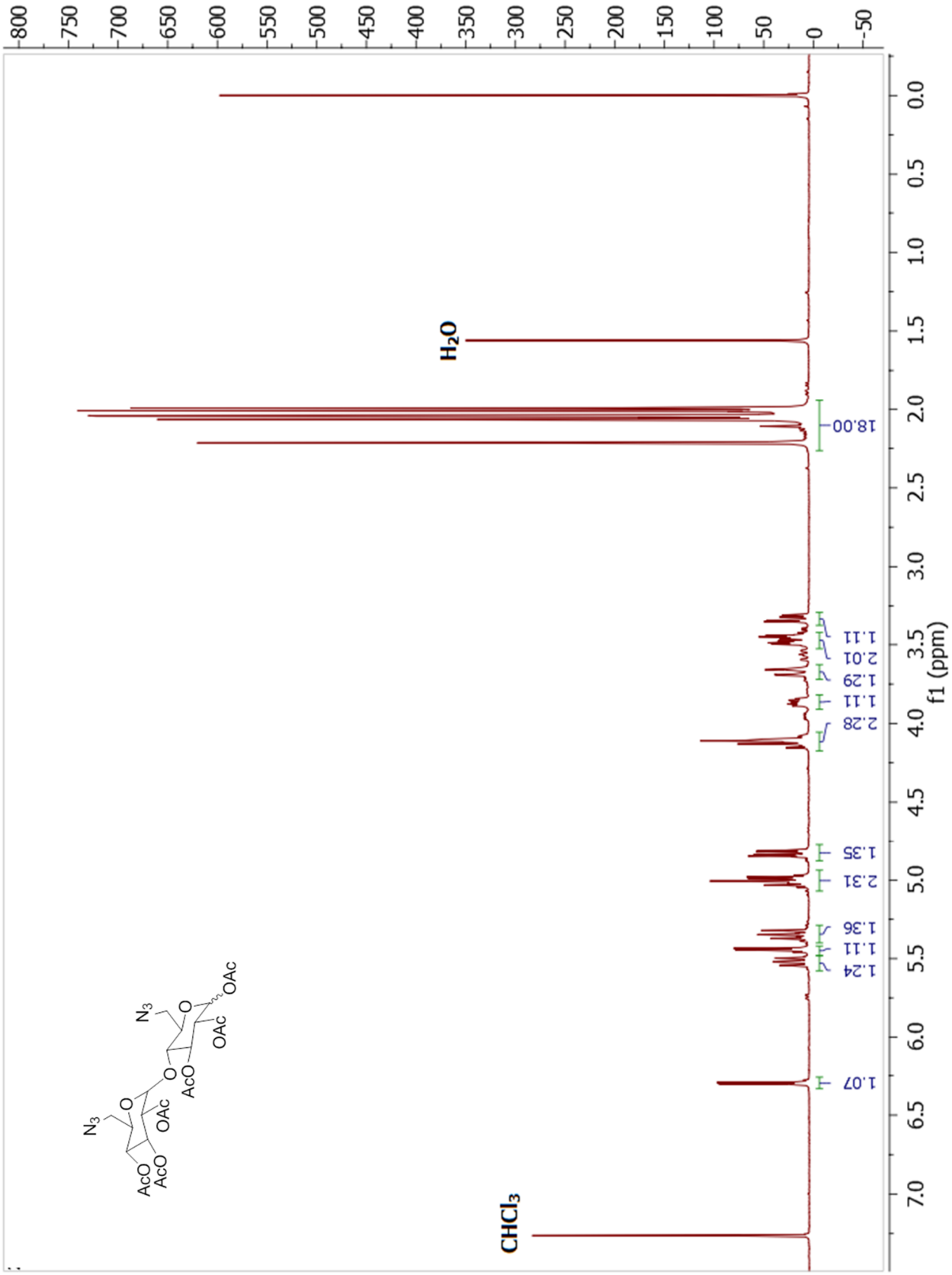
CHCl3
H2O
18.00
2.28
1.11
1.29
2.01
1.11
1.35
2.31
1.36
1.11
1.24
1.07
f1 (ppm)
N3
AcO
AcO
OAc
O
AcO
OAc
N3
OAc

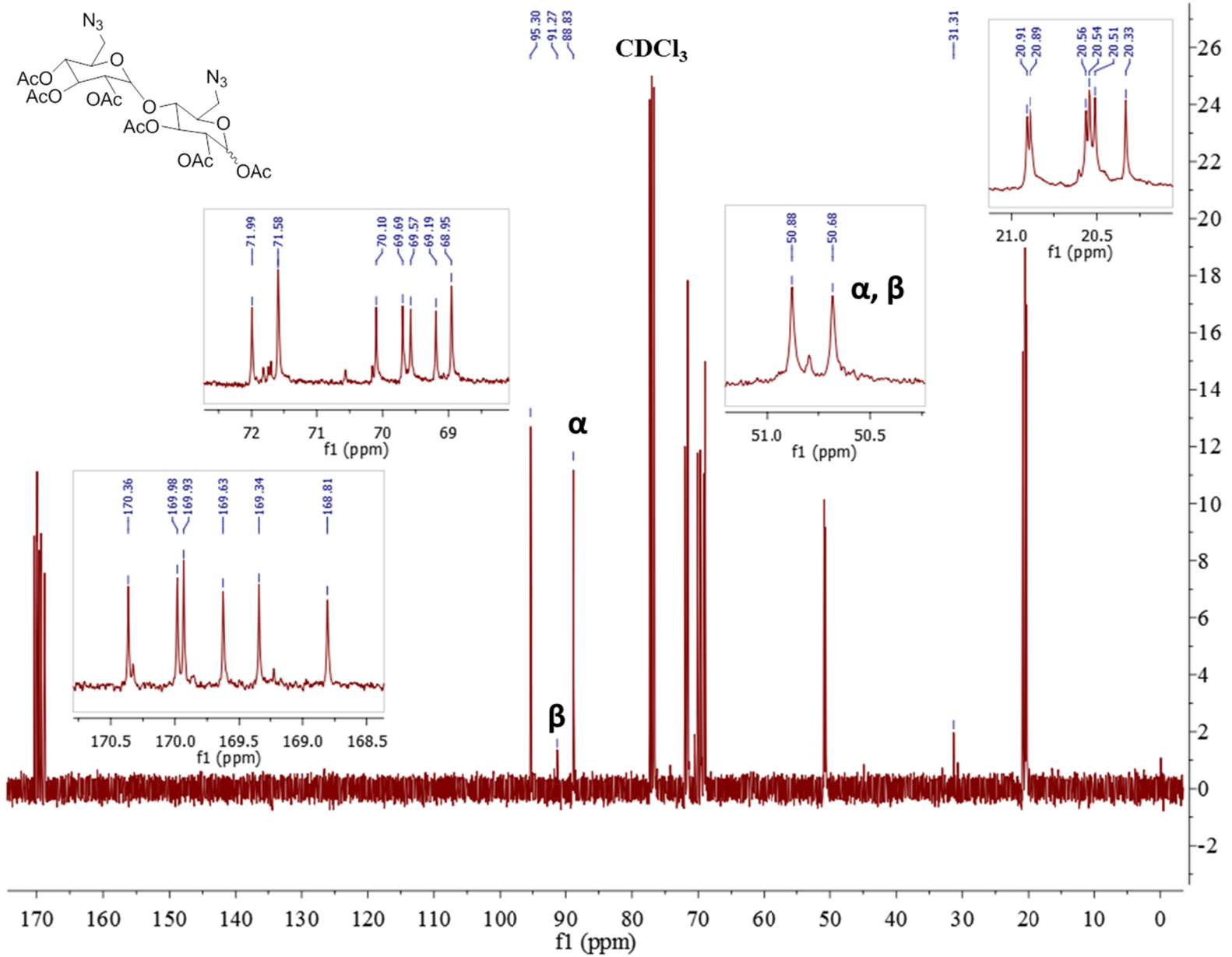
N3
AcO
AcO
OAc
O
AcO
N3
O
OAc
OAc
95.30
91.27
88.83
CDCl3
31.31
20.91
20.89
20.56
20.54
20.51
20.33
71.99
71.58
70.10
69.69
69.57
69.19
68.95
50.88
50.68
α, β
α
β
170.36
169.98
169.93
169.63
169.34
168.81
f1 (ppm)

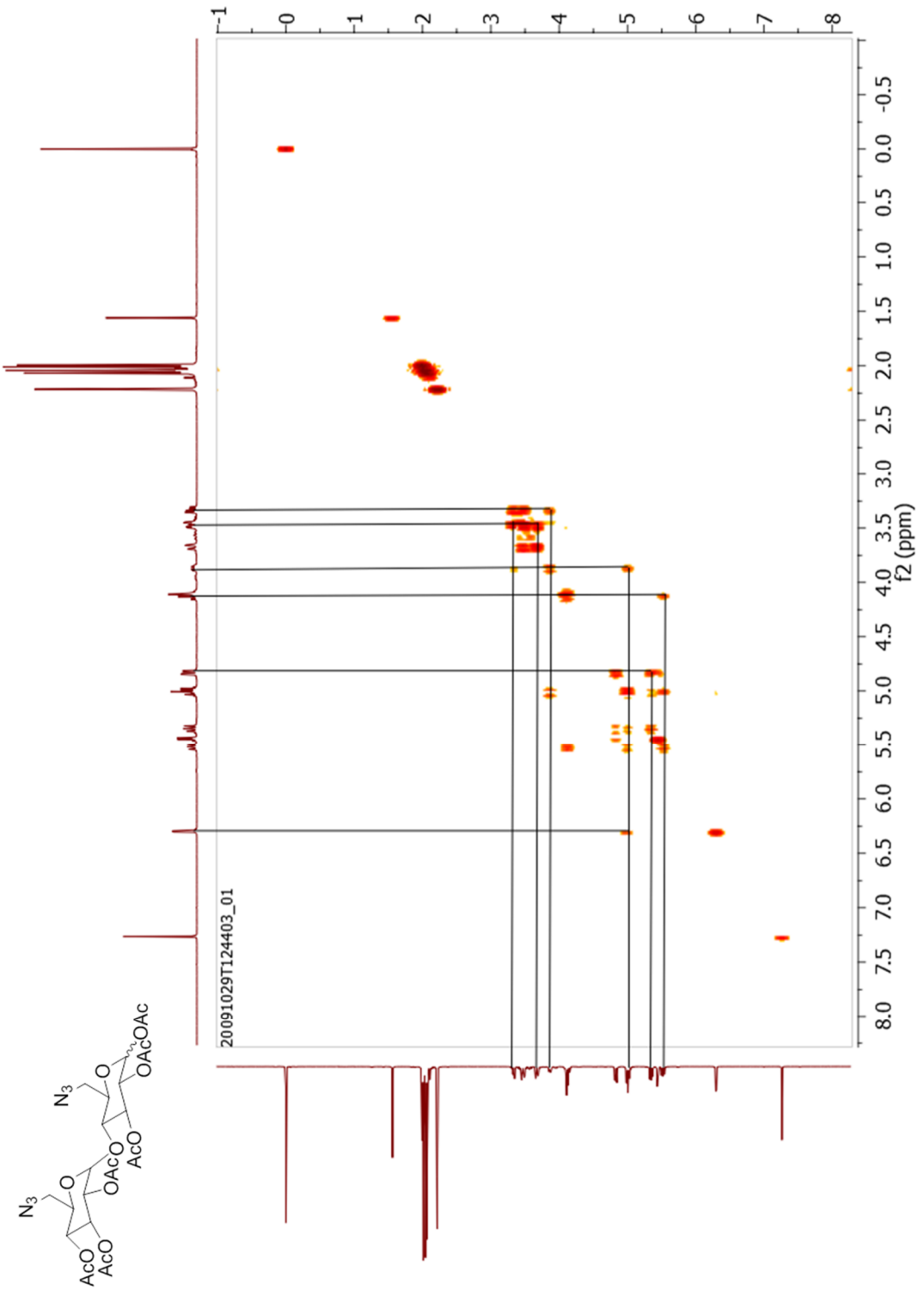
f1 (ppm)
f2 (ppm)
20091029T124403_01
N3
AcO
AcO
OAcO
AcO
OAcOAc

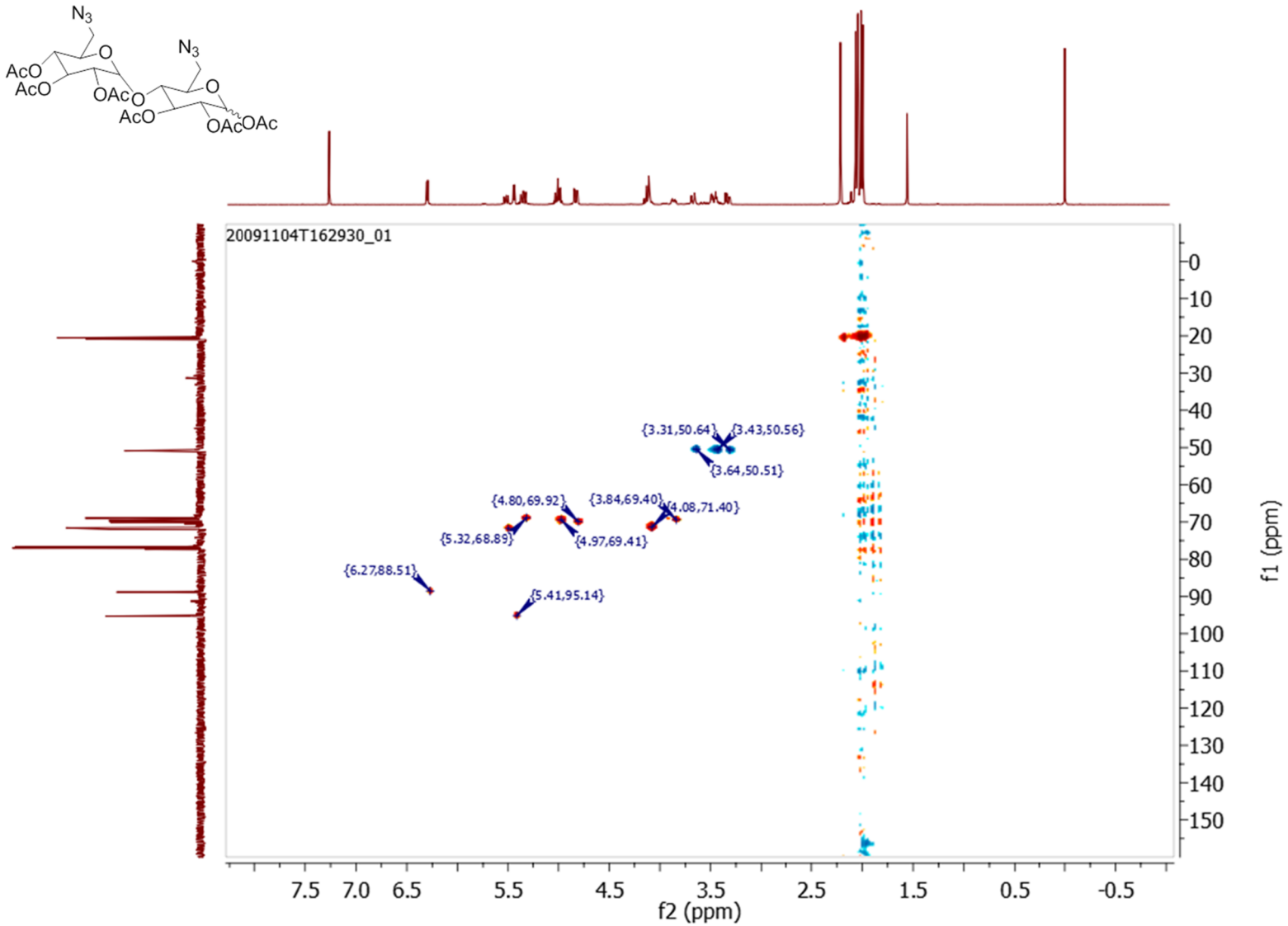
N3
N3
AcO
AcO
OAc
AcO
OAc
OAc
20091104T162930_01
{3.31,50.64}
{3.43,50.56}
{3.64,50.51}
{4.80,69.92}
{3.84,69.40}
{4.08,71.40}
{5.32,68.89}
{4.97,69.41}
{6.27,88.51}
{5.41,95.14}
7.5
7.0
6.5
5.5
4.5
3.5
2.5
1.5
0.5
-0.5
f2 (ppm)
f1 (ppm)
0
10
20
30
40
50
60
70
80
90
100
110
120
130
140
150

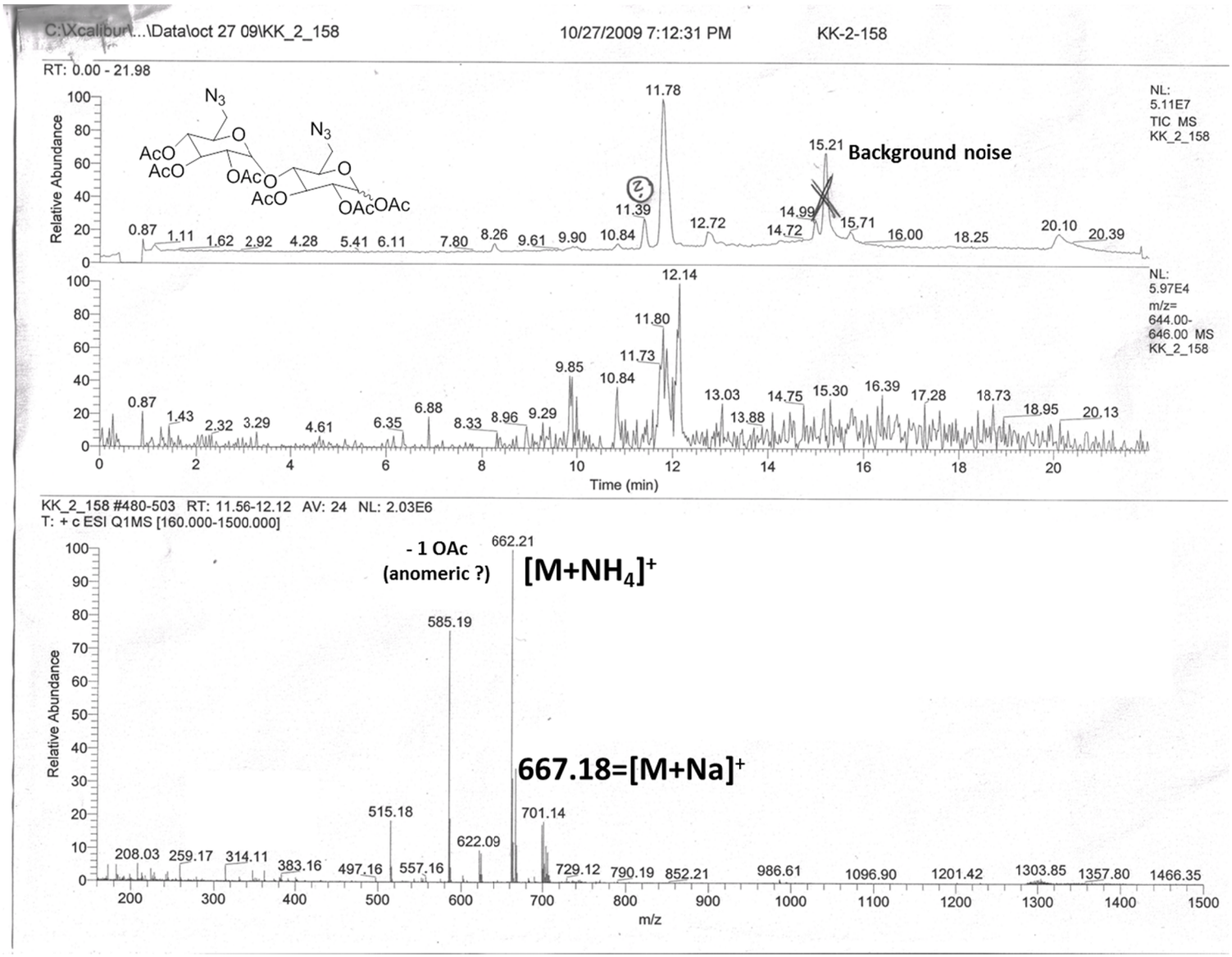
C:\Xcalibur\...\Data\oct 27 09\KK_2_158
10/27/2009 7:12:31 PM
KK-2-158
RT: 0.00 - 21.98
Relative Abundance
Time (min)
NL: 5.11E7 TIC MS KK_2_158
NL: 5.97E4 m/z= 644.00-646.00 MS KK_2_158
Background noise
KK_2_158 #480-503 RT: 11.56-12.12 AV: 24 NL: 2.03E6
T: + c ESI Q1MS [160.000-1500.000]
- 1 OAc (anomeric ?)
[M+NH4]+
667.18=[M+Na]+
m/z

Appendix B: Other Supporting Information

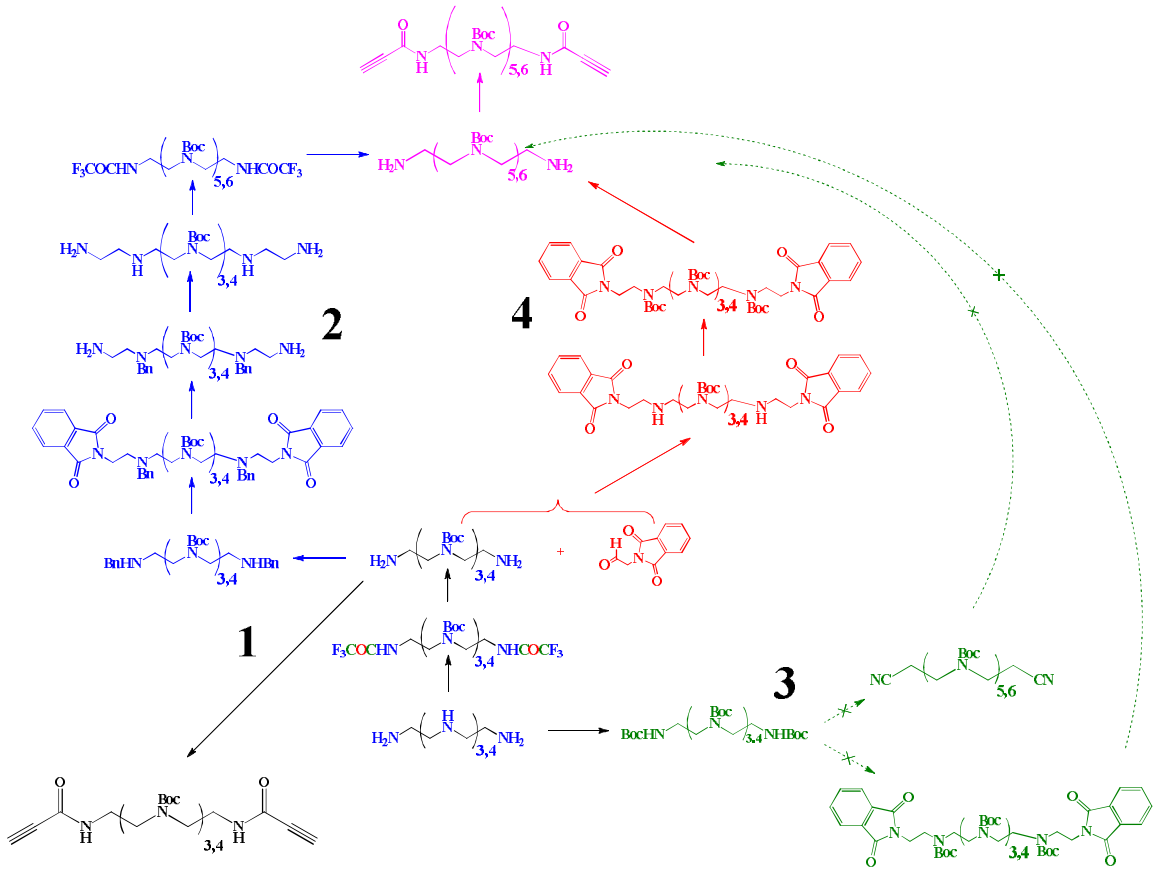

The synthetic routes utilized for the synthesis of oligoethyleneamine monomers.

Route 1: The original synthesis of oligoethyleneamines of shorter length (with 1 to 4 secondary amines).

Route 2: The synthetic scheme used by the former group member, Chen-Chang Lee, and slightly modified towards the desired goal products. The scheme has too many steps and gives very low total yields.

Route 3: This route failed since no conditions were found for the alkylation of the carbamates on the ends of fully Boc-protected oligoethyleneamines.

Route 4: The current route used for the synthesis of oligoethyleneamine monomer of extended length (with 5 and 6 secondary amines).

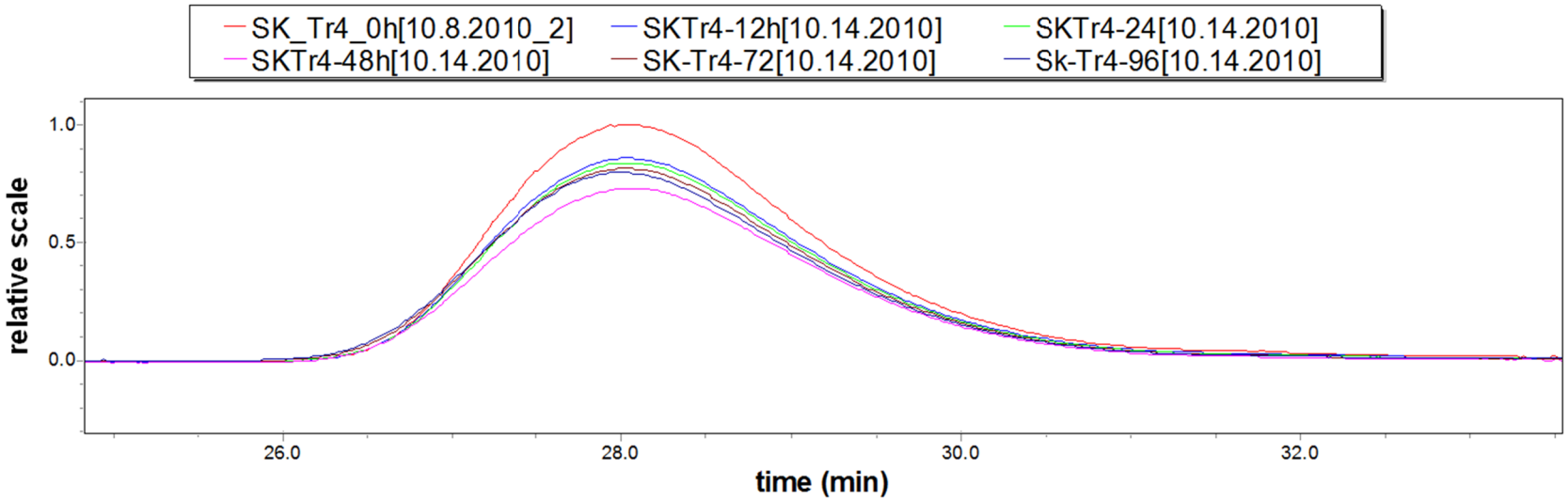

Degradation studies of **Tr4** polymer (DP=77) via GPC. Preliminary studies.

Tr4 was dissolved in aqueous buffer (pH 5.5). The aliquots were taken from this solution at the certain time points (0 h, 12 h, 24 h, 48 h, 72 h, and 96 h), freeze-dried and subjected to a GPC analysis. Conditions: eluent of 0.48 M sodium acetate solution in water:acetonitrile-80:20 (pH 7) at a flow rate of 0.3 mL/min at 25 ºC with an injection volume of 100 µL, Eprogen, Inc. CATSEC columns (100, 300, and 1000 Å), Waters 2489 UV/vis detector (λ = 274 nm), Wyatt Optilab rex refractometer (λ = 658 nm), and Wyatt DAWN Heleos-II multiangle laser light scattering (MALLS) detector (λ = 662 nm). The data was analyzed using ASTRA software version 5.3.4.14. The chromatogram is representing light scattering (LS) signal. The lack of the shift of the signal toward the higher retention time is indicating that the polymer did not degrade.

Experiment was performed by Sneha Kelkar. We thank Lian Xue for **Tr4**.